Dissertation

submitted to the

Combined Faculty of Natural Sciences and Mathematics

of the Ruperto Carola University Heidelberg, Germany

for the degree of

Doctor of Natural Sciences

Presented by

M.Sc. Martin Roßmanith

born in: Zwickau, Germany

Oral examination: 26.07.2021

Characterization and modulation of neuronal ensembles involved in reward learning

Examining neuronal ensembles encoding for drug and natural reward seeking

Referees: Prof. Dr. Rainer Spanagel

Prof. Dr. Andreas Draguhn

ACKNOWLEDGEMENTS

The following PhD thesis was accomplished at the Institute of Psychopharmacology, Central Institute of Mental Health (CIMH), Mannheim and the University of Heidelberg under guidance and supervision of Prof. Dr. Rainer Spanagel, Dr. Anita Hansson, Dr. Valentina Vengeliene and Dr. Georg Köhr.

This work was financially supported by the German Research Foundation within the framework of the Collaborative Research Centre 1134, subproject B05.

Over the past few years, a lot of people accompanied and helped me on my greatest scientific journey to date. With their unswerving scientific as well as moral support they have laid the foundation for the success of my dissertation. Thus, I would like to deeply thank each and every one of them.

First and foremost, I would like to express my sincere gratitude towards all of my supervisors:

Prof. Dr. Rainer Spanagel for his excellent advice and guidance throughout the entire PhD thesis and beyond. Thank you very much for the great opportunity to join your renowned laboratory and work on such an interesting and challenging project. Even though it has not always been easy, it was an exciting experience that helped me to become a better scientist and person.

Dr. Anita Hansson thank you so much for your guidance and your deep knowledge that covered the largest part of my PhD thesis. I am incredibly grateful that I could benefit from your expertise in neuroanatomy, radioactive *in situ* hybridizations and double antibody stainings. Moreover, I am thankful for your moral support during the more challenging times.

Dr. Valentina Vengeliene my deepest thanks goes to you for all your outstanding guidance during the last couple of years. Your unfailing encouragement and enthusiasm that already supported me during my Master thesis just carried on during my PhD thesis and motivated me to give my best. Thank you very much for your expertise and wisdom regarding conditioning experiments and reward learning behaviour, it laid the foundation for this thesis. And most important, thank you for your friendship, it made everything so much better!

Dr. Georg Köhr I am incredibly grateful that I had your excellent guidance and support during one of the toughest parts of my PhD thesis. Thanks a lot for your knowledge as well as for

supporting me, during my 12-hour days, helping me tirelessly with my electrophysiological recordings and everything that came along during this part of the project.

Moreover, I would like to thank all members of my PhD examination committee for their time, effort and scientific input: Prof. Dr. Andreas Draguhn, Prof. Dr. Stephan Frings and Dr. Ana M.M. Oliveira.

A very special thanks goes to our wonderful technicians Elena Büchler, Sabrina Koch, Elisabeth Röbel and Claudia Schäfer-Arnold. Thank you very much Elena for all your great help regarding the cocaine self-administration experiments. All your knowledge, your help with surgeries and catheter implantations, it has been a fantastic support and I am deeply grateful. And of course, thanks a lot for your friendship and all the fun we had inside and outside the lab. Sabrina I am deeply grateful for your fantastic help in managing and taking care of the animal breedings. Not to mention the hours we spent together tailing animals for genotyping. You supported me from the very beginning, and I always could count on you! Dear Elisabeth, I would like to deeply thank you for your endless support and encouragement during my excursions to the third and now second floor. For all your aid with brain slicing, all the PFA preparations, your professional knowledge and all the other countless things you supported me with or taught me. You really are the good soul of our lab. Claudia thank you very much for your great help in the radioactive laboratory when I was running endless *in situ* hybridizations. And of course, thanks a lot for all the genotyping you did for my transgenic animals.

A huge thanks goes to Janet Barroso-Flores, who taught me whole-cell recordings and analysed the acquired data.

Moreover, I would like to express my gratitude to Dr. Peter Bengtson, who was so kind to let me use his microscope and patch clamp set up in Heidelberg for all my electrophysiological recordings.

I furthermore would like to thank Marvin Pätz and Arian Hach for their help with double immunostainings.

A special thanks goes to my fellow PhD students Simone Pfarr, Tatiane Takahashi and Shoupeng Wei. Together we shared the same path and scientifically and morally supported each other along the way. Thanks for the great times during conferences, retreats and the daily lab routine.

Furthermore, I would like to thank all my friends and colleagues in the lab for their help, support and advice during all these years. It was a pleasure working with all of you: Chris Friemel, Peggy Schneider, Christine Roggenkamp, Nazzareno Cannella, Anne Mallien, Natasha Pfeifer, Wolfgang Sommer, Sandra Helinski, Catarina Luis, Tianyang Ma, Thorsten Lau, Sarah Leixner, Rebecca Hoffmann, Laura Schaaf, Thomas Enkel and Rick Bernardi.

An enormous thanks goes to all my friends outside the laboratory. First and foremost, this thanks goes to all my "Heidelberg friends", most of whom I have known since my first semester in Heidelberg and whose support and friendship I could always count on: Anki, Andi, Björn, Caro, Janina, Kristin, Lena, Philipp and Robin. Another deep thanks goes to my two best friends at home: Dennis and Meister. Even though we are separated by more than 400 km your friendship and support lasted since our time at the Käthe-Kollwitz Gymnasium Zwickau.

In the end my deepest gratitude goes to my parents and my family! Without your everlasting support and help I would not be where I am today. Thank you for everything! Tanja, you were there when I first started this journey and you unconditionally supported me with all your patience, help and love during all these years. You always motivated me during the good times and cheered me up during the hard times. I am deeply grateful for that!

Even though I cannot mention each and every name of the people who supported me during my PhD journey and beyond, I am truly grateful for each and every one of you!

SUMMARY

Our daily life activities are highly dependent on rewards and their ability to drive our motivational and goal-directed behaviours. Rewards are essential for all individuals as they enable us to satisfy our most basic needs and desires. The processing of exteroceptive and interoceptive stimuli within the reward system help us to evaluate the rewarding value of certain actions and reward entities. In this regard, the reward system is originally responsible for processing of information related to natural rewards including food, water and sex. However, it can also be hijacked by drugs of abuse, which are able to manipulate the system with their reinforcing properties. Drugs of abuse are thereby able to drive learning processes, as a result of which external stimuli, such as odours, sounds or visual cues, become associated with the respective drug. For addicts, exposure to these stimuli triggers drug seeking, which results in drug consumption and, for abstinent individuals, relapse of compulsive drug use. In order to improve relapse prevention with pharmacological or therapeutical interventions the underlying mechanisms must be understood on a neuronal level. Today, it is widely accepted that distinct memories, such as learned cue-reward associations, are encoded in sparsely distributed subsets of neurons, so called neuronal ensembles, to achieve given tasks. Rewarding stimuli are thereby thought to activate distinct neurobiological patterns within the reward system. Thus, the associative learning process might result in the formation of neuronal ensembles that encode cue-reward associations, which are reward specific.

This thesis therefore aimed to examine the shared and distinct properties of neuronal ensembles encoding different cue-reward associations, investigating different drugs of abuse and the natural reward saccharin.

In a first set of experiments, we identified co-active neurons encoding for the investigated cue-induced reward seeking behaviour within the extended reward system. The natural reward saccharin as well as the three drugs of abuse (ethanol, cocaine, nicotine) showed broadly overlapping neuronal activity patterns within the prefrontal cortex, specifically within its orbitofrontal part. On a subcortical level similar activation patterns could be found within the caudate putamen. Despite these similarities, each reward also displayed distinct changes in neuronal activity. Cue-induced ethanol seeking, for example, increased activity within the basolateral amygdala, whereas cue-induced seeking for both psychostimulants displayed elevated activity within the nucleus accumbens core. Saccharin trained animals, however, showed activity reduction within the ventral tegmental area. A second set of experiments characterized the previously identified ensembles on a neurochemical level. The focus was

thereby put on ensembles activated within the orbitofrontal cortex, the brain region with the highest activity during cue-induced reward seeking. Immunohistochemical co-localizations showed that all ensembles activated during reward seeking were entirely neuronal and did not comprise any neuroglia. Most remarkably however was the finding that neuronal ensembles within the orbitofrontal cortex displayed a reward specific neurochemical composition. Whereas the neuronal ensemble activated by cue-induced saccharin seeking showed a balanced participation of glutamatergic and GABAergic neurons, the ensemble induced by ethanol seeking was primarily GABAergic and the ensemble triggered by cocaine seeking was predominantly glutamate driven. In a further experiment, the previously identified neuronal ensembles within the orbitofrontal cortex were functionally validated for their involvement in cue-induced saccharin seeking or cue-induced cocaine seeking behaviour. It was found that inactivation of neuronal ensembles responsible for cue-induced saccharin seeking within the orbitofrontal cortex had an impact on reward seeking behaviour whereas abolition of neuronal ensembles involved in cue-induced cocaine seeking showed no effect on the behavioural output. Finally, neuronal ensembles within the infralimbic cortex mediating ethanol and saccharin seeking were investigated. Examination of participating neurons revealed that both ensembles were largely overlapping but also displayed distinct components specific to each reward.

Overall, the present work contributes to a better understanding of the organisation and functionality of neuronal ensembles involved in cue-induced reward seeking behaviour. The discovered reward dependent neurochemical distinctness of neuronal ensembles encoding cue-reward associations may provide the opportunity for new therapeutical approaches focusing on the distinct features. However, further studies are necessary to further clarify the role of these distinct reward specific components. Nevertheless, the findings of this thesis provide a good starting point to gain more knowledge about neuronal ensembles and their underlying mechanisms and how these might be addressed in a drug-specific manner during addiction treatment.

ZUSAMMENFASSUNG

Unser tägliches Leben sowie unsere Aktivitäten werden von Belohnungen geprägt, die unsere Motivation und unser zielgerichtetes Verhalten steuern. Belohnungen sind dabei essenziell für jedes Individuum, da sie es befähigen seine Grundbedürfnisse und sein Verlangen zu stillen. Das Belohnungszentrum verarbeitet dabei verschiedene externe und interne Reize, um jede Aktivität hinsichtlich ihres Belohnungswertes zu evaluieren. Obwohl das Belohnungszentrum ursprünglich für die Informationsverarbeitung natürlicher Belohnungen, wie Nahrung, Wasser und Sex, zuständig ist, kann es von verschiedenen rauscherzeugenden Substanzen beeinflusst werden. Drogen stoßen dabei Lernprozesse an bei denen externe Reize, wie Gerüche, Geräusche oder visuelle Stimuli, mit der jeweiligen Droge assoziiert werden. Diese Reize können bei drogenabhängigen Personen sogenanntes Belohnungssuchverhalten auslösen, welches in der Regel zum Drogenkonsum und im Falle von abstinenten Personen zu einem Rückfall mit unkontrolliertem Drogenmissbrauch führt. Um die Rückfallprävention durch pharmakologische oder therapeutische Interventionen zu verbessern, ist ein tiefgehendes Verständnis zugrundeliegender neuronaler Mechanismen erforderlich. Ein Hauptaugenmerk liegt dabei auf Erinnerungen, wie jenen Reiz/Belohnungsassoziationen, welche auch nach Jahren noch einen Rückfall bei Betroffenen auslösen können. Diese Assoziationen werden von kleinen, weit verteilten neuronalen Populationen kodiert, die als neuronale Ensembles bezeichnet werden. Es wird vermutet, dass sowohl verschiedene Reize als auch unterschiedliche Belohnungen spezifische neuronale Strukturen im Belohnungszentrum aktivieren. Das heißt assoziative Lernprozesse können zur Entstehung von individuellen, belohnungsspezifischen und reizspezifischen neuronalen Ensembles führen.

Die vorliegende Doktorarbeit hat sich daher zum Ziel gesetzt die Gemeinsamkeiten und Unterschiede neuronaler Ensembles, welche Reiz/Belohnungsassoziationen kodieren, zu untersuchen und dabei verschiedene psychoaktive Substanzen und die natürliche Belohnung Saccharin zu berücksichtigen. In einem ersten Schritt wurden dafür ko-aktive Neurone, welche reizinduziertes Suchverhalten im Belohnungszentrum kodieren, identifiziert. Suchverhalten für Saccharin sowie die drei untersuchten Drogen Alkohol, Kokain und Nikotin, zeigte weitreichende und überlappende neuronale Aktivität im präfrontalen Kortex und dort besonders im orbitofrontalen Teil. Auf subkortikaler Ebene wurde im Striatum dorsale ähnliche Aktivität für alle getesteten Belohnungen beobachtet. Unabhängig von den beobachteten Gemeinsamkeiten zeigte jede Belohnung auch spezifische Veränderungen in neuronaler Aktivität. Reizinduziertes Alkoholsuchverhalten wies verstärkte Aktivität in der basolateralen

Amygdala auf, wohingegen reizinduziertes Suchverhalten nach den beiden getesteten Psychostimulanzien erhöhte Aktivität im Kernbereich des Nucleus accumbens zur Folge hatte. Versuchstiere, die auf Saccharin trainiert wurden, zeigten wiederum reduzierte Aktivität in der Area tegmentalis ventralis. In einem weiteren Experiment wurden die neurochemischen Eigenschaften zuvor identifizierter Ensembles in der Hirnregion mit der höchsten Aktivität, dem orbitofrontalen Kortex, charakterisiert. Die immunhistochemische Analyse offenbarte eine rein neuronale Zusammensetzung der aktiven Ensembles, wodurch die Beteiligung von Neuroglia ausgeschlossen werden konnte. Am interessantesten jedoch war die Entdeckung, dass die untersuchten neuronalen Ensembles eine belohnungsspezifische neurochemische Zusammensetzung aufwiesen. Das neuronale Ensemble zuständig für reizinduziertes Saccharinsuchverhalten wies gleichermaßen Anteile von GABAergen und glutamatergen Neuronen auf, wohingegen das Ensemble für reizinduziertes Alkoholsuchverhalten vorwiegend von GABAergen Neuronen und das Ensemble für reizinduziertes Kokainsuchverhalten überwiegend von glutamatergen Neuronen gebildet wurde. In einem weiteren Schritt wurde die funktionelle Beteiligung der zuvor charakterisierten neuronalen Ensembles am Saccharinsuchverhalten oder Kokainsuchverhalten untersucht. Dabei konnte gezeigt werden, dass Inaktivierung der neuronalen Ensembles im orbitofrontalen Kortex, welche während des reizinduzierten Saccharinsuchverhaltens aktiv waren, einen Einfluss auf das untersuchte Verhalten haben. Für die Inaktivierung der neuronalen Ensembles, welche während des reizinduzierten Kokainsuchverhaltens aktiv waren, konnte keine Verhaltensbeeinflussung nachgewiesen werden. Abschließend wurden neuronale Ensembles des infralimbischen Kortex, welche Alkohol- und Saccharinsuchverhalten kodieren, untersucht. Dabei wurde nachgewiesen, dass beide Ensembles zu einem Großteil überlappen aber auch individuelle und belohnungsspezifische Anteile besitzen.

Alles in allem ermöglicht die vorliegende Doktorarbeit einen neuen Einblick in die Organisation und Funktion der am reizinduzierten Suchverhalten beteiligten neuronalen Ensembles. Die Entdeckung belohnungsspezifischer Unterschiede neuronaler Ensembles, welche bestimmte Reiz/Belohnungsassoziationen kodieren, könnte die Möglichkeit für neue therapeutische Ansätze bieten. Ungeachtet dessen sind weitere Untersuchungen nötig um die Rolle dieser belohnungsspezifischen Komponenten weitergehend aufzuklären. Dennoch bieten die vorliegenden Ergebnisse einen guten Ausgangspunkt, um das Wissen über neuronale Ensembles und ihre zugrundeliegenden Mechanismen zu erweitern und um die Behandlung von Suchterkrankungen potentiell zukünftig noch individueller und spezifischer gestalten zu können.

TABLE OF CONTENTS

ACKNOWLEDGEMENTS ..... **I**

SUMMARY ..... **IV**

ZUSAMMENFASSUNG ..... **VI**

TABLE OF CONTENTS ..... **VIII**

LIST OF FIGURES ..... **XIII**

LIST OF TABLES ..... **XVI**

SYMBOLS AND ABBREVIATIONS ..... **XVII**

LIST OF PUBLICATIONS ..... **XXII**

1. INTRODUCTION **1**

1.1 Reward seeking behaviour **2**

1.2 Drugs of abuse and their mechanism of action **6**

1.3 The brain reward system **13**

1.4 Prefrontal cortex **16**

1.4.1 Orbitofrontal cortex 19

1.4.1.1 Role of the orbitofrontal cortex in reward seeking 20

1.4.2 Medial prefrontal cortex 22

1.4.2.1 Role of the medial prefrontal cortex in reward seeking 23

1.5 The role of neuronal ensembles in reward seeking **25**

1.6 Immediate early genes - cFOS **29**

1.7 Animal disease models **34**

1.7.1 Animal model of drug self-administration and reinstatement of reward seeking 34

1.8 Transgenic animals **37**

1.8.1 *c-fos*-GFP transgenic rats 37

1.8.2 *c-fos*-lacZ transgenic rats 38

1.9 Hypothesis and Aims **39**

1.10 Study list **40**

2. MATERIALS AND METHODS **41**

2.1 Subjects **41**

2.2 Experimental study design **42**

2.2.1 Study 1A: Identification of neuronal ensembles within the extended reward system encoding for natural reward and drug reward seeking 42

2.2.2 Study 1B: Immunohistochemical analysis of neuronal ensembles following cue-induced reinstatement of reward seeking behaviour 43

2.2.3 Study 1C: Characterization of the physiological properties of GFP positive (active) versus GFP negative (inactive) neurons after reinstatement of reward seeking 44
2.2.4 Study 2: Validation of functional neuronal ensembles encoding for natural reward and drug reward seeking behaviour 45
2.2.5 Study 3: Comparison of neuronal ensembles within the infralimbic cortex following reinstatement of saccharin and ethanol seeking behaviour 46

2.3 Behavioural experiments 48
2.3.1 Operant conditioning experiments 48
2.3.1.1 Operant conditioning chamber 48
2.3.1.2 Operant self-administration training 48
2.3.1.3 Extinction training/Extinction test session (Study 1A) 50
2.3.1.4 Cue-induced reinstatement of reward seeking behaviour 51

2.4 Surgical interventions and associated procedures 52
2.4.1 Intravenous catheter implantation 52
2.4.1.1 Catheter preparation 52
2.4.1.2 Catheter implantation 53
2.4.1.3 Catheter maintenance 54
2.4.2 Stereotaxic surgery 55
2.4.2.1 Guide cannula implantation 55
2.4.3 Daun02/vehicle infusions 56
2.4.3.1 Daun02 preparation 57
2.4.3.2 Vehicle preparation 57

2.5 Tissue collection and preparation 58
2.5.1 Brain harvesting 58
2.5.1.1 Decapitation 58
2.5.1.2 Transcardial perfusions 58
2.5.2 Brain slice preparation 59
2.5.2.1 Cryosectioning 59
2.5.2.2 Vibratome sectioning 60

2.6 *In situ* Hybridization 61
2.6.1 Radioactive *in situ* hybridization (Study 1A) 61
2.6.1.1 Probe generation 61
2.6.1.2 Fixation 63
2.6.1.3 Siliconizing coverslips 63
2.6.1.4 Probe labelling - *In vitro* transcription 64
2.6.1.5 Prehybridization and Hybridization 65
2.6.1.6 Post-hybridization washing steps 65
2.6.1.7 Autoradiography 66
2.6.1.8 Autoradiography analysis 66
2.6.2 Fluorescent *in situ* hybridization (Study 3B) 68
2.6.2.1 RNAscope *in situ* hybridization 68
2.6.2.2 Image acquisition 69

2.7 Immunohistochemical examination 70
2.7.1 Double immunofluorescence stainings (Study 1B) 70
2.7.1.1 Image acquisition 71
2.7.1.2 Image analysis 72

2.7.2 Double immunofluorescence stainings (Study 3A) ... 73
2.7.2.1 Image acquisition ... 73
2.7.2.2 Image analysis ... 73
2.7.3 ß-galactosidase immunohistochemical stainings (Study 2) ... 74
2.7.3.1 Infusion validation ... 74
2.8 Electrophysiological examination ... 75
2.8.1 Whole-cell patch clamp recordings ... 75
2.8.2 Data analysis ... 76
2.9 Statistical analysis ... 77
3. RESULTS ... 78
3.1 Study 1A: Identification of neuronal ensembles within the extended reward system encoding for natural reward and drug reward seeking ... 79
3.1.1 Operant conditioning to identify neuronal ensembles encoding cue-reward associations ... 79
3.1.2 Mapping of *c-fos* mRNA expression patterns following natural reward and drug reward seeking ... 82
3.2 Study 1B: Neurochemical characterization of neuronal ensembles within the OFC active during reinstatement of reward seeking ... 86
3.2.1 Operant conditioning to characterize the neurochemical nature of neuronal ensembles encoding natural reward and drug reward seeking ... 86
3.2.2 Immunohistochemical analysis of neuronal ensembles following cue-induced reinstatement of reward seeking behaviour ... 88
3.3 Study 1C: Characterization of the physiological properties of GFP positive (active) versus GFP negative (inactive) neurons after reinstatement of reward seeking ... 96
3.3.1 cFOS-ir and GFP-ir co-localization ... 96
3.3.2 Operant conditioning to investigate the functional properties of neuronal ensembles involved in cue-induced reinstatement of cocaine seeking ... 97
3.3.3 Whole-cell patch clamp analysis to characterize physiological properties of neuronal ensembles ... 99
3.4 Study 2: Validation of functional neuronal ensembles encoding for natural reward and drug reward seeking behaviour ... 102
3.4.1 Investigating the functional relevance of neuronal ensembles involved in saccharin reward seeking behaviour ... 102
3.4.2 Investigating the functional relevance of neuronal ensembles involved in cocaine reward seeking behaviour ... 107
3.5 Study 3: Comparison of neuronal ensembles within the infralimbic cortex following reinstatement of saccharin and ethanol seeking behaviour ... 111
3.5.1 Study 3A: Two-reward operant conditioning for characterization of neuronal ensemble size following cue-induced reinstatement of EtOH or saccharin seeking behaviour ... 111
3.5.2 Study 3A: Immunohistochemical analysis of neuronal ensemble size ... 114

3.5.3 Study 3B: Two-reward operant conditioning for characterization of neuronal ensemble distinctness following cue-induced reinstatement of natural and drug reward seeking 115
3.5.4 Study 3B: Double *c-fos* fluorescent *in situ* hybridization following EtOH and saccharin cue-induced reinstatement 117

3.6 Troubleshooting 120

4. DISCUSSION 123

4.1 Study 1: Identification of neuronal ensembles within the extended reward system encoding for natural reward and drug reward seeking 124
4.1.1 Operant conditioning to identify neuronal ensembles within the extended reward system encoding for natural reward and drug reward seeking 124
4.1.2 Study 1A: Mapping of *c-fos* mRNA expression patterns following natural reward and drug reward seeking 126
4.1.2.1 *c-fos* mRNA expression during cue-induced reinstatement of reward seeking 126
4.1.2.2 *c-fos* mRNA expression during extinction 130
4.1.2.3 Summary 132
4.1.3 Study 1B: Immunohistochemical analysis of neuronal ensembles following cue-induced reinstatement of reward seeking behaviour 132
4.1.3.1 Summary 138
4.1.4 Study 1C: Characterization of the physiological properties of GFP positive (active) versus GFP negative (inactive) neurons after reinstatement of reward seeking 138
4.1.4.1 cFOS-ir and GFP-ir co-localization 138
4.1.4.2 Whole-cell patch clamp analysis to characterize physiological properties of neuronal ensembles 139
4.1.4.3 Summary 140

4.2 Study 2: Validation of functional neuronal ensembles encoding for natural reward and drug reward seeking behaviour 140
4.2.1 Investigating the functional relevance of neuronal ensembles involved in saccharin reward seeking behaviour 140
4.2.2 Investigating the functional relevance of neuronal ensembles involved in cocaine reward seeking behaviour 143
4.2.3 Summary 145

4.3 Study 3: Comparison of neuronal ensembles within the infralimbic cortex following reinstatement of saccharin and ethanol seeking behaviour 146
4.3.1 Two-reward operant conditioning for characterization of neuronal ensemble size and distinctness following cue-induced reinstatement of EtOH or saccharin seeking behaviour 146
4.3.2 Study 3A: Immunohistochemical analysis of neuronal ensemble size 147
4.3.3 Study 3B: Double *c-fos* fluorescent *in situ* hybridization following EtOH and saccharin cue-induced reinstatement 148
4.3.4 Summary 148

4.4 Study limitations 149

5. CONCLUSION 150

6. OUTLOOK **152**

6.1 CAMPARI method **152**

6.2 Cell-type specific silencing of active neurons using a Cre-dependent viral gene transfer approach **153**

7. REFERENCES **156**

8. SUPPLEMENTARY **180**

7.1 Supplementary Materials & Methods **180**

7.1.1 Antibodies 180

7.1.2 Drugs 181

7.1.3 Solutions 182

7.2 Supplementary Results **185**

7.2.1 Immunohistochemical analysis of neuronal ensembles following cue-induced reinstatement of reward seeking behaviour 185

LIST OF FIGURES

Figure 01) Illustration of the gradual progression of drug 'liking' and drug 'wanting' according to the Incentive-Sensitization theory 4

Figure 02) Estimated prevalence of drug dependence throughout lifetime 5

Figure 03) Simplified schematic illustration of major projections within the rat's brain reward system 15

Figure 04) Illustration of the different neocortical lobes of the rat brain 16

Figure 05) Subregional division of rodent prefrontal cortex 17

Figure 06) Schematic representation of OFC subregions 20

Figure 07) Schematic representation of mPFC subregions 23

Figure 08) Schematic representation of two neuronal ensembles activated by specific afferent input 26

Figure 09) Daun02 inactivation method 27

Figure 10) Interaction of neuronal ensembles within the brain reward system 29

Figure 11) Calcium-depended regulation of *c-fos* expression 33

Figure 12) Animal model of drug self-administration and reinstatement of reward seeking 36

Figure 13) Illustration of the structure of the *c-fos*-GFP transgene 38

Figure 14) Illustration of the structure of the *c-fos*-lacZ transgene 38

Figure 15) Time schedule for the identification of neuronal ensembles within the extended reward system 42

Figure 16) Experimental time plan for the neurochemical characterization of neuronal ensembles encoding cue-induced reward seeking behaviour 43

Figure 17) Schedule for the electrophysiological characterization of neuronal ensembles active during cue-induced cocaine seeking behaviour 44

Figure 18) Experimental timeline for the functional validation of previously identified neuronal ensembles encoding for cue-induced reward seeking behaviour 45

Figure 19) Time schedule for two-reward operant conditioning to investigate size differences between neuronal ensembles involved in EtOH or saccharin seeking 46

Figure 20) Timeline for experimental processes during two-reward operant conditioning to compare neuronal ensembles encoding for EtOH and saccharin seeking behaviour within the same animal 47

Figure 21) Schematic representation of brain regions of interest and representative autoradiograms of *c-fos* mRNA *in situ* hybridizations 67

Figure 22) Schematic representation of brain regions of interest as well as representative ß-galactosidase stainings and bright field images of infusion positions 75

Figure 23) Self-administration and extinction training 80

Figure 24) Active and inactive responses during cue-induced reinstatement compared to the average responses during the last four extinction sessions 81

Figure 25) Active and inactive responses during extinction test session compared to the average responses during the last four extinction sessions 82

Figure 26) *c-fos* mRNA expression levels within the extended reward system after cue-induced reinstatement 83

Figure 27) *c-fos* mRNA expression levels within the extended reward system after an additional extinction session 85

Figure 28) Self-administration and extinction training 87

Figure 29) Active and inactive responses during cue-induced reinstatement compared to the average responses during the last four extinction sessions 88

Figure 30) Co-localization of cFOS-ir positive and NeuN-ir positive cells in brain slices of ethanol, saccharin, cocaine and control animals after cue-induced reinstatement 90

Figure 31) Co-localization of cFOS-ir positive and GFAP-ir positive cells in brain slices of ethanol, saccharin, cocaine and control animals after cue-induced reinstatement 91

Figure 32) Co-localization of cFOS-ir positive and CaMKII-ir positive cells in brain slices of ethanol, saccharin, cocaine and control animals after cue-induced reinstatement 92

Figure 33) Co-localization of cFOS-ir positive and GAD67-ir positive cells in brain slices of ethanol, saccharin, cocaine and control animals after cue-induced reinstatement 93

Figure 34) Overview over the neurochemical composition of the cFOS-ir positive neuronal population for different rewards displayed as percentage of Δ RE-control 95

Figure 35) Co-localization of cFOS-ir positive and GFP-ir positive cells in brain slices of cocaine trained rats after cue-induced reinstatement 97

Figure 36) Self-administration and extinction training for cocaine trained animals 98

Figure 37) Active and inactive responses during cue-induced reinstatement compared to average responses during the last four extinction sessions for cocaine trained animals 99

Figure 38) Whole-cell recording of a GFP positive cell 99

Figure 39) Representative voltage traces from GFP negative and GFP positive neurons 100

Figure 40) Current-voltage relationship of GFP^-, GFP^+ type 1 and GFP^+ type 2 neurons.... 100

Figure 41) Comparison of different electrophysiological properties between GFP negative and GFP positive neurons 101

Figure 42) Saccharin self-administration training and extinction sessions for animals implanted into the lateral OFC 102

Figure 43) Active and inactive responses during cue-induced reinstatement before and after Daun02/vehicle infusions into the lateral OFC of saccharin trained rats compared to extinction 104

Figure 44) Infusion site mapping for saccharin trained animals 104

Figure 45) Saccharin self-administration training and extinction sessions for animals implanted into the ventral OFC 105

Figure 46) Active and inactive responses during cue-induced reinstatement before and after Daun02/vehicle infusions into the ventral OFC of saccharin trained rats compared to extinction 106

Figure 47) Infusion site mapping for saccharin trained animals 106

Figure 48) Cocaine self-administration training and extinction sessions for animals implanted into the lateral OFC 107

Figure 49) Active and inactive responses during cue-induced reinstatement before and after Daun02/vehicle infusions into the lateral OFC of cocaine trained rats compared to extinction 108

Figure 50) Mapping of infusion sites for cocaine trained rats 108

Figure 51) Cocaine self-administration training and extinction sessions for animals implanted into the ventral OFC 109

Figure 52) Active and inactive responses during cue-induced reinstatement before and after Daun02/vehicle infusions into the ventral OFC of cocaine trained rats compared to extinction 110

Figure 53) Location mapping of infusion sites for cocaine trained rats 110

Figure 54) Average lever press responses during the different stages of the two-reward self-administration training paradigm to investigate ensemble size 112

Figure 55) Co-localization of cFOS-ir positive and NeuN-ir positive cells in brain slices after ethanol or saccharin cue-induced reinstatement 114

Figure 56) Average lever press responses during the different stages of the two-reward self-administration training paradigm to examine the distinctness of involved ensembles 116

Figure 57) Fluorescent *in situ* hybridization for nascent and mature *c-fos* mRNA following cue-induced reinstatement of EtOH and saccharin seeking 118

Figure 58) Bootstrap analysis of cell populations expressing both, one or none of the *c-fos* mRNA species examined 119

Figure 59) Differential interference contrast image of an acute OFC brain slice 121

Figure 60) Schematic representation of the CaMPARI method 153

Figure 61) Schematic representation of the viral rAAV-CRAM-d2tTA::TRE-FLEX-hM4Di-mCherry construct and the Tet-OFF system 155

LIST OF TABLES

Table 01) PCR reaction pipetting scheme 62

Table 02) Primary and secondary antibody combinations for immunohistochemical co-localizations 71

Table 03) Statistics for comparison of *c-fos* mRNA expression levels within the extended reward system for control animals vs. animals undergoing reinstatement 84

Table 04) Statistics for comparison of *c-fos* mRNA expression levels within the extended reward system for control animals vs. animals subjected to an additional extinction session 85

Table 05) Statistical analysis for two-reward operant conditioning cFOS-ir/NeuN-ir co-localization 113

Table 06) Statistical analysis for two-reward operant conditioning double fluorescent *in situ* hybridization 117

Table 07) Summary of *c-fos* activation within the PFC following cue-induced reward seeking 128

Table 08) Summary of *c-fos* activation within subcortical brain regions following cue-induced reward seeking 129

Table 09) Summary of *c-fos* activation within the PFC during extinction 131

Table 10) Summary of *c-fos* activation within subcortical brain regions following extinction 131

Table 11) List of antibodies 180

Table 12) List of rewards and active compounds used for self-administration and infusion 181

Table 13) List of solutions and preparation protocols 182-184

Table 14) Number of cells labelled by the different antibodies within the OFC after cue-induced reinstatement and percentage of co-localized cells within each population 187

Table 15) Statistics for the comparison of cell numbers, number of active cells between rewards/between stainings and percentage of merged immune reactivity within the respective population 188

Table 16) Statistical analysis for cell number comparisons 189

Table 17) Statistical analysis of cFOS-ir reward/control-specific 190

Table 18) Statistical analysis for active cell number comparisons 191

Table 19) Statistical analysis of cell activity counts between different antibody stainings within each reward group 192

Table 20) Statistical analysis for the percentage of merged immune reactivity 193

SYMBOLS AND ABBREVIATIONS

%	Percentage
°C	Degree Celsius
µl	Microlitre
µm	Micrometre
35S-UTP	S-35 labelled uridine triphosphate
5'-ITR	5' inverted terminal repeat
5-HT/5-HT$_3$	5-hydroxytryptamine/5-hydroxytryptamine-3
a.m.	Ante meridiem
Acb	Nucleus accumbens
AcbC	Nucleus accumbens core
AcbS	Nucleus accumbens shell
aCSF	Artificial cerebrospinal fluid
AI	Agranular insular cortex
AID	Dorsal agranular insular cortex
AIV	Ventral agranular insular cortex
AMP	Adenosine monophosphate
AMPA	α-amino-3-hydroxy-5-methyl-4-isoxazolepropionic acid
Amy	Amygdala
AP	Anterior/posterior
BLA	Basolateral amygdala
BNST	Bed nucleus of the stria terminalis
BSA	Bovine serum albumine
Ca^{2+}	Calcium ion
CaM	Calmodulin
CaMKII	Ca^{2+}/calmodulin-dependent protein kinase II
CaMPARI	Calcium modulated photoactivatable ratiometric integrator
CaRE	Calcium response element
cDNA	Complementary deoxyribonucleic acid
Cg/Cg1/Cg2	Cingulate cortex/cingulate cortex 1/2
CIMH	Central Institute of Mental Health
cm	Centimetre
CNO	Clozapine-N-oxide

CNS	Central nervous system
cpEOS	Circularly permuted photoactivatable green to red fluorescent protein
cpm	Counts per minute
CPu	Caudate putamen
CRAM	Cre-dependent robust activity marking system
CRE	Cyclic AMP response element
CREB	Cyclic AMP response element-binding protein
CS	Conditioned stimulus
d2tTA	Destabilized tetracycline transactivator
DAPI	4′,6-diamidino-2-phenylindole
df	Degrees of freedom
DLO	Dorsolateral orbitofrontal cortex
DMSO	Dimethyl sulfoxide
DNA	Deoxyribonucleic acid
DNaseI	Deoxyribonuclease I
dNTP	Deoxynucleotide
DOX	Doxycycline
DSM-5	Diagnostic and Statistical Manual of Mental Disorders, 5th edition
DV	Dorsal/ventral
EDTA	Ethylenediaminetetraacetic acid
EGFP	Enhanced green fluorescent protein
ELK1	ETS transcription factor
ERK	Extracellular signal-regulated kinase
EXT	Extinction
F	F-value
FR 1	Fixed ratio 1
g	Gram
GA	Gauge
GABA/GABA$_A$	γ-Aminobutyric acid/γ-Aminobutyric acid A
GAD/GAD67	Glutamic acid decarboxylase/Glutamic acid decarboxylase 67
GDP	Guanosine diphosphate
GEF	Guanine nucleotide exchange factors
GFAP	Glial fibrillary acidic protein
GFP	Green Fluorescence Protein

GTP	Guanosine triphosphate
h	Hour(s)
$HCl_{(aq)}$	Hydrochloric acid
Hipp	Hippocampus
hM4D	Modified human M4 muscarinic receptor
hSYN1	Human synapsin1 promoter
I.U.	International units
IC	Insular cortex
IEG	Immediate early genes
IL	Infralimbic Cortex
Rinput	Input resistance
ir	Immune reactivity
K^+	Potassium ion
KCl	Potassium chloride
kg	Kilogram
KH_2PO_4	Potassium dihydrogen phosphate
LDTg	Laterodorsal tegmental nucleus
LH	Lateral hypothalamus
LO	Lateral orbitofrontal cortex
lox2272/loxP	Recombination sites
LTDg	Laterodorsal tegmental nucleus
M13	M13 peptide
MAP	Mitogen-activated protein
MAPK	Mitogen-activated protein kinase
mCherry	Red fluorescent protein mCherry
MEK 1/MEK 2	Mitogen-activated protein kinase kinase
mg	Milligram
$MgCl_2$	Magnesium chloride
min	Minute(s)
ML	Medial/lateral
ml	Millilitre
mm	Millimetre
mM	Millimolar
MO	Medial orbitofrontal cortex

mPFC	Medial prefrontal cortex
mRNA	Messenger ribonucleic acid
ms	Millisecond
mV	Millivolt
n	Number
nA	Nanoampere
Na^+	Sodium ion
Na_2HPO_4 * 2 H_2O	Disodium hydrogen phosphate dihydrate
nACh	Nicotinic acetylcholine
NaCl	Sodium chloride
NaOH	Sodium hydroxide
nCi	Nanocurie
NeuN	Neuronal nuclei (protein marker)
NF-κB	Nuclear factor kappa B
ng	Nanogram
nM	Nanomolar
NMDA	N-methyl-D-aspartate
OFC	Orbitofrontal cortex
p	p-value
P	Phosphate group
p.m.	Post meridiem
pA	SV40 polyadenylation signal
PBS	Phosphate-buffered saline
PCR	Polymerase chain reaction
PFA	Paraformaldehyde
PFC	Prefrontal cortex
P_{RAM}	Robust activity marking promoter
PrL	Prelimbic Cortex
rAAV	Recombinant adeno-associated virus
Raf	Rapidly accelerated fibrosarcoma
Ras	Rat sarcoma (a small guanine nucleotide-binding protein)
RE	Cue-induced reinstatement
RMTg	Rostromedial tegmentum
RNase	Ribonuclease

rpm	Rounds per minute
RSK2	Ribosomal S6 kinase 2
SA	Self-administration
Sacc	Saccharin
SEM	Standard error of mean
SN	Substantia nigra
SRE	Serum response element
SRF	Serum-response factor
SSC	Saline-sodium citrate buffer
t	t-value
TBE	Tris/Borate/EDTA
TBS	Tris-buffered saline
Tet	Tetracycline
TH	Thalamus
TRE	tTA-responsive element
tTA	Tetracycline-controlled transactivator
VGCC	L-type voltage-gated calcium channel
VLO	Ventrolateral orbitofrontal cortex
VO	Ventral orbitofrontal cortex
Vrest	Resting membrane potential
VTA	Ventral tegmental area
WPRE	Woodchuck hepatitis virus post-transcriptional regulatory element
$\bar{x}$ EXT	Average of last extinction sessions

LIST OF PUBLICATIONS

1. Thesis related publications:

Choice for Drug or Natural Reward Engages Largely Overlapping Neuronal Ensembles in the Infralimbic Prefrontal Cortex.

Pfarr S, Schaaf L, Reinert JK, Paul E, Herrmannsdorfer F, **Roßmanith M**, Kuner T, Hansson AC, Spanagel R, Korber C, Sommer WH. J Neurosci. 2018; 38:3507-3519.

2. Thesis unrelated publications:

Targeting Glycine Reuptake in Alcohol Seeking and Relapse

Vengeliene V, **Roßmanith M**, Takahashi TT, Alberati D, Behl B, Bespalov A, Spanagel R. Journal of Pharmacology and Experimental Therapeutics. 2018; 365:202-211.

Towards trans-diagnostic mechanisms in psychiatry: neurobehavioral profile of rats with a loss-of-function point mutation in the dopamine transporter gene.

Vengeliene V*, Bespalov A*, **Roßmanith M***, Horschitz S, Berger S, Relo AL, Noori HR, Schneider P, Enkel T, Bartsch D, Schneider M, Behl B, Hansson AC, Schloss P, Spanagel R. Dis Model Mech, 2017; 10:451-461. (* equal contribution)

Flexible, AAV-equipped Genetic Modules for Inducible Control of Gene Expression in Mammalian Brain.

Dogbevia GK, **Roßmanith M**, Sprengel R, Hasan MT. Mol Ther Nucleic Acids. 2016; 5:e309.

Convergent evidence from alcohol-dependent humans and rats for a hyperdopaminergic state in protracted abstinence.

Hirth N, Meinhardt MW, Noori HR, Salgado H, Torres-Ramirez O, Uhrig S, Broccoli L, Vengeliene V, **Roßmanith M**, Perreau-Lenz S, Kohr G, Sommer WH, Spanagel R, Hansson AC. Proc Natl Acad Sci U S A. 2016; 113:3024-3029.

1. INTRODUCTION

Substance use is not a phenomenon of modern civilisation but can be traced back through human history, to their origin and beyond. Early humans as well as our hominoid ancestors, living in substance-rich environments, were already exposed to psychotropic substances, which they consumed through their plant diet and therefore established a million-year-old co-evolutionary relationship (Dudley, 2000; Sullivan and Hagen, 2002). Plants, being stationary organisms, developed a wide variety of highly potent secondary metabolites, as effective defence mechanism against herbivores, microorganisms, viruses and fungi. These allelochemicals are able to interfere with the metabolism, reproduction and neuronal signal transduction as their chemical structure mimic that of endogenous neurotransmitters (Wink, 2003; Wink, 2018). Mammals, on the other hand, developed detoxifying mechanisms, such as the cytochrome P-450 system, to metabolize such harmful plant neurotoxins (Sullivan et al., 2008). Sullivan and Hagen argue that over the co-evolutionary relationship, adaptive mechanisms may have evolved in humans to profit from the potential benefits of plant secondary metabolites. Over time the adaptive benefits of those plant chemicals may have driven evolutionary changes resulting in basic principles of substance seeking behaviour as consumption of those substances provided a survival advantage (Sullivan and Hagen, 2002; Sullivan et al., 2008). This might be the reason why plant chemicals, like nicotine, caffeine, cocaine and others are able to trigger reward and approach behaviour in humans and other animals.

From an evolutionary standpoint rewards might be seen as entities that provide beneficial advantages to our daily survival and thus exert positive effects on behaviour, daily drive and overall wellbeing. A more technical standpoint refers to rewards as stimuli with the potential to reinforce behaviour and in consequence result in conditioned approach behaviour (Ikemoto and Bonci, 2014).

Rewards can thereby be categorized in two groups. One group comprises rewards such as water, food, sex and social interactions, the so-called natural rewards. Drugs of abuse like alcohol, cocaine, nicotine or heroin fall into the second category (Parsons and Hurd, 2015; Pfarr, 2018). Both groups are strong reinforcers that act upon the mesocorticolimbic dopamine system by altering neurotransmitter signalling (DePoy et al., 2017). These changes will influence the future behaviour of the individual. For example, the organism will learn to associate certain environmental stimuli with the positive effects of rewards, which gives them a predictive value.

Thus, individuals will engage in opportunities that predict reward availability to satisfy their needs and desires (Ikemoto and Bonci, 2014).

However, rewards, especially drug rewards, can have a high addictive potential and some individuals are more vulnerable to develop addictions to them, then others. Once addicted to a drug like cocaine, it is exceedingly difficult for an individual to stop engaging in behaviours that facilitate the addiction. Even if the disorder is overcome there are still chances of relapse, even after years of abstinence. As such a relapse can be triggered by the environmental stimuli that were once associated with the drug, a better understanding of the underlying neuronal mechanisms of this association must be gained to prevent further fall-backs.

In order to do so, this thesis aimed to provide a deeper insight into how stimuli-induced natural and drug reward seeking are encoded on a neuronal level. Therefore, neuronal ensembles were characterized for natural (saccharin) and drug (alcohol, nicotine, cocaine) reward seeking behaviours.

1.1 Reward seeking behaviour

Engagement in rewarding activities, be it consumption of food, sexual intercourse or the use of drugs, results in the experience of pleasure. The hedonic sensation leads to changes in neuroplasticity in order to link the positive feeling with the rewarding goal, to memorize the actions necessary to achieve it and to establish stimulus/reward associations (Kelley and Berridge, 2002; Arias-Carrión and Pöppel, 2007; Berridge and Kringelbach, 2008). With the ability to learn from the experiences and how to use the acquired associations to predict future rewards, an organism evolutionary gained great advantages in survival, reproduction and fitness (Kelley and Berridge, 2002; Berridge and Kringelbach, 2008). But even in our modern society rewards play an important role during our daily life activities, since pleasurable experiences are crucial for normal well-being (Berridge and Kringelbach, 2008). However, due to the sheer abundance in our modern environment the pleasure system can also malfunction like it happens during addiction development (Berridge and Kringelbach, 2015).

The entity of reward is based on a complex interplay of different psychological components, each with its distinct underlying neurobiological mechanisms. The core process underlying the pursuit of an organism to engage in rewarding activities due to their reinforcing and hedonic effects, is the component of ‘liking’. An individual ‘likes’ the pleasurable feature of the reward and consequently ‘wants’ it. ‘Wanting’, as second component, describes the incentive motivation and desire of an organism to achieve the pleasurable stimulus (reward)

and therefore driving approach behaviour. Learning the different associations, representations and predictions, that are linked to reward as well as subsequent behavioural events, is the third element in the trinity of psychological components of rewards (Berridge, 2003; Berridge and Kringelbach, 2008; Berridge et al., 2009; Berridge and Kringelbach, 2015).

Naturally individuals 'want' rewards because they 'like' their pleasurable feature, which drives initial engagement and voluntary reward consumption. Over time however, this normal and healthy behaviour can transition towards loss of control over the amount of reward consumed, until it develops into a habitual behaviour, which finally becomes compulsive despite negative or aversive outcomes (Everitt and Robbins, 2005; Everitt et al., 2008). This transition from initial drug use towards the full developed addiction goes hand in hand with the switch of the ordinary incentive motivation to achieve a pleasurable stimulus into excessively and intensely 'wanting' the reward, which is termed drug craving. Drug craving can be seen as the major component behind the compulsive behaviour as it drives drug seeking and drug taking, with almost no chance for the individual to resist (Robinson and Berridge, 1993). According to a survey among human addicts, drug 'wanting' and drug 'liking' evolve in a distinct manner during the development of an addiction. Whereas the pleasurable effect ('liking') of a given drug does not rise over time but rather declines, the incentive value of the drug ('wanting') increases strongly (Fig. 01). During the development of addictive behaviours, individuals therefor experience progressively increasing compulsive episodes of drug-seeking and drug-taking (Robinson and Berridge, 1993).

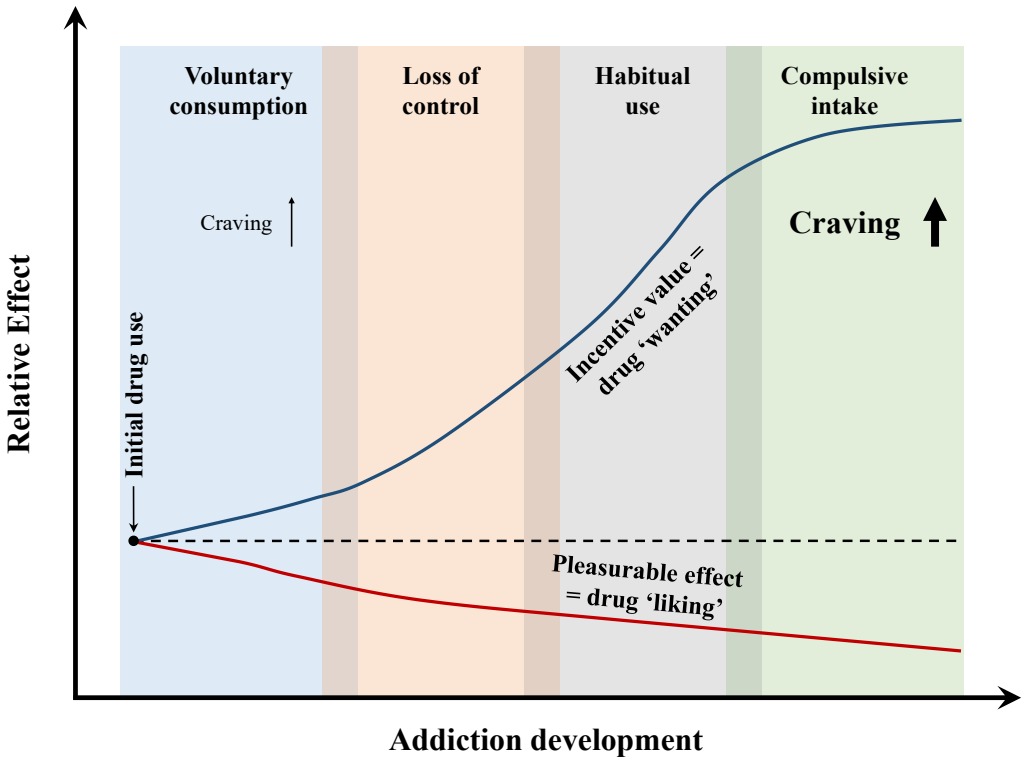

Figure 01) Illustration of the gradual progression of drug 'liking' and drug 'wanting' according to the Incentive-Sensitization theory

Starting with the initial use, drug consumption happens on a voluntary basis whereby the pleasurable effect of the drug and its incentive value are closely related. During the transition from initial drug use, through loss of control and habitual use towards compulsive intake, both drug 'wanting' and drug 'liking' dissociate from each other. As addiction develops gradually the incentive properties of a given drug increase over time together with the craving for it. The experienced pleasure of drug consumption on the other hand decreases as addiction progresses. Figure adapted from (Robinson and Berridge, 1993; Pfarr, 2018).

A crucial role in the development of an addiction is played by external stimuli, as they are able to trigger the excessive increase in the psychological component of 'wanting' that occurs over time (Berridge and Robinson, 2016). During initial drug use/voluntary consumption, environmental stimuli, that enable an individual to recognise an incentive, are associated with the pleasurable effect of the given drug. The associative learning process therefore links pleasure to a specific cue, it becomes conditioned. Via attribution of incentive salience these cues become attention-grabbing and attractive to the individual. For this reason, drug-associated cues are able to trigger the incentive motivation and desire to obtain and consume the associated reward (Robinson and Berridge, 1993; Berridge and Robinson, 2016). In this way they instigate drug consumption and promote its maintenance, leading to the transition from loss of control, over habit formation to compulsive drug intake. These cues can trigger such a strong 'wanting' response and urge that even recovered addicts, that consciously want to stay away from drugs, relapse when exposed to drug-associated cues (Berridge and Robinson, 2016).

However, not everyone consuming addictive drugs will experience the aforementioned transitions from initial drug use to a full-grown addiction. In fact, only a small proportion of drug users will experience drug dependence throughout their lifetime, depending on the drug consumed (Fig. 02). Drugs with the highest prevalence for dependence are tobacco, heroin, alcohol and cocaine. For these drugs lifetime prevalence for dependence ranges from 15.4 % for alcohol to 31.9 % for tobacco (Anthony et al., 1994).

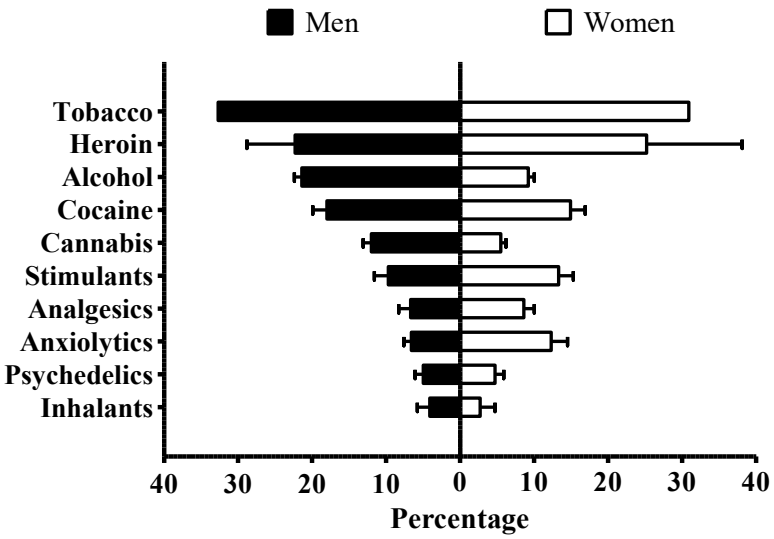

Figure 02) Estimated prevalence of drug dependence throughout lifetime

The graph displays the lifetime prevalence of drug dependence in extramedical drug users as estimated from data compiled by the National Comorbidity Survey in 1990-1992. The large majority of drug users did not proceed through the different stages of addiction development after initial usage. However, highly addictive drugs, such as tobacco and heroin, still lead to drug dependence with a prevalence of 20-30 %. Figure adapted from (Anthony et al., 1994).

As prevalence for dependence is at the high end of the spectrum for alcohol, cocaine and tobacco, these drugs were chosen as reinforcer for cue-paired operant conditioning within this thesis. The next chapter will give an overview about all three drugs of abuse and their detailed mechanism of action.

1.2 Drugs of abuse and their mechanism of action

Drugs of abuse are substances that are consumed in excessive manner to alter mood and behavioural states. This can result in compulsive seeking and use of these drugs. Consequently, the behaviour can develop into drug addiction, a chronic and relapsing neurological disorder, in which drugs are used despite severe impairments of one's social and occupational obligations, significant and prolonged health issues or death. A huge variety of natural and synthetic substances is able to cause drug addictions through a wide range of different mechanisms of action in the central nervous system.

The present study examined three different drugs of abuse, namely ethanol, nicotine and cocaine and compared their effects on neuronal ensembles involved in cue-induced reinstatement behaviour with those of the natural reward saccharin.

Ethanol:

Ethanol, commonly referred to as alcohol, is a legal drug in most parts of the world and one of the most commonly abused amongst the population. Each year 5.3 % of all deaths worldwide are a result of harmful ethanol usage, which is a total of three million deaths, respectively. Furthermore 5.1 % of the global disease burden is linked to ethanol consumption. Intoxicating the organism with ethanol is causally linked to more than 200 conditions associated with disease and injury (World Health Organization, 2018). Health problems associated with ethanol consumption range from mental and behavioural disturbances caused by the alcohol effects on the central nervous system to severe damage at other organs like heart, stomach, liver and pancreas. Furthermore, ethanol consumption is associated with several types of cancer like colon cancer, oesophageal cancer, rectal cancer or stomach cancer. In addition, ethanol intake can result in severe injuries due to accidental injuries, self-inflicted injuries and interpersonal violence, to name a few (Rehm et al., 2003; Rehm et al., 2010; Rehm et al., 2017). Alcohol intoxication also takes a toll on the ability of the immune system to fight of infections, making consumers more vulnerable to infectious diseases (World Health Organization, 2018).

Even though the harmful effects of alcohol are widely known, the drug is socially well accepted. Its consumption, e.g., volume and pattern, is influenced by a variety of risk factors on the individual (i.e., gender, genetics, socio-economic status) and societal level (i.e., culture, level of development, alcohol production, distribution and marketing) (Sudhinaraset et al., 2016; World Health Organization, 2018). In Germany 71.6 % of the 18-64 old population,

which corresponds to 36.9 million people, consumed alcohol within the last 30 days. Whereas most consumers showed controlled alcohol intake, 34.5 % underwent heavy drinking episodes on at least one day with five or more alcoholic beverages and 18.1 % of the population displayed hazardous consumption behaviour (> 12 g pure alcohol/day for women and > 24 g pure alcohol/day for men). Within the 18-64 years old German population, 2.8 % abuse alcohol and 3.1 % are alcohol-dependent, which corresponds to 1.4 million and 1.6 million individuals respectively (Atzendorf et al., 2019). Therefore, according to the Diagnostic and Statistical Manual of Mental Disorders, 5th edition (DSM-5) (American Psychiatric Association, 2013), which combines alcohol abuse and alcohol-dependence into the diagnosis of alcohol use disorder, a total of 3 million Germans suffer from the disease. The classification of the disorder into mild, moderate or severe, depends on how many of the eleven clinical diagnostic criteria are met by the individual (Reilly et al., 2017). Alcohol use disorder is a chronic relapse disorder during which phases of abstinence and return to drug use are alternating. Loss of control over alcohol drinking behaviour, compulsive alcohol seeking and drinking behaviour as well as withdrawal symptoms associated with a negative emotional state are characteristics of an alcohol use disorder (Koob and Volkow, 2010; Reilly et al., 2017).

Alcohol can interact with a huge variety of molecular and cellular targets and lead to severely altered neuronal communication in the CNS. Some of the main molecular targets of ethanol are γ-Aminobutyric acid A ($GABA_A$) receptors, 5-hydroxytryptamine-3 (5-HT_3) receptors, neuronal nicotinic acetylcholine (nACh) receptors, *N*-methyl-D-aspartate (NMDA) receptors, Dopamine receptors D1/D2 and a variety of channels, like G protein-coupled inwardly-rectifying potassium channels, L-type Ca^{2+} channels and Hyperpolarization-activated cyclic nucleotide-gated channels (Lüscher and Ungless, 2006; Spanagel, 2009; Abrahao et al., 2017). The psychotropic effects of alcohol, like anxiolytic, sedative and stimulating euphoric are mediated by the changes and the interplay within the neurotransmitter/ion channel system. These changes include inhibition of glutamatergic neurotransmission, facilitation of $GABA_A$ receptor function, modulation of neuronal nACh receptor function, potentiation of 5-HT_3 receptors and increased activation of dopaminergic neurons (von Wartburg, 1990; Vengeliene et al., 2008). In a second wave ethanol displays a series of indirect effects on different neurotransmitter and neuropeptide systems, mainly involving monoamines, opioids and endocannabinoids (Vengeliene et al., 2008; Spanagel, 2009). By activation of various signalling pathways, alcohol consumption leads to an alteration in gene expression, which results in changes on the cellular as well as neurophysiological level within the reinforcement system of the brain, including brain regions like prefrontal cortex (PFC), nucleus accumbens (Acb),

amygdala and the ventral tegmental area (VTA) (Vengeliene et al., 2008; Spanagel, 2009; Hansson et al., 2019). These changes facilitate alcohol intake pushing the initial acquisition phase of alcohol drinking towards an established yet controlled alcohol-seeking behaviour (Spanagel, 2009). Continued long-term alcohol intake can severely alter inhibitory and excitatory neurotransmitter homeostasis due to enhanced glutamatergic neurotransmission, neuroadaptations within γ-Aminobutyric acid (GABA)-ergic synapses, changes in dopamine release and changes in the endocannabinoid system, which leads to long lasting adaptions within these systems (Vengeliene et al., 2008; Abrahao et al., 2017; Roberto and Varodayan, 2017). Dependent on genetic predisposition and environmental factors some of these changes can lead from controlled alcohol drinking behaviour to compulsive alcohol consumption in about 10-15 % of users, during which they lose control over their alcohol seeking and intake behaviour (Wolffgramm and Heyne, 1995; Vengeliene et al., 2008).

Nicotine:

Tobacco with its addictive ingredient nicotine is another legal drug in most parts of the world consumed by 1.1 billion smokers. While killing up to 50 % of its user's, 7 million people per year, tobacco is also deadly for around 1.2 million people per year exposed to second-hand smoke. Tobacco is therefore one of the biggest health threats of modern times (World Health Organization, 2019). Containing more than 7000 chemicals of which several hundred are toxic and approximately 70 are carcinogenic, tobacco smoke damages almost every organ in the human body. It does so from the very first cigarette and accumulates over time, leading to a multitude of diseases including smoking-related cancer (e.g., mouth, nose and throat cancer, trachea cancer, lung cancer, stomach cancer), cardiovascular diseases (e.g., atherosclerosis, coronary heart disease, stroke), metabolic diseases (e.g., diabetes) and pulmonary diseases (e.g., chronic bronchitis, asthma). Moreover, smoking causes inflammation and decreases immune system function (U.S. Department of Health and Human Services, 2010, 2014; Die Drogenbeauftragte der Bundesregierung, 2019). Even though public awareness about the hazardous health consequences of tobacco consumption increased over the past years, the proportion of smokers (15 + years) within the German population remains high although numbers decreased over the last two decades. However, within the group of adolescents, aged 12-17 years, the trend of smoking was more than halved from 1997 to 2010 (Deutsche Hauptstelle für Suchtfragen e.V., 2013; Seitz et al., 2019). The proportion of current tobacco smokers within the German population aged 14 + years amounts to 28.3 % (Kotz et al., 2018).

5.4 % of the 18-64 years old German population are heavy users, with a daily consumption of at least 20 cigarettes. With only 4 % and 0.8 % the usage of e-cigarettes and heat-not-burn products remains low even though numbers increased over the last years (Atzendorf et al., 2019). The DSM-5 lists eleven diagnostic criteria upon which a problematic tobacco use is determined. Tobacco use disorder is diagnosed if at least two of the diagnostic criteria manifested over a 12-month period. Its severity is classified by the number of criteria met by the individual into mild, moderate and severe (American Psychiatric Association, 2013). As other drug addictions, tobacco use disorder is characterised by chronic abstinence-relapse cycles with episodes of tobacco craving, uncontrollable tobacco consumption and withdrawal symptoms (Koob and Volkow, 2010). Within the German population the 12-month prevalence for tobacco dependence is approximately 8.6 % for adults aged 18-64 years (Atzendorf et al., 2019).

Tobacco addiction is caused by nicotine a substance naturally produced in tobacco leaves. Smoking tobacco releases nicotine, which is inhaled with the cigarette smoke into the lunges from where it enters the cardiovascular system. Within seconds nicotine arrives in the brain where it targets nACh receptors, which become cation-permeable resulting in a sodium ion (Na^+), potassium ion (K^+) or calcium ion (Ca^{2+}) influx. This influx in turn activates voltage-gated calcium channels resulting in a strong depolarization of the cell (Lüscher and Ungless, 2006; Benowitz, 2010; Herman et al., 2014). The activation of presynaptic nACh receptors by nicotine mediates the release of a variety of neurotransmitters, like acetylcholine, dopamine, GABA, glutamate and serotonin. The major pathways activated by nicotine are the mesolimbic pathway and the mesocortical pathway, whose activation lead to increased dopamine levels in the nucleus accumbens shell (AcbS) or the PFC via projections from the VTA (Dajas-Bailador and Wonnacott, 2004; Herman et al., 2014). Nicotine also acts at GABAergic and glutamatergic synapses, which leads to inhibition of dopamine release and stimulation of dopamine release, respectively. This well-balanced system gets affected by long-term nicotine exposure as nACh receptors get desensitized with time. Since desensitization happens at different rates for the various nACh subtypes (glutamate release controlling subtypes desensitize slower than GABA release controlling ones) the foremost well-balanced system of inhibition and facilitation of dopaminergic neurons gets shifted, resulting in a decreased GABAergic inhibition and therefore elevated dopamine release in the Acb (Benowitz, 2010; Herman et al., 2014). Another mechanism through which nicotine increases dopamine levels in the Acb is the involvement of the endogenous opioid system. To do so nicotine induces the release of beta-endorphin, which in turn acts at GABAergic mu-opioid receptors within the VTA, resulting in the inhibition of

GABA release and reduced inhibition of dopamine neurons (Herman et al., 2014). Thus activation and desensitization of nACh receptors by nicotine results in elevated dopamine levels throughout the mesocorticolimbic dopamine system, driving the rewarding nature of tobacco smoking. Part of the rewarding nature is the ability for mood regulation through nicotine's pleasurable effects as well as its stress relieving properties. Withdrawal from nicotine however results in strong mood disturbances ranging from irritability to anxiety (Benowitz, 2010). Furthermore, conditioned cues like environmental factors or specific emotional states that are associated with the pleasurable effects of nicotine, are able to trigger activation of mesocorticolimbic circuits (Picciotto et al., 2008; Benowitz, 2010). Taken together these modalities play a critical role in the development and the behavioural phenotype displayed by tobacco addiction.

Cocaine:

It is estimated that 18.1 million people worldwide or 0.4 % of the world population aged 15 - 64 are using cocaine nowadays (United Nations, 2019). In 2017 approximately 7287 deaths were accounted to cocaine use disorder worldwide (Institute for Health Metrics and Evaluation, 2017). However, numbers of cocaine involved deaths are considerably higher since in the United States alone 13942 people died of drug overdoses involving cocaine in the same year (Kariisa et al., 2019). In Germany, the 12-month prevalence for cocaine use is 1.1 % within the population aged 18-64 years, whereas 4.1 % of the population report cocaine usage of at least once within their lifetime (Atzendorf et al., 2019; Die Drogenbeauftragte der Bundesregierung, 2019). The Federal Criminal Police Office states that 93 individuals died in 2018 because of cocaine intoxication, both monovalent and polyvalent intoxication (Bundeskriminalamt, 2018). In Germany approximately 57000 individuals suffer from cocaine abuse and 41000 individuals suffer from cocaine dependence. According to DSM-5 criteria, where cocaine abuse and dependence diagnosis are combined, a total of 0.2 % of the German population aged 18-64 years thus suffer from cocaine use disorder (Atzendorf et al., 2019). The disorder is characterized by chronic relapse episodes, a loss of control of cocaine intake, severe withdrawal symptoms and compulsive seeking and consumption behaviour (Koob and Volkow, 2010). Cocaine consumption is associated with acute (e.g. consciousness disturbance, hallucinations, seizures, shock) and long-term (e.g. impairment of immune system function, damage to cardiovascular system, liver, heart and kidneys, psychological damage) adverse health effects (Die Drogenbeauftragte der Bundesregierung, 2019).

Cocaine is primarily administered intranasally ("snorting"), orally, via intravenous injection or inhalation (crack cocaine) (Cregler, 1989). Depending on the route of administration absorption speed as well as intensity and duration of the effects of cocaine vary. The faster the absorption of cocaine, the more intense and shorter are the effects (Goldstein et al., 2009). Lower doses of cocaine result in effects like euphoria, increased self-confidence, excitement and social inhibition whereas higher doses might lead to aggressiveness, hallucinations and disorientation (Cregler, 1989; Goldstein et al., 2009). Cocaine's mechanism of action is the inhibition of neurotransmitter reuptake transporters. In this way cocaine blocks the reuptake of dopamine, norepinephrine and serotonin, leading to elevated extracellular levels of the before-mentioned monoamines (Goldstein et al., 2009; Drake and Scott, 2018). Cocaine therefore interferes with the neuronal communication process, resulting in intensified signal transduction through the accumulation of neurotransmitters in the synaptic cleft. Thereby activation of the mesocorticolimbic dopamine system is triggered, which contributes to the reinforcing nature of cocaine and the reinstatement of cocaine seeking (Pierce and Kumaresan, 2006; Schmidt and Pierce, 2010) Even though the dopaminergic system is considered to be the main factor for the reinforcing aspects of cocaine, the serotonergic system plays an important role in the rewarding or aversive effects of cocaine whereas the norepinephrine system only seems to contribute to the aversive effects (Filip et al., 2005; Wee et al., 2006; Nonkes et al., 2011). However, cocaine indirectly also modulates other neurotransmitter systems like the glutamatergic, the GABAergic and the endocannabinoid system (Karila et al., 2008). Cocaine administration and repetitive use result in short-term as well as long-term neuroadaptations in the central nervous system (Schmidt and Pierce, 2010). Some of these neuroadaptations include changes to dopamine release, regulation of dopamine receptor sensitivity and number, reduced dopamine transporter synthesis as well as dopamine synthesis (Trulson and Ulissey, 1987; Volkow et al., 1990; Volkow et al., 1993; Tsukada et al., 1996; White and Kalivas, 1998). Another neurotransmitter system highly effected by alterations due to repeated cocaine use is the glutamatergic neurotransmitter system particularly in the Acb but also the dorsal striatum. Changes comprise glutamate release and reuptake, alterations in receptor expression and trafficking as well as intracellular signalling (Schmidt and Pierce, 2010; Parikh et al., 2014). The neuroadaptations induced by cocaine among the different neurotransmitter systems have a major impact on the brain's reward and motivation system as well as on learning and memory circuits making the individual more susceptible to the drug. Over time behavioural changes are induced, which can eventuate in cocaine addiction (Pierce and Kumaresan, 2006; Karila et al., 2008; Schmidt and Pierce, 2010).

Saccharin:

Saccharin is an artificial sweetener, discovered in 1879 with a sweetness of about three hundred times of that of sucrose. The compound is non-caloric as it cannot be metabolized by mammals, whereby it was initially and still is used for diabetics, obesity treatment and patients with metabolic syndrome (Arnold et al., 1983; Kumar and Chail, 2019). Over the course of its history, the safety of saccharin for use in humans was controversially discussed, especially after two-generation studies in rats provided evidence of an association with urinary bladder carcinogenicity. However, several follow up studies, mechanistical and epidemiological, demonstrated lack of evidence for negative effects in humans (Arnold et al., 1983; Ellwein and Cohen, 1990; Chappel, 1992).

Saccharin is approved as food additive by the U.S. Food and Drug Administration and is still used in beverages and food products today (Kumar and Chail, 2019). In research saccharin is utilised in a wide variety of topics, ranging from addiction to cancer, nutrition and learning studies (Rehn et al., 2018; Koruza et al., 2019).

After getting a better understanding about the pleasurable substances used, the next chapter will provide a deeper inside about the neural circuitry targeted by these rewards.

1.3 The brain reward system

The first discovery of brain regions mediating reinforcing effects of rewards that trigger certain behaviours, was made in 1954 by James Olds and Peter Milner, when both scientists conducted their famous electrical self-stimulation experiments in rats. In these experiments animals were allowed to freely press a lever, which resulted in a brief electrical stimulation of the rat's brain via an implanted electrode. By moving the electrode to different brain regions, Olds and Milner identified brain areas whose stimulation was rewarding for the animals, which expressed itself by frequent and continuous pressing of the lever that in some cases animals even stopped the consumption of food and water (Spanagel and Weiss, 1999; Bear et al., 2016). In the following years scientists started to examine the neuroanatomical and neurochemical nature of these brain circuitries identifying three dopaminergic circuitries crucial for drug reward and addiction development. These three dopaminergic pathways were the mesolimbic, the mesocortical and the nigrostriatal pathway (Fig. 03a) (Volkow et al., 2011). Dopaminergic neurons originating in the VTA that project to the Acb are part of the mesolimbic pathway, which is essential for the regulation of reward related behaviours. Activation of the pathway by natural rewards (e.g. food, sex) or drugs of abuse (e.g. cocaine, alcohol, nicotine) leads to increased extracellular mesolimbic dopamine levels (Spanagel and Weiss, 1999). Dopaminergic neurons from the VTA also innervate the prefrontal cortex, insular cortex and to a lesser extent some motor cortices. These connections make up the mesocortical dopamine system, which is involved in motivation, reinforcement, emotion and executive functions (Settell et al., 2017; Wan et al., 2017). In addition, the VTA is the origin of a more complex dopaminergic circuitry, which involves connections to the amygdala, the hippocampus, the lateral hypothalamus, the ventral pallidum and the bed nucleus of the stria terminalis (BNST), amongst others (Klitenick et al., 1992; Spanagel and Weiss, 1999; Adinoff, 2004; Russo and Nestler, 2013; Settell et al., 2017; Wan et al., 2017). The third dopaminergic pathway involved in reward and addiction is the nigrostriatal pathway whose origin is the dopamine neuron dense substantia nigra (SN). The SN is anatomically but also functionally closely related to the VTA. The dopaminergic neurons that project from the SN to the dorsal striatum, the Acb, the PFC and the amygdala, are involved in habit formation, reward value, reward processing and reward-prediction (Heimer et al., 1997; Wise, 2009; Sesia et al., 2014).

However, signalling within the dopaminergic reward system is regulated and modified by a variety of direct or indirect inputs from different brain regions. For example, most of the connections that the VTA establishes are reciprocal, meaning that the VTA itself receives

inhibitory and excitatory signals from brain regions it innervates. Afferent connections to the VTA include GABAergic and glutamatergic innervations from Acb, amygdala, PFC, caudate putamen (CPu), BNST, lateral hypothalamus, lateral habenula, laterodorsal tegmental nucleus and ventral pallidum, among others (Fig. 03b) (Oades and Halliday, 1987; Volkow et al., 2011; Russo and Nestler, 2013; Cooper et al., 2017; Settell et al., 2017; Wan et al., 2017; Pardo-Garcia et al., 2019). The SN also receives feedback and direct/indirect projections from a variety of brain regions like dorsal striatum, Acb, globus pallidus, subthalamic nucleus and PFC (Strahlendorf and Barnes, 1983; Oades and Halliday, 1987; Haber et al., 2000; Lee and Tepper, 2009; Volkow et al., 2011; Poulin et al., 2018). About 70 % of these projections are GABAergic, whereas the remaining 30 % are mostly glutamatergic (Fig. 03b) (Tepper and Lee, 2007; Lee and Tepper, 2009). In addition, most brain regions named above, that are involved in regulation of the dopaminergic system, are themselves densely connected to one another as well as to other structures related to reward behaviour and addiction development. For example, the Acb, as part of the mesolimbic pathway, not only receives dopaminergic input from the VTA but is also influenced by glutamatergic innervations from PFC, hippocampus, and amygdala, which are able to modify dopaminergic signals (Fig. 03b) (Russo and Nestler, 2013).

The large number of different brain regions involved as well as the various neurotransmitters utilised for communication between these regions make it particularly challenging to shed light on this immensely complex reward circuitry and its mode of operation in reward behaviour and addiction development. However, the prefrontal cortex, which counts to “one of the most complex anatomical and functional structures of the mammalian brain” (Abernathy et al., 2010) is considered to be strongly involved in reward related behaviour and addiction (Everitt and Robbins, 2005; Kalivas and Volkow, 2005; Everitt et al., 2007; Pfarr et al., 2018). Thus, the next chapter focuses on this brain region and its role in exactly those entities.

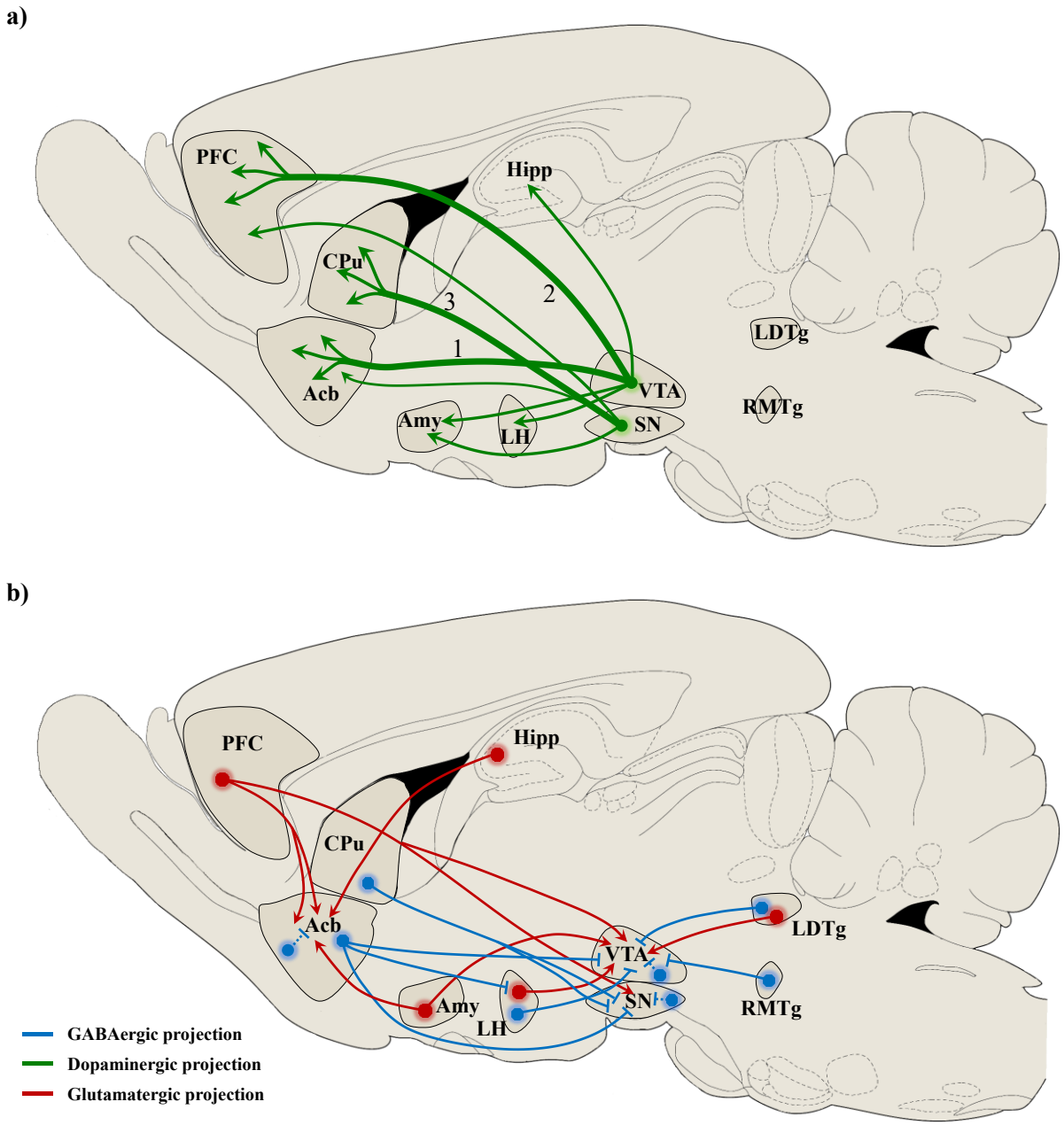

Figure 03) Simplified schematic illustration of major projections within the rat's brain reward system

a) Illustration of the different dopaminergic projections originating in the VTA and SN. The three major dopaminergic pathways involved in reward behaviour and addiction development are the mesolimbic pathway (1), the mesocortical pathway (2) and the nigrostriatal pathway (3). The mesolimbic pathway (1), which sends dopaminergic projections from the VTA to the Acb, is the primary dopaminergic reward circuit. It gets activated by rewards and their associated stimuli. The motivational and reinforcement aspects of reward related behaviours are mediated by the mesocortical pathway (2), which projects from the VTA to PFC regions. The nigrostriatal pathway (3), which projects from the VTA into the CPu, is involved in habit formation, reward prediction and processing. In addition, the VTA sends dopaminergic projections towards Amy, LH, and Hipp, whereas the SN innervates PFC, Acb and amygdala. b) Simplified schematic of the major GABAergic and glutamatergic projections that affect and modify dopaminergic neurotransmission. The VTA receives excitatory innervations from PFC, Amy, LH and LDTg, whereas inhibitory signals arrive from Acb, LDTg, RMTg and LH. Glutamatergic input to the SN comes from the PFC. Dopaminergic neurons of the SN are influenced by GABAergic signals emerging from CPu and Acb. In addition, both VTA and SN utilise dense interneuronal communication. Abbreviations: PFC = prefrontal cortex, CPu = caudate putamen, Acb = nucleus accumbens, Hipp = Hippocampus, Amy = amygdala, LH = lateral hypothalamus, VTA = ventral tegmental area, SN = substantia nigra, LDTg = laterodorsal tegmental nucleus, RMTg = rostromedial tegmentum. Adapted and modified from (Paxinos and Watson, 1998; Russo and Nestler, 2013).

1.4 Prefrontal cortex

The brain is one of the most complex structures in the universe comprising 86 billion neurons and a similar amount of non-neuronal cells (Azevedo et al., 2009). With up to 1000 trillion synaptic connections neuronal cells built an extremely complex network (Sporns et al., 2005). The evolutionary youngest part of the brain, the neocortex, is a brain structure unique to mammals and centre for higher functions of cognition and behaviour. It has expanded notably throughout evolution, especially in humans, and can be divided into functionally distinct neocortical areas. The lissencephalic neocortex of rodents, which is by far less complex than in humans, can be subdivided into three lobes (Fig. 04) (Florio and Huttner, 2014; Castillo-Morales et al., 2016)

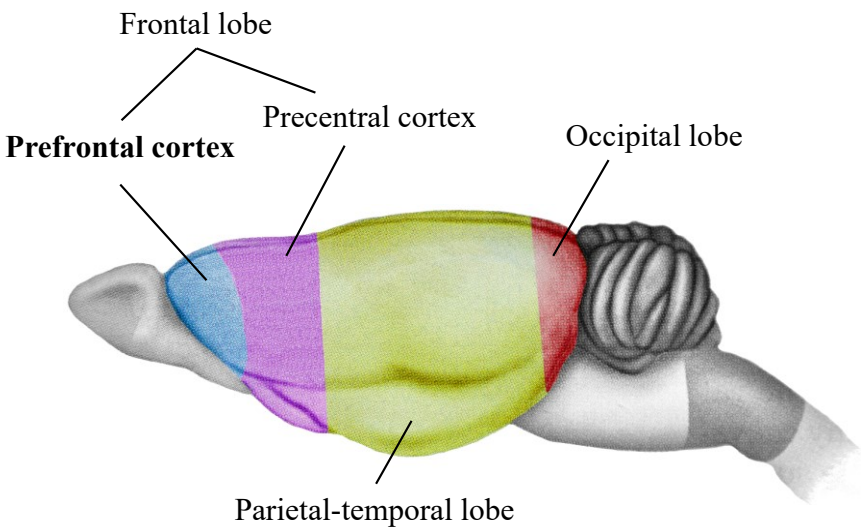

Figure 04) Illustration of the different neocortical lobes of the rat brain

The graphic displays a lateral view of the rat brain. The coloured parts visualise the neocortex with its different lobes: the occipital lobe (red), the parietal-temporal lobe (green/orange), and the frontal lobe comprising the precentral cortex (pink) and the prefrontal cortex (blue). Adapted and modified from (Paxinos and Watson, 1998; Dorr et al., 2007; Bear et al., 2016).

The PFC, as part of the frontal lobe, grew in size relative compared to the rest of the region and is considered to be the most complex brain structure in mammals whereby huge discrepancies can be found between different species. Humans and rodents, for example, have their last common ancestor about 96 million years ago, which led to a divergent phylogenetic development of the PFC. As a result of this development the human PFC possesses a higher anatomical and cognitive complexity than the PFC of rodents. Some of the differences between the human and rodent PFC include spatial orientation of prefrontal areas, the functional subdivision of the PFC and their connectivity to others brain areas (Wise, 2008; Kesner and

Churchwell, 2011; Carlén, 2017). However, despite these differences, subregions of the rodent PFC seem to participate in similar functions as subregions of the human PFC. In a review by Kesner and Churchwell (2011), the scientists concluded that the different subregions of both species feature subregional specificity whereby homologous subregions show parallels in cognitive functioning. For example, the rodent PFC shows features similar to the ones in the medial and orbital areas of the primate PFC and even a few features of the dorsolateral PFC (Uylings et al., 2003). In addition, the PFC was found to fulfil an overall role, as it processes complex higher-order functions that would not be possible be simple adding up the specific functions of the different subregions (Wilson et al., 2010; Carlén, 2017). Furthermore, evolution does not select for the anatomical structure of the brain but its functions and resulting behaviours. Thus, even though the rodent PFC is not a miniature replica of the human PFC, both share class-common behaviours and functions (Wilson et al., 2010; Carlén, 2017). Despite the obvious differences between the two species, rodents provide a simpler yet useful model system to study PFC functions and their impact on complex behavioural processes (Kesner and Churchwell, 2011). Functionally the rodent PFC can be divided into the following subregions: secondary motor cortex, anterior cingulate cortex, prelimbic cortex, infralimbic cortex, agranular insular cortex and the orbitofrontal cortex (OFC) (Fig. 05) (Carlén, 2017).

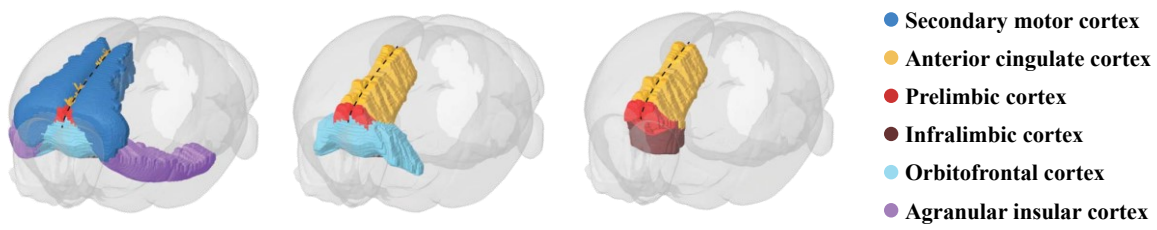

Figure 05) Subregional division of rodent prefrontal cortex

The three-dimensional brain graphs show the functional subdivision of the rodent PFC. The left illustration displays the secondary motor cortex (blue) and the agranular insular cortex (purple), whereas the middle panel shows the anterior cingulate cortex (bright orange) and orbitofrontal cortex (turquoise). The right illustration gives view of the prelimbic cortex (red) and the infralimbic cortex (brown). The sagittal midline is indicated by a dashed black line. Adapted and modified from (Carlén, 2017).

Each of the PFC subregions mainly consists of two neuronal types, which are pyramidal cells and interneurons. Both, pyramidal cells as well as interneurons, show a high diversity with subtypes that differ in size and shape, the neurotransmitters utilized and their electrophysiological properties (Rudy et al., 2011; Fan et al., 2017; Radnikow and Feldmeyer, 2018). The neuronal population within the prefrontal cortex is made of approximately 70 % - 80 % excitatory pyramidal neurons and 20 % - 30 % of interneurons that are primarily inhibitory, even though interneurons such as the spiny stellate cells are of excitatory nature

(Markram et al., 2004; Wonders and Anderson, 2006). The primary neurotransmitter of excitatory pyramidal cells is the neurochemical glutamate whereas the main neurotransmitter utilized by inhibitory interneurons is the neurotransmitter GABA. Behavioural and cognitive processes are controlled by a close interaction of these two neurotransmitter systems whereby the inhibitory control of GABAergic interneurons over afferent and efferent pyramidal neuron activity is a key component (Wonders and Anderson, 2006; Girgenti et al., 2019). In addition to neurons, the central nervous system contains an even larger amount of neuroglia in the human brain with ten times more neuroglia than neurons. The key function of these cells is the maintenance of homeostasis within the central nervous system. Thereby they not only support neuronal function but are actively involved in brain metabolism and the communication processes between neurons (Rajkowska and Miguel-Hidalgo, 2007; Rodríguez-Arellano et al., 2016). Even though the number of neurons and glia cells is of similar magnitude in the rat brain, the cerebral cortex volume of these animals consists of 90 % astrocytes, the most common type of neuroglia, whereas only 10 % of the volume are made up by neurons and blood vessels (Rajkowska and Miguel-Hidalgo, 2007).

The PFC receives a myriad of different sensory and motor inputs with detailed information about the environment and is provided with a multitude of actions available. This results in a variety of available possibilities that require cognitive control along an internal goal. In contrast to automatic behaviours, which only require the execution of a certain behaviour in response to a particular stimulus ("bottom-up" processing), the PFC is mainly involved in "top-down" processing. During this process, the PFC incorporates and analyses the input and information it receives in order to guide and control complex behavioural responses and decisions, considering past, present or future goals (Miller and Cohen, 2001; Abernathy et al., 2010).

In its function to orchestrate behavioural adaptations in response to sensory inputs from the environment the PFC executes a series of different high-level cognitive processes, such as decision making, working memory, response initiation, planning, attention, autonomic control, behavioural flexibility, emotion, inhibition of unwanted behaviours and temporal processing (Heidbreder and Groenewegen, 2003; Kesner and Churchwell, 2011; Carlén, 2017; Dixon et al., 2017; Hika and Al Khalili, 2020). Thereby the PFC is critically involved in the regulation of reward behaviour and addiction development as it is a key player in limbic reward area modulation and higher-level processes. PFC dysfunction results in highly increased salience to the reward and reward predicting cues, which in turn enhances the internal drive for reward seeking and reward consumption for the affected individual (Goldstein and Volkow, 2002, 2011). Two subregions of the PFC, the orbitofrontal cortex and the infralimbic cortex, are

involved in a majority of the processes mentioned above and are therefore heavily implicated in reward seeking behaviours. Thus, the next paragraphs will give a closer look at these brain regions.

1.4.1 Orbitofrontal cortex

The OFC is part of the prefrontal cortex and found within the central nervous system of all mammals. Even though the OFC of humans and other mammals is not identical, all mammals have a structure that resembles the human OFC with its afferent and efferent projections from and to similar brain regions indicating functional and anatomical homology between species (Rudebeck and Rich, 2018). For example, afferent and efferent connections of the rodent OFC suggest analogous function between human and rat orbitofrontal cortices. Moreover, the ventral OFC, the lateral OFC and the agranular insular cortex are considered to be homologous with the human OFC (McCracken and Grace, 2007).

Even though the organisation of the rat OFC is less complex than in other species, the subdivision of the orbitofrontal area as well as their boundaries vary across authors throughout the literature (Reep et al., 1996; Paxinos and Watson, 1998; Van De Werd and Uylings, 2008; Alcaraz et al., 2016; Izquierdo, 2017; Murphy and Deutch, 2018; Reiner et al., 2020). Izquierdo et. al. 2017 and other scientists subdivide the OFC into the following areas: medial OFC (MO), ventral OFC (VO), ventrolateral OFC (VLO), lateral OFC (LO), dorsolateral OFC (DLO) and agranular insular cortices (AI) (Van De Werd and Uylings, 2008; Izquierdo, 2017; Murphy and Deutch, 2018). The brain atlas used in this thesis, however, divides the OFC into four regions, namely the medial OFC, the ventral OFC, the lateral OFC and the dorsolateral OFC (Fig. 06) (Paxinos and Watson, 1998). This subdivision is also used throughout the literature (Alcaraz et al., 2016; Reiner et al., 2020). Therefore, potential discrepancies with other studies might depend on the brain atlas used and the question whether or not certain areas are included (Alcaraz et al., 2016).

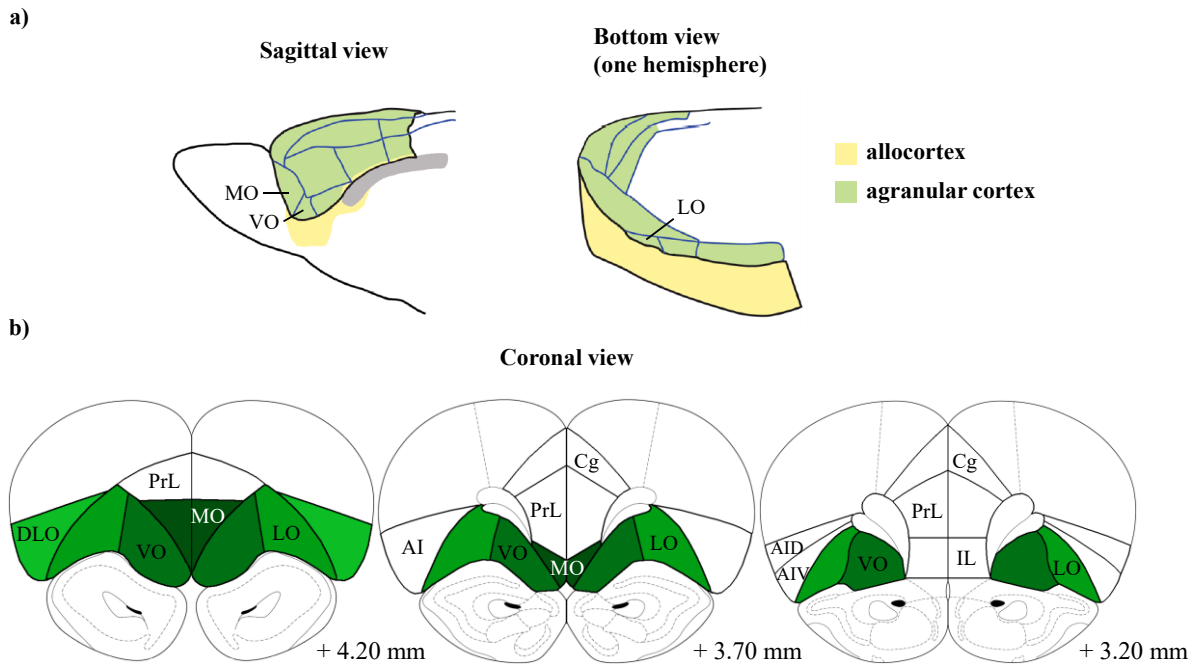

Figure 06) Schematic representation of OFC subregions

a) Schematic of the rat frontal lobe from a sagittal and horizontal view with OFC subregions labelled. b) Illustration of the different subregions of the rat OFC at three different rostrocaudal levels. Different OFC subdivisions are labelled in distinct shades of green. Abbreviations: DLO = dorsolateral orbitofrontal cortex, LO = lateral orbitofrontal cortex, VO = ventral orbitofrontal cortex, MO = medial orbitofrontal cortex, PrL = prelimbic cortex, Cg = cingulate cortex, AI = agranular insular cortex, IL = infralimbic cortex, AIV = ventral agranular insular cortex, AID = dorsal agranular insular cortex. Adapted and modified from (Paxinos and Watson, 1998; Wallis, 2011).

1.4.1.1 Role of the orbitofrontal cortex in reward seeking

The OFC is functionally a very heterogeneous area. Its multiple connections to cortical and subcortical areas get the OFC involved in top-down control of a wide variety of behaviours and executive functions. With its functional spectrum the OFC mainly acts at the interface of cognitive and emotional processes. Neurons of the orbitofrontal cortex are able to establish associations between incoming environmental stimuli and internal emotional states integrating them into ongoing cognitive processing, such as learning and motivation (Rudebeck and Rich, 2018; Shields and Gremel, 2020).

Therefore, it is no wonder that impairments of the OFC can be found in several neuropsychiatric diseases like major depression disorder (Drevets, 2007), obsessive-compulsive disorder (Nakao et al., 2014), bipolar disorder (Huber et al., 2019), social anxiety disorder (Sladky et al., 2012) and substance use disorders (Goldstein and Volkow, 2011).

The OFC is activated by different sensory stimuli, primarily those that are linked to food or drinks. Through modulation, combination and integration of the different olfactory, visual,

auditory or gustatory stimuli with both exteroceptive and interoceptive factors, neurons of the OFC generate representations of the rewarding value of the different stimuli at a very high level of information processing. The rewarding value of these stimuli, positive or negative, are then linked via associative learning processes, which are driven by the OFC, to the respective behaviour (Rolls, 2015; Moorman, 2018). The OFC can then use this information to predict the consequences or value of certain actions or expected outcomes and integrate this knowledge into economic decision making. Once a decision is made the OFC is also involved in revaluating the actual outcome, categorizing it, whether it was better or worse than expected and on basis of this information guide future decision making. As this decision-making process is controlled by previous experiences, the OFC is also crucially involved in goal-directed behaviours (Moorman, 2018; Rudebeck and Rich, 2018). Furthermore, the OFC is participating in response regulation to environmental changes. It is therefore essential for flexible behavioural adaptations such as changes of choice or action in response to changed outcomes (Roberts, 2006; Rempel-Clower, 2007; Arinze and Moorman, 2020). This characteristic of the OFC was demonstrated by various studies using different experimental tasks such as reversal learning, Wisconsin Card sort task and the attentional set shift task (Boulougouris et al., 2007; Chase et al., 2012; Dalton et al., 2016; Sleezer et al., 2016; Sleezer et al., 2017; Moorman, 2018). The previously discussed features of the OFC make it a crucial part of the reward system as the different attributes play a central role in reward seeking and drug addiction. There are several studies both from humans and animals that demonstrate the involvement of the OFC in these behaviours. Neuroimaging studies in humans, for example, showed that the OFC gets activated in individuals suffering from an addiction when they get exposed to drug-related cues that trigger craving. Another indication is the fact that the compulsive behaviour displayed by addicts shows similarities with behavioural traits from patients suffering OFC impairments. In addition, the OFC of addicted individuals shows various functional changes on a metabolic or neurochemical level. And lastly, several processes that are impaired in addiction are associated with OFC function such as emotion regulation, motivation, awareness and interoception, learning and memory and salience attribution (London et al., 2000; Volkow and Fowler, 2000; Goldstein and Volkow, 2002; Volkow et al., 2003; Bechara, 2005; Everitt et al., 2007; Goldstein and Volkow, 2011; Wilcox et al., 2011). In animals the OFC was indicated to play a crucial role in cue-, context- or cocaine-induced reinstatement of cocaine seeking behaviour (Fuchs et al., 2004; Lasseter et al., 2009; Arguello et al., 2017; Bal et al., 2019), in cue- and context-induced reinstatement of ethanol seeking behaviour (Bianchi et al., 2018; Arinze and Moorman, 2020), in opioid seeking behaviour (Reiner et al., 2020), the control of alcohol consumption in

dependent animals (den Hartog et al., 2016), reward value encoding (Malvaez et al., 2019), reward learning (Izquierdo, 2017), regulation of incentive motivation for drugs of abuse (Minogianis et al., 2019; Hernandez and Moorman, 2020) and reward prediction (Stalnaker et al., 2018).

Furthermore, as the OFC can be divided into different subregions, each of which has distinct connection patterns to other brain regions, it is not surprising that they were also shown to execute distinct functions in addition to their shared functional repertoire. Medial OFC and ventral OFC share robust projection patterns to cortical and subcortical areas, which might reflect shared complementary function, whereas the lateral OFC, which only shares some connections with the other OFC subregions, might differ more functionally (Izquierdo, 2017). The medial OFC in humans, for example, was shown to encode for the reward value of reinforcers, in contrast to the lateral OFC, which serves in the evaluation of punishers (Kringelbach, 2005). Also reward learning processes seem to differ between subregions as the medial OFC is implicated in reward-guided learning, whereas the lateral OFC is essential for reversal learning processes (Fettes et al., 2017). In animals these dichotomies between the orbitofrontal subregions could also be observed. The ventral and lateral OFC, for example, were found to be involved in cue-induced reward seeking behaviour whereas the medial OFC was not (Bal et al., 2019). A comprehensive review by Alicia Izquierdo (2017), showed that the rat OFC displays functional heterogeneity with the medial OFC mainly involved in value representation, the ventral OFC involved in reward learning and the lateral OFC in reversal learning and outcome prediction.

All in all, these findings nicely demonstrate the crucial role of the OFC and its importance for the reward system and its functions.

1.4.2 Medial prefrontal cortex

The medial prefrontal cortex (mPFC) is a subregion of the PFC and can be found across different mammalian species. Like the OFC the mPFC establishes a wide network of afferent and efferent connections with other cortical and subcortical areas (Öngür and Price, 2000; Xu et al., 2019). Over the years a lot of studies investigated the rodent mPFC with the intent to compare findings and transfer them to humans. However, the anatomical nomenclature used, and the way certain areas were related across species, were found to be critically inconsistent between studies, leading to poor clarity, rigor and reproducibility (Laubach et al., 2018). As most scientists subdivide the rodent mPFC into anterior cingulate cortex (Cg), prelimbic cortex

(PrL) and infralimbic cortex (IL) (Fig. 07) (Heidbreder and Groenewegen, 2003; Dalley et al., 2004), Laubach et al., 2018 used these subregions to propose an alternative scheme to handle cross-species homologies. The authors suggest that the rodent Cg is homologue to human anterior midcingulate cortex, the rodent PrL is homologue to human pregenual anterior cingulate cortex and the rodent IL is thought to be homologue to human subgenual anterior cingulate cortex. By pointing out the necessity of clear anatomical nomenclature the authors hope that future translational studies involving the rodent mPFC become clearer and more reproducible, improving the value of these studies for human use (Laubach et al., 2018).

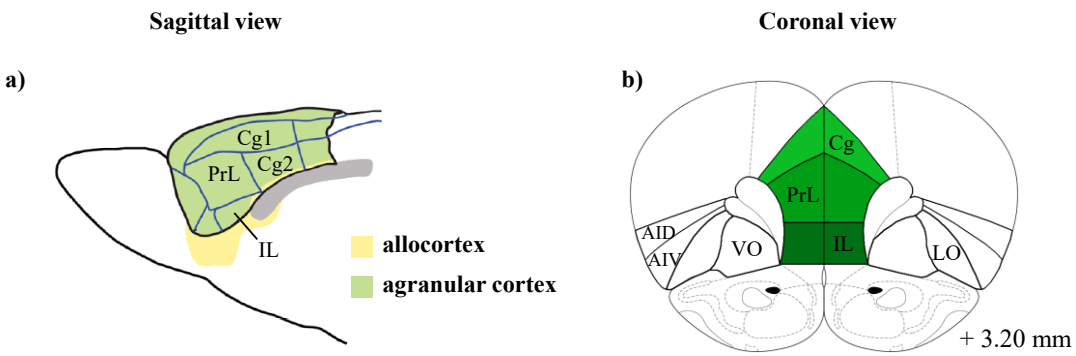

Figure 07) Schematic representation of mPFC subregions

a) The graph displays the rat frontal lobe from a sagittal view with the different mPFC subregions indicated. b) Illustration of the different mPFC subregions in a rat brain at rostrocaudal level + 3.20mm. mPFC subregions are labelled in distinct shades of green. Abbreviations: LO = lateral orbitofrontal cortex, VO = ventral orbitofrontal cortex, PrL = prelimbic cortex, Cg 1/2 = cingulate cortex 1/2, IL = infralimbic cortex, AIV = ventral agranular insular cortex, AID = dorsal agranular insular cortex. Adapted from (Paxinos and Watson, 1998; Wallis, 2011).

1.4.2.1 Role of the medial prefrontal cortex in reward seeking

Like the OFC the mPFC is functionally a heterogeneous area participating in a wide range of different behaviours. With its dense network of afferent and efferent connections the mPFC controls different executive functions like attention, decision-making, working memory and goal directed behaviours in a top-down manner (Öngür and Price, 2000; Heidbreder and Groenewegen, 2003; Hoover and Vertes, 2007; Moorman et al., 2015; Pfarr, 2018). Furthermore, the mPFC is implicated in reward seeking and drug-taking behaviours as the brain region is part of the mesocorticolimbic dopamine system. Thereby, the mPFC is involved in the evaluation of inputs coming from various sensory and limbic regions and most importantly from the VTA. Extrinsic and intrinsic stimuli can be integrated in this way and depending on their salience and motivational significance, they can trigger reward seeking behaviour via efferent connections to the Acb, Amy and related regions (Hoover and Vertes, 2007; Moorman et al., 2015; Heilig et al., 2017). The mPFC is often divided into a dorsal part comprised of the

Cg and the dorsal PrL and a ventral part composed of ventral PrL and IL. Both subdivisions are thought to fulfil functionally differential roles in line with their vastly varying projection patterns (Heidbreder and Groenewegen, 2003; Moorman et al., 2015). Traditionally the PrL was thought to be crucial for executive behaviours whereas the IL was proposed to be essential for response inhibition. This dichotomous function of PrL and IL was found to be true especially during fear conditioning and drug seeking (Moorman et al., 2015). However, research conducted over the last years challenges this dichotomous view on PrL/IL function (Heilig et al., 2017). Studies conducted to investigate the effect of non-selective or selective inactivation of PrL and IL neurons showed that the involvement of the mPFC in reward seeking is more complex than just PrL-driven behavioural execution ("go") and IL-driven behavioural suppression ("stop"). Non-selective inhibition experiments, for example, that targeted the rodent IL were not able to clearly demonstrate involvement of the subregion in only one function of behavioural control. Some studies could show suppressive function of the IL, whereas others could demonstrate executive function of the IL, yet some studies reported no effect on behavioural inhibition or execution at all (Peters et al., 2008; Koya et al., 2009a; Bossert et al., 2011; LaLumiere et al., 2012; Willcocks and McNally, 2013; Pfarr et al., 2015; Suto et al., 2016). Similar contradictory findings were made for the PrL (Bossert et al., 2011; Willcocks and McNally, 2013; Limpens et al., 2015; Moorman and Aston-Jones, 2015; Palombo et al., 2017; Trask et al., 2017). Specific inactivation of neuronal ensembles involved in reward seeking also resulted in contradictory reports. A study conducted by Bossert et al., 2011, for example, found that selective inactivation of neuronal ensembles within the IL supressed the behavioural response to heroin associated context (Bossert et al., 2011). However, selective inhibition of a neuronal ensemble in the IL responsive to ethanol associated cues was found to increase ethanol seeking (Pfarr et al., 2015). One explanation for the contradictory results between the different studies is the existence of several distinct neuronal ensembles within either subregion reacting to different environmental cues, that were previously conditioned, and which encode opposing effects on reward seeking (George and Hope, 2017). Evidence for this hypothesis is provided by several studies that showed that distinct neuronal ensembles coexist within the same brain region and that these neuronal ensembles are also able to mediate opposing effects on different behaviours in reaction to environmental cues (Suto et al., 2016; Warren et al., 2016; George and Hope, 2017; Warren et al., 2019; Kane et al., 2020).

Overall, these findings nicely demonstrate the essential involvement of PrL and IL in reward seeking behaviours, irrespective of the exact functional role on behavioural control each mPFC subregions fulfils.

1.5 The role of neuronal ensembles in reward seeking

The first idea of brain processes being controlled by close interaction of neuronal populations was proposed by D.O. Hebb in 1949. In his book, “The Organization of Behavior” (1949), he stated that neurons work together in groups, rather than working in isolation, to achieve a given task, forming the basis of learning and memory. Hebb named these populations “cell assemblies” (Hebb, 1949; Nicolelis et al., 1997). If certain neurons receive repeated input from afferent connections “that convey information about interoceptive stimuli, exteroceptive stimuli, and previous experience” (Cruz et al., 2015). The strongest activated neurons can be recruited together via strong synaptic connections and form a closed system. This system embodies the formation of functional neuronal ensembles in which the received information and learned associations are encoded via specific activity patterns. Upon memory recall the particular neuronal ensemble can be reactivated by synchronous activation of participating neurons which gives raise to coordinated spatiotemporal activity patterns. The output generated by these patterns will then initiate learned behaviours that are mediated by the learned associations (Fig. 08) (Hebb, 1949; Cruz et al., 2013; Mayford, 2013; Sompolinsky, 2014; Cruz et al., 2015; Holtmaat and Caroni, 2016).

Neurons of a certain ensemble encoding a specific behaviour do not have to be located in close proximity to each other but can be located in different brain areas. In addition, a certain brain area can comprise several neuronal ensembles encoding different learned behaviours (Fig. 08). Moreover, individual neurons are not tied to only one neuronal ensemble but can participate in several different ensembles and thus be involved in various behavioural outcomes. A single neuronal ensemble is considered to consist of only about 1-5 % of neurons of a given brain region, which is composed of up to several million neurons. Given a hypothetical brain region, which consists of 300 neurons and only 1 % of neurons form an ensemble, there are almost 4.46 million combinations of different ensembles possible. This and the fact, that individual neurons can be part of different ensembles, gives rise to an enormous complexity and variety of neuronal ensemble patterns and coding space (Hebb, 1949; Nicolelis et al., 1997; Cruz et al., 2015; Holtmaat and Caroni, 2016; Warren et al., 2017). During the learning process the strength of synaptic connections between neurons is changed on a regular basis depending on the afferent input each neuron receives. Therefore, it is not surprising that neuronal ensembles that encode specific learned associations are highly dynamic. Depending on the input participating neurons receive, they can be formed, modified or diminished (Holtmaat and Caroni, 2016).

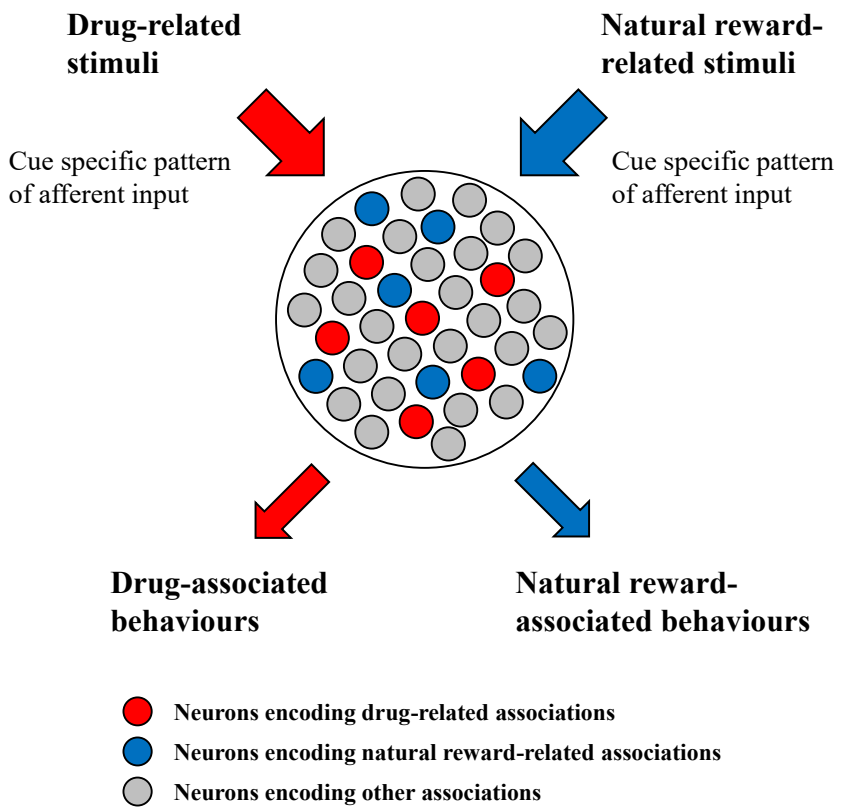

Figure 08) Schematic representation of two neuronal ensembles activated by specific afferent input

The specific afferent input pattern, triggered by a distinct drug-related stimulus, activates a set of neurons within the targeted brain region (large black circle). Nerve cells receiving the strongest and most persistent input will thereby form the neuronal ensemble (red circles), which encodes for the drug-related learned association. This ensemble will then initiate the specific drug-associated behaviours upon recall of the engrained memory. However, another stimulus, which is related to a natural reward, triggers the activity of another set of neurons within the same brain region, via specific afferent input patterns. Neurons that are activated the most by this input, will form a neuronal ensemble (blue circles) encoding for the natural reward-related associations. Recall of the engrained memory, by presentation of the cue associated with the natural reward, will activate the specific neuronal ensemble (blue) triggering the respective behavioural response. Adapted and modified from (Cruz et al., 2015; Pfarr, 2018).

The scientific world got intrigued by the idea of subpopulations of cells working in synchrony to encode memories and behaviours and slowly started investigating the matter. Up to today (24.10.2020), PubMed lists 3291 search results for publications about neuronal ensembles, with about 187 papers on the topic published on average each year over the last decade (PubMed.gov, 2020). Thereby neuronal ensembles were investigated in a wide context range from memory encoding in the hippocampus (Leutgeb et al., 2005), over rats being able to control a robotic arm by neuronal ensembles (Fetz, 1999), to social fear research (Sakurai et al., 2016). Several of those studies on neuronal ensembles, however, also investigated their involvement in reward seeking and addiction. Electrophysiological studies on drug self-administration, for example, revealed participation of different neuronal ensembles across several brain regions, like nucleus accumbens (Carelli et al., 1993; Peoples and West, 1996;

Chang et al., 1997), VTA (Kiyatkin and Rebec, 1997), basolateral amygdala (BLA) (Carelli et al., 2003) and ventral pallidum (Root et al., 2010), in a correlative manner (Cruz et al., 2013). However, in order to examine neuronal populations that are synchronously active in response to drug-associated cues or the drug itself and therefore might mediate drug seeking or conditioned drug associated behaviours, new techniques had to be developed to directly target and manipulate these groups of cells. One technique that nicely fulfilled this task was the Daun02 inactivation method (Koya et al., 2009b; Cruz et al., 2013; Koya et al., 2016). This technique allowed scientists to selectively inactivate neurons that were previously active in response to exteroceptive stimuli using *c-fos*-lacZ transgenic rats (Fig. 09). Thus, it was possible to establish a causal relationship between an active neuronal ensemble and learned behaviours.

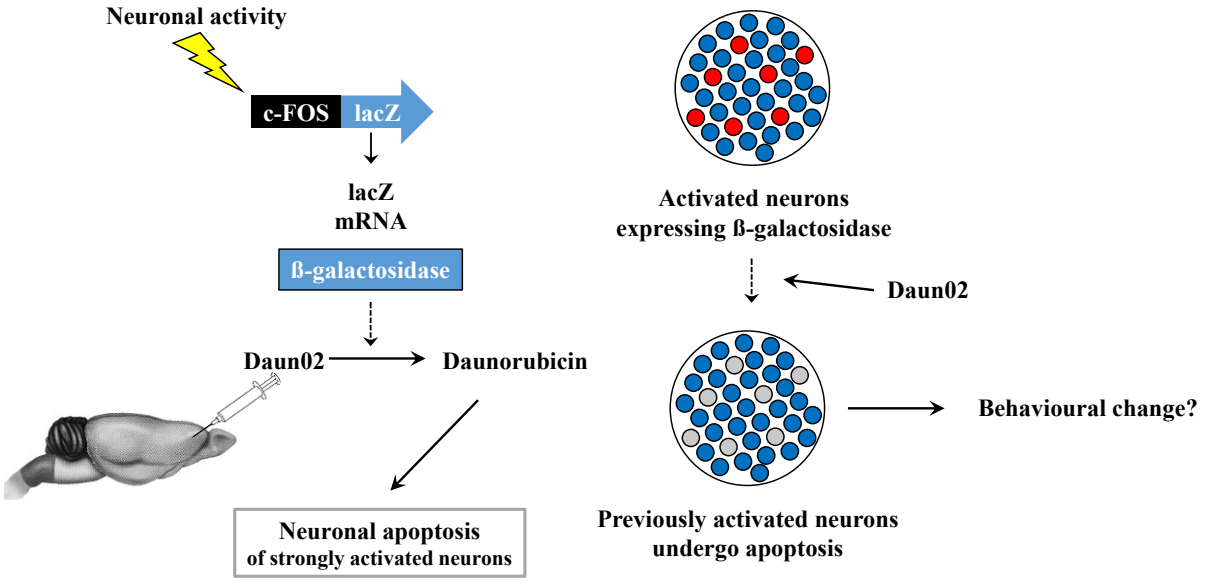

Figure 09) Daun02 inactivation method

The *c-fos*-lacZ transgenic rat strain carries a lacZ gene under control of a *c-fos* promotor. Each time, when sufficiently strong neuronal activity is induced by afferent input, the *c-fos* promotor gets activated and transcription of the lacZ coding sequence is induced. The resulting lacZ messenger ribonucleic acid (mRNA) is translated and ß-galactosidase is produced. Thus, ß-galactosidase is expressed in all strongly activated neurons (red circles) that are cFOS-positive, but not in other neurons of the brain region that are inactive (blue circles) and therefore cFOS-negative. Infusion of Daun02 into the target brain region then results in conversion of the prodrug into daunorubicin, which is mediated by ß-galactosidase. Conversion of Daun02 into its active form leads to neuronal apoptosis of previously strongly activated neurons. The elimination of the neuronal ensemble responsible for the specific behaviour (e.g., drug seeking behaviour) might then lead to changes in the behavioural outcome once the animal is challenged again by exteroceptive stimuli that triggered the behaviour. Adapted and modified from (Cruz et al., 2013).

Over the years, since its first introduction in 2009, the Daun02 inactivation method helped to identify several neuronal ensembles within the mesocorticolimbic system that were involved in reward seeking and addiction behaviour. Synchronously active neuronal populations within the medial prefrontal cortex, for example, were found to be involved in context-induced heroin

seeking (Bossert et al., 2011), alcohol seeking (Pfarr et al., 2015), food reward seeking (Warren et al., 2016), seeking for a glucose-saccharin solution (Suto et al., 2016) as well as cocaine seeking and cocaine self-administration (Warren et al., 2019; Kane et al., 2020). Neuronal ensembles involved in the incubation of methamphetamine craving were found in the dorsal striatum (Caprioli et al., 2017). The nucleus accumbens as crucial component of the mesocorticolimbic system was associated with context-induced reinstatement of cocaine seeking behaviour (Cruz et al., 2014). The different nuclei of the amygdala were also found to give raise to neuronal ensembles involved in drug-related behaviour. Neuronal ensembles in the central amygdala were found to be crucial in excessive alcohol consumption and incubation of nicotine craving (de Guglielmo et al., 2016; Funk et al., 2016). In the basolateral amygdala, however, neuronal ensembles involved in nicotine craving and relapse were identified (Xue et al., 2017).

Neuronal ensembles of the OFC were also investigated in the context of reward and addiction research where they were found to be crucial for the prediction of expected outcomes (Riceberg and Shapiro, 2017), the discrimination between natural rewards and reward probability (van Duuren et al., 2009), adaptation to changing reward contingencies (Simmons and Richmond, 2007), coding of reward magnitude (van Duuren et al., 2008) and for the response to acute drug exposure (Wall et al., 2019). One study also used the previously described Daun02 inactivation method to target neuronal ensembles within the OFC to prove the importance of these ensembles in cue-induced heroin seeking behaviour (Fanous et al., 2012).

All these different studies on functional neuronal ensembles provided a deeper inside on how these subpopulations of cells might encode specific behaviours, how they might work together and co-exist within the same brain region or across a network of different brain areas such as the mesocorticolimbic reward system. And even though the importance of different ensembles was proven for various drugs and slightly varying behavioural tasks the general underlying mechanism of action, of how these ensembles might interact within the mesocorticolimbic reward system, is thought to be similar (Fig. 10) (Cruz et al., 2013).

With novel techniques like the Daun02 inactivation method, that are based on the use of immediate-early genes, scientists were able to shed light on the theory of “cell assemblies” proposed by D.O. Hebb in 1949 and proved their involvement in a wide range of various behaviours. In the next paragraph a deeper understanding of immediate-early genes will be given.

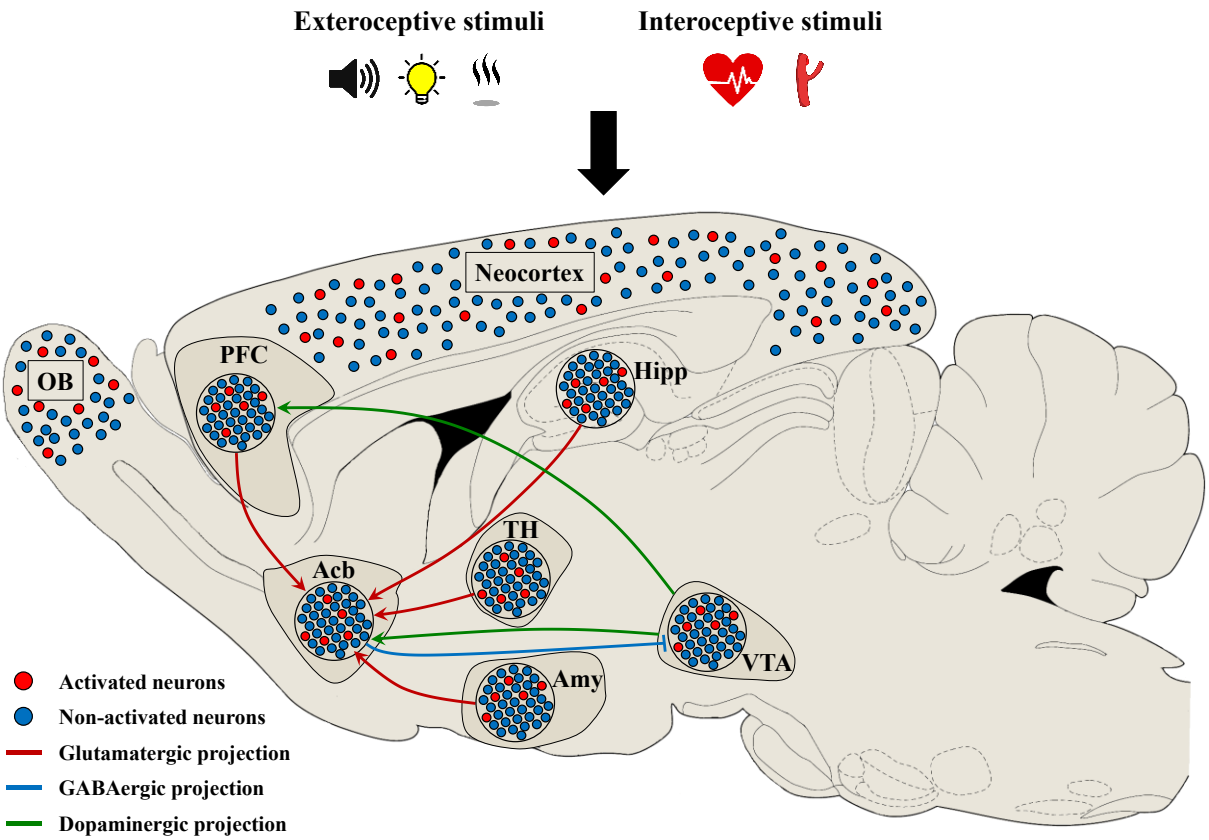

Figure 10) Interaction of neuronal ensembles within the brain reward system

The schematic illustrates how various drug-related factors like interoceptive stimuli, exteroceptive stimuli and previous experience might be integrated into information processing and how, consequently, coordinated patterns of neurons are activated to encode this information and interact with each other across different brain regions. In a first instance, neuronal ensembles involved in sensory processing in both neocortex and OB are activated by reward/drug consumption. These ensembles integrate the received information and transmit it to ensembles in PFC, Hipp, Amy and TH. After processing the afferent input, these brain regions send excitatory signals to the Acb via glutamatergic projections. In the Acb, the received information is integrated and neurons that receive the strongest input are recruited to form neuronal ensembles that respond to a specific set of stimuli and their involvement in reward-related behaviours. Dopaminergic projections from the VTA innervate PFC and Acb to further stimulate the coordinated neuronal activity of these ensembles in response to reward value and salience of incoming stimuli. The VTA also receives inhibitory input from neuronal ensembles of the Acb after afferent inputs to the Acb have been processed. Abbreviations: OB = olfactory bulb, PFC = prefrontal cortex, Acb = nucleus accumbens, Hipp = Hippocampus, Amy = amygdala, TH = thalamus, VTA = ventral tegmental area. Adapted and modified from (Cruz et al., 2013; Pfarr, 2018).

1.6 Immediate early genes - cFOS

Adaptations made by an organism in response to environmental changes or other extrinsic stimuli require alterations in gene expression. The cellular response can thereby involve the expression of two different classes of genes, the class of immediate early genes (IEG) and the class of late response genes. Whereas IEGs are rapidly and transiently expressed within minutes, as they do not require *de novo* protein synthesis, the expression of late response genes happens within hours since this process is normally dependent on *de-novo* protein synthesis

(Sheng and Greenberg, 1990). The class of IEGs can be grouped into two categories: the group of regulatory IEGs, that encode for transcription factors, and the group of effector IEGs, which encode for effector proteins. Regulatory IEGs can affect cellular function by regulation of downstream gene expression, through their gene products, whereas the group of effector IEGs expresses proteins, which can control cellular functions in a more direct manner (Davis et al., 2003; Barbosa and Silva, 2018). The expression of IEGs will alter the phenotype of a cell in response to environmental stimuli, which is the basis for a wide range of adaptations that should benefit an organism's competitive fitness and survival (Causton et al., 2001). IEGs are, in comparison to other genes, rather short, with an average length of 19 kilo base pairs vs. 58 kilo base pairs. They also contain fewer exons but are rich in TATA boxes and CPG islands. Their promoter regions are furthermore equipped with binding sites for different transcription factors such as cyclic adenosine monophosphate (AMP) response element-binding protein (CREB), nuclear factor kappa B (NF-κB) and serum-response factor (SRF) (Bahrami and Drabløs, 2016). It is estimated that the class of IEGs contains a few hundred genes of which about 30-40 are responsible for early responses in neurons. Approximately 10-15 of those IEGs encode transcription factors such as *c-fos* and *zif-268,* which are associated with long-term potentiation and long-term depression, the cellular correlates of learning and memory processes in the central nervous system (Richardson et al., 1992; Lanahan and Worley, 1998; Bahrami and Drabløs, 2016; Gandolfi et al., 2017; Barbosa and Silva, 2018). The proto-oncogene *c-fos* was one of the first IEGs to be described and up to today belongs to one of the best characterized ones. Its expression can be induced by a wide range of different stimuli and environmental factors like stress, fear, heat, odours and different convulsive- (e.g., lindane, t-hexachlorocyclohexane) and pharmacological substances (e.g., cocaine, caffeine, morphine), to name a few. *c-fos* is also activated during various forms of brain injury (mechanical, ischaemic, seizures) but also during developmental processes in the brain. As already mentioned, *c-fos* is also induced during learning and memory processes and therefore crucial for synaptic plasticity and behavioural adaptations (Herrera and Robertson, 1996; Cohen and Greenberg, 2008; Barros et al., 2015).

In the central nervous system *c-fos* is known to be regulated in a neuronal activity-dependent manner. Its expression can be induced by a variety of different extracellular signals and stimuli, to which its response is transient, but *c-fos* is also expressed under basal conditions. Thus, *c-fos* messenger ribonucleic acid (mRNA) and the cFOS protein are perfect candidates for activity mapping in the brain and can be used to identify populations of cells that are synchronously active in response to specific stimuli. Other reasons, why *c-fos* is widely used as neuronal

activity marker, are its simple detection, the possibility to label it in combination with a variety of other biomarkers and the fact that it can be used to examine its role in the regulation of other genes (Herrera and Robertson, 1996; Kovács, 1998; Kovács, 2008; Cruz et al., 2013; Barros et al., 2015; Cruz et al., 2015).

The exact molecular and cellular mechanisms that lead to *c-fos* gene transcription upon neuronal activation will be discussed in the following. cFOS belongs to the family of FOS proteins, which also includes FosB and its splice variants FosB2 and deltaFosB2 as well as Fra-1 and Fra-2. The cFOS protein possesses two conserved domains, which are a deoxyribonucleic acid (DNA)-binding region and the leucine zipper motif. The latter mediates dimerization with proteins of the Jun family (c-Jun, Jun B and Jun D), leading to formation of the AP-1 transcription factor complex. The Jun-FOS heterodimer can bind to the 12-O-tetradecanoylphorbol-13-acetate responsive elements, that are located in the promoter and enhancer regions of AP-1 regulated genes, leading to expression of proteins, which are involved in functional and morphological changes of neuronal cells (Angel and Karin, 1991; Hoffman et al., 1993; Milde-Langosch, 2005; Pérez-Cadahía et al., 2011). Strong neuronal activation, which results in calcium influx into the cell through NMDA-type glutamate receptors or L-type voltage-gated calcium channels (VGCCs), is the main driver for *c-fos* expression in neurons. However, all calcium signals are not created equal, meaning that additional properties of the signal such as duration and amplitude determine the type of transcription factor expressed. If intracellular calcium levels are sufficiently high the extracellular signal-regulated kinase (ERK)/mitogen-activated protein (MAP) kinase (MAPK) pathway is activated (Fig. 11). This includes the conversion of Rat sarcoma (Ras), a small guanine nucleotide-binding protein, from its guanosine diphosphate (GDP)-bound inactive form into its guanosine triphosphate (GTP)-bound active form. This molecular switch is regulated by guanine nucleotide exchange factors (GEFs), which catalyse the reaction (Bading et al., 1997; Agell et al., 2002; Bengtson and Bading, 2012). The Ras-GTP complex is then able to interact with and activate different downstream targets. One of them is the serine/threonine kinase rapidly accelerated fibrosarcoma (Raf), a *MAP-kinase-kinase-kinase*, which is phosphorylated by the GTP-bound Ras to initiate the ERK/MAPK pathway. Raf in turn activates the *MAP-kinase-kinases* MEK 1 and MEK 2 via phosphorylation on two serotonin residues. The MEK 1 and MEK 2 can now regulate the activity of the *MAP-kinase* ERK 1 and ERK 2 by phosphorylation on a threonine and a tyrosine residue (Alessi et al., 1994; Alberts B, 2002; McCubrey et al., 2007). The active ERK 1 and 2 can enter the nucleus and phosphorylate the ribosomal S6 kinase 2 (RSK2) and the ETS transcription factor Elk-1. Elk-1 forms a complex with another transcription factor, the

serum response factor (SRF). The Elk-1/SRF complex binds to one of two crucial elements of the *c-fos* promotor, the serum response element (SRE). The second element of the *c-fos* promotor, critical for *c-fos* expression, is the calcium response element (CaRE), which is also known as cyclic AMP response element (CRE). This region is the binding side for the transcription factor CREB. CREB is activated via phosphorylation by RSK2. Both transcription factors, Elk-1 and CREB, are therefore necessary to drive *c-fos* expression (Bading et al., 1997; McCubrey et al., 2007; Cruz et al., 2015). Once the *c-fos* promotor is activated, the *c-fos* coding sequence, consisting of four exons and three introns, is transcribed into *c-fos* mRNA. The *c-fos* transcript is already existent 5 min after neuronal activation but it cannot be translated due to its unspliced form. Thus, the unspliced isoform has first to be spliced before the cFOS protein can be generated. The underlying mechanism is called alternative splicing, which is a way to regulate gene expression even after transcription. The spliced *c-fos* mRNA reaches its peak at around 30-60 min after neuronal activation. Translation of the spliced *c-fos* mRNA results in the production of the cFOS protein, which reaches its maximum levels in the cell nucleus at about 90 minutes after neuronal activation and stays detectable as long as 4-6 hours after stimulation (Morgan et al., 1987; Hoffman et al., 1993; Kovács, 1998; Feng et al., 2001; Jurado et al., 2007; Lin et al., 2011). In order to control expression of AP-1 regulated genes, even after cFOS translation, cFOS activity can be regulated by posttranscriptional modification. Different enzymes like protein kinase A, protein kinase C, MAP kinase and cyclin-dependent kinase 1 are able to do so via phosphorylation of cFOS (Milde-Langosch, 2005). The ERK/MAPK pathway is thereby the main route of *c-fos* expression in drug-associated behaviours even though alternative pathways exist (Cruz et al., 2015).

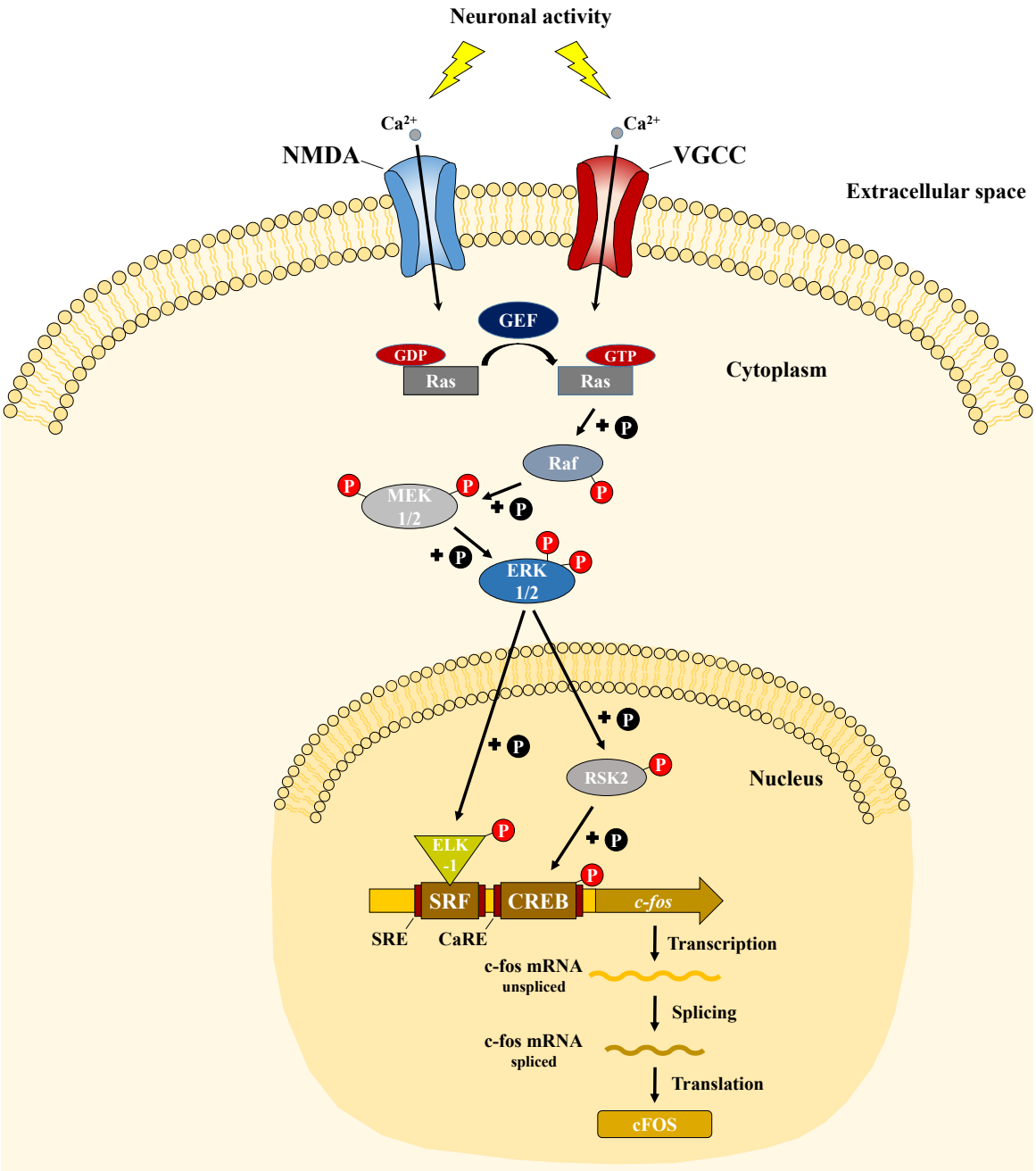

Figure 11) Calcium-depended regulation of *c-fos* expression

Illustration of the molecular mechanisms involved in initiation, transcription and translation of *c-fos* mRNA and cFOS protein, following reward-associated behaviours. Neuronal activation results in Ca^{2+}-ion influx into the cytoplasm through NMDA and VGCC receptors. This leads to the recruiting of GEFs, which catalyse the conversion of Ras-GDP to Ras-GTP. Ras-GTP phosphorylates the serine/threonine kinase Raf, which in turn phosphorylates MEK 1 and MEK 2. The *MAP-kinase-kinases* MEK 1 and MEK 2 catalyse the phosphorylation of ERK 1 and ERK 2, which allows them to phosphorylate Elk-1 and RSK2 in the cell nucleus. Elk-1 binds to SRF enabling the complex to interact with the SRE of the *c-fos* promotor. RSK2 phosphorylates CREB, which allows the transcription factor to bind the CaRE of the *c-fos* promotor. Activation of both response elements, by the transcription factors, leads to transcription of the downstream *c-fos* coding sequence. The resulting unspliced *c-fos* mRNA is spliced into mature *c-fos* mRNA, which is then translated into the final cFOS protein. Abbreviations: NMDA = N-meythyl-D-aspartate receptor, VGCC = L-type voltage-gated calcium channel, GEF = guanine nucleotide exchange factor, Raf = rapidly accelerated fibrosarcoma, Ras = Rat sarcoma, MEK = mitogen-activated protein kinase kinase, ERK = extracellular signal-regulated kinase, RSK2 = ribosomal S6 kinase 2, Elk-1 = ETS transcription factor ELK1, SRF = serum response factor, CREB = cAMP response element-binding protein, SRE = serum response element, CaRE = calcium response element, P = phosphate group, Ca^{2+} = calcium ion. Adapted and modified from (Cruz et al., 2013; Pfarr, 2018).

1.7 Animal disease models

Animal disease models are important tools to help scientists to decipher underlying mechanisms of human disease and with this knowledge develop treatments for those illnesses. In order to model a disease an animal model should ideally display similarities in disease symptoms, aetiology, underlying biochemical processes and treatment. However, in reality animal disease models are only able to model a restricted set of these aspects for complex clinical conditions such as Alzheimer's disease, Parkinson's disease or cardiovascular disease. (Ellenbroek and Cools, 1990; Sams-Dodd, 2006). In order to determine the relevance of an animal model to resemble a specific disorder it must undergo a critical evaluation and validation system. This system consists of three levels, which are face validity, predictive validity and construct validity. The degree by which the clinical condition and the animal model share phenomenological similarities e.g., similar symptomatology, is indicated by face validity. Predictive validity refers to the predictive value of the model, such as the aspect of how responses to pharmacological treatments or other manipulatory interventions resemble the clinical condition. Construct validity examines whether the underlying mechanism of the disease is equal between the human disorder and the condition modelled by the animal (Ellenbroek and Cools, 1990; Willner et al., 1992; Sams-Dodd, 1999; Sams-Dodd, 2006).

1.7.1 Animal model of drug self-administration and reinstatement of reward seeking

Drug addiction is a complex chronic brain disorder characterized by different factors like compulsive use and seeking of the drug, loss of control to restrict drug consumption and in case of drug abstinence the development of negative symptoms (Koob and Volkow, 2010). One of the most prominent problems for individuals undergoing withdrawal or during successful abstinence is relapse to drug consumption. Drug relapse can be triggered by different factors such as the re-exposure to the drug itself, exposure to exteroceptive cues that were previously associated with drug intake and stress (Marchant et al., 2013). In order to gain better understanding of drug relapse and to develop successful treatment options, preclinical research depends on animal models that resemble this complex disorder. The reinstatement model, which is widely used to study relapse-like behaviours, is such a model (Fig. 12) (Sanchis-Segura and Spanagel, 2006). It is essentially composed of three different phases. The first is the operant conditioning or self-administration phase, where the animals learn that responding to the active lever, which is paired with a distinct cue (e.g., light stimulus) leads to reward delivery. On the

other hand, animals learn that responding to the inactive lever, which is not paired with any cue, does not result in reward delivery. Pressing of the active lever is thus reinforced by the distinct cue, making it a conditioned stimulus (CS). The model is suitable for both oral as well as intravenous self-administration (Sanchis-Segura and Spanagel, 2006; García Pardo et al., 2017; Spanagel, 2017). After successful acquisition of reward self-administration and association of the conditioned stimulus with the reward, the second phase is initiated, which is extinction training. During extinction training animals progressively decrease their response until their operant responding behaviour is extinguished in consequence of the lack of cues predicting the reward or the reward itself. Once a certain extinction criterion is reached animals are subjected to test their reinstatement of reward seeking behaviour. Reward seeking can thereby be reinstated by drug priming, a technique where a small dose of the previously conditioned reward is presented (de Wit and Stewart, 1981; Pfarr, 2018). Furthermore, seeking behaviour can be initiated by presentation of environmental contexts or cues that were previously associated with the reward (Meil and See, 1996; Weiss et al., 2000; Crombag and Shaham, 2002), or it can be induced by exposure to stressors (Shaham and Stewart, 1995; Shepard et al., 2004; Bossert et al., 2013; Marchant et al., 2013).

As the reinstatement of reward seeking in this model is triggered by similar factors as in human addicts during abstinence, the reinstatement model shows excellent face validity. In addition, the model seems to provide predictive validity as pharmacological compounds used in drug treatment of humans like, naltrexone, buprenorphine, or methadone, are also functional in the reinstatement model as they decrease drug seeking triggered by drug-priming or conditioned cues (Marchant et al., 2013; Spanagel, 2017). In addition, Spanagel (2017) argues that the model also provides construct validity as underlying neurochemical and neuroanatomical mechanisms of the disorder are similar between species (Spanagel, 2017).

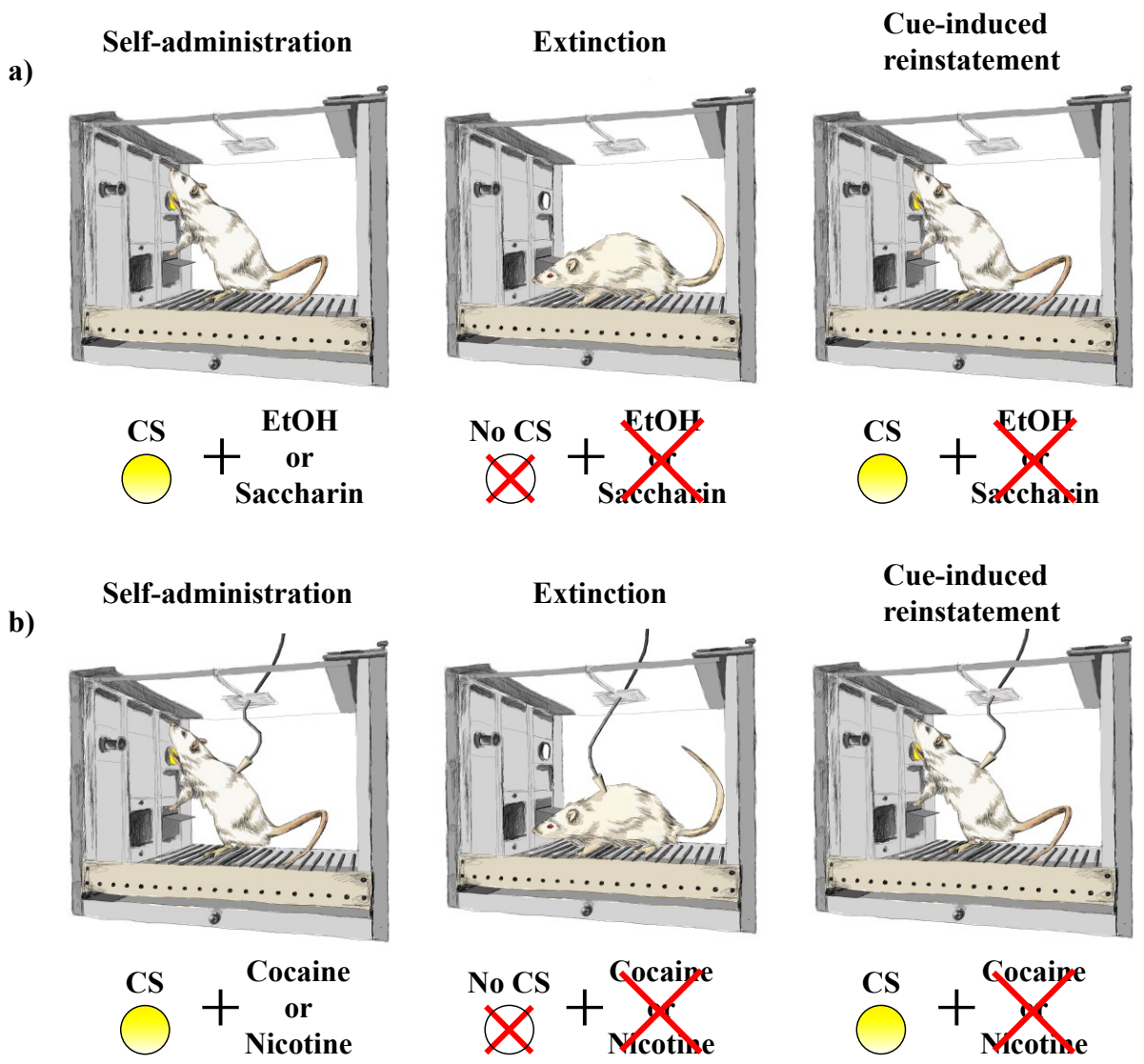

Figure 12) Animal model of drug self-administration and reinstatement of reward seeking

The illustration shows the operant conditioning model of drug self-administration and reinstatement of reward seeking behaviour. Animals are placed in an operant conditioning chamber, which is equipped with two response levers, one on the left side and one on the right side. A light source (cue light) is placed above each lever. During the self-administration phase response to the active lever (left) results in delivery of either EtOH or saccharin (a) into a small metal receptacle next to the lever or the intravenous infusion of either cocaine or nicotine (b) through the drug delivery assembly. Simultaneous to reward delivery a blink light stimulus is presented. During the self-administration phase the animals learn to associate the cue light with reward availability. Once animals show robust reward seeking behaviour, they undergo extinction training. During extinction, response to the lever does neither result in reward delivery nor in cue light presentation. Extinction training is followed by a test session to examine the animal's cue-induced reinstatement of reward seeking behaviour. During the test session response to the left lever results in cue light presentation but no rewards are delivered. Abbreviation: CS = conditioned stimulus. Drawings modified and used with permission of Wolfgang Sommer.

1.8 Transgenic animals

With the introduction of the first transgenic animals in 1980, the generation of animal models to study molecular mechanisms of specific diseases improved significantly. With these models new compounds and methods could be developed to stop the onset of disorders, slow down their progress or improve their symptomology (Gordon et al., 1980; Merlino, 1991). There are different methods to introduce genetic information into animals. The first step thereby is the construction of a DNA fragment of interest that will result in the expression of the desired gene product. This so-called transgene can be introduced in different ways into the genome of animals. Two of the most common techniques are the insertion of gene knockouts via specifically engineered genomic DNA in embryonic stem cells or the microinjection of the transgene into the pronucleus of fertilized ova, which leads to the random integration of the transgene into the germ-line DNA of the host (Shuldiner, 1996; Schönig et al., 2012).

As discussed previously, *c-fos* is an ideal marker to map neuronal activity. First, *c-fos* expression is not only triggered by a huge variety of different environmental stimuli but it is expressed at low basal levels, both *c-fos* mRNA and protein display a wide dynamic range and their half-life is rather short (Gall et al., 1998). In addition, the underlying mechanisms of both induction and expression of the *c-fos* gene are well studied. Because of its usefulness to identify brain regions involved in several different behaviours and map activity down to cellular level, several *c-fos* transgenic animals were generated.

Two of these transgenic rat strains, the *c-fos*-green fluorescent protein (GFP) transgenic rats and the *c-fos*-lacZ transgenic rats, were used in this thesis in order to investigate functional ensembles during reinstatement of reward seeking behaviour.

1.8.1 *c-fos*-GFP transgenic rats

The *c-fos*-GFP transgenic rats used in this thesis were developed by Bruce Thomas Hope's laboratory. The c-*fos-gfp* transgene was first described by Barth *et al.* (2004), who generated the first *c-fos*-GFP transgenic mouse model. The transgenic rat strain was generated on a Long-Evans background by injecting the c-*fos-gfp* transgene (Fig. 13) into pronuclei of fertilized ova. Offspring from the *c-fos-gfp* transgene positive founder expressed GFP under control of the *c-fos* promotor. Since the *c-fos* promotor is induced by strong neuronal activity, GFP can be

utilised to identify activated neurons in ex-vivo electrophysiological slice preparations, characterizing their physiological properties (Barth et al., 2004; Cifani et al., 2012b).

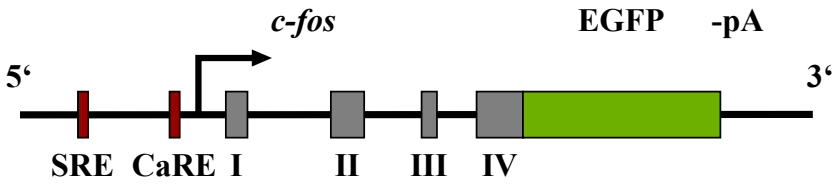

Figure 13) Illustration of the structure of the *c-fos*-GFP transgene

The 5'untranslated part of *c-fos* contains two crucial transcription regulatory sequences of the *c-fos* promotor, which are the serum response element (SRE) and the calcium response element (CaRE). These response elements are followed by the transcription start site, which is indicated by the black arrow. The four grey boxes (I. II, III, IV) illustrate the exons of the *c-fos* coding sequence. The last exon of the *c-fos* gene was fused to the coding sequence of enhanced GFP (EGFP), which is indicated by the green rectangle. It contains a stop codon to terminate transcription of the coding sequence. After the EGFP gene follows the 3' untranslated region, which contains the SV40 polyadenylation signal (pA). Adapted and modified from (Barth et al., 2004).

1.8.2 *c-fos*-lacZ transgenic rats

The *c-fos*-lacZ transgenic rats were generated by James I. Morgan's laboratory about 25 years ago. The scientists microinjected the *c-fos*-lacZ transgene (Fig. 14), which was previously described by Schilling *et al.* (1991), into the pronuclei of fertilized ova of female Sprague-Dawley rats (Kasof et al., 1995; Koya et al., 2009b). Transgenic *c-fos*-lacZ rats transcribe the *lacZ* coding sequence under control of the *c-fos* promotor, resulting in translation into the protein ß-galactosidase in strongly activated neurons (Cruz et al., 2013). The rats can be used to study the selective inactivation of neurons, that were previously activated following a specific behaviour or challenge in a given brain region, with help of the Daun02 inactivation method (paragraph 1.5, Fig. 9). Thus, they are a useful tool to investigate neuronal ensembles involved in cue-induced reward seeking (Koya et al., 2009b; Cruz et al., 2013; Cruz et al., 2015).

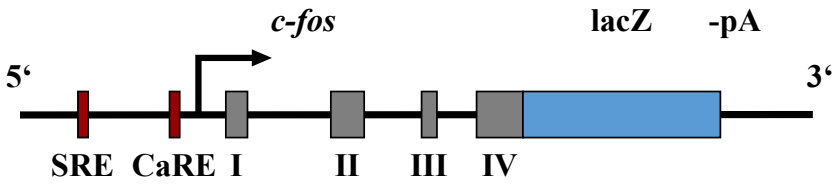

Figure 14) Illustration of the structure of the *c-fos*-lacZ transgene

The *c-fos* promotor is equipped with the two transcription regulatory sequences of the serum response element (SRE) and the calcium response element (CaRE). After those elements, the transcription start site, which is indicated by the black arrow, was introduced. The *c-fos* coding sequence contains four exons (I. II, III, IV) illustrated by grey rectangles. The lacZ gene (blue box) was fused to the last exon of the *c-fos* coding sequence. lacZ also contains the stop codon to terminate the transcription. The 3' untranslated region of *c-fos* furthermore contains the SV40 polyadenylation signal (pA). Adapted and modified from (Schilling et al., 1991).

1.9 Hypothesis and Aims

Repeated drug use leads to the formation of distinct memories, that encode for specific stimuli/cue-reward associations. These stimuli can develop a predictive value and acquire powerful control over an individual's motivational behaviour, capable of triggering craving and spurring drug seeking, eventually resulting in compulsive drug use. Re-exposure to conditioned stimuli is therefore one of the major causes of drug relapse. Even though reward seeking plays a key role in addiction, its underlying molecular and cellular mechanisms are not well understood.

Over the last few years, several studies could demonstrate that neuronal ensembles play a crucial role in reward seeking for different rewards. However, due to different study designs, a comprehensive comparison between distinct reward-encoding neuronal ensembles is not feasible. Thus, the overall goal of this work is to examine whether neuronal ensembles that encode for cue-reward associations are distinct or share properties between different rewards.

The hypothesis of this thesis is that different rewards, natural rewards and drugs of abuse, activate distinct neuronal ensembles within the major reward-related brain regions.

Our hypothesis will be tested by the following aims:

Aim 1: Identification and characterization of neuronal ensembles within activated reward-related brain regions, that encode either cue-induced natural (saccharin) or drug-induced (ethanol/nicotine/cocaine) reward seeking responses.

Aim 2: Functional validation of neuronal ensembles involved in the reinstatement of reward seeking behaviour.

Aim 3: Characterization of the shared and distinct properties of neuronal ensembles encoding ethanol and saccharin reward seeking.

1.10 Study list

Study 1: Identification and characterization of neuronal ensembles within the extended reward system encoding for natural reward and drug reward seeking (Aim 1).

Study 2: Validation of functional neuronal ensembles encoding for natural reward and drug reward seeking behaviour (Aim 2).

Study 3: Comparison of neuronal ensembles within the infralimbic cortex following reinstatement of saccharin and ethanol seeking behaviour (Aim 3).

2. MATERIALS AND METHODS

2.1 Subjects

c-fos-GFP transgenic rats

Male *c-fos*-GFP transgenic rats generated on a Long Evans genetic background (Cifani et al., 2012a) were bred in the on-site breeding facility of the CIMH Mannheim. Animals being heterozygous carriers of the cFOS-GFP fusion protein (Barth et al., 2004) were used for *in situ* hybridization, immunostaining and whole-cell patch clamp experiments.

All animals were single housed in Makrolon™ cages (Eurostandard type III H) under a reverse 12 h/12 h light-dark cycle (lights off at 5:00 a.m./lights on at 5 p.m.) with *ad libitum* tap water and food supply (ssniff Spezialdiäten GmbH, Germany).

c-fos-lacZ transgenic rats

Male *c-fos*-lacZ transgenic rats bred on a Sprague-Dawley genetic background (Kasof et al., 1995) were used in the Daun02 inactivation study. Animals were bred in the on-site breeding facility of the CIMH Mannheim. Rats were exposed to a reverse 12 h/12 h light-dark cycle (lights off at 5:00 a.m./lights on at 5 p.m.) with tap water and food (ssniff Spezialdiäten GmbH, Germany) available *ad libitum*. Animals were kept single-housed in Makrolon™ cages (Eurostandard type III H) with begin of the experimental phase.

Wild type Wistar rats

Male Wistar rats, used in Study 3 were sourced from Charles River Germany. Rats were kept group housed in Makrolon™ cages (Eurostandard type IV) on a 12 h/12 h light-dark cycle, with experiments being performed during the dark phase. Animals had *ad libitum* excess to both water and food (ssniff Spezialdiäten GmbH, Germany).

All experimental procedures were approved by the local animal care committee (Regierungspräsidium Karlsruhe, Germany) and performed in accordance with directive 2010/63/EU of the European Parliament and of the Council on the protection of animals used for scientific purposes.

2.2 Experimental study design

2.2.1 Study 1A: Identification of neuronal ensembles within the extended reward system encoding for natural reward and drug reward seeking

In order to identify neuronal ensembles within the reward system that encode cue-induced reward seeking responses for different drugs of abuse and a natural reward, *c-fos*-GFP transgenic rats were trained under an operant conditioning paradigm to either self-administer one of the three drugs of abuse (EtOH, cocaine, nicotine) or the natural reward saccharin. Self-administration training was then followed by extinction learning of the previously acquired lever press behaviour. Subsequently, animals were divided into two groups according to their performance during self-administration and extinction. On the test day group 1 underwent an additional extinction session whereas group 2 was subjected to a cue-induced reinstatement session. Immediately after the experiment animals were sacrificed, their brains harvested and stored at - 80 °C until further processing. In the following coronal slices of the obtained brains were taken, *c-fos* mRNA radioactively labelled and the resulting autoradiographs analysed to identify the brain region with strongest activation during the behavioural task (Fig. 15).

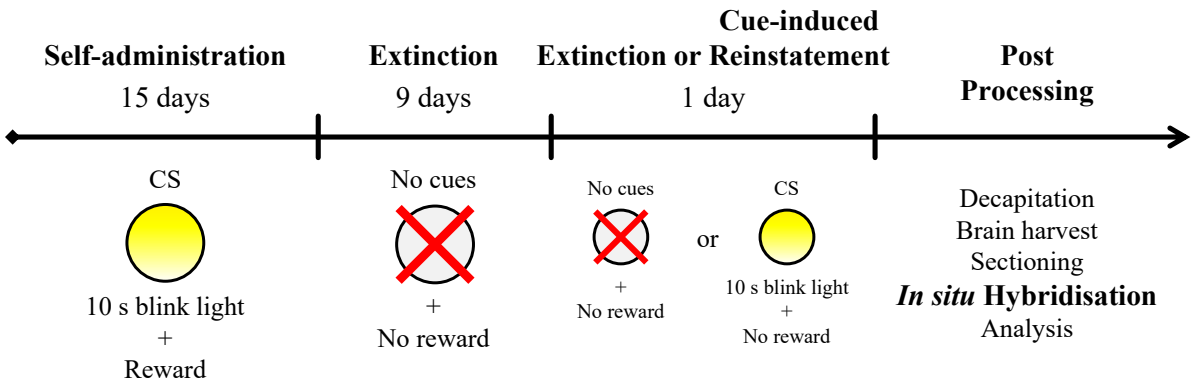

Figure 15) Time schedule for the identification of neuronal ensembles within the extended reward system

Animals were trained to self-administer either EtOH, saccharin, cocaine or nicotine for three weeks until they reached a stable lever press response rate. Afterwards, they underwent extinction training and were grouped according to their performance in the previous tasks. Following extinction, animals were subjected to an additional extinction or a cue-induced reinstatement session according to their group. Immediately after, animals were sacrificed and their brains processed. Then, c-*fos* mRNA was radioactively labelled and the resulting autoradiographs analysed. Abbreviation: CS = conditioned stimulus.

2.2.2 Study 1B: Immunohistochemical analysis of neuronal ensembles following cue-induced reinstatement of reward seeking behaviour

For the neurochemical characterization of neuronal ensembles different batches of *c-fos*-GFP transgenic rats were trained to self-administer either EtOH, saccharin or cocaine. Afterwards animals were subjected to extinction training, which was followed by a cue-induced reinstatement session the next day. Thirty minutes after the end of the reinstatement session animals were perfused, their brains harvested and sliced. In the following the previously acquired coronal slices underwent double-immunohistochemical stainings to co-localize cFOS with different cell markers. Afterwards slides were investigated with help of a confocal microscope and images acquired. For quantitative analysis of the different co-localizations, cells labelled with the respective markers were counted subsequently, in order to identify the neurochemical composition of neuronal ensembles. Figure 16 shows the time schedule for Study 1B.

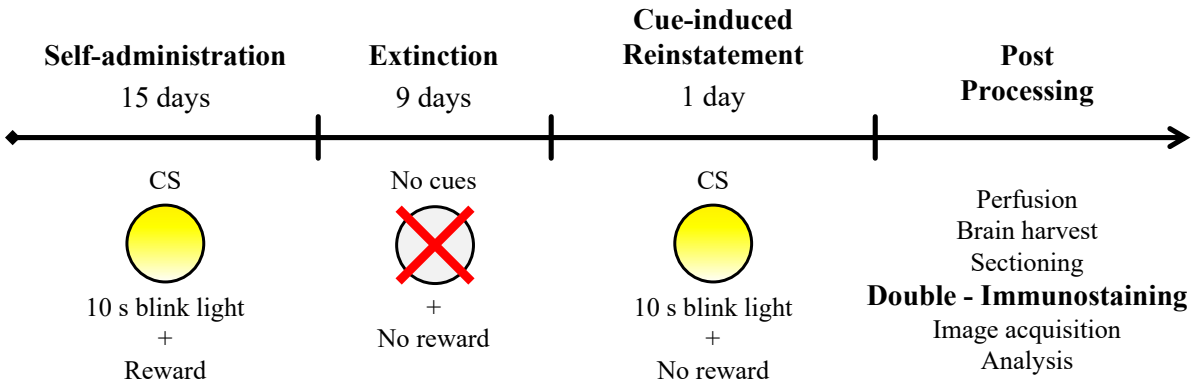

Figure 16) Experimental time plan for the neurochemical characterization of neuronal ensembles encoding cue-induced reward seeking behaviour

First *c-fos*-GFP transgenic rats were trained to self-administer either one of the drugs of abuse (EtOH, cocaine) or the natural reward saccharin. Afterwards, they performed extinction training until they reached less than 20 % of their baseline response rate. Extinction learning was then followed by a cue-induced reinstatement session. Ninety minutes after beginning of the test session animals were perfused and their brains processed. Coronal slices were then treated with different antibodies for the different co-localizations. Afterwards images were recorded and analysed. Abbreviation: CS = conditioned stimulus.

2.2.3 Study 1C: Characterization of the physiological properties of GFP positive (active) versus GFP negative (inactive) neurons after reinstatement of reward seeking

For the physiological characterization of neuronal ensembles mediating cue-induced reward seeking behaviour *c-fos*-GFP transgenic rats were trained to self-administer cocaine, one of the drugs of abuse. After reaching stable response rates animals underwent extinction training of their lever press behaviour. Following successful extinction animals were subjected to a cue-induced reinstatement session. 30 min after the test session animals were perfused and their brains harvested. Afterwards acute slices with the brain region of interest were acquired. Then electrophysiological properties were examined using the whole-cell patch clamp method. Measurements were subsequently followed by data analysis. The time schedule for Study 1C is displayed in Figure 17.

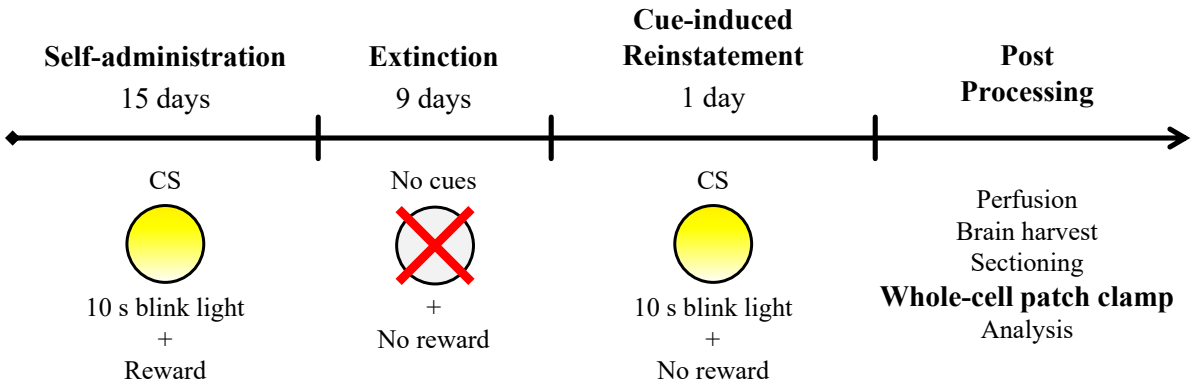

Figure 17) Schedule for the electrophysiological characterization of neuronal ensembles active during cue-induced cocaine seeking behaviour

c-fos-GFP transgenic animals were trained to self-administer the psychostimulant cocaine over the course of three weeks. Afterwards, the rats underwent extinction learning until their lever press behaviour was extinguished. Animals were then tested for their reward seeking behaviour in a cue-induced reinstatement session. Ninety minutes after beginning of the test session, all rats were perfused and their brains processed. Electrophysiological recordings of active vs. inactive neurons were recorded in the following. Finally, recordings were analysed. Abbreviation: CS = conditioned stimulus.

2.2.4 Study 2: Validation of functional neuronal ensembles encoding for natural reward and drug reward seeking behaviour

In order to examine the functional relevance of the previously identified neuronal ensembles, they were inactivated with help of the Daun02 method. Therefore, *c-fos*-lacZ transgenic rats were trained to self-administer either saccharin or cocaine over the course of three weeks. Afterwards the rats had to undergo extinction training until they reached less than 20 % of their baseline response rate. After successful extinction, all animals were implanted bilaterally with guide cannulas into the OFC. This was followed by a recovery period of one week. Next, the rats were examined for their cue-induced reinstatement of reward seeking behaviour. Thirty minutes after the end of the test session animals were either intracranially infused with Daun02 or vehicle depending on their group assignment, which was based on their performance during self-administration, extinction and the first cue-induced reinstatement. After a break of four days the rats were tested in a second cue-induced reinstatement for changes in their reward seeking behaviour. Following the second cue-induced reinstatement animals were perfused and their brains harvested. Brains were then sliced and coronal slices immunohistochemically stained. Afterwards brain slices were analysed. Figure 18 depicts the time schedule for Study 2.

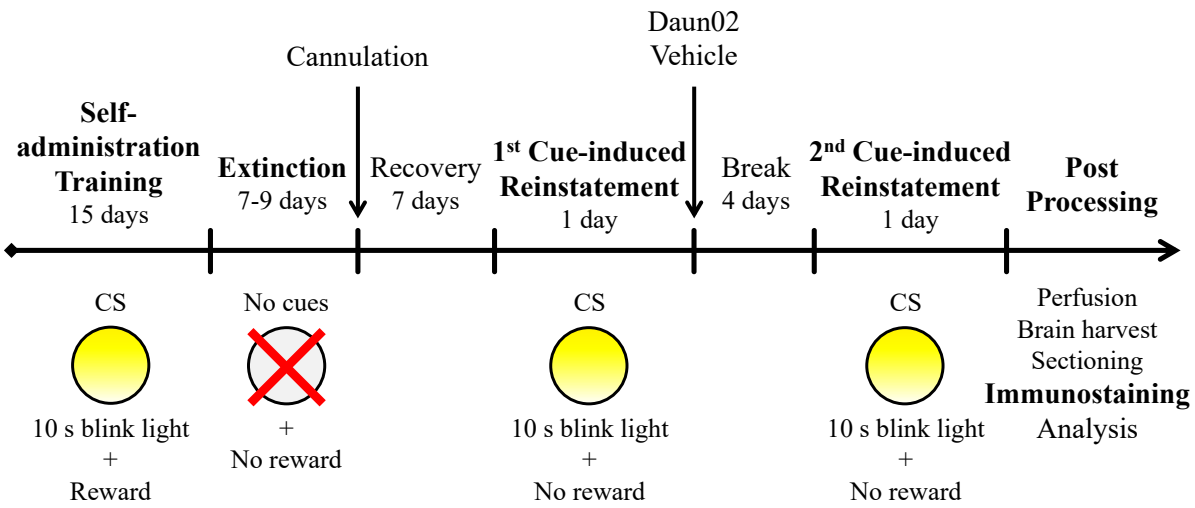

Figure 18) Experimental timeline for the functional validation of previously identified neuronal ensembles encoding for cue-induced reward seeking behaviour

Animals were trained to self-administer either saccharin or cocaine which was followed by extinction of the lever press behaviour. Afterwards, animals were bilaterally implanted with guides cannulas into the OFC. Next, animals recovered for one week before they were subjected to the first cue-induced reinstatement. After the test session, animals were either infused with Daun02 or vehicle into the OFC. Four days of break later, the rats were subjected to the second cue-induced reinstatement. Ninety minutes after the final test session animals were perfused and their brains processed. Finally, brain slices were immunohistochemically stained and analysed. Abbreviation: CS = conditioned stimulus.

2.2.5 Study 3: Comparison of neuronal ensembles within the infralimbic cortex following reinstatement of saccharin and ethanol seeking behaviour

In order to compare neuronal ensembles active during EtOH and saccharin seeking a two-reward conditioning approach was used. Two batches of animals were trained to self-administer 10 % ethanol, which was paired with an orange odour (olfactory cue) and a 5 s blink light (visual cue), and saccharin (Study 3A: 0.08 % saccharin; Study 3B: 0.025 %), which was paired with lemon grass odour (olfactory cue) and a 5 s blink light (visual cue). After achieving a stable baseline for both rewards, the rats were subjected to extinction training. Following extinction, animals underwent matched cue-induced reinstatement (RE) for ethanol and saccharin seeking (RE 1 + 2).

Animals of Study 3A were subjected to retrograde tracer injection (data not shown), grouped according to their performance during reinstatement and after a recovery period of 5 days they were once more tested for their relapse-like behaviour during cue-induced reinstatement for EtOH or saccharin (RE 3) (Fig. 19). Afterwards animals were sacrificed and brains processed for double immunohistochemistry against cFOS-immune reactivity (ir) and Neuronal nuclei (NeuN)-ir.

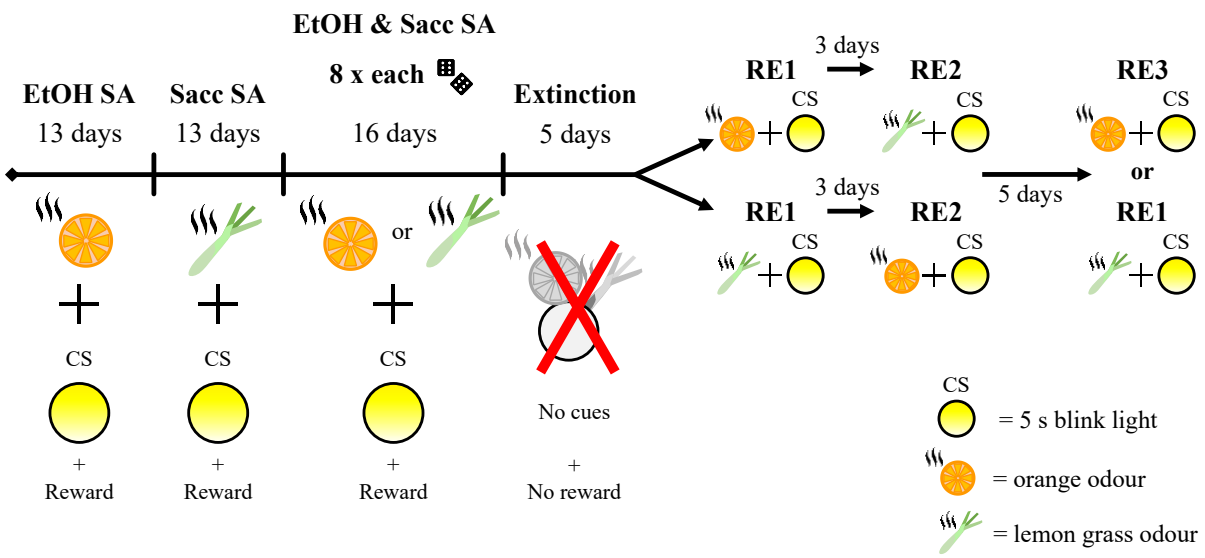

Figure 19) Time schedule for two-reward operant conditioning to investigate size differences between neuronal ensembles involved in EtOH or saccharin seeking

Wistar rats were trained to self-administer 10 % EtOH (olfactory cue: orange odour) and 0.08 % saccharin (olfactory cue: lemon grass odour). Both rewards were paired with a 5 s blink light upon active lever press/reward delivery. After achieving a robust performance for both rewards, animals underwent extinction training where no rewards or cues were presented. Extinction was followed by matched cue-induced reinstatement sessions for EtOH or saccharin seeking (RE 1 + 2). After retrograde tracer injection and five days of recovery animals were subjected to a cue-induced reinstatement for EtOH or saccharin (RE 3). Abbreviation: CS = conditioned stimulus, RE = cue-induced reinstatement, SA = self-administration, Sacc = saccharin. Modified from (Pfarr, 2018; Pfarr et al., 2018).

In Study 3B, which aimed to compare cue-responsive neuronal ensembles during reinstatement of EtOH and saccharin within the same animal, rats were grouped according to their performance during RE 1 + 2 and subjected to two additional cue-induced reinstatement sessions (RE 3 + 4) (Fig. 20). Both sessions were 5 min in length and separated by a 30 min time period. After RE 4 animals were sacrificed and their brains processed for double *c-fos* fluorescent *in situ* hybridization using RNAscope.

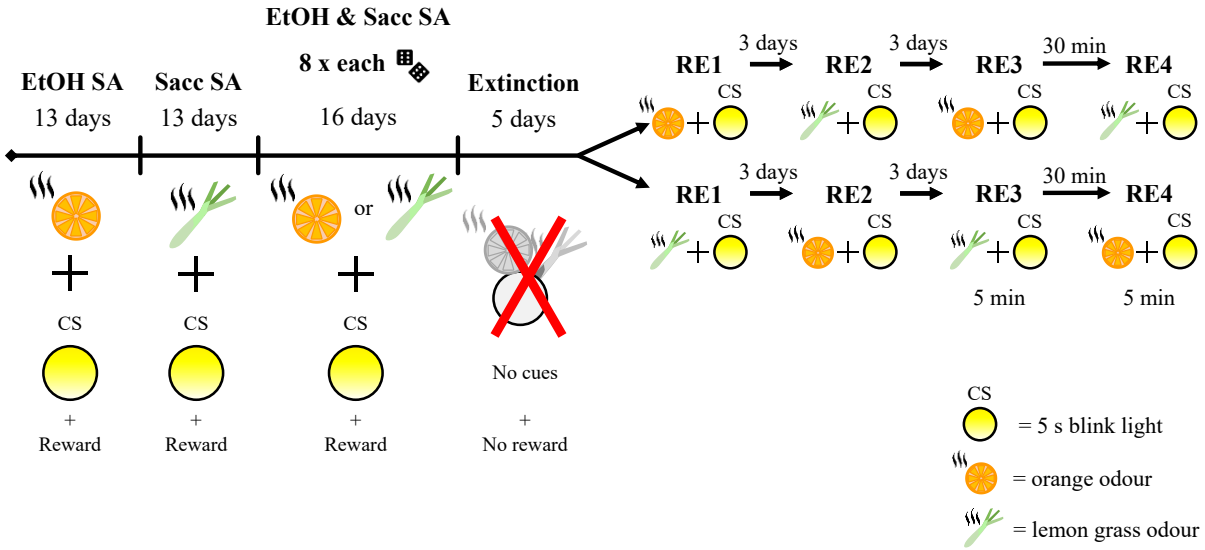

Figure 20) Timeline for experimental processes during two-reward operant conditioning to compare neuronal ensembles encoding for EtOH and saccharin seeking behaviour within the same animal

First a batch of Wistar rats was trained to self-administer 10 % EtOH and 0.025 % saccharin. Each reward was paired with its respective olfactory cue (EtOH: orange odour; saccharin: lemon grass odour) and a visual stimulus (5 s blink light). After reaching a stable baseline for self-administration for both rewards, training was continued with extinction learning. When the animal's lever press behaviour was successfully extinguished, the rats underwent matched cue-induced reinstatement for EtOH and saccharin seeking (RE 1 + 2). After a break of three days two more cue-induced reinstatement sessions were performed. Both sessions had a length of 5 min and were 30 min apart (RE 3 + 4). Abbreviation: CS = conditioned stimulus, RE = cue-induced reinstatement, SA = self-administration, Sacc = saccharin. Modified from (Pfarr, 2018; Pfarr et al., 2018).

2.3 Behavioural experiments

2.3.1 Operant conditioning experiments

2.3.1.1 Operant conditioning chamber

All operant conditioning and reward seeking experiments were conducted in standard operant conditioning chambers (Med. Associates) housed in sound attenuating cubicles. Each operant chamber was equipped with two retractable response levers on either side as well as white stimulus lights positioned above the response levers. Next to each lever, in the middle of the side panel, a liquid receptacle was placed. In addition, each operant chamber was equipped with a drug delivery arm assembly and the appropriate tether/infusion system, which did exit the chamber in the middle of the top, for intravenous drug self-administration. Upon response at the appropriate lever (active lever) reward delivery was initiated either by activation of the liquid dispenser, in case of EtOH or saccharin rewards or by activation of the single speed syringe pump for intravenous administration of cocaine or nicotine. Besides drug delivery, response at the active lever led to activation of the cue light.

The entire system was controlled and all actions recorded with the behavioural software Med PC IV via Med Associates interfaces.

2.3.1.2 Operant self-administration training

Study 1 & 2

Animals were conditioned to self-administer one of the three drugs of abuse (alcohol, cocaine, nicotine) or the natural reward saccharin under a fixed ratio 1 (FR 1) schedule in one-hour sessions five times a week. Sessions started three to five hours after the dark phase of the reverse 12 h/12 h light-dark cycle was initiated. Animals were kept water deprived for 22 hours prior to the training sessions for the first two days of self-administration training. Whereas EtOH and saccharin trained animals were simply placed inside the operant chamber before start of a session, cocaine and nicotine trained animals had to be connected to the infusion system to be able to receive their intravenous reward infusions. Therefore, the tubing of the infusion system was connected to the top projection of the back mount cannula of the intravenous catheter and secured by a screwable adaptor. Each of the self-administration sessions started

with the presentation of two response levers (active: left side; inactive: right side). Response at the active lever was recorded and resulted in delivery of one of the four rewards. Saccharin and alcohol were delivered orally in 30 µl droplet portions whereas cocaine and nicotine were delivered as intravenous infusion with a volume of 106 µl. In order to equalize response rates at the active lever between rewards, the following reward concentrations were used: 10 % EtOH, 0.125 mg/kg cocaine, 0.01 mg/kg nicotine and 0.04 % saccharin (Long-Evans)/0.2 % saccharin (Sprague Dawley). Upon response at the active lever and simultaneous to reward delivery, a discrete visual stimulus in the form of a 10-second blink light was presented. Animals therefore learned to closely associate the visual cue with reward availability upon response to the active lever. Within the 10 s cue light presentation, which served as "time out", animals were able to continue lever pressing, which was recorded, but no rewards were delivered. In addition, inactive lever responses were recorded but had no programmed consequences.

Animals were trained until they reached stable self-administration baseline performance, which was generally reached after fifteen cue-conditioning sessions.

Study 3

In the two-reward operant conditioning paradigm Wistar rats were trained to self-administer EtOH and saccharin under a FR1 schedule in daily 30 min sessions for five days a week. Operant training was conducted 3 hours after onset of the animal's dark phase. Rats were kept water deprived for 18 hours prior to the training sessions for the first 3 days of self-administration. In order to successfully condition the animals to both rewards, each reward was coupled with a unique set of stimuli of which one targeted the olfactory domain and the other the visual domain. EtOH was paired with an orange odour (orange oleum aurantii dulcis g420, Caelo, Hilden, Germany) and saccharin with a lemon grass odour (lemon grass oil w861, Caelo, Hilden, Germany) as contextual olfactory stimulus. For each session that was paired with an olfactory cue, few drops of either oil (max. 4 - 6) were drippled over bedding material, which was placed onto a drawer in the operant chamber. Thus, the operant chamber was equipped with the respective olfactory cue throughout the session. The visual cue, a 5 s blink light, was presented if the animal made a response at the active lever. Every session started with the presentation of a left response lever and a right response lever. During EtOH paired sessions, response at the left lever resulted in reward delivery and presentation of the cue light, whereas during saccharin paired sessions response at the right lever led to reward delivery and cue light

presentation. The 5 s, during which the cue light was presented, served as "time out", meaning that responses to the active lever were recorded but no rewards were delivered. Responses to the inactive lever (EtOH: right; saccharin: left) were recorded but had no consequences.

At first animals were trained to self-administer 10 % EtOH. During the first nine conditioning sessions the rats had only access to the active lever, whereas in the next four training sessions the inactive lever was presented in addition, so that the rats learned to discriminate between the two levers. After these thirteen days of EtOH conditioning the identical process was repeated, only this time for saccharin (Fig. 19 + 20). To match responses during EtOH conditioning, the saccharin concentration had to be adjusted accordingly (Study 3A: 0.08 % saccharin; Study 3B: 0.025 % saccharin). After the animals were conditioned for both rewards, they were subjected to eight randomised training sessions for each reward. The goal of the additional self-administration sessions was to obtain a robust baseline for self-administration performance (mean of the last three SA sessions) for each reward.

2.3.1.3 Extinction training/Extinction test session (Study 1A)

Study 1 & 2

Following self-administration training animals underwent extinction training, until they reached the extinction criterion, defined as active lever response rate of < 20 % of baseline activity averaged over the last few extinction sessions. Sessions lasted one hour each and were performed in the same operant chambers as described before. During extinction training both levers were presented but in contrast to the self-administration sessions, response to the active lever did not result in presentation of the conditioned cue light nor reward delivery. Responses to the inactive lever were recorded but had no outcome for the animal.

As previously described (paragraph 2.2.1) one group of animals in Study 1A was subjected to an additional extinction session on test day. This test extinction session was performed in the same way as a normal extinction session. However, immediately after end of the session animals were sacrificed (paragraph 2.5.1.1).

Study 3

After self-administration training, animals underwent five days of extinction learning to achieve the goal extinction criterion, defined as active lever response rate of < 10 % of baseline

activity averaged over the last few extinction sessions. Extinction sessions were 30 min long and both levers were presented during these sessions. However, no cues, neither visual nor olfactory, were presented and no rewards were delivered.

2.3.1.4 Cue-induced reinstatement of reward seeking behaviour

Study 1 & 2

On test day, one day after successfully finishing extinction training, animals were subjected to a one-hour cue-induced reinstatement session during which both response levers were presented. Response to the active lever resulted in activation of the visual conditioned stimulus, the 10 s blink light, however no rewards were delivered. Inactive responses had no programmed outcome. Responses to active and inactive lever were recorded for further analysis. Animals that responded > 90 % above their baseline extinction training performance (average performance of the last four extinction sessions) and achieved at least 18 lever presses at the active lever, were classified as having successfully established reinstatement of reward seeking behaviour. A few animals performed slightly below this criterion but were still included if they pressed at least 16 times on the active lever and were 100 % above their extinction performance or that achieved 50 % - 90 % above their extinction performance but pressed at least 26 times on the active lever.

Animals subjected to Study 1A were sacrificed sixty minutes after onset of the cue-induced reinstatement session (paragraph 2.5.1.1). Rats assigned to Study 1B were transcardially perfused as described in paragraph 2.5.1.2. Animals used for the characterization of physiological properties of co-active neurons (Study 1C), were sacrificed ninety minutes after onset of cue-induced reinstatement (paragraph 2.5.1.2). Animals undergoing the Daun02 inactivation experiment were divided into two groups according to their performance during reward self-administration, extinction and cue-induced reinstatement. Depending on the group, animals received a bilateral intracranial infusion of either Daun02 or vehicle into the ventral OFC or lateral OFC ninety minutes after start of the cue-induced reinstatement session (paragraph 2.4.3). After a recovery period of four days animals were subjected to a second cue-induced reinstatement session to examine potential changes in their reward seeking behaviour. Ninety minutes after onset of the second cue-induced reinstatement of reward seeking animals were transcardially perfused (2.5.1.2).

Study 3

After successful extinction training all animals were tested in counterbalanced cue-induced reinstatement sessions. Depending on which reward condition was reinstated, the respective olfactory cue was used (EtOH: orange odour; saccharin: lemon grass). During the 30 min long reinstatement sessions both levers were presented. Response at the active lever (EtOH: left; saccharin: right) resulted in presentation of the 5 s blink light but in contrast to the conditioning sessions no rewards were delivered. Responses to the inactive lever were recorded but had no consequences for the animals.

In Study 3A two counterbalanced cue-induced reinstatement sessions, one for each reward, which were separated by a 3-day break, were performed (RE 1 + 2). Depending on their performance animals were grouped and subjected to either one more EtOH or saccharin cue-induced reinstatement session (RE 3) (Fig. 19).

Animals subjected to Study 3B also performed two initial counterbalanced cue-induced reinstatement sessions, one for either reward (RE 1 + 2). Both sessions were also separated by a 3-day break. Three days after RE 2 the previously grouped animals performed two more reinstatement sessions (RE 3 + 4). Each animal underwent a 5 min reinstatement session for EtOH and a 5 min reinstatement session for saccharin. Re 3 + 4 were again counterbalanced. Both reinstatement sessions were separated by 30 min (Fig. 20).

Ninety minutes after onset of reinstatement session RE 3 animals were perfused as described in paragraph 2.5.1.2 (Study 3A). Animals of Study 3B were sacrificed 35 min after onset of the last cue-induced reinstatement session (paragraph 2.5.1.1).

2.4 Surgical interventions and associated procedures

2.4.1 Intravenous catheter implantation

2.4.1.1 Catheter preparation

Catheters were built by connecting 16 cm Silastic® silicone laboratory tubing (0.51 mm x 0.94 mm) to a 22 gauge (GA) stainless steel Back-Mount Cannula (PlasticsOne: 313000 BM - 10) by sliding the tubing over the side projection of the Back-Mount Cannula. To protect the silicone tubing the connection point was encased with 1.5 cm shrinking tube (1.17 mm, shrink ratio 2:1) and secured with superglue (Loctite 401). To keep the catheter in place, after inserting

it into the vein, two anchor points (1st: 1.5 cm from the end of the tube, 2nd: 4 mm after the 1st) were created by the use of superglue and two pieces of 3 mm shrinking tube. In addition, a 2.5 cm x 2.5 cm piece of a monofilament polypropylene mesh (Bard Mesh) was attached to the Back-Mount Cannula to allow for better integration and resilience of the catheter after implantation. To enable an easier insertion of the tube into the vein its end was cut pointed. After the catheter assembly was finished, they were autoclaved at 121 °C for 20 min in small sterilization pouches.

2.4.1.2 Catheter implantation

Animals undergoing intravenous cocaine or nicotine self-administration were implanted with silicon catheters into their jugular vein. At the beginning of the intervention the surgery table and all necessary instruments were prepared and sterilized. To guaranty most sterile working conditions, instruments were sterilized using a hot bead sterilizer during the surgery if necessary.

The surgery started by anaesthetizing the animal inside an anaesthesia box supplied with 4 % isoflurane. After the rat went unconscious it was transferred to a heating pad (39 °C), which was covered with a sterile plain drape. To keep the animal in deep anaesthesia for the whole procedure it was constantly breathing an air-isoflurane mixture at a flow rate of 405 ml/min, which was supplied with 1.8 % - 2.2 % isoflurane. The animal's eyes were protected from drying out with an ophthalmic gel. The incision areas on the back, between the shoulder plates and in front above the jugular vein were shaven and cleaned repetitively with iodine and ethanol pads. Then a 2 cm incision was made orthogonal to the rat's body axis slightly caudal from the scapulae. Another small incision was made approximately 10 cm caudal from the first incision in the middle of the back. To form a channel for the catheter tubing the skin between the two incisions was carefully separated from the surrounding tissue. In order to insert the catheter into the jugular vein a small incision was made above the right jugular vein on the ventral side of the body. To enable the implantation of the catheter from the back to the jugular vein a connection between the ventral incision and the scapulae incision was created under the skin. After inserting the catheter from the back to the front, the tissue below the incision was gently pushed aside to expose the jugular vein. To keep it in place a metal stick was inserted below the blood vessel. With help of a 0.7 mm needle a small incision was pierced into the vein followed by a gentle insertion of the tubing into the blood vessel until both anchor points of the catheter were inside the vein. The correct position of the catheter was checked by gently

flushing the-tubing with heparinized (50 I.U./ml) saline containing 1 mg/ml Baytril. Then three non-absorbable strings were placed under the vein (below the 1st anchor point (string 1), between the anchor points (string 2), above the 2nd anchor point (string 3)) and sewed each with a simple interrupted suture connecting both catheter and vein. Now the ends of string 2 and 3 were sewed crosswise with each other using a simple interrupted suture. Another string was used to connect the catheter between the anchor points and the fat tissue. After securing the catheter in place the fat tissue above it was sewed together. Then the skin incision was closed using re-absorbable suture. The catheter was then inserted through the incision at the scapulae to let the top projection of the Back-Mount Cannula exit at the small incision in the middle of the back. All remaining skin incisions were closed with simple interrupted sutures. Before closing the top projection of the Back Mount Cannula with a small tubing cap and a screwable metal cap the catheter was once more flushed with the heparinized Saline/Baytril solution. For pain relief all animals were treated with 5 mg/kg Carprofen (Rimadyl) during the surgery.

In the end animals were transferred back into their home cage and monitored until they became conscious again.

Post-surgery monitoring was done on a daily basis to check for infections and increased levels of distress or pain so animals could immediately be nursed back to health if necessary. In addition, catheters were flushed daily post-surgery with the heparinized Saline/Baytril solution to ensure catheter patency and reduce infection risk.

Surgeries were executed one week prior to start of the experiments to guarantee animal recovery.

2.4.1.3 Catheter maintenance

In order to maintain optimal function and prevent blockage of the catheter, each catheter was flushed daily with 0.1 ml of the heparinized Saline/Baytril solution. During self-administration training catheters were flushed twice; before the animals got connected to the infusion system and when they were disconnected at the end of the session. On weekends catheters were flushed once per day.

In case the proper function of a catheter was questionable (e.g., an animal was not responding during the self-administration session), its patency was tested by flushing it with 4 mg/kg ketamine. This resulted in an immediate yet very light anaesthetic response by the animal, if the catheter was functioning well. When the catheter was dysfunctional the rat underwent

another surgery where the catheter was replaced and a new catheter was implanted into the other jugular vein.

2.4.2 Stereotaxic surgery

2.4.2.1 Guide cannula implantation

Stereotaxic surgeries were performed in order to prepare the animals for the Daun02 inactivation experiments. During the experiment, an infusion cannula was inserted into the brain region of interest to infuse either the compound Daun02 or the vehicle. To precisely target the investigatory brain region a guide cannula (C313G/SPC, 4 mm, Plastics One) was implanted beforehand using coordinates from the rat brain atlas (George Paxinos and Charles Watson, 1998). At the start of the intervention the surgery table and all necessary instruments were prepared and sterilized.

To start the surgery, animals were deeply anaesthetised using an anaesthesia box with a constant (405 ml/min) vaporised isoflurane (4 %) flow. Afterwards animals were placed on a heating pad, which was set to 39 °C. They were then mounted to the stereotaxic apparatus by securing the mouth of the rats to the anterior mount of the apparatus, which was followed by ear bar placement into the bony ear canal. Correct ear bar position was indicated by ipsilateral eye blinking and when the head of the animal was completely fixed. Subjects were kept under anaesthesia throughout the whole procedure at a constant isoflurane concentration of 1.8 - 2.2 % and a flow rate of 405 ml/min. The eyes were protected from dryness with help of an ophthalmic gel. The incision area on top of the skull was shaven and sterilized using iodine and alcohol pads in a repetitive manner. After disinfecting the skin, an anterior/posterior incision was made starting in the middle of the skull (between the eyes) and extending until the cross point of sagittal and lambdoid suture, named lambda. For better accessibility, the incision was kept open by two bulldog serrefines. The skull was cleaned with cotton pads and treated with hydrogen peroxide to increase the visibility of bregma, the cross point of sagittal and coronal suture and lambda. In the following bregma and lambda were used to bring the skull to a horizontal level. This was done by comparing their coordinates (anterior/posterior: AP (x); medial/lateral: ML (y); dorsal/ventral: DV (z)) and equating the z-coordinate. Afterwards the guide cannula was placed directly over bregma, which is used as reference point in the rat brain atlas, and its coordinates were set to zero. Then the coordinates of the brain region of interest were used to move the guide cannula to the correct position on the skull and mark it. Since Daun02

inactivation was done bilaterally the location for the guide cannula was marked for both hemispheres. In order to fix the guide cannulas sufficiently, three holes for anchoring screws were drilled into the skull. A ring drill was then used to generate one hole each at the already marked positions for the guide cannulas. After cleaning the holes from debris, the anchoring screws were fastened. Then the position of the guide cannula was checked once more with the coordinates of the desired brain region. If coordinates were correct, it was carefully lowered into the brain until its desired depth was reached (depth of guide cannula = depth of investigatory brain region - length of infusion cannula projection). The brain regions of interest were the ventral OFC (AP: 3.45 mm, ML: +/- 2.0 mm, DV: - 5.1 mm) and the lateral OFC (AP: 3.45 mm, ML: +/- 2.8 mm, DV: - 5.1 mm). Since the projection of the infusion cannula was 1.1 mm the resulting depth for the guide cannula was - 4.0 mm.

After inserting the first guide cannula, it was fixed with liquid dental cement before the second guide cannula was implanted into the other hemisphere. To secure both guide cannulas three additional layers of dental cement were applied connecting cannulas and anchoring screws to the skull. The resulting cement cap was then smoothened to rule out skin irritation and promote wound healing. To prevent clogging of the guide cannulas they were closed with special dummy cannulas. Furthermore, the margins of the wound were closed with simple interrupted sutures, if necessary. After surgery, animals were removed from the stereotaxic apparatus und transferred into their home cages to be monitored until they came back to consciousness.

During the surgery, all animals were injected with 5 mg/kg Carprofen (Rimadyl) for pain relief.

Animals were checked daily post-surgery for signs of infections and increased pain levels so they could be treated immediately, if necessary.

After surgery, animals could recover for one week before Daun02 inactivation experiments were executed.

2.4.3 Daun02/vehicle infusions

One week prior to the Daun02 inactivation experiments, animals were bilaterally implanted with guide cannulas into the brain region of interest (paragraph) 2.4.2.1.

On the day of the Daun02 inactivation experiment all animals underwent the first cue-induced reinstatement test, which lasted 60 min. As ß-galactosidase activity peaked 90 min after

session onset, animals were transferred back into their home cages for the remaining 30 min until the Daun02 or vehicle infusion took place.

All equipment necessary for the infusion procedure was prepared beforehand. Therefore, internal cannulas (C313G/SPC, Plastics One) with a projection of 1.1 mm, to precisely hit the ventral OFC or the lateral OFC, were connected to fluorinated ethylene propylene tubing (CMA Microdialysis), via tubing adaptors. The tubing was then attached to a 25 µl syringe (Hamilton), which was fitted into the syringe pump (PHD 22/2000, Harvard apparatus). Two sets of syringes were prepared containing either Daun02 or vehicle. Depending on their performance during reward self-administration, extinction and the first cue-induced reinstatement, animals were assigned to one of two groups. The first group was bilaterally infused with Daun02 infusions whereas the other group was bilaterally infused with vehicle. Each infusion lasted 2 min and allowed the application of 2 µg/5 µl of Daun02 or the same volume of vehicle per hemisphere (Koya et al., 2009). Comprehensive distribution of the infused liquid into the brain tissue via diffusion was enabled by a 1 min break before the internal cannula was removed. After application of both infusions, animals were returned to their home cages.

Four days after infusion, the rats were examined in a second cue-induced reinstatement task before they were sacrificed to ensure correct infusion placement.

2.4.3.1 Daun02 preparation

Daun02 was prepared and made ready for infusion by dissolving it in 100 % dimethyl sulfoxide (DMSO) to a concentration of 80 µg/µl. Then 2.5 µl of the mixture were given to 15 µl of a 20 % Tween-80 stock. After adding up the reagents the mixture was shortly vortexed, halved into aliquots and frozen at - 80 °C.

On the day of the experiment a frozen aliquot was thawed and filled up with 16.5 µl of 1 x Phosphate-buffered saline (PBS) to a final working concentration of 4 µg/µl Daun02 in 5 % DMSO and 5 % Tween-80.

2.4.3.2 Vehicle preparation

The vehicle was prepared by mixing 0.5 ml 100 % DMSO and 0.5 ml 100 % Tween-80 with 10 ml PBS to a final concentration of 5 % DMSO and 5 % Tween-80.

2.5 Tissue collection and preparation

2.5.1 Brain harvesting

2.5.1.1 Decapitation

Study 1A

Animals were decapitated 60 min after start of the cue-induced reinstatement session, the point in time at which *c-fos* mRNA translation peaked (Morgan et al., 1987; Kovács, 1998). Immediately after decapitation the brains were carefully harvested and rapidly frozen in 2-Methylbutane (- 40 °C) for 2 min and stored at - 80 °C until further processing.

Study 3B

35 min after onset of the last cue-induced reinstatement session animals were decapitated. Then their brains were harvested in a carful manner and frozen in 2-Methylbutane (- 40 °C) for 2 min and stored at - 80 °C until further processing.

2.5.1.2 Transcardial perfusions

Study 1B & 2

In order to detect cells activated during cue-induced reward seeking behaviour, animals were perfused 90 min after onset of the cue-induced reinstatement session, when expression of the cFOS protein reached its maximum (Sheng and Greenberg, 1990). Therefore, animals received the inhalation anaesthetic isoflurane until they became deeply unconscious and were then transcardially perfused with 1 x PBS until they were bled out. Afterwards the tissue was pre-fixated by perfusion of the body with ice cold 4 % paraformaldehyde (PFA) in 1 x PBS until all muscle contractions stopped. Then brains were harvested and post-fixed at room temperature in 4 % PFA/1 x PBS. After 1.5 h brains were transferred into a 10 % sucrose/1 x PBS solution and stored at 4 °C until further processing.

Due to time constraints, processing of brains collected for Study 2 was delayed. Thus, brains were rapidly frozen with liquid carbon dioxide and stored at - 80 °C until further processing.

Study 1C

Animals were perfused 90 min after onset of the cue-induced reinstatement session as cFOS and therefore also GFP concentrations peaked. The aim of Study 1C was to electrophysiologically analyse neurons within the brain region of interest, thus the main priority was to keep the cells alive and in a healthy condition. Therefore, the animals were perfused transcardially with slightly frozen artificial cerebrospinal fluid (aCSF) solution containing 20 % sucrose until they were bled out. Afterwards the rats were decapitated and the brains harvested. The brains were placed into a beaker with slightly frozen aCSF with 20 % sucrose for transportation. For optimal conditions aCSF was saturated with carbogen. Then the beaker was placed inside a transportation box and surrounded with ice. The box was saturated with carbogen and sealed to make it ready for the 30 min transportation to our collaboration partners in Heidelberg, where the whole cell recordings were done.

Study 3A

Rats were perfused 90 min after onset of the last cue-induced reinstatement session. They received the inhalation anaesthetic isoflurane until they became deeply unconscious and were then transcardially perfused with 1 x PBS. This procedure was followed by perfusion with ice cold 4 % paraformaldehyde (PFA) in 1 x PBS until muscle contractions terminated. Afterwards brains were harvested and post-fixed overnight at 4 °C in 4 % PFA/1 x PBS. Before sectioning, brains were washed with 1 x PBS to remove remaining PFA.

2.5.2 Brain slice preparation

2.5.2.1 Cryosectioning

Study 1A

Brain slice preparation was done with help of a cryostat-microtome (Leica Biosystems). The frozen brains were fixed on the specimen stage using Tissue-Tek® O.C.T™ Compound and sectioned into 12 µm slices with a sharp blade at - 20 °C. Slices were collected on labelled Super Frost Plus slides (Thermo Fisher) and stored at - 80 °C until further analysis.

Study 2

Brains used for ß-gal immunostainings were sliced using a cryostat-microtome (Leica Biosystems). Therefore, they were fixed on the specimen stage and slices of the brain region of interest were obtained at a thickness of 55 µm. Slices were collected into 12 well plates containing 1 x PBS + 0.01 sodium azide and stored at 4 °C until further processing.

Study 3B

Brain sections were obtained using a cryostat-microtome (Leica Biosystems). 20 µm slices were cut at - 20 °C after the brains were fixed to the specimen stage with Tissue-Tek® O.C.T™ Compound. Slices were collected via thaw-mounting on Super Frost Plus slides (Thermo Fisher) and stored at - 80 °C until further processing.

2.5.2.2 Vibratome sectioning

Study 1B

Brain slices for immunohistochemical analysis were prepared with help of a vibrating blade microtome (Leica Biosystems). Therefore, the brains were mounted to the specimen-mounting disc with superglue (Loctite 410) and fixed to the vibratome, whose buffer chamber was filled with 1 x PBS. Afterwards 40 µm thick slices of the brain region of interest were obtained and collected into 12 well plates filled with 1 x PBS + 0.01 sodium azide. Slices were stored at 4 °C until further processing.

Study 1C

Brain sectioning was done with help of a vibrating blade microtome (Leica Biosystems), whose buffer chamber was filled with aCSF/20 % sucrose and kept at a temperature of 4 °C. The solution was saturated with carbogen during the whole process. Before slicing, the brain was cut into a tissue block of appropriate size without damaging the target regions and mounted to the specimen-mounting block, which in turn was fixed to the vibratome. In the following, 250 µm thick slices of the PFC were taken and collected into a carbogenated aCSF bath for further processing.

Study 3A

Brain sections for double immunohistochemical analysis of cFOS and NeuN were prepared with help of a vibrating blade microtome (Leica Biosystems). Brains were mounted to the specimen-mounting block and fixed to the vibratome. 70 µm thick slices of the brain region of interest were acquired and stored in cryoprotectant solution at - 20°C until further processing.

2.6 *In situ* Hybridization

2.6.1 Radioactive *in situ* hybridization (Study 1A)

In order to detect brain sides of the extended reward system, exhibiting the highest levels of activity during cue-induced reward seeking behaviour, brain slices of the tested animals were examined for their *c-fos* mRNA expression levels. Therefore, *c-fos* mRNA was targeted by its complementary nucleic acid probe, which was radioactively labelled with ^{35}S.

To prevent degradation of the target nucleic acid and therefore loss of signal all procedures were carried out very carefully to avoid Ribonuclease (RNase) contaminations.

2.6.1.1 Probe generation

The rat specific riboprobe for *c-fos* [gene reference sequence in Pub-Med database (http://www.ncbi.nlm.nih.gov/Entrez/); NM_022197.1, position 306–864 bp at cDNA) has been used.

In order to generate radioactively labelled ribonucleic acid (RNA) probes targeting the mRNA of interest in both antisense and sense direction, an adequate amount of template DNA had to be generated. Therefore, previously reverse transcribed *c-fos* cDNA was amplified via polymerase chain reaction (PCR) using primer containing T3 or SP6 sequences for the RNA polymerase promoter. For a 500 µl PCR reaction the reagents were thawed on ice and pipetted together (Table 01).

Amount	Reagent	Final concentration
360 µl	Nuclease free water	-
50 µl	10 x PCR buffer	1 x
10 µl	dNTP mix (10 µM)	0.2 µM
15 µl	$MgCl_2$ (50 mM)	1.5 mM
25 µl	Primer T3 FW (10 µM)	0.5 µM
25 µl	Primer T7 RV (10 µM)	0.5 µM
10 µl	DNA template	200 ng
5 µl	Taq-polymerase (5 units/µl)	0.05 units/µl

Table 01) PCR reaction pipetting scheme

Then the PCR reaction was run following the described scheme: Step 1 was run for three minutes at a temperature of 94 °C. This was followed by steps 2 (94 °C/1 min), step 3 (58 °C/1 min) and step 4 (72 °C/1 min). Step 5 was a repetition of steps 2 - 4 for 34 times. Step 7 was run at 72 °C for ten minutes. During the last step, the sample was cooled down to 4 °C and kept at this temperature until further processing or storage at - 20 °C.

In the meantime, a 1.5 % agarose gel was prepared by dissolving 1.5 g agarose-powder in 100 ml Tris/Borate/EDTA (TBE)-buffer and boiling it shortly. Then 5 µl ethidium-bromide were added and the solution poured into the gel-apparatus with a comb with big teeth.

After the PCR reaction finished, the gel solidified and the gel was covered with TBE buffer, the gel could be loaded with the samples and the DNA ladder. Then the gel was run for 40 min at 45 Volt. The *c-fos* PCR template could be detected at 558 base pair height. In the next step, DNA was extracted from the agarose gel with help of a QIAGEN MinElute® Gel Extraction Kit. DNA fragments of the appropriate size were cut out of the gel and the weight of these small gel blocks was determined. Then three volumes of buffer were added to the gel blocks and incubated for 10 min at 55 °C. After the gel dissolved, one volume of isopropanol was added and mixed by inverting the tube. In the following the sample was applied on a MinElute column and centrifuged at 13,000 rpm for 60 s. Then 500 µl of QG buffer were added and centrifuged at 13,000 rpm for 60 s. Afterwards 750 µl PE were applied and again centrifuged at 13,000 rpm for 60 s. After each centrifugation step the flow-through was discarded. For elution of the DNA sample 12 µl EB buffer were added to the column, incubated for 60 s at room temperature and centrifuged for 60 s at 13,000 rpm. In a last step DNA concentration was measured and the tube labelled with the relevant information.

2.6.1.2 Fixation

All slices were fixated onto glass slides to preserve the morphology of the brain tissue. In order to fixate the brain slices they had to undergo a series of steps where they were exposed to different buffer solutions and washed with sterile water and dehydrated with ethanol.

Before starting the fixation, all buffers were prepared carefully as displayed in the supplementary and filled into beakers. In addition, the working space was thoroughly cleaned with water, 70 % ethanol and RNase away.

The procedure started by getting the slides from the - 80 °C freezer and sorting them into slide holders in the cold room, which was also cleaned before with 70 % EtOH and RNase away. Afterwards the holders with the slides were brought to the experimental set up, where they were allowed to adjust to room temperature for 5 min. Then the holders were incubated in 4 % PFA for 15 min to cross-link the proteins in the brain samples and therefore to fix the tissue. In the following the slices were washed in 1 x PBS for 10 min and twice in sterile water, 5 min each. After the washing steps, the slices were exposed to 0.1 M HCl for 10 min.
This was followed by two steps of washing in 1 x PBS for 5 min each. Then the slides were placed into 500 ml 0.1 M Triethanolamine to which 1.25 ml acetic anhydride were added immediately. After carefully mixing the solution, slides were incubated for 20 min in order to acetylate positively charged amino groups, which reduces unspecific binding of the RNA probe to them. Afterwards all slides were washed again twice in 1 x PBS for 5 min each and remaining salts were removed by washing for 1 min in sterile water. Then the slides were dehydrated by exposing them for 2 min each to an increasing EtOH concentration array (70 %, 80 %, 95 %, 99 %). Finally, the slides were air dried and sorted into boxes together with silica gel. The boxes were sealed with tape and shrink-wrapped before they were stored at - 80 °C.

2.6.1.3 Siliconizing coverslips

For siliconizing the coverslips, one beaker with Sigmacote, one beaker with nuclease-free water and one beaker with ethanol absolute, were prepared. Before starting the working gloves were cleaned thoroughly with water, ethanol and RNase away. First the coverslips were taken out of their box and placed into Sigmacote separately. Then they were transferred into the nuclease-free water with sterile forceps. Afterwards they were placed into the pure ethanol. Then each of the coverslips was taken from the ethanol and put onto filter paper inside a glass

bowl. After filling up the glass bowl layer by layer (filter paper + coverslips) it was placed in the desiccator over night at 37 °C.

2.6.1.4 Probe labelling - *In vitro* transcription

In this step of the *in-situ* Hybridization the RNA probes were transcribed *in vitro* from the template DNA (paragraph 2.6.1) and labelled radioactively. In order to do so the working space was cleaned carefully to make it RNase free. Then all reagents were prepared (10x transcription buffer, dNTPs, template DNA, ^{35}S-UTP, RNase inhibitor and RNA polymerase) and placed into the radioactivity laboratory.

For antisense transcription, a total volume of 30 µl transcription mix were prepared whereas for sense strands only a total volume of 15 µl was prepared. For the 30 µl reaction mix the appropriate amount of water was pipetted into the reaction tube before 3 µl 10 x transcription buffer, 6 µl dNTPs and 200 ng plasmid DNA were added. Then 15 µl ^{35}S-UTPs were added very carefully to the mix. To prevent RNase activity 2µl RNase inhibitor were added before 2.5 µl RNA polymerase were pipetted to the mix. Then the whole mixture was incubated for 120 min at 37 °C and at the end 1 µl RNase inhibitor and 1.5 µl RNA polymerase were added. For the following steps samples were kept on ice. 2 µl RNase inhibitor were put into the mix before 2 µl DNaseI were added. After a short exposure to a vortex and a short centrifugation step, samples were incubated for 20 min at 37 °C. Again, samples were kept on ice. Next the labelled RNA probes needed to be purified. Therefore, purification columns (New England Biolabs GmbH) were prepared as described in their manual. Then samples were carefully pipetted onto the matrix of the purification column and centrifuged at 2800 rpm for 2 min. Afterwards the eluate was transferred into clean Eppendorf tubes and 5 µl RNase inhibitor were added. Finally, the freshly labelled RNA probes were stored at - 80 °C.

In order to test the ionizing radiation of the freshly labelled probes their counts per minute were checked using a scintillator. Therefore, three scintillation tubes were filled with 4 ml scintillation fluid each and 1 µl of the probe was added to each of them. After mixing them thoroughly counts per minute (cpm) were measured in the scintillator. The resulting mean of all three measurements had to be 500,000-1,000,000 cpm for a successful radioactive labelling of the RNA probe.

2.6.1.5 Prehybridization and Hybridization

Before starting prehybridization and hybridization a few preparatory steps had to be taken. First Plexiglas boxes, which were used for both the prehybridization and hybridization, were cleaned with 70 % ethanol as well as RNase away. Then all spaces in between glass slide holders were covered with filter paper. Afterwards 2 x prehybridization buffer was diluted with deionized Formamide 1:1 to working concentration (1 x prehybridization buffer).

After preparing everything all filter paper strips inside the Plexiglas boxes were saturated with 1 x prehybridization buffer. Then the fixed brain slices on their glass slides were sorted into the Plexiglas boxes and each glass slide was covered with 800 µl of 1 x prehybridization buffer. After all slides were covered entirely with 1 x prehybridization buffer the Plexiglas boxes were carefully transferred into an incubator where the slices incubated for 2 h at 37 °C.

In the meantime, the radioactive hybridization mix was prepared. The final probe activity of the hybridization mix had to be 1,000,000 cpm per 100 µl. Therefore, the volume of ^{35}S-RNA needed was calculated from measurements taken with the scintillator.

Based on a final volume of 6 ml of the hybridization mix, 3 ml deionized Formamide were mixed together with 600 µl of 10 x Grundmix, 750 µl 1.5 M Dithiothreitol, 400 µl 5 M NaCl, and 11.5 µl sterile water. Then, assuming an example activity of 1,558,243 cpm, 38.5 µl of ^{35}S-RNA were added to the mixture. Afterwards the mix was vortexed and centrifuged, then 1.2 ml 50 % dextran sulphate were carefully added. Finally, the hybridization mix was thoroughly vortexed and centrifuged for 10 min at 5000 rpm until all bubbles inside the mixture were eliminated.

After incubating the glass slides for two hours with prehybridization buffer the prehybridization mixture was removed from the glass slides and they were dried by pressing them on lint-free tissue. Again, the slides were sorted into the Plexiglas boxes. Then 100 µl hybridization mix were pipetted on each glass slide before they were carefully covered with siliconized cover slips. Afterwards, the Plexiglas boxes were sealed with tape and the slides incubated overnight at 55 °C.

2.6.1.6 Post-hybridization washing steps

To finalize the *in situ* hybridization unspecific bound probes had to be removed together with the surplus of single-stranded probes. Therefore, the slides had to undergo different washing steps before the radioactive signal could be detected by autoradiography.

First, all cuvettes needed for the different washing conditions were prepared and filled with 1 x Saline-sodium citrate buffer (SSC) buffer. Then the glass slides were taken from the Plexiglas boxes and sorted into slide holders fitting the cuvettes. Afterwards the holders were placed into preheated 1 x SSC buffer at 42 °C for 30 min to wash off all coverslips before they were transferred into fresh 1 x SSC buffer to incubate again for 30 min at 42 °C. To remove unspecific or weakly bound RNA strands the next washing step was carried out in 1 x SSC mixed with formamide at ratio 1:1 for 60 min at 42 °C. This was followed by washing the slides twice in fresh 1 x SSC for 30 min each at 42 °C. Meanwhile RNase buffer was prepared by mixing 250 ml 5 M NaCl, 25 ml 1 M Tris pH 8.0 and 5 ml ethylenediaminetetraacetic acid (EDTA) pH 7.5. Then 200 ml of the previously prepared buffer were poured into a fresh cuvette. The cuvette was placed into a water bath and heated to 37 °C. After placing the holders into the preheated buffer, 200 µl of 20 mg/ml RNAse were added and the incubation time of 60 min was started. Then the glass slides were washed twice in fresh 1 x SSC for 30 min each at 55 °C. Afterwards slides were washed in deionized water for 60 s and dehydrated in a series of increasing ethanol concentrations (70 %, 80 %, 99 %) for 2 min each. In the end the glass slides were air dried.

2.6.1.7 Autoradiography

In order to visualize the radioactive signal on the brain slices, autoradiograms of the samples were generated using storage phosphor screens and digitalized with help of a Phosphoimager. To do so glass slides were sorted into exposure boxes together with a ^{14}C-standard. A BAS-IP storage phosphor screens (GE Healthcare Life Sciences) was placed on top of the sections. Then the exposure box was closed and light protected. The BAS-IP storage phosphor screens were exposed to the ionizing radiation of the labelled samples for 1 week before they were scanned using a Typhoon FLA7000 IP Phosphoimager. After scanning images were named and saved as GEL files.

2.6.1.8 Autoradiography analysis

For analysis of the obtained autoradiograms the MCID analysis software was used. After retrieval of the image by the software, a calibration to the radiolabel standard (^{14}C) was initialized. By measuring the different values of the ^{14}C-standard and proper curve fitting a

standard curve was established. Then density measures of the background noise were obtained. Finally, each of the brain regions of interest (Fig. 21) was encircled for all brain slices and their antisense and sense density values measured. Anatomical landmarks as described in the rat brain atlas (Paxinos and Watson, 1998), were used to define the brain regions of interest. Based on the known radioactivity in the 14C standards, the obtained values were converted to nCi⁄g. All values were exported into an excel file, sorted, sense values of each region were subtracted from antisense values and an average calculated from the mean values of each rat respective to reward and brain region. Afterwards the mean value of the control animal's brain region was subtracted from the average of the reward group's respective brain region resulting in a Δ *c-fos* mRNA [nCi/g] value for each brain region and reward.

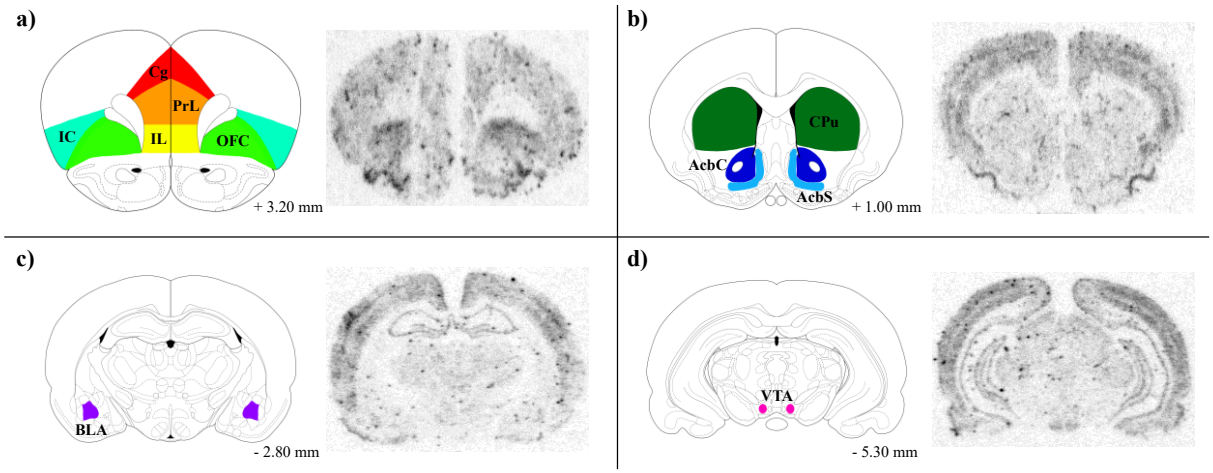

Figure 21) Schematic representation of brain regions of interest and representative autoradiograms of *c-fos* mRNA *in situ* hybridizations

a) Schematic representation of brain regions of the prefrontal cortex (left panel) (cingular cortex (Cg - red), prelimbic cortex (PrL - orange), infralimbic cortex (IL - yellow), orbitofrontal cortex (OFC - bright green) and insular cortex (IC - turquoise)) that were measured utilizing autoradiograms of coronal slices at around + 3.20 mm from bregma (right panel) b) Schematic representation of a coronal slice at bregma + 1.00 mm with labelled brain regions of interest (left panel) (nucleus accumbens core (AcbC - dark blue), nucleus accumbens shell (AcbS - bright blue) and caudate putamen (CPu - green)) and a representative *c-fos in situ* hybridization autoradiogram (right panel) c) The basolateral amygdala (BLA - purple) is shown in a representative schematic coronal slice at - 2.80 mm from bregma together with a respective *c-fos in situ* hybridization autoradiogram (right panel) d) The left panel shows a scheme of the ventral tegmental area (VTA - pink) at bregma - 5.30 mm, whereas the right panel shows its respective autoradiogram. Schematics of the coronal section used were adapted from (Paxinos and Watson, 1998).

2.6.2 Fluorescent *in situ* hybridization (Study 3B)

Study 3B aimed to characterize the distinctness of neuronal ensembles in the IL encoding for EtOH and saccharin seeking within the same animal. In order to do so different *c-fos* mRNA species, each with its own temporal profile, were labelled with help of fluorescent *in situ* hybridization. Upon stimulus presentation (e.g., cue light), *c-fos* mRNA expression is induced within the activated neuronal ensemble. The first form is nascent or unspliced *c-fos* mRNA, which forms within 5 minutes after induction. However, unspliced *c-fos* mRNA is rapidly spliced resulting in mature *c-fos* mRNA, which reaches maximum levels approximately 30 min after induction (Jurado et al., 2007; Lin et al., 2011). This specific temporal expression profile of different *c-fos* mRNA species was used to design the time schedule for RE 3 and RE 4 (Fig. 20). Neuronal ensembles active during the first cue-induced reinstatement (RE 3) could be detected by labelling of mature *c-fos* mRNA and the neuronal ensemble active during the second cue-induced reinstatement (RE 4) could be identified by nascent *c-fos* mRNA.

2.6.2.1 RNAscope *in situ* hybridization

Double *c-fos* mRNA fluorescent *in situ* hybridization was performed using the RNAscope *in situ* hybridization technology. The kit used was the RNAscope Multiplex Fluorescent Reagent Kit (Advanced Cell Diagnostics, Newark, USA). Experiments were performed in accordance with the manufacturer's instructions for freshly frozen brain tissue. Brain slices were prepared as described in paragraph 2.5.2.1. At the day of the RNAscope *in situ* hybridization, brain slices were taken from - 80 °C and incubated at 4 °C for 15 min in sterile 4 % PFA/1 x PBS. Afterwards slices were washed thrice in fresh 1xPBS. This washing step was followed by an increasing EtOH ladder (50% (5min), 70% (5 min), 2 x 100% (5 min each)) to dehydrate the slices. After drying the sections at room temperature for approximately 5 min a hydrophobic barrier pen (ImmEdgeTM Hydrophobic Barrier Pen, Vector Laboratories) was utilised to encircle each slice. The hydrophobic barrier, that was built in this way, was used to create a small room around each slice for all the upcoming washing and reaction steps. Next the protease IV solution (PN 322340, ACD) was pipetted on each section to incubate for 15 min at room temperature. Protease IV treatment was followed by two washing steps with 1xPBS. Afterwards brain slices were hybridized with the 1 x target probe solution (Rn-Fos-O1-C2: mature *c-fos* mRNA; Rn-Fos-Intron1-C3: nascent *c-fos* mRNA) and help of the HybEZ Hybridization Oven for 2 hours at 40 °C. Hybridization was followed by two more washing

steps in 1 x RNAscope® Wash Buffer at room temperature for 2 min each. Next brain sections were treated with AMP1 for 30 min at 40°C using the HybEZ Hybridization Oven followed by washing the slices twice for 2 min at room temperature with washing buffer. Afterwards sections were hybridized with AMP 2 for 15 minutes at 40 °C. Two more washing steps (1 x washing buffer, 2 min at room temperature) later, slices were incubated with AMP 3 for 30 min at 40°C. The last hybridization step (15 min, 40 °C) with fluorescently labelled probes (C2 with Alexa 488; C3 with Atto 647) was preceded by two washing steps. Another two washing steps later the brain sections were finally counterstained with DAPI for 30 s at room temperature. Brain slices were coverslipped using Thermo Scientific™ Shandon™ Immu-Mount and stored at 4 °C until further analysis.

2.6.2.2 Image acquisition

For quantitative analysis brain slices were investigated with a confocal microscope. Per animal two sections containing the IL were examined and of each slice three z-stacks of the IL were acquired at random positions. Images were taken at a resolution of 512 x 512 pixels and saved for further analysis.

2.6.2.3 Image analysis

Fluorescent signals of both fluorescent channels were analysed in a semi-automated manner with help of the cell counter macro in Fiji, a distribution of ImageJ. The 4′,6-diamidino-2-phenylindole (DAPI) counterstaining helped with the verification of the specificity of fluorescent signals. Co-localizations of markers for nascent and mature *c-fos* mRNA were analysed manually. Therefore, the number of DAPI-positive cells expressing mature *c-fos* mRNA was calculated and the amount of nascent *c-fos* mRNA was determined by the mean grey value per cell. In order to differentiate between basal activity and activity induced expression of nascent *c-fos* mRNA all grey values were graded. The proportion of cells displaying highest expression levels of nascent *c-fos* mRNA, similar to the one shown by the mature *c-fos* mRNA expressing proportion, were considered for analysis.

2.7 Immunohistochemical examination

2.7.1 Double immunofluorescence stainings (Study 1B)

To identify the neurochemical nature of co-active neurons a fluorescent immunohistochemical co-labelling approach was chosen. cFOS was co-labelled with an antibody against one of the following antigens: GFP, NeuN, Glial fibrillary acidic protein (GFAP), Glutamic acid decarboxylase 67 (GAD67) or Ca^{2+}/calmodulin-dependent protein kinase II (CaMKII).

Brain samples were sliced using a vibrating blade vibratome (paragraph 2.5.2.2). Before starting the co-labelling procedure, all necessary buffers were prepared (supplementary).

In the beginning brain slices were transferred into 6 well plates filled with 1 x PBS and washed for 10 min. Then slices were fixed for 15 min with 4 % PFA in 1 x PBS. The fixation was followed by another washing step in 1 x PBS for 10 min. Afterwards the sections were washed three times for 10 min each in 1 x Tris-buffered saline (TBS), which was exchanged each time. Then brain slices were incubated in blocking solution (7.5 % Donkey serum + 2.5 % bovine serum albumine (BSA) in TBS with 0.2 % Triton X-100) at room temperature for 1 h. After blocking, sections were incubated in blocking solution mixed with the different primary antibody combinations overnight at 4 °C (Table 02).

The second day started by washing the brain slices three times in 1 x TBS for 10 min each. Afterwards the sections were incubated with the secondary antibodies in TBS 0.2 % Triton X-100 for 1 h at room temperature (Table 02). With introduction of the secondary antibodies all remaining steps were executed with minimal light exposure. After the 1 h incubation all brain slices were washed once more for three times in 1 x TBS for 10 min each. Then the sections were shortly washed with ultrapure water. Afterwards sections were mounted onto glass slides and coverslipped using Thermo Scientific™ Shandon™ Immu-Mount. Then the slides were sorted into light-tight boxes and stored at 4 °C until further analysis.

Combination	Primary antibody	Species	Dilution	Secondary antibody	Species	Dilution
A	cFOS	rabbit	1:250	Alexa Fluor 594, anti-rabbit	donkey	1:200
	GFP	mouse	1:250	Alexa Fluor 488, anti-mouse	donkey	1:200
B	cFOS	rabbit	1:250	Alexa Fluor 488, anti-rabbit	donkey	1:200
	NeuN	mouse	1:700	Alexa Fluor 594, anti-mouse	donkey	1:200
C	cFOS	rabbit	1:250	Alexa Fluor 488, anti-rabbit	donkey	1:200
	GFAP	mouse	1:200	Alexa Fluor 594, anti-mouse	donkey	1:200
D	cFOS	rabbit	1:250	Alexa Fluor 488, anti-rabbit	donkey	1:200
	GAD67	mouse	1:400	Alexa Fluor 594, anti-mouse	donkey	1:200
E	cFOS	rabbit	1:250	Alexa Fluor 488, anti-rabbit	donkey	1:200
	CaMKII	mouse	1:250	Alexa Fluor 594, anti-mouse	donkey	1:200

Table 02) Primary and secondary antibody combinations for immunohistochemical co-localizations

Table 02 displays the different primary and secondary antibody combinations used for the different co-localizations as well as the specific dilutions utilised. As shown, cFOS was labelled in combination with different antibodies against GFP, NeuN, GAD67, GFAP and CAMKII.

2.7.1.1 Image acquisition

For quantitative analysis of the different co-localization's slides were investigated with help of a Leica TCS SP5 confocal microscope and a HC PL APO 20 x /0.70 IMM CORR CS objective. Z-stacks were obtained with sections every 0.49 µm at a zoom factor of 3.15, corresponding to a magnification of 63 x. For quantification, six z-stacks were taken per hemisphere for cFOS/NeuN co-labelled brain slices, three at random position within the ventral OFC and three within the lateral OFC. Four z-stacks per hemisphere were acquired for all the other co-localizations, with two images taken within the ventral OFC and two within the lateral OFC. Images were acquired at an image resolution of 512 x 512 pixels and saved as TIFF files for further analysis.

2.7.1.2 Image analysis

Image analysis was carried out with Fiji, a distribution of ImageJ. Before analysis images were sorted and stacks organized. Then each stack was loaded into the software and the beforehand programmed macros were run in order to create a single image from the stack and enhance image quality for analysis. Afterwards the number of cFOS-ir, NeuN-ir, GFAP-ir, GAD67-ir, CaMKII-ir and GFP-ir positive cells was manually counted as well as their position marked for all different rewards and control animals using the cell counter plugin of Fiji. Then the number of cells for each co-localization was determined by merging the respective images and counting the overlapping cells. For each staining the average number of cells was determined from all animals and slices for both lateral and ventral OFC. Afterwards the percentage of cFOS-ir positive cells within the population of either NeuN-ir, GFAP-ir, GAD67-ir or CaMKII-ir positive cells was calculated. For the cFOS/GFP co-localization the percentage of GFP positive cells within the cFOS-ir positive cell population was calculated. However, for the examination of the neurochemical composition of the cFOS-ir positive neuronal population for the different rewards, the percentage calculated for the control animals was subtracted from the respective percentage for the different rewards resulting in Δ RE-control. For each reward the total percentage of cFOS-ir positive cells was determined either by summation of the percentage of subpopulations (CaMKII-ir and GAD67-ir) or by determination of the percentage amount of cFOS-ir positive cells within the neuronal population after subtraction of control percentage. From the resulting percentage of cFOS positive neurons, the amount of cFOS negative neurons could be determined. Last, the proportion of CamKII-ir and GAD67-ir positive cells within the cFOS-ir positive neuronal population was calculated.

2.7.2 Double immunofluorescence stainings (Study 3A)

For comparison of neuronal ensemble size induced by EtOH or saccharin seeking within the IL, brain slices were prepared as described in paragraph 2.5.2.2. Afterwards slices were stained using the protocol described under paragraph 2.7.1 starting with the second 1 x PBS washing step. The primary antibody used against cFOS (Cell Signaling Technology, catalogue #2250, RRID: AB_2247211, rabbit, monoclonal) was used add a dilution of 1:500, whereas the primary antibody against NeuN (Millipore, catalogue #MAB377, RRID:AB_2298772, mouse, monoclonal) was used with a dilution of 1:250. Secondary antibodies used were the appropriate Alexa 568 (cFOS) and Alexa 405 (NeuN) antibodies from Thermo Fisher. They were used at a dilution of 1:1000. At the end slices were mounted onto microscope slides and coverslipped with Mowiol.

2.7.2.1 Image acquisition

For quantitative analysis of cFOS-ir/NeuN-ir co-localization's, slices were examined with help of a Leica TCS SP5 confocal microscope. The objective used was a Leica HCX PL APO 63x (1.45 NA). Per hemisphere a total of four z-stacks was recorded at random positions in the IL. For each animal three different brain sections of the IL were investigated. Images were saved for further analysis with a resolution of 512 x 512 pixels.

2.7.2.2 Image analysis

Co-localization analysis of cFOS-ir and NeuN-ir was conducted semiautomatically using a Matlab algorithm written by Dr. Frank Herrmannsdörfer (Anatomy and Cell Biology, Heidelberg University). Each of the recorded channels was quantitatively analysed for the signal of cFOS-ir and NeuN-ir. Therefore, a 2D Gaussian filter (sigma = 3 pixels, 1 pixel = 0.459 µm) was applied, followed by binarization of channel intensities, which defined 98 % of the cFOS-ir signal and 95 % of the NeuN-ir signal as background pixels. To compensate for declining signal intensities in deeper tissue layers, thresholds were calculated per frame. Furthermore, each channel was analysed by connected components analysis (connectivity = 26) and all connected components smaller than 500 voxels were excluded from analysis. In order to examine co-localizations, each connected component's centre of mass was defined and each

connected component's centre of mass the lay within the range of 10 µm was identified as co-localized. The semi-automated analysis was counter-checked by manual inspection.

2.7.3 ß-galactosidase immunohistochemical stainings (Study 2)

In order to being able to validate the functional relevance of neuronal ensembles identified during reward seeking the infusion success during the Daun02 inactivation experiment had to be investigated. Therefore, ß-galactosidase was immunohistochemically labelled and the infusion placement validated.

Frozen brain samples were sliced using a cryostat-microtome (Leica Biosystems) (paragraph 2.5.2.1) and transferred into 12-well plates. They were then washed for 10 min in 1 x PBS. Afterwards slices were fixed for 15 min in 4 % PFA in 1 x PBS. Then all slices were washed once more in 1 x PBS for 10 min. This step was followed by three washing steps in 1 x TBS for 10 min each. Afterwards brain slices were incubated in blocking solution (7.5 % Donkey serum + 2.5 % BSA in TBS with 0.2 % Triton X-100) at room temperature for one hour. Then slices were exposed to the primary antibody (beta Galactosidase Antibody (A-11132), Thermo Fisher, rabbit, 1:100) diluted in blocking solution and incubated at 4 °C over night. The next day slices were washed again for three 10 min rounds in 1 x TBS. Afterwards slices were incubated at room temperature for one hour with the secondary antibody (Alexa Fluor 488, donkey, 1:200). With introduction of the secondary antibodies all remaining steps were executed with minimal light exposure. Then brain slices were washed three times in 1 x TBS for 10 min each. After shortly washing the slices in Millipore water, they were mounted onto glass slides and coverslipped using Thermo Scientific™ Shandon™ Immu-Mount. Then the slides were sorted into light-tight boxes and stored at 4 °C until further analysis.

2.7.3.1 Infusion validation

Brain slices were investigated with an epifluorescence microscope (ZEISS Axioscope 5). The correct position of the infusion into ventral or lateral OFC as well as successful inactivation of neuronal ensembles was examined for each brain slice (Fig. 22). Infusion sides were mapped and animals with misplaced or unsuccessful infusion were excluded from the experiment.

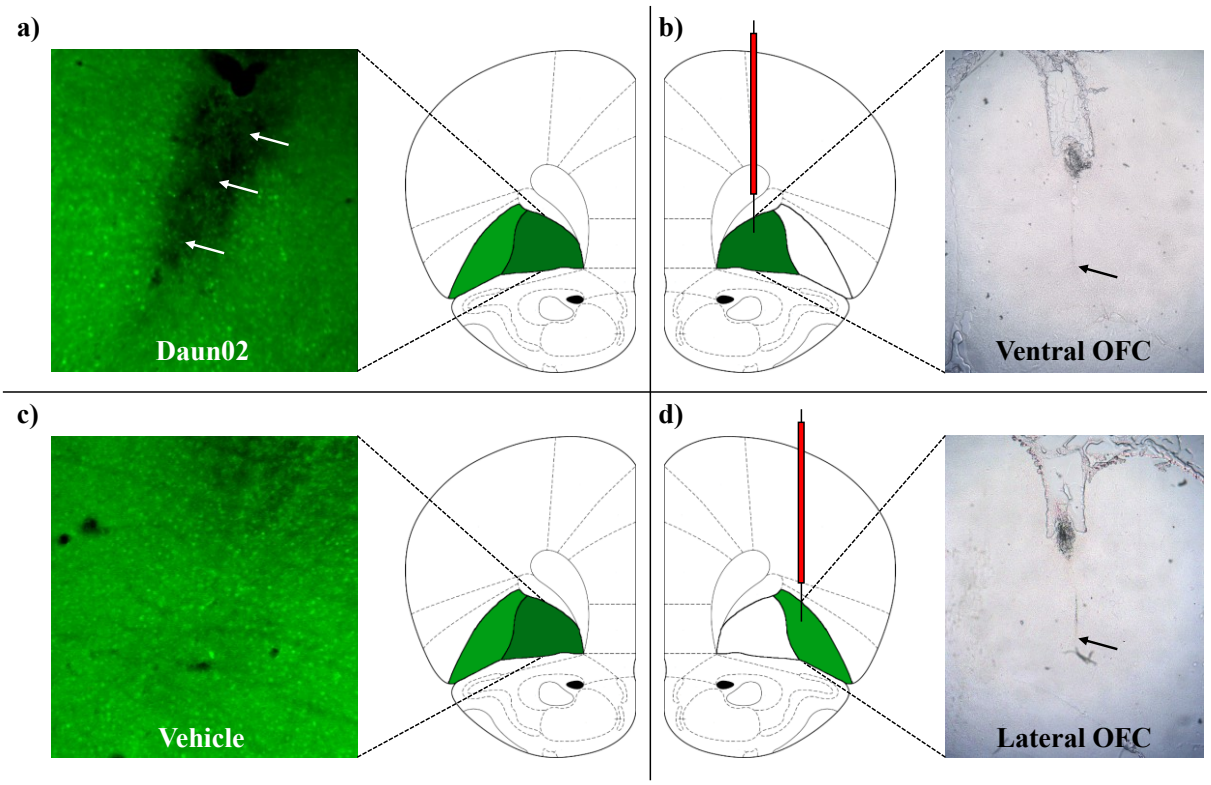

Figure 22) Schematic representation of brain regions of interest as well as representative ß-galactosidase stainings and bright field images of infusion positions

a) + c) Representative ß-galactosidase immunostainings of lacZ positive cells in the OFC of *c-fos*-lacZ transgenic rats after the second cue-induced reinstatement. White arrows indicate successful Daun02 infusion. Coronal section schemes show the targeted brain region (OFC) in green. b) + d) Representative images of infusion positions within the ventral OFC (b) and the lateral OFC (d). Black arrows show the exact infusion locations. Schematic drawings depict guide cannula and infusion needle for ventral OFC (dark green (b)) and lateral OFC (green (d)). Schematics of brain slices adapted from (Paxinos and Watson, 1998).

2.8 Electrophysiological examination

2.8.1 Whole-cell patch clamp recordings

In order to investigate the physiological characteristics of co-active neurons whole-cell recordings were performed *in vitro*. Tissue preparation was executed as described in paragraphs 2.5.1.2 and 2.5.2.2. After vibratome sectioning, brain slices were incubated at 37 °C in carbogenated aCSF for 30 min. In the meantime, the whole-cell patch clamp set up was prepared for recordings. The entire equipment was switched on, carbogenated aCSF was prepared to constantly wash through the recording chamber at an approximate flow rate of 1.5 ml per minute, internal solution was filled into a 1 ml syringe equipped with a 0.2 µm pore filter attached to a micro loader tip and recording pipettes were prepared from borosilicate glass capillaries with help of a glass capillary puller.

After incubation one brain slice at a time was placed inside the recording chamber for electrophysiological manipulations whereas the other slices stayed in constantly carbogenating aCSF at room temperature. To hold the brain slice in place a small metal harp was placed on top of it. Then the laser equipped microscope was used to detect GFP fluorescent cells, indicating previously activated neurons, within the OFC. Once a cell was detected, a recording pipette was filled halfway with the filtered internal solution, the solution was made air bubble free and the pipette placed inside the set ups pipette holder. The pipette was moved inside the aCSF bath with the stage control unit and light positive pressure was applied through the mouthpiece of the pressure control system. To keep the pressure constant, the three-way valve was closed. Next the pipette was moved carefully towards the target cell by moving the micromanipulator and focusing directly on or below the pipette tip. As soon as the tissue was coming in sight the micromanipulators motion was changed to slow and smooth. Next the pipette offset was corrected in voltage-clamp mode, so all currents measured inside the aCSF bath were considered as 0 picoampere. In the following the pipette was moved closer so the target cell until its tip touched the cell membrane and formed a small dimple. Then the positive pressure was released to form a G Ω seal of 1 - 2 G Ω. After having obtained a stable G Ω seal the voltage clamp was changed to - 70 mV, to mimic the expected resting potential of the neuron and corrected for fast capacitance. Next the seal had to be broken to gain electrical and molecular access to the neurons intracellular space. This was done by applying short and careful suction pulses through the mouthpiece. After successfully breaking through the membrane, recordings could be acquired both in “voltage-clamp” mode, to examine the transmembrane current, and in “current-clamp” mode, to investigate changes in the membrane potential. This was done with help of the appropriate software and respective programs. Once a GFP positive cell was recorded a neighbouring GFP negative cell was targeted for later comparison of physiological properties. Recorded data was stored as .abf files.

2.8.2 Data analysis

Recorded data was analysed with MATLAB R2018a. The first script used was written to pre-process raw data and calculate intrinsic properties of each neuron. This produced a MATLAB object with the aforementioned information. In addition, two scripts (one for GFP negative cells and one for GFP positive cells) were written to calculate current voltage relationship, resting membrane potential, input resistance, rheobase and latency from the pre-processed data. Data analysis was performed by Janet Barroso.

2.9 Statistical analysis

Statistical analysis was carried out with STATISTICA 10.0 (StatSoft, Inc.). All data are expressed as mean ± SEM. The threshold for statistical significance was set to 0.05.

Study 1A: Behavioural data were analysed using two-way ANOVA. Newman-Keuls *post hoc* tests were carried out where appropriate. *c-fos* mRNA levels were analysed utilising the two-tailed unpaired t-test.

Study 1B: Two-way ANOVA was used to analyse behavioural data for the different rewards as well as immunohistochemical data. Following two-way ANOVA analysis, Newman-Keuls *post hoc* tests were run, where applicable.

Study 1C: Behavioural data were examined by two-way ANOVA analysis. Newman-Keuls *post hoc* tests were run where appropriate. The statistical analysis for the comparison of physiological properties was done using two-tailed unpaired t-tests.

Study 2: Two-way ANOVA with repeated measures was used to analyse behavioural data, which was followed by *post hoc* analysis (Newman-Keuls), where applicable.

Study 3: Behavioural data were analysed by two-way ANOVA with repeated measures, followed by *post hoc* analysis (Newman-Keuls), where applicable or by two-tailed paired t-test. Immunohistochemical analysis and fluorescent *in situ* hybridization analysis was statistically evaluated using two-way ANOVA and two-tailed unpaired t-tests. Bootstrap analysis and the significance of co-localization of the two *c-fos* mRNA species was analysed with custom written IGOR macros (100.000 repetitions, RRID:SCR_000325, Wavemetrics, Lake Oswego, OR) by Janine K Reinert (Institute of Anatomy and Cell Biology, Heidelberg University).

Testimony:

All experiments of Study 3 and their analysis were performed by Simone Pfarr. Both was published before (Pfarr, 2018; Pfarr et al., 2018). Methodological descriptions were taken from either publication and re-written in own words, thus similarities cannot be excluded.

3. RESULTS

In Study 1A the extend reward system was analysed for peak *c-fos* mRNA activity following cue-induced reinstatement of reward seeking behaviour to identify regions with the highest neuronal activity following behavioural onset. The tested animals were trained in an operant conditioning paradigm to self-administer either one of three drugs of abuse (ethanol, cocaine, nicotine) or the natural reward saccharin. The identification of co-active neurons was done by a reward system wide analysis of *c-fos* responses during cue-induced reinstatement using an *in situ* hybridization approach. After identification of the brain region with the highest activity during cue-induced reinstatement of reward seeking, further experiments, except Study 3, focused on that region.

Study 1B aimed to characterize the neurochemical nature of the previously identified co-active neurons mediating reward seeking responses for ethanol, cocaine and saccharin. Thus, a double immunohistochemistry approach labelling cFOS in combination with different cell-type markers (NeuN- ir (neurons), CaMKII-ir (glutamatergic cells), GAD67-ir (GABAergic cells) and GFAP-ir (glial cells)) was utilized. In addition, a co-expression analysis of cFOS-ir and GFP-ir was performed using the respective antibodies.

Study 1C characterized cue-induced reinstatement activated neuronal ensembles on a physiological level. This was done by whole-cell patch clamp recordings of GFP positive (active) versus nearby GFP negative (inactive) neurons measuring the cells' electrophysiological properties.

Study 2 examined the functional relevance of neuronal ensembles using the Daun02 inactivation method, which is based on the conversion of Daun02 into daunorubicin by ß-galactosidase. Daunorubicin leads to neurodegeneration and therefore to irreversible inactivation of neurons (Pfarr et al., 2015). The rat strain used, carries a lacZ gene under control of *c-fos* promotor and therefore expresses ß-galactosidase in active neurons. Thus, Daun02 was infused into the brain region of interest after cue-induced reinstatement of reward seeking to selectively inactivate neuronal ensembles. A second cue-induced reinstatement was then performed to examine potential changes to reward seeking behaviour.

In Study 3, we asked the question whether activated neuronal ensembles are distinct or overlapping. In this experimental approach a two-reward conditioning model was used to investigate ensembles encoding EtOH and saccharin seeking within the same animal. First the size of both ensembles within the IL was determined by double antibody stainings against NeuN and cFOS. Afterwards a new batch of animals was used to investigate the distinctness of the

involved neuronal ensembles with the help of a double *c-fos* fluorescent *in situ* hybridization approach. Co-localization analysis of different *c-fos* mRNA species (spliced and unspliced) in combination with DAPI counterstaining was then used to differentiate between neuronal ensembles encoding for EtOH and saccharin seeking. Experiments of Study 3 (paragraph 3.5) were performed, analysed and published by Simone Pfarr in The Journal of Neuroscience, April 4, 2018 and her PhD thesis (Pfarr, 2018; Pfarr et al., 2018).

3.1 Study 1A: Identification of neuronal ensembles within the extended reward system encoding for natural reward and drug reward seeking

3.1.1 Operant conditioning to identify neuronal ensembles encoding cue-reward associations

In order to identify ensembles during cue-induced reward seeking behaviour *c-fos*-GFP transgenic rats were trained to self-administer either one of three drugs of abuse (ethanol, cocaine, nicotine) or the natural reward saccharin. During the training, the rats were conditioned to press an active lever, which led to reward delivery and simultaneous presentation of a specific cue (blink light). Animals therefore learned to associate the cue light with reward availability. Training sessions were performed until the animals reached a stable reward seeking response. Cocaine and nicotine trained animals showed similar responding on average over the last four training session (cocaine: 53 ± 9; nicotine: 56 ± 5). Animals trained to ethanol reached a slightly higher average response of 79 ± 9 lever presses. The average response for saccharin trained rats during their last four training sessions was the highest with 119 ± 15 lever presses (Fig. 23). The conditioning phase was followed by extinction training, where all animals showed fading of the non-reinforced response behaviour over time reaching < 20 % of their baseline responses on average (ethanol: 14 ± 2; saccharin: 13 ± 1; cocaine: 12 ± 1; nicotine: 9 ± 1) (Fig. 23).

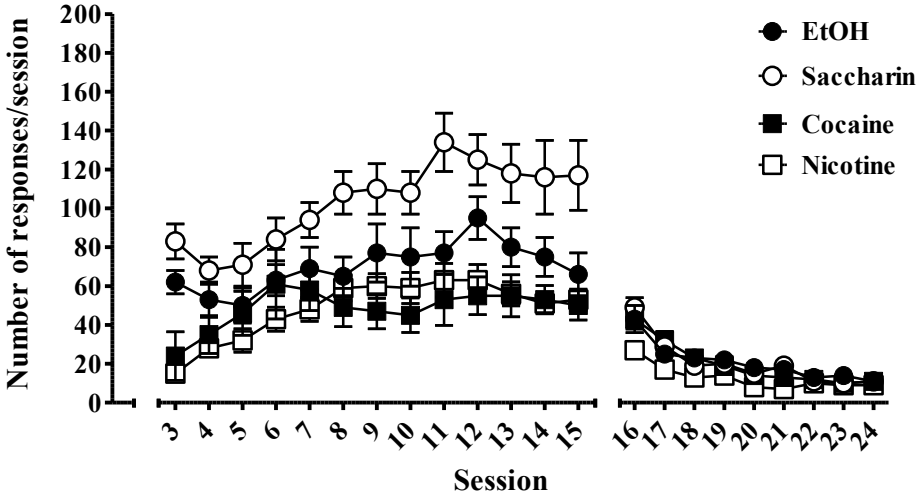

Figure 23) Self-administration and extinction training; data for water deprivation (day 1 & 2) not shown

The graph shows the animal's performance during self-administration (days 3-15) and extinction (days 16-24). Rats were trained to lever press for either 10 % EtOH, 0.04 % saccharin, 0.125 mg/kg cocaine or 0.01 mg/kg nicotine. EtOH: n = 14; Saccharin: n = 20; Cocaine: n = 14; Nicotine: n = 14; Values presented as mean ± Standard error of mean (SEM).

To identify potential differences in cellular ensemble activation in the reward system between extinction training and cue-induced reward seeking behaviour animals were grouped in two cohorts for each reward (extinction & reinstatement) according to their performance at the active lever during operant conditioning and extinction training. Then one day after the last extinction session animals were subjected to either one additional 1 h extinction session or a 1 h cue-induced reinstatement session. For all three drugs of abuse as well as the natural reward saccharin animals showed a significant increase in their reward seeking response compared to the average of their last four extinction sessions (two-way ANOVA; EtOH: main effect of sessions, $F(1,20) = 16.181$, $p < 0.001$; of active vs. inactive lever press, $F(1,20) = 55.023$, $p < 0.001$; and interaction, $F(1,20) = 13.893$, $p = 0.0013$; Newman-Keuls *post hoc* test $\bar{x}$ EXT active vs RE active $p < 0.001$; saccharin: main effect of sessions, $F(1,28) = 33.444$, $p < 0.001$; of active vs. inactive lever press, $F(1,28) = 116.60$, $p < 0.001$; and interaction, $F(1,28) = 32.594$, $p < 0.001$; Newman-Keuls *post hoc* test $\bar{x}$ EXT active vs RE active $p < 0.001$; cocaine: main effect of sessions, $F(1,28) = 32.288$, $p < 0.001$; of active vs. inactive lever press, $F(1,28) = 29.305$, $p < 0.001$; and interaction, $F(1,28) = 29.570$, $p < 0.001$; Newman-Keuls *post hoc* test $\bar{x}$ EXT active vs RE active $p < 0.001$; nicotine: main effect of sessions, $F(1,24) = 19.042$, $p < 0.001$; of active vs. inactive lever press, $F(1,24) = 38.902$, $p < 0.001$; and interaction, $F(1,24) = 14.811$, $p < 0.001$; Newman-Keuls *post hoc* test $\bar{x}$ EXT active vs RE active $p < 0.001$) (Fig. 24). Inactive lever presses showed no statistically significant differences between sessions as

revealed by Newman-Keuls *post hoc* test (EtOH: p = 0.837; saccharin: p = 0.959; cocaine: p = 0.864; nicotine: p = 0.719).

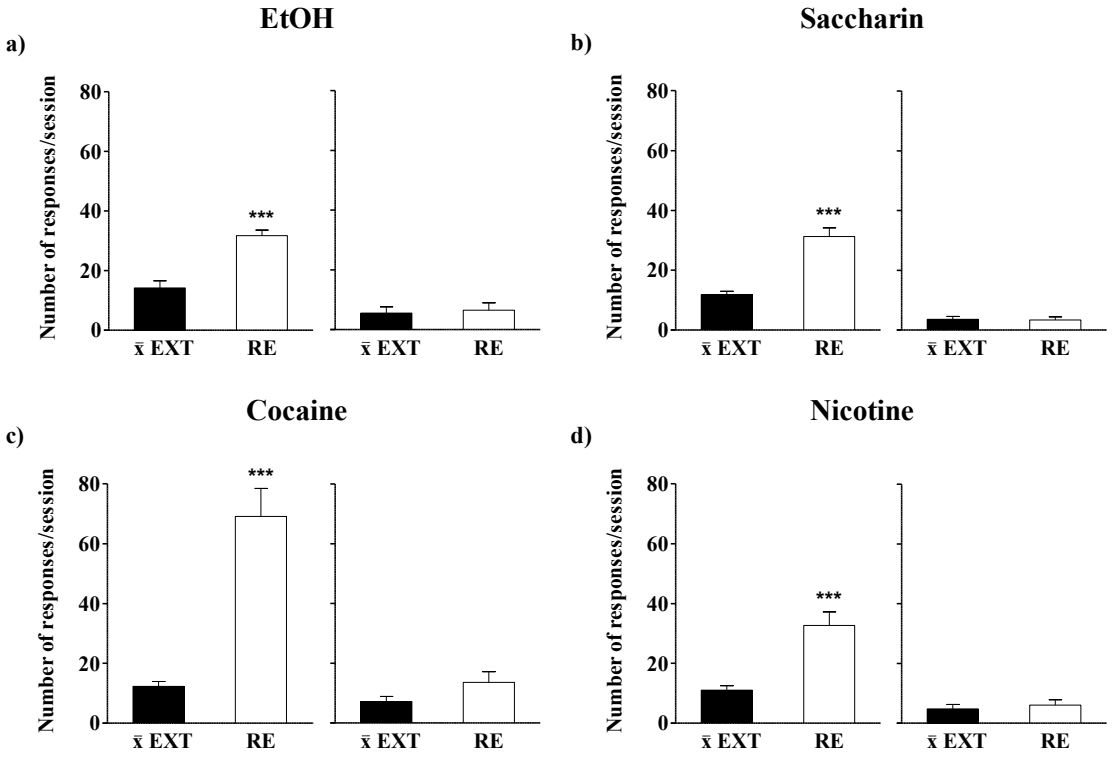

Figure 24) Active and inactive responses during cue-induced reinstatement compared to the average responses during the last four extinction sessions

a) Data displayed for ethanol trained animals with active responses shown in the left panel and inactive responses shown in the right panel; b) Responses (left panel active and right panel inactive) shown for saccharin trained animals; c) Active lever presses in the left panel and inactive lever presses in the right panel shown for cocaine trained rats; d) Active (left panel) and inactive (right panel) responses displayed for nicotine trained animals. Ethanol: n = 6; Saccharin: n = 8; Cocaine: n = 8; Nicotine: n = 7; All values are expressed as mean ± SEM. *** p < 0.001; Abbreviations: x̄ EXT = average of last extinction sessions, RE = cue-induced reinstatement.

Within the extinction group no significant difference was detected for either reward between the number of active responses for the test extinction session and the average of the last four extinction sessions (two-way ANOVA; EtOH: main effect of sessions, F (1,28) = 1.505, p = 0.230; of active vs. inactive lever press, F (1,28) = 10.451, p = 0.003; and interaction, F (1,28) = 1.024, p = 0.320; Newman-Keuls *post hoc* test x̄ EXT active vs EXT active p = 0.125; saccharin: main effect of sessions, F (1,44) = 0.253, p = 0.617; of active vs. inactive lever press, F (1,44) = 15.736, p < 0.001; and interaction, F (1,44) = 3.722, p = 0.060; Newman-Keuls *post hoc* test x̄ EXT active vs EXT active p = 0.093; cocaine: main effect of sessions, F (1,20) = 0.027, p = 0.871; of active vs. inactive lever press, F (1,20) = 0.619, p = 0.441; and interaction, F (1,20) = 0.747, p = 398; Newman-Keuls *post hoc* test x̄ EXT active vs EXT active p = 0.750; nicotine: main effect of sessions, F (1,24) = 1.311, p = 0.263; of active vs. inactive lever press,

F (1,24) = 13.534, p = 0.001; and interaction, F (1,24) = 0.314, p = 0.580; Newman-Keuls *post hoc* test x̄ EXT active vs EXT active p = 0.240; Fig. 25). Inactive lever presses showed no statistically significant differences between sessions as revealed by Newman-Keuls *post hoc* test (EtOH: p = 0.880; saccharin: p = 0.319; cocaine: p = 0.875; nicotine: p = 0.683).

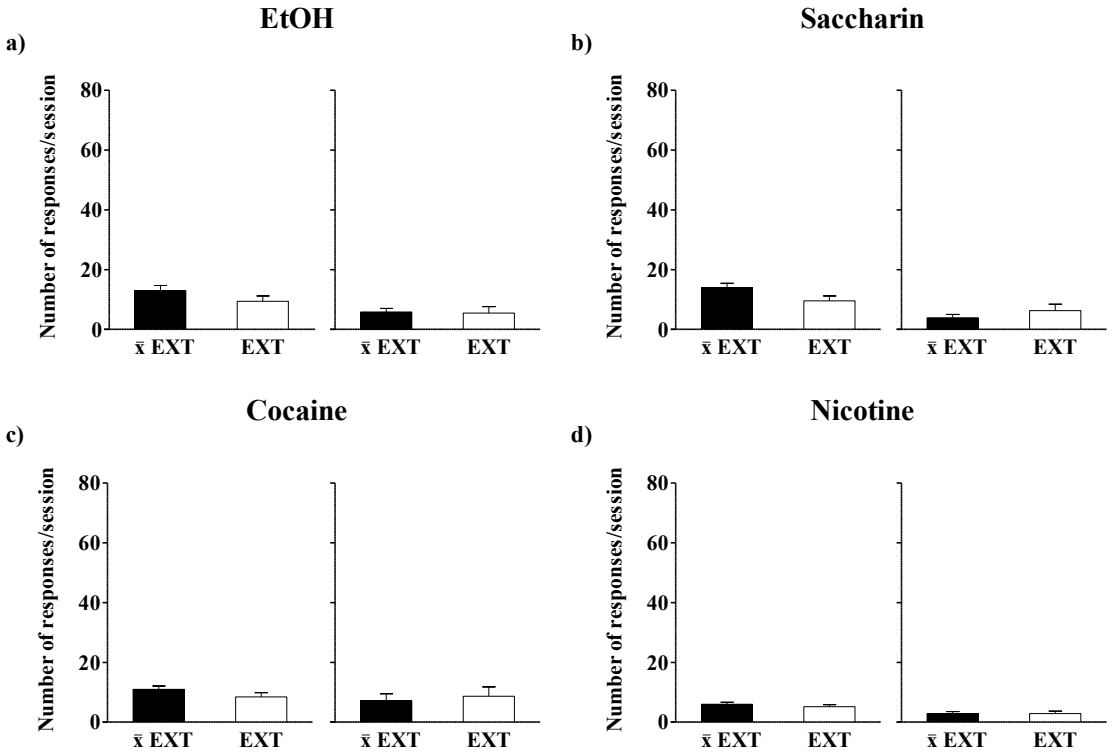

Figure 25) Active and inactive responses during extinction test session compared to the average responses during the last four extinction sessions

a) Data displayed for ethanol trained animals with active responses shown in the left panel and inactive responses shown in the right panel; b) Responses (left panel active and right panel inactive) shown for saccharin trained animals; c) Active lever presses in the left panel and inactive lever presses in the right panel shown for cocaine trained rats; d) Active (left panel) and inactive (right panel) responses displayed for nicotine trained animals. Ethanol: n = 8; Saccharin: n = 12; Cocaine: n = 6; Nicotine: n = 7; All values are expressed as mean ± SEM. Abbreviations: x̄ EXT = average of last extinction sessions, EXT = extinction test.

3.1.2 Mapping of *c-fos* mRNA expression patterns following natural reward and drug reward seeking

At the end of the additional extinction session or the cue-induced reinstatement session animals were decapitated, brains harvested and rapidly frozen using - 40 °C cold 2-Methylbutane. In the following brain slices were prepared, which then underwent ^{35}S-*in situ* hybridisation in order to label *c-fos* mRNA for mapping of brain regions with highest activity during the respective behavioural task. The resulting autoradiographs revealed broadly

overlapping activation patterns within the extended reward system, especially for the PFC, for the different rewards comparing control animals vs. animals that performed cue-induced reinstatement (Fig. 26 + Table 03). All parts of the PFC investigated showed a significant increase in activity compared to control animals for all four rewards, with the most prominent change in the OFC. Another brain region that changed its activity significantly for all four conditions was the CPu. Apart from the broad overlap between *c-fos* mRNA expression levels, distinct changes for the different rewards could be detected as well. Ethanol trained animals displayed additional significant changes within the insular cortex and the basolateral amygdala whereas saccharin showed a significant change for the VTA. Both psychostimulants had significantly increased *c-fos* mRNA expression within the AcbC. Nicotine in addition showed increased activity levels in the insular cortex (IC).

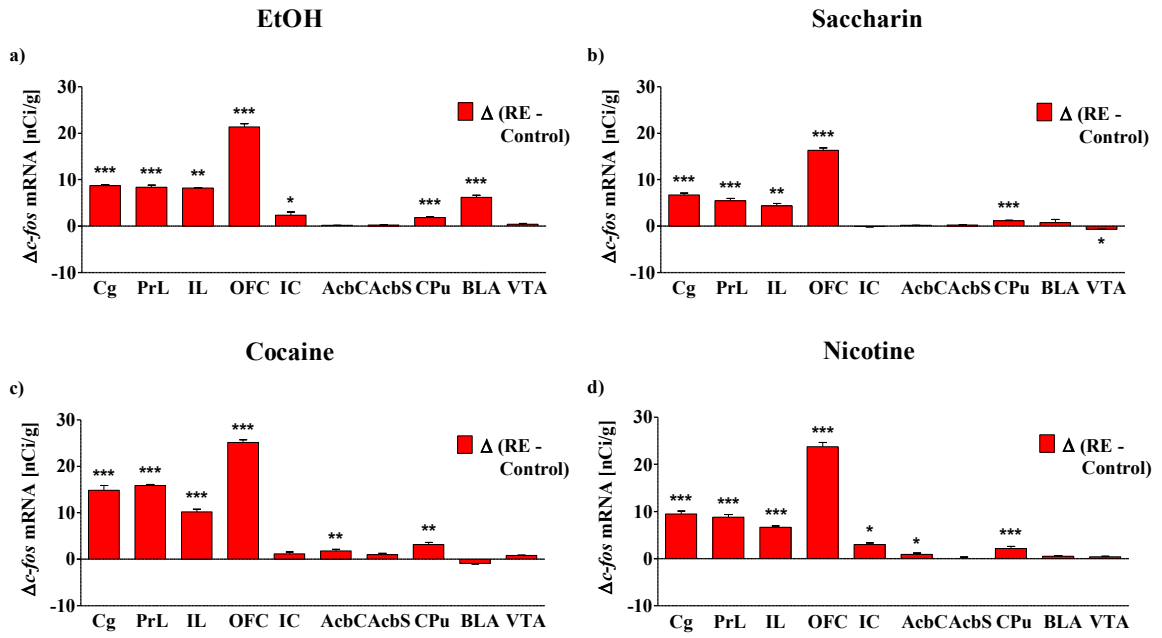

Figure 26) *c-fos* mRNA expression levels within the extended reward system after cue-induced reinstatement

a) Expression levels of *c-fos* mRNA displayed as Δ of ethanol trained animals vs. control animals; b) *c-fos* mRNA expression levels after cue-induced reinstatement of saccharin trained rats; c) Transcription levels of *c-fos* mRNA from cocaine trained animals vs. control animals; d) Δ *c-fos* mRNA expression levels after cue-induced reinstatement of nicotine trained animals. All values are expressed as mean ± SEM. * $p < 0.05$; ** $p < 0.01$; *** $p < 0.001$, Detailed statistical analysis can be found in Table 03. Abbreviations: Cg = cingular cortex, PrL = prelimbic cortex, IL = infralimbic cortex, OFC = orbitofrontal cortex, IC = insular cortex, AcbC = nucleus accumbens core, AcbS = nucleus accumbens shell, CPu = caudate putamen, BLA = basolateral amygdala, VTA = ventral tegmental area, RE = cue - induced reinstatement.

	EtOH			Saccharin			Cocaine			Nicotine		
	t	df	p	t	df	p	t	df	p	t	df	p
Cg	15.667	7	0.000001	8.771	7	0.000050	8.260	10	0.000009	7.986	10	0.000012
PrL	15.227	11	0.000000	7.942	13	0.000002	8.994	11	0.000002	6.003	11	0.000089
IL	5.694	5	0.002330	4.929	6	0.002634	7.320	9	0.000045	5.963	10	0.000139
OFC	13.751	9	0.000000	10.063	11	0.000001	10.313	8	0.000007	11.184	9	0.000001
IC	2.418	9	0.038707	-0.112	12	0.912848	0.922	16	0.370437	2.439	17	0.025977
AcbC	1.264	11	0.232338	1.217	13	0.245385	3.952	14	0.001447	2.150	15	0.048315
AcbS	0.942	11	0.366444	1.588	13	0.136289	1.803	18	0.088153	0.004	18	0.996546
CPu	6.925	10	0.000041	4.530	11	0.000858	5.670	15	0.000045	3.779	16	0.001643
BLA	11.317	11	0.000000	0.915	12	0.377966	-1.060	16	0.304921	0.592	16	0.562203
VTA	1.123	10	0.287823	-2.772	10	0.019705	1.691	17	0.109177	0.799	18	0.434668

Table 03) Statistics for comparison of *c-fos* mRNA expression levels within the extended reward system for control animals vs. animals undergoing reinstatement

Results are displayed for two-tailed unpaired t-tests, groups. Abbreviations: t = t-value, df = degrees of freedom, p = p-value, Cg = cingular cortex, PrL = prelimbic cortex, IL = infralimbic cortex, OFC = orbitofrontal cortex, IC = insular cortex, AcbC = nucleus accumbens core, AcbS = nucleus accumbens shell, CPu = caudate putamen, BLA = basolateral amygdala, VTA = ventral tegmental area.

Comparing *c-fos* mRNA expressions levels of control animals vs. animals that underwent an additional extinction session revealed a similar pattern throughout the extended reward system as animals subjected to a cue-induced reinstatement session (Fig. 27). All four rewards showed significant increases of *c-fos* mRNA in the PFC with the strongest elevation in the OFC. The CPu also showed significantly elevated *c-fos* mRNA expression levels for all four rewards. Distinct activity increases were detected for ethanol and saccharin trained animals within the basolateral amygdala and for nicotine conditioned rats within the insular cortex (Table 04).

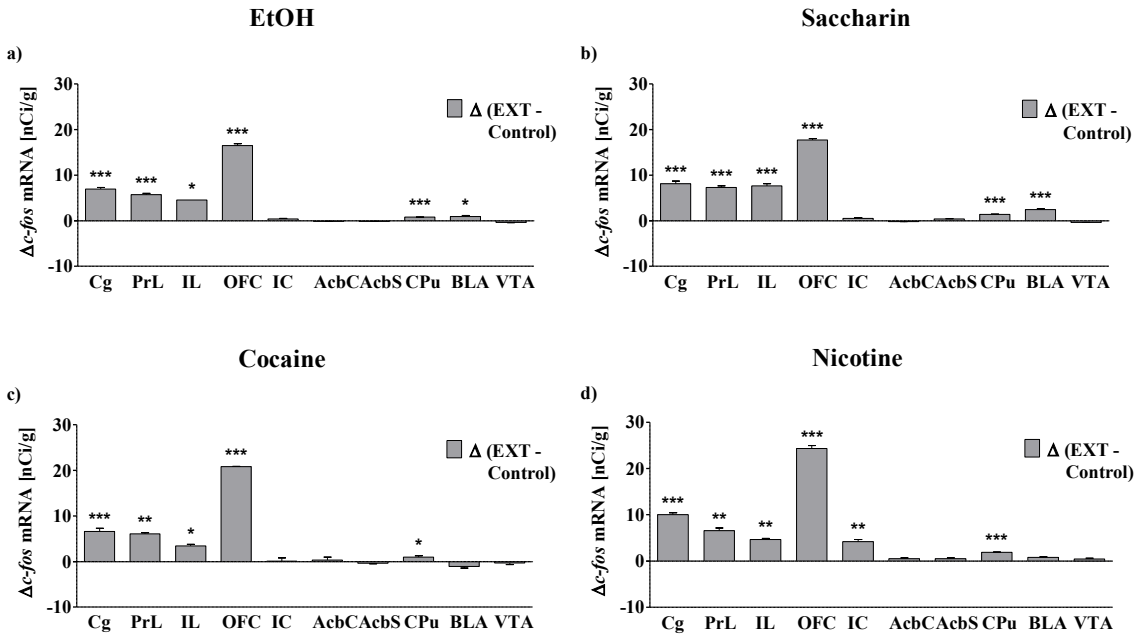

Figure 27) *c-fos* mRNA expression levels within the extended reward system after an additional extinction session

a) Expression levels of *c-fos* mRNA displayed for EtOH trained animals after the extinction test b) *c-fos* mRNA transcription levels for saccharin trained rats after additional extinction c) Transcription levels of *c-fos* mRNA from cocaine trained animals after additional extinction d) *c-fos* mRNA expression levels after extinction test of nicotine trained rats. Values are expressed as mean ± SEM. * $p < 0.05$; ** $p < 0.01$; *** $p < 0.001$. See Table 04 for a full statistical analysis. Abbreviations: Cg = cingular cortex, PrL = prelimbic cortex, IL = infralimbic cortex, OFC = orbitofrontal cortex, IC = insular cortex, AcbC = nucleus accumbens core, AcbS = nucleus accumbens shell, CPu = caudate putamen, BLA = basolateral amygdala, VTA = ventral tegmental area, EXT = extinction test.

	EtOH			Saccharin			Cocaine			Nicotine		
	t	df	p	t	df	p	t	df	p	t	df	p
Cg	9.265	8	0.000015	6.123	11	0.000075	6.358	7	0.000382	10.817	9	0.000002
PrL	14.723	11	0.000000	11.175	16	0.000000	3.519	9	0.006528	4.437	10	0.001260
IL	3.422	4	0.026743	8.006	9	0.000022	3.316	8	0.010610	4.759	9	0.001031
OFC	11.084	11	0.000000	12.216	14	0.000000	6.558	7	0.000316	10.401	8	0.000006
IC	0.962	12	0.354803	1.446	15	0.168820	0.066	14	0.947925	3.287	16	0.004649
AcbC	-1.217	13	0.245217	-0.940	16	0.361333	0.633	11	0.539357	1.578	14	0.136951
AcbS	-0.833	13	0.419872	1.415	15	0.177481	-0.848	16	0.409205	1.184	17	0.252867
CPu	5.398	11	0.000217	7.570	14	0.000003	2.256	13	0.041934	6.764	15	0.000006
BLA	2.405	13	0.031804	6.296	15	0.000014	-0.986	14	0.340915	0.874	14	0.396942
VTA	-1.784	12	0.099627	-1.291	13	0.219075	-0.484	15	0.635606	0.719	17	0.481814

Table 04) Statistics for comparison of *c-fos* mRNA expression levels within the extended reward system for control animals vs. animals subjected to an additional extinction session

Results are displayed for two-tailed unpaired t-tests, groups. Abbreviations: t = t-value, df = degrees of freedom, p = p-value, Cg = cingular cortex, PrL = prelimbic cortex, IL = infralimbic cortex, OFC = orbitofrontal cortex, IC = insular cortex, AcbC = nucleus accumbens core, AcbS = nucleus accumbens shell, CPu = caudate putamen, BLA = basolateral amygdala, VTA = ventral tegmental area.

Since the main goal of the thesis was to examine neuronal ensembles that are active during cue-induced reinstatement of reward seeking and the OFC displayed the highest activity during this behaviour, the brain region was chosen as target for further investigation.

3.2 Study 1B: Neurochemical characterization of neuronal ensembles within the OFC active during reinstatement of reward seeking

3.2.1 Operant conditioning to characterize the neurochemical nature of neuronal ensembles encoding natural reward and drug reward seeking

After identifying the region of the extended reward system with the highest activity during cue-induced reward seeking behaviour, the region was further investigated on a neurochemical level. Therefore, the next experiment aimed to characterize the shared and distinct neurochemical composition of the co-active cell ensembles activated during cue-induced reinstatement for the different rewards within the OFC. In order to do so animals were trained to self-administer either EtOH, cocaine or saccharin under the same operant conditioning paradigm used before. After the rats learned to associate the cue light with reward availability, animals were subjected to extinction learning. Responses on the active lever were similar on average over the last four sessions for ethanol with 49 ± 10 presses and cocaine with 42 ± 11 lever presses. Saccharin trained animals however showed much higher and more variable response rates on the active lever with 120 ± 33 lever presses. The huge difference in reward seeking between saccharin, ethanol and cocaine did not manifest during extinction where all animals displayed fading of the non-reinforced response behaviour below 20 % of their baseline response (ethanol: 9 ± 1; saccharin: 11 ± 3; cocaine: 8 ± 1) (Fig. 28).

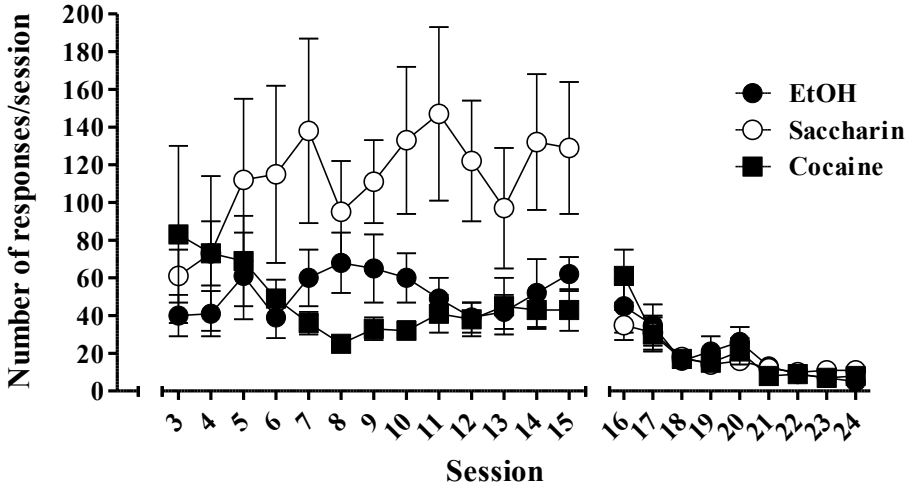

Figure 28) Self-administration and extinction training; data for water deprivation (day 1 & 2) not shown

The graph shows active lever press responses of 10 % ethanol, 0.04 % saccharin and 0.125 mg/kg cocaine trained animals for self-administration training (days 3-15) and extinction training (days 16-24). Ethanol: n = 5; Saccharin: n = 5; Cocaine: n = 5; All values are expressed as mean ± SEM.

Following extinction training the animal's cue-induced reinstatement of reward seeking behaviour was examined. As depicted in Figure 29 all animals showed a significant increase of their reward seeking compared to the average of the last four extinction sessions for all three rewards (two-way ANOVA; EtOH: main effect of session, $F(1,16) = 33.102$, $p < 0.001$; of active vs. inactive lever press, $F(1,16) = 101.98$, $p < 0.001$; and interaction, $F(1,16) = 26.938$, $p < 0.001$; Newman-Keuls *post hoc* test $\bar{x}$ EXT active vs RE active $p = 0.000159$; Saccharin: main effect of sessions, $F(1,16) = 5.7955$, $p = 0.0285$; of active vs. inactive lever press, $F(1,16) = 27.441$, $p < 0.001$; and interaction, $F(1,16) = 12.413$, $p = 0.0028$; Newman-Keuls *post hoc* test $\bar{x}$ EXT active vs RE active $p = 0.000817$; Cocaine: main effect of sessions, $F(1,16) = 17.016$, $p < 0.001$; of active vs. inactive lever press, $F(1,16) = 12.230$, $p < 0.00298$; and interaction, $F(1,16) = 9.5789$, $p = 0.00695$; Newman-Keuls *post hoc* test $\bar{x}$ EXT active vs RE active $p = 0.000431$). Inactive lever presses showed no statistically significant differences between sessions as revealed by Newman-Keuls *post hoc* test (EtOH: $p = 0.696$; saccharin: $p = 0.442$; cocaine: $p = 0.751$).

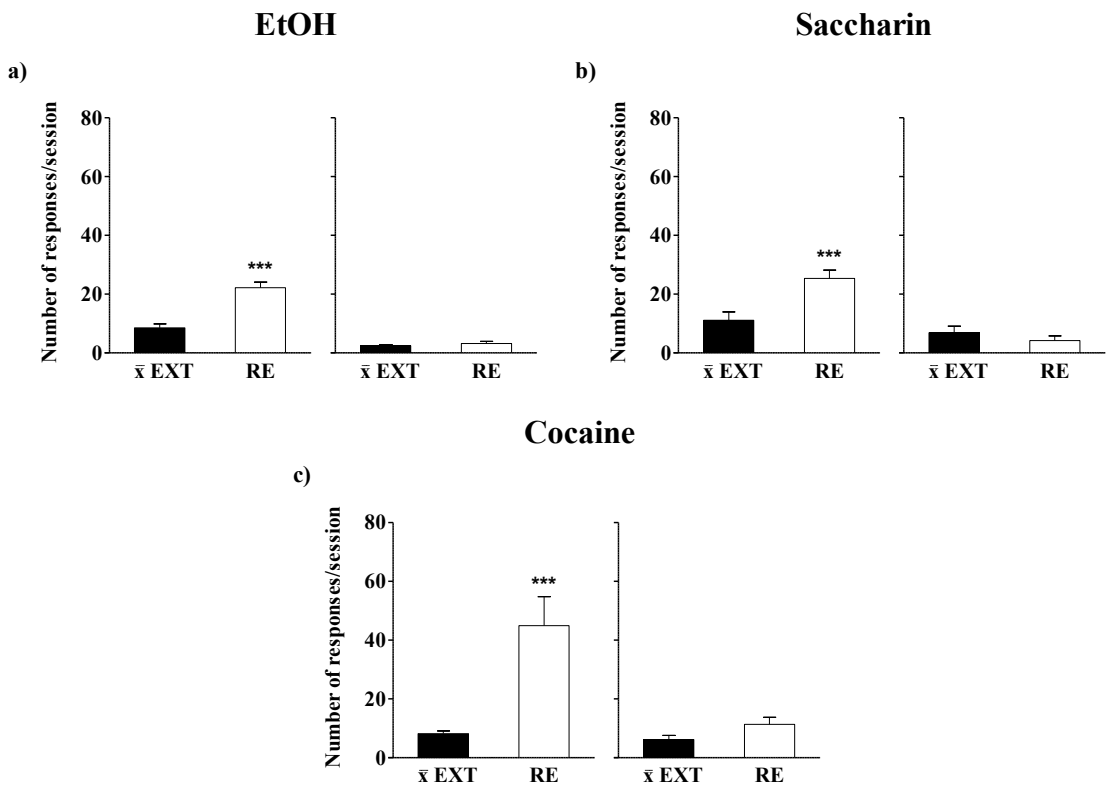

Figure 29) Active and inactive responses during cue-induced reinstatement compared to the average responses during the last four extinction sessions

a) Data displayed for ethanol trained animals with active responses shown in the left panel and inactive responses shown in the right panel; b) Active (left panel) and inactive (right panel) responses displayed for saccharin trained animals; c) Active lever presses in the left panel and inactive lever presses in the right panel shown for cocaine trained rats; Ethanol: n = 5; Saccharin: n = 5; Cocaine: n = 5; All values are expressed as mean ± SEM. *** $p < 0.001$, Abbreviations: $\bar{x}$ EXT = average of last extinction sessions, RE = cue-induced reinstatement.

3.2.2 Immunohistochemical analysis of neuronal ensembles following cue-induced reinstatement of reward seeking behaviour

Animals were perfused 90 min after onset of the cue-induced reinstatement session. Their brains were then processed to undergo the different double immunohistochemistry stainings. In order to characterize the co-active cell ensembles on a neurochemical level cFOS was co-labelled with different cell-type-specific markers. NeuN-ir was used to study the co-localization of cFOS expressing cells and neurons. To examine possible participation of glia in our co-active cell ensembles cFOS-ir was tested together with GFAP-ir. To further characterize the co-active cell ensembles, cFOS-ir was investigated together with GAD67-ir or CaMKII-ir to identify co-localization with GABAergic and glutamatergic cells, respectively. Analysis of double-immunolabeling was done by image acquisition at a confocal laser scanning microscope and investigation of the individual cell markers as well as their co-localization using ImageJ (Fig.

30a-33a). Total cell numbers counted as well as detailed statistical analysis can be found in the supplementary (Table 14-20).

cFOS-ir and NeuN-ir was investigated for ethanol, saccharin and cocaine trained animals after cue-induced reinstatement and compared to control animals. The distribution of NeuN-ir within the OFC was very homogeneous throughout the entire region whereas cFOS-ir was not as dense and a little bit more clustered but equally distributed within the region. However, image acquisition was done focusing on segments with high cFOS expression. Cells were counted for cFOS-ir, NeuN-ir as well as their overlap and expressed as percentage of cFOS-ir positive cells within the NeuN-ir positive cell population (Fig. 30b). Analysis revealed that with only 30 % cFOS expression in the NeuN-ir positive cell population control animals showed significantly the lowest activity. During reinstatement, however, cFOS expression increased strongly for all rewards, with a similar raise for ethanol and cocaine trained animals (23 % and 19 % respectively) and a significant increase for saccharin trained rats (about 35.5 %) (Table 20). There were only slight and non-significant differences (1 % - 3 %) in cFOS activation between the lateral and ventral OFC as can be seen in Fig. 30b.

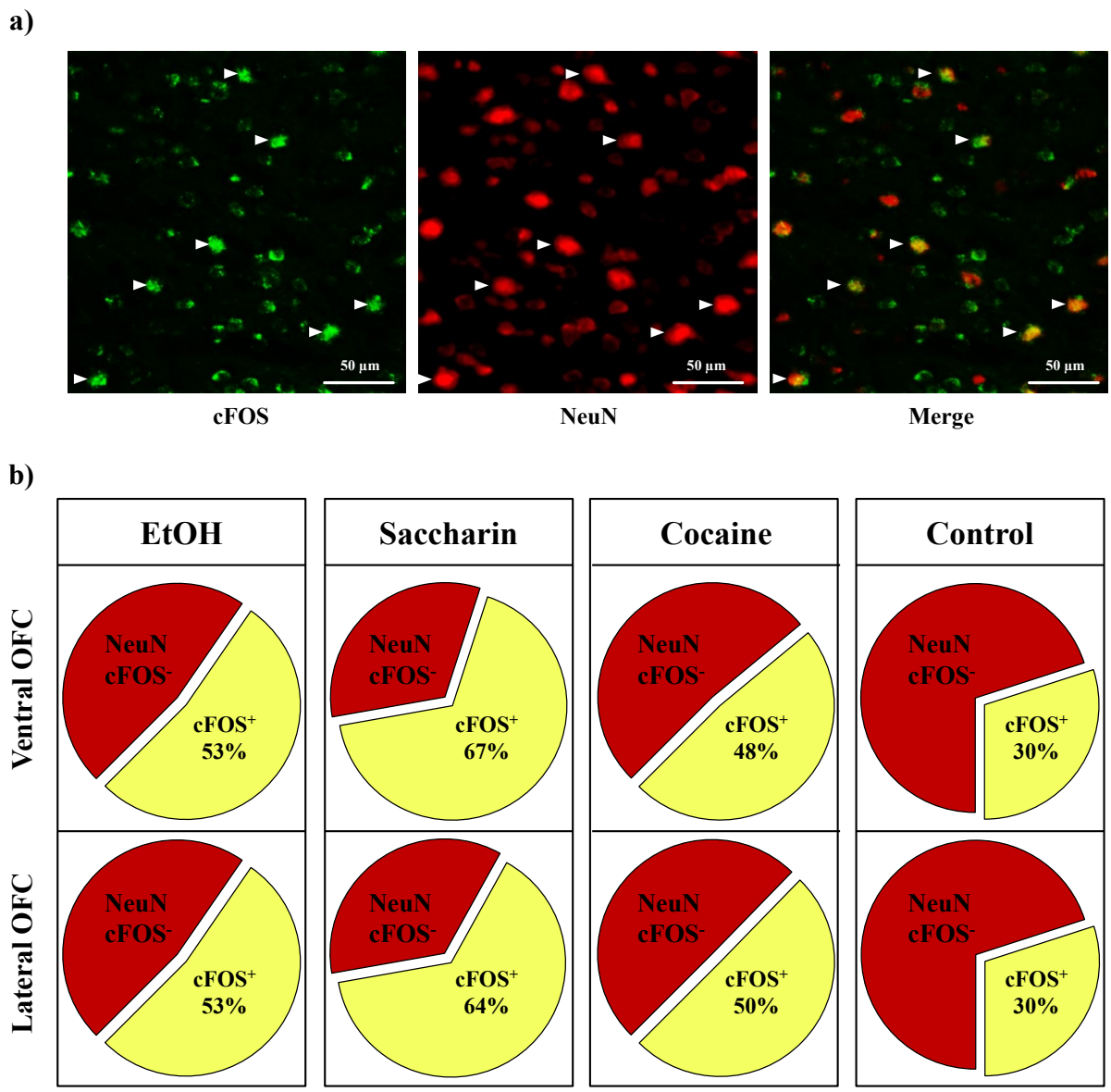

Figure 30) Co-localization of cFOS-ir positive and NeuN-ir positive cells in brain slices of ethanol, saccharin, cocaine and control animals after cue-induced reinstatement

a) Confocal laser scanning microscopy sample images of cFOS-ir/NeuN-ir double immunostainings (cFOS-ir = green, NeuN-ir = red, cFOS-ir/NeuN-ir merge = yellow). Arrows indicate co-localization b) Percentage of cFOS-ir positive cells within the neuronal population of control animals and rats trained to the different rewards, shown for the ventral and lateral OFC.

The double staining for cFOS-ir and GFAP-ir (Fig. 31b) showed no overlap between the different biomarkers neither for control animals nor for any of the reward trained rats. Taking the results of the cFOS-ir/NeuN-ir and the cFOS-ir/GFAP-ir together it can be concluded that all co-active cell ensembles are entirely neuronal and we can therefore relate to them as neuronal ensembles.

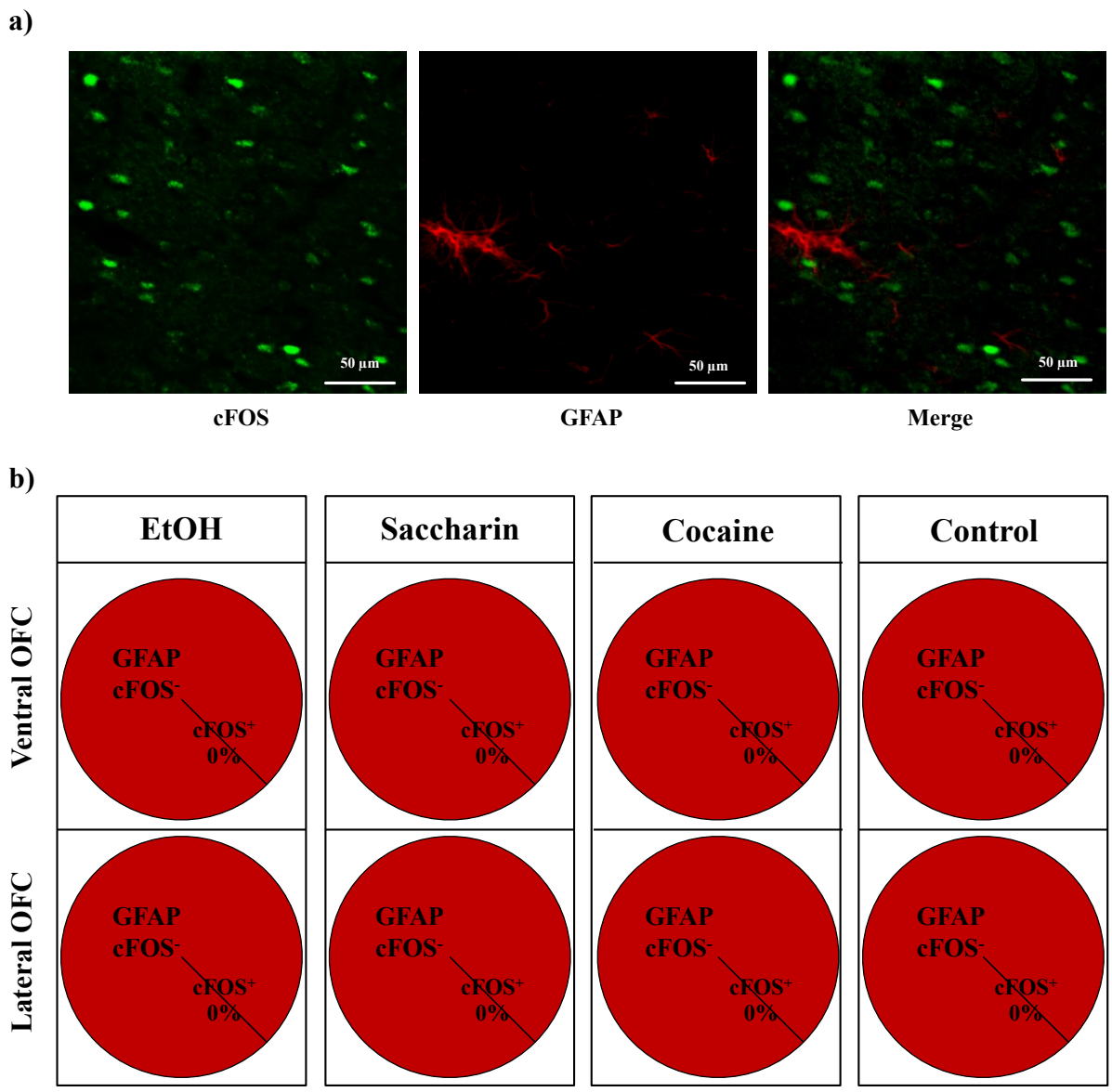

Figure 31) Co-localization of cFOS-ir positive and GFAP-ir positive cells in brain slices of ethanol, saccharin, cocaine and control animals after cue-induced reinstatement

a) Confocal laser scanning microscopy sample images of cFOS-ir/GFAP-ir double immunostainings (cFOS-ir = green, GFAP-ir = red). Arrows indicate co-localization b) Percentage of cFOS-ir positive neurons within the population of GFAP-ir positive cells for control animals and rats trained to the different rewards, shown for the ventral and lateral OFC.

In order to further characterize the active neuronal ensembles, double stainings of cFOS-ir/CaMKII and cFOS-ir/GAD67-ir were performed for all four conditions.

Co-localization of cFOS-ir and CaMKII-ir revealed increased cFOS expression levels within the CAMKII positive cell pool during reinstatement compared to control animals (Fig. 32b). Saccharin showed the smallest increase in cFOS activity within the CAMKII pool with 9.5 % whereas EtOH trained animals had an increased cFOS activity of 19 % and cocaine trained rats showed increases of 24 %. Again, the lateral and ventral OFC showed only slight differences in activity between each other (1 % - 5 %).

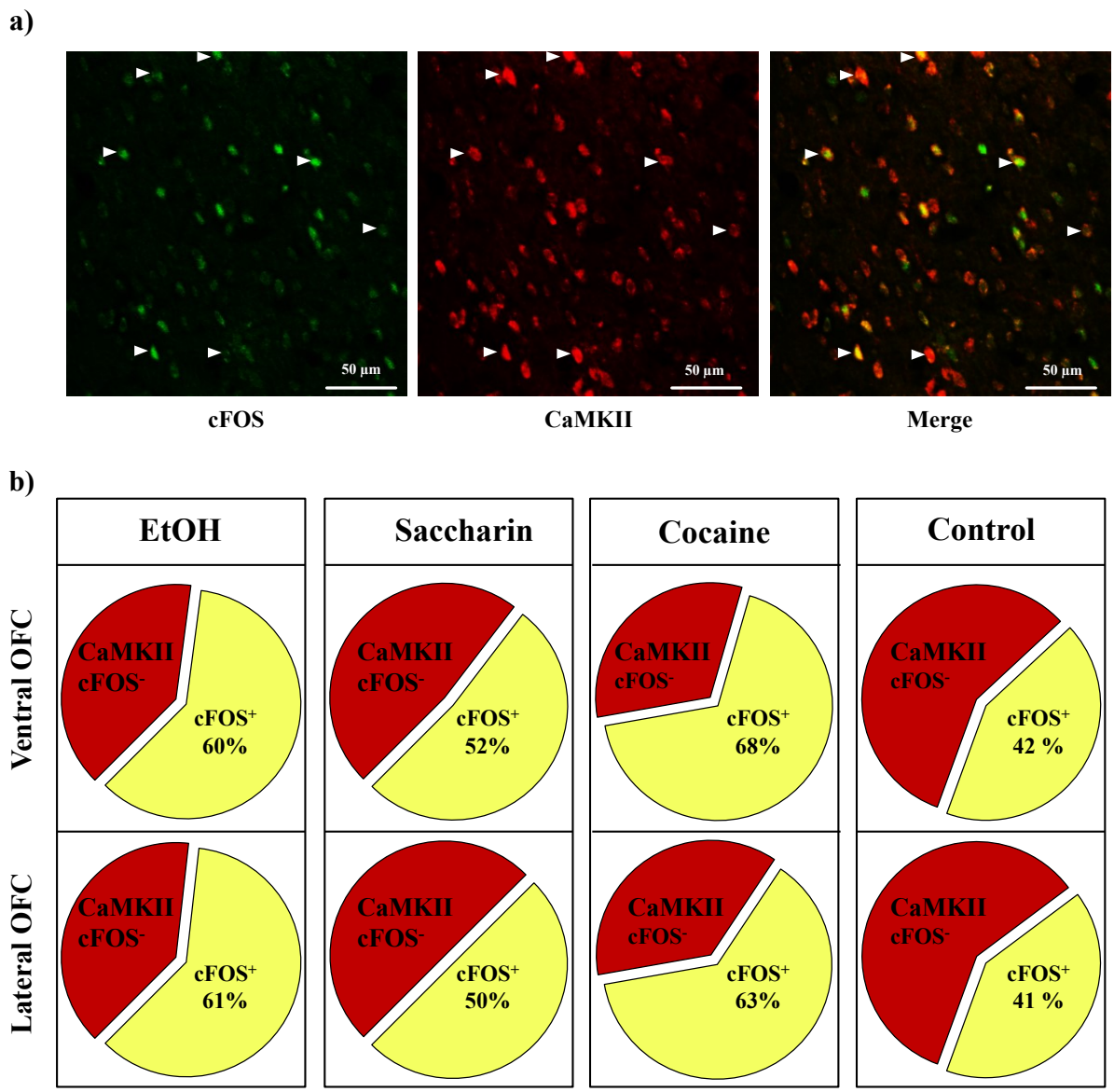

Figure 32) Co-localization of cFOS-ir positive and CaMKII-ir positive cells in brain slices of ethanol, saccharin, cocaine and control animals after cue-induced reinstatement

a) Confocal laser scanning microscopy sample images of cFOS-ir/CaMKII-ir double immunostainings (cFOS-ir = green, CaMKII-ir = red, cFOS-ir/CaMKII-ir merge = yellow). Arrows indicate co-localization b) Percentage of cFOS-ir positive neurons within the CaMKII-ir positive cell population of control animals and rats trained to the different rewards, shown for the ventral and lateral OFC.

Double staining of cFOS and GAD67 showed that only 16 % of the GAD67 cell population were cFOS-ir positive for control animals. Also, the amount of cFOS-ir positive cells within the GAD67 population for cocaine and saccharin was rather low, with 26.5 % and 27 % respectively. However, for ethanol trained animals almost half of the GAD67 population was cFOS-ir positive (Fig. 33b). Differences between lateral and ventral OFC were neglectable with only 1 % difference.

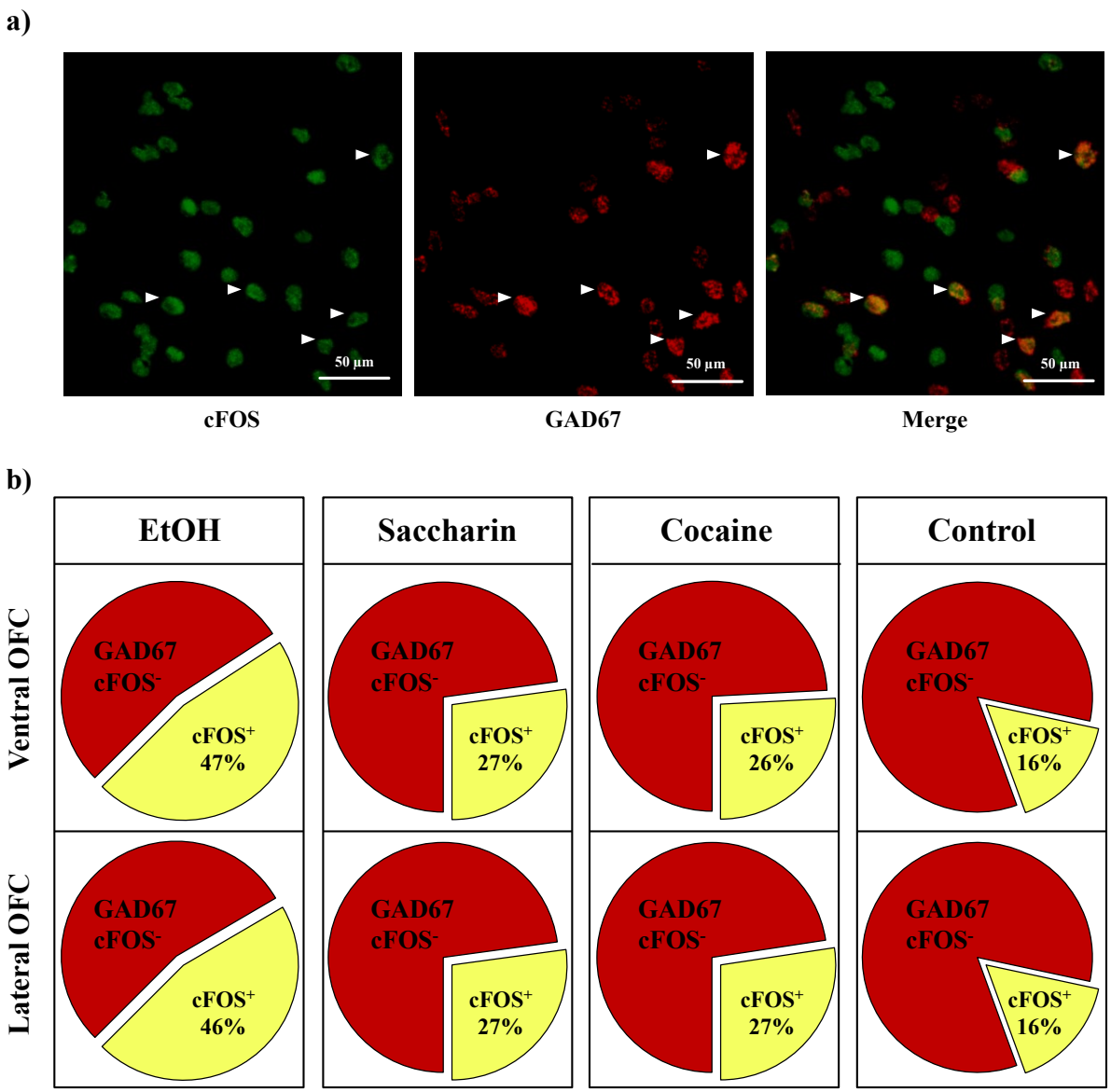

Figure 33) Co-localization of cFOS-ir positive and GAD67-ir positive cells in brain slices of ethanol, saccharin, cocaine and control animals after cue-induced reinstatement

a) Confocal laser scanning microscopy sample images of cFOS-ir/GAD67-ir double immunostainings (cFOS-ir = green, GAD67-ir = red, cFOS-ir/GAD67-ir merge = yellow). Arrows indicate co-localization b) Percentage of cFOS-ir positive neurons within the GAD67-ir positive cell population of control animals and rats trained to the different rewards, shown for the ventral and lateral OFC.

After analysis of cFOS-ir positive cells within the respective cell populations the neurochemical composition of the cFOS-ir positive population for each reward was investigated. For this analysis the percentage amount of activated cells within control animals was subtracted from the respective percentage amount for each reward during reinstatement, resulting in percentage Δ of RE - control. The resulting percentage composition for each reward can be seen in Fig. 34. As already detected before, the differences in cFOS activation between the lateral and the ventral OFC for the different rewards are marginal (1 - 5 %). The amount of cFOS-ir positive cells for saccharin trained animals was about 8.5 % or 15.5 % higher than for

ethanol or cocaine trained rats, respectively. However, the most interesting finding was that the composition of the different cFOS-ir positive populations was reward specific. For the natural reward saccharin, the amount of CaMKII-ir and GAD67-ir positive cells was quite balanced even though the lateral OFC showed a higher amount of cFOS-ir/CaMKII-ir positive cells than the ventral OFC (Fig. 34b). However, ethanol and cocaine trained animals displayed a highly drug specific composition of their neuronal ensembles. The composition of the cFOS-ir positive neuronal population of ethanol trained animals was 75 % GAD67-ir and 25 % CaMKII-ir for the lateral OFC and 67 % GAD67-ir and 33 % CaMKII-ir for the ventral OFC (Fig. 34a). Cocaine trained rats on the other hand displayed high levels of CaMKII-ir positive cells within the cFOS-ir positive population, with 82 % for the ventral OFC and 79 % for the lateral OFC. Consequently, the amount of GAD67-ir positive cells within the cFOS-ir positive neuronal population was low with only 18 % (ventral OFC) or 21 % (lateral OFC) (Fig. 34c).

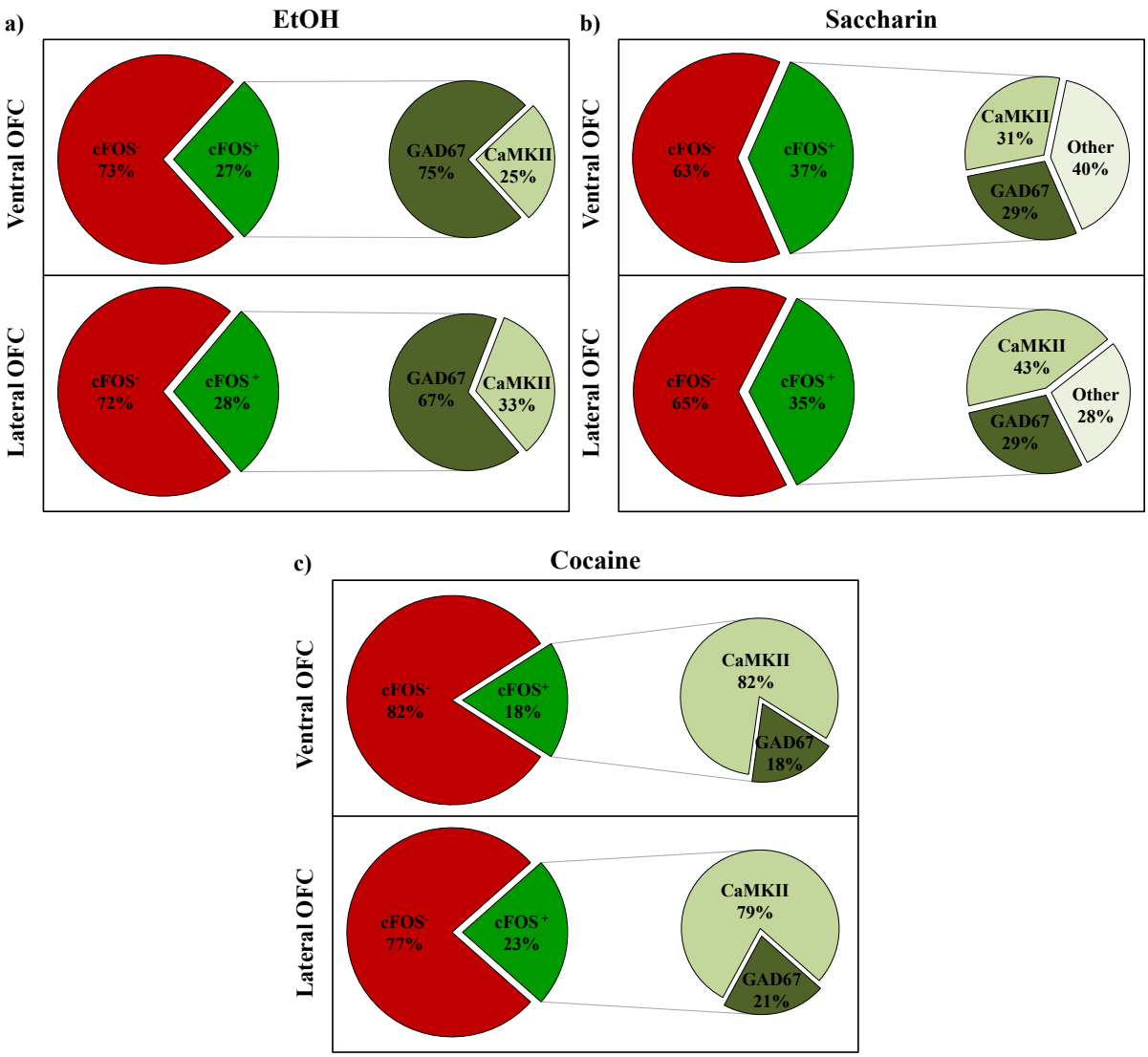

Figure 34) Overview over the neurochemical composition of the cFOS-ir positive neuronal population for different rewards displayed as percentage of Δ RE-control

a) Proportion of CaMKII-ir and GAD67-ir positive neurons within the cFOS-ir positive pool of ethanol trained animals b) Ratio of GAD67-ir positive, CaMKII-ir positive and other neurons within the cFOS-ir positive population of saccharin trained animals c) Amount of CaMKII-ir and GAD67-ir positive neurons within the cFOS-ir positive pool of cocaine trained animals.

After characterization of the neurochemical nature of neuronal ensembles active during cue-induced reinstatement of reward seeking behaviour and the finding that the neuronal ensembles are reward specific in their composition, a next set of experiments should determine their physiological properties.

3.3 Study 1C: Characterization of the physiological properties of GFP positive (active) versus GFP negative (inactive) neurons after reinstatement of reward seeking

After assessment of the neurochemical composition of neuronal ensembles mediating cue-induced reward seeking responses a detailed investigation of their basic physiological parameters was intended. For this purpose, *c-fos*-GFP transgenic rats were used as GFP expression allowed for identification of strongly activated neurons in acute coronal slices under the microscope. Whole-cell recordings of GFP-positive neurons were obtained and compared with nearby non-active neurons (GFP-negative) to enable physiological characterization. Data analysis of the whole cell patch clamp data was performed by Janet Barroso-Flores at the Central Institute of Mental Health, Mannheim.

3.3.1 cFOS-ir and GFP-ir co-localization

In a first step cFOS and GFP induction were characterized in the OFC by co-labelling of the respective proteins (Fig. 35a) in animals that were trained to self-administer cocaine and underwent cue-induced reinstatement of cocaine seeking behaviour (Fig. 28 & 29 in Results 3.2.1). Analysis of cFOS-ir and GFP-ir in the ventral and lateral OFC revealed that 84 % and 82 % of cFOS-ir neurons were GFP-ir positive (Fig. 35b).

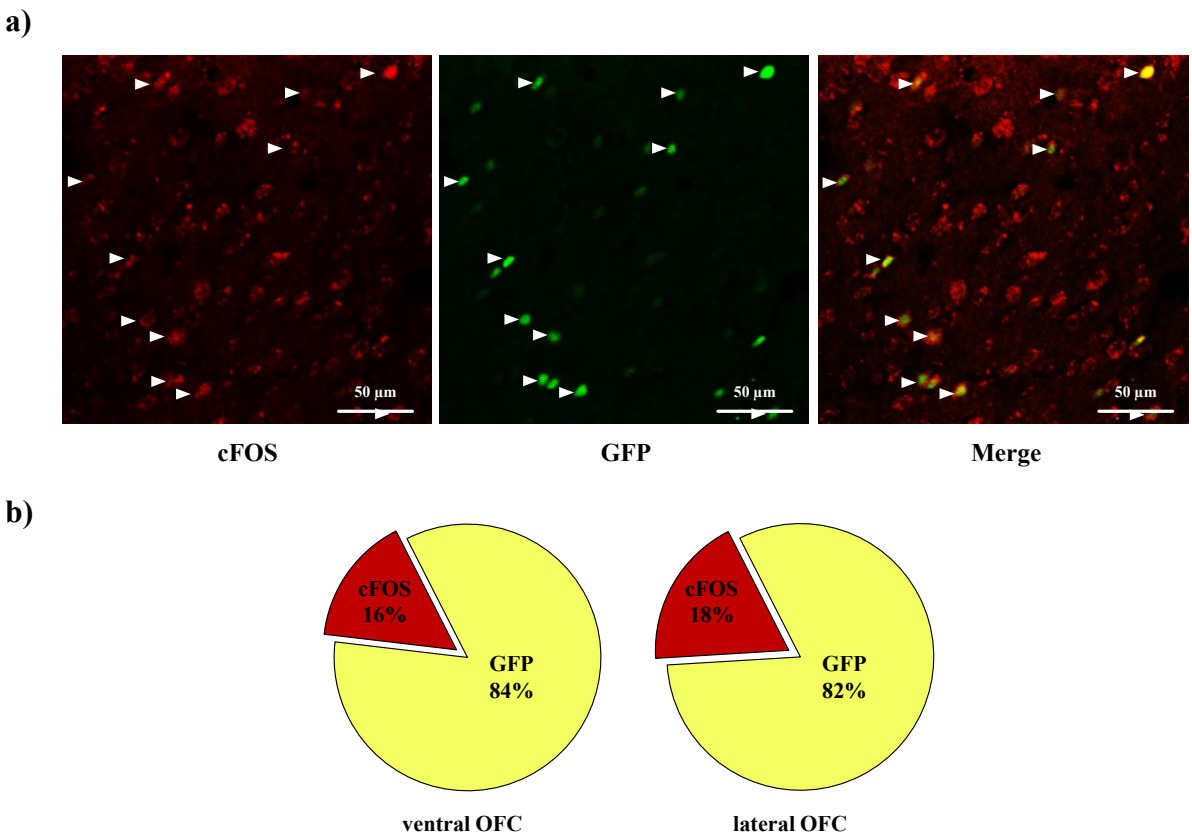

Figure 35) Co-localization of cFOS-ir positive and GFP-ir positive cells in brain slices of cocaine trained rats after cue-induced reinstatement

a) Confocal laser scanning microscopy sample images of cFOS-ir/GFP-ir double immunostainings (cFOS-ir = red, GFP-ir = green, cFOS-ir/ GFP-ir merge = yellow), arrows indicate co-localization b) Percentage of GFP-ir positive neurons within the cFOS-ir positive cell population shown for the ventral and lateral OFC.

3.3.2 Operant conditioning to investigate the functional properties of neuronal ensembles involved in cue-induced reinstatement of cocaine seeking

For the physiological characterization animals were trained to self-administer cocaine until they reached a stable baseline. On average animals lever pressed 77 ± 18 times during the last four training sessions. Self-administration training was then followed by extinction learning during which animals showed fading of non-reinforced seeking behaviour. Animals reached a response rate of 11 ± 1 lever presses on average and therefore less than 20 % of baseline responses (Fig. 36).

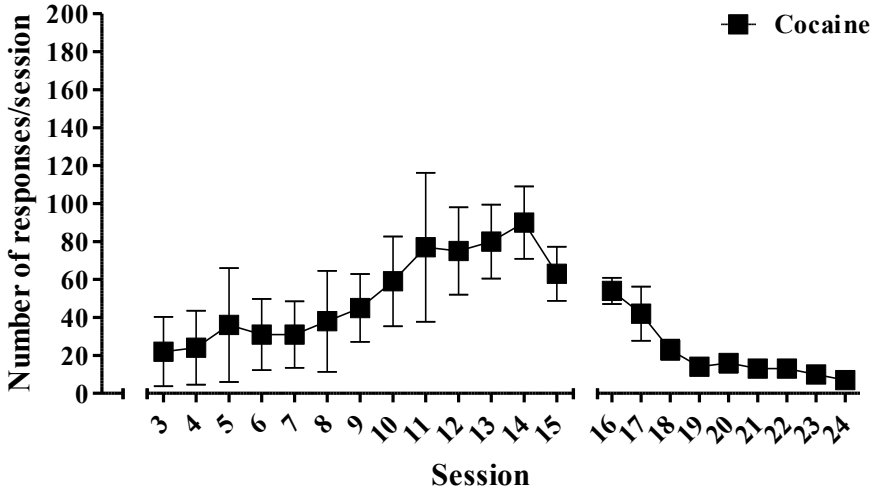

Figure 36) Self-administration and extinction training for cocaine trained animals; data for water deprivation (day 1 & 2) not shown

The graph displays lever press responses during self-administration training (days 3-15) for 0.125 mg/kg cocaine trained animals. Additionally, responses to the active lever are shown for extinction training (days 16-24). Cocaine: n = 5; All values are expressed as mean ± SEM.

After successfully finishing extinction training animals were subjected to a cue-induced reinstatement session in order to activate neuronal ensembles mediating cue-induced reward seeking behaviour. During the test session animals displayed a significant increase in their reward seeking behaviour (Fig. 37a) (two-way ANOVA; main effect of sessions, $F(1,16) = 17.135$, $p < 0.001$; of active vs. inactive lever press, $F(1,16) = 15.741$, $p = 0.001$; and interaction, $F(1,16) = 12.944$, $p = 0.002$; Newman-Keuls *post hoc* test $\bar{x}$ EXT active vs RE active $p < 0.001$). No significant change was detected on the inactive lever (Fig. 37b) (Newman-Keuls *post hoc* test $\bar{x}$ EXT inactive vs RE inactive $p = 0.923$). Figure 37c shows the individual responses made by each animal as well as the kind of neuron (GFP positive/GFP negative) that was analysed for each animal.

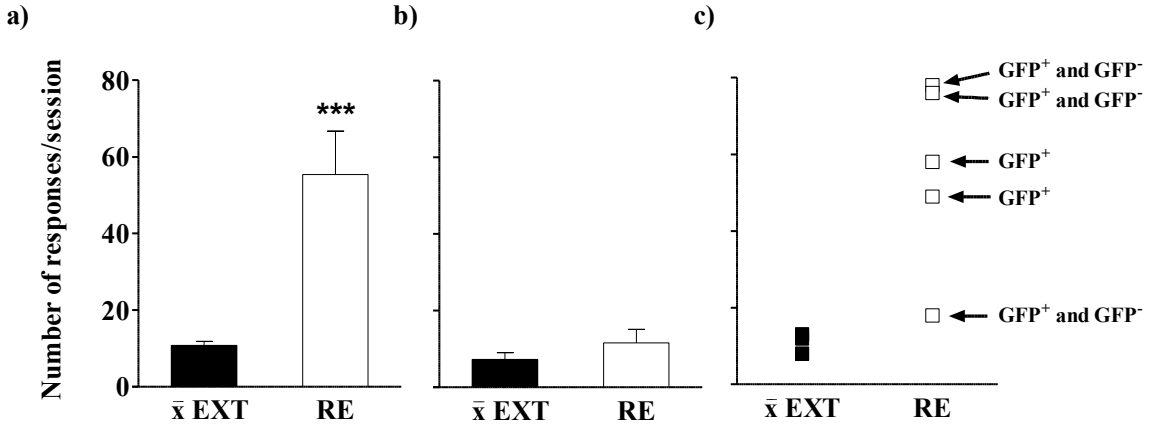

Figure 37) Active and inactive responses during cue-induced reinstatement compared to average responses during the last four extinction sessions for cocaine trained animals

The graph shows the active lever responses (a) and inactive lever responses (b) during cue-induced cocaine seeking behaviour in comparison to responses during extinction training. c) Individual responses for each animal together with the indication what kind of neuron (GFP positive/GFP negative) was electrophysiologically characterized; n = 5; All values are expressed as mean ± SEM. *** $p < 0.001$.

3.3.3 Whole-cell patch clamp analysis to characterize physiological properties of neuronal ensembles

Thirty minutes after the cue-induced reinstatement session was finished, animals were perfused with aCSF/20 % sucrose and their brains processed for electrophysiological whole-cell recordings. Once acquired, coronal brain slices of the OFC were placed inside the recording chamber and investigated for fluorescent cells under the laser microscope. As soon as a cell was successfully targeted and a stable access to the neurons intracellular space was established, recordings could be initiated (Fig. 38).

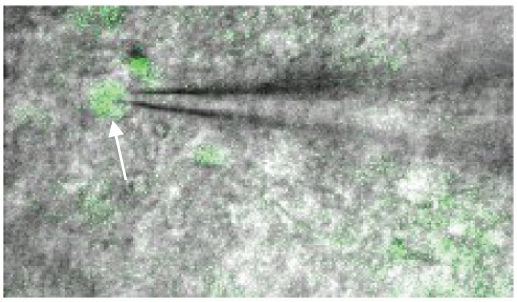

Figure 38) Whole-cell recording of a GFP positive cell

Merged image (fluorescent/differential interference contrast) from an acute brain slice during whole-cell patch clamp recordings (see pipette tip). The recording was acquired from a GFP positive cell (white arrow) in the OFC.

First, changes in membrane potential were investigated by applying a known current to the cell and measuring the resulting voltage change. Figure 39 depicts voltage traces for representative GFP negative and GFP positive neurons. All GFP negative neurons measured (n = 3) displayed similar spike patterns after current injection whereas GFP positive neurons (n = 5) could be grouped into GFP positive type 1 neurons (n = 2) and GFP positive type 2 neurons (n = 3). GFP positive type 1 neurons showed rapid and high action potential firing rates. GFP positive type 2 neurons however, fired just one action potential (Fig. 39).

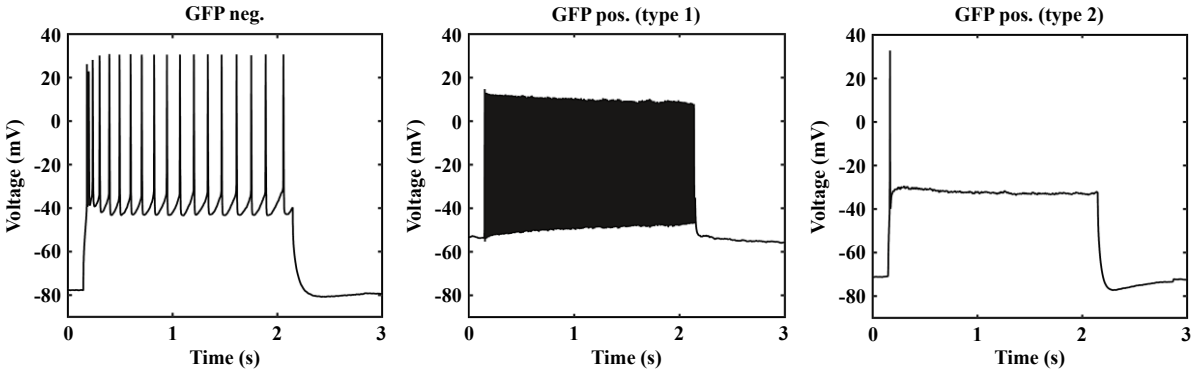

Figure 39) Representative voltage traces from GFP negative and GFP positive neurons

Example voltage traces from one GFP negative and two representative GFP positive neurons. Action potentials were evoked from the resting membrane potential with somatic current injections.

From the same neurons current voltage-relationships were established. Therefore, ionic currents were evoked with hyperpolarizations and depolarizations in steps of 10 mV (Fig. 40). The group of GFP negative neurons displayed similar current voltage relationships whereas GFP positive neurons were highly variable especially looking at outward currents.

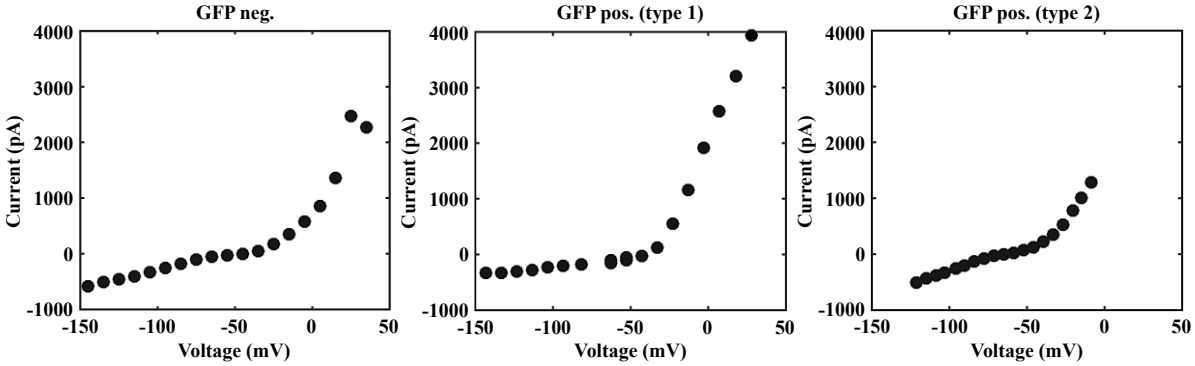

Figure 40) Current-voltage relationship of GFP$^-$, GFP$^+$ type 1 and GFP$^+$ type 2 neurons

Current voltage relationship from the same neurons shown in Figure 39. Currents were evoked by hyper - and depolarizations in steps of 10 mV. Inward currents are plotted below 0 mV, whereas outward currents are plotted above 0 mV.

In addition different physiological properties were compared between GFP negative and GFP positive neurons in the OFC (Fig. 41). Properties investigared were resting membrane potential, input resistance, the latency to evoke the first action potential with a somatic current injection and rheobase, which resambles the current required to elicit an action potential. For none of the examined physiological properties a significant difference could be detected (two-tailed unpaired t-test; Vrest: t (6) = 0.047, p = 0.964; Rinput: t (6) = - 0.893, p = 0.406; Latency: t (6) = -2.291, p = 0.062; Rheobase: t (6) = -1.798, p = 0.122)

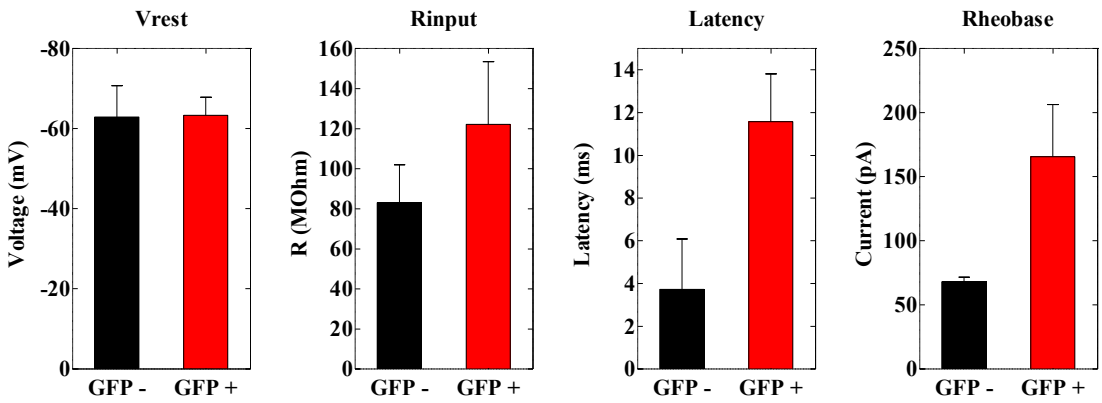

Figure 41) Comparison of different electrophysiological properties between GFP negative and GFP positive neurons

The graph shows the comparison of the resting membrane potential (Vrest), the input resistance (Rinput), the latency to evoke the first action potential with somatic current injection and rheobase, the currents required to elicit an action potential, between GFP negative and GFP positive neurons. All values are expressed as mean ± SEM.

After in depth identification and characterization of neuronal ensembles active during cue-induced reinstatement of natural reward and drug reward seeking behaviour, a next set of experiments aimed to determine their functional role in cue-induced reward seeking.

3.4 Study 2: Validation of functional neuronal ensembles encoding for natural reward and drug reward seeking behaviour

To investigate the functional role of neuronal ensembles within the OFC active during cue-induced reinstatement of reward seeking for different rewards a *c-fos*-lacZ transgenic Sprague-Dawley rat strain was used to specifically inactive neuronal ensembles via Daun02 silencing. As the OFC is functionally a very heterogeneous region (Izquierdo, 2017) and several studies showed a differential role of OFC subregions (Fuchs et al., 2004; den Hartog et al., 2016; Bianchi et al., 2018) we targeted both the lateral and the ventral OFC.

3.4.1 Investigating the functional relevance of neuronal ensembles involved in saccharin reward seeking behaviour

In a first set of experiments animals were trained to self-administer 0.2 % saccharin followed by extinction training until animals reached less than 20 % of their baseline response. Animals showed a high variability in their response rate during self-administration settling at 160 ± 30 lever presses on average for their last four sessions. Extinction learning was successful at 12 ± 1 lever presses on average over the last 4 extinction sessions (Fig. 42).

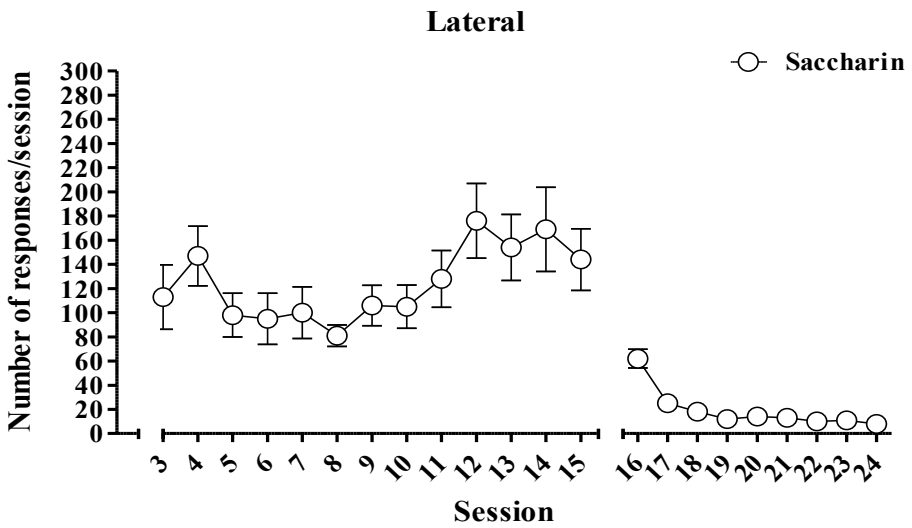

Figure 42) Saccharin self-administration training and extinction sessions for animals implanted into the lateral OFC; data for water deprivation (day 1 & 2) not shown

The graph shows response behaviour of 0.2 % saccharin trained animals, that were implanted with a guide cannula into the lateral OFC, during self-administration training (days 3-15) and extinction training (days 16-24). Saccharin: n = 15; All values are expressed as mean ± SEM.

Following extinction training animals were implanted with a guide cannula targeting the lateral OFC. After one week of recovery animals were tested in the first cue-induced reinstatement session (RE 1) to activate the neuronal ensembles of interest. Animals were then assigned to either the vehicle or Daun02 group according to their performance during self-administration, extinction and RE 1. Both groups of animals showed significant increase in responding to the active lever between the average of the last extinction sessions and RE 1 (Fig. 43) (two-way repeated measures ANOVA; saccharin lateral: main effect of sessions, $F(1,26) = 23.521$, $p < 0.001$; assigned groups, $F(1,26) = 0.587$, $p = 0.450$; and interaction $F(1,26) = 0.099$, $p = 0.755$; Newman-Keuls *post hoc* test $\bar{x}$ EXT vs RE 1, Daun02 group: $p < 0.001$ and vehicle group $p = 0.002$). 30 min after RE 1 the animals were infused with either Daun02 or vehicle into the lateral OFC (see Fig. 44 for respective infusion placement). Following the intracranial infusions animals recovered for four days before they were subjected to the second cue-induced reinstatement (RE 2). Daun02 infused animals displayed a significant decrease in their cue-induced saccharin seeking response compared to their RE 1 response rate. On the other hand, vehicle animals showed no significant reduction in their reward seeking response (Fig. 43) (two-way repeated measures ANOVA; main effect of sessions, $F(1,26) = 6.289$, $p < 0.0187$; assigned groups, $F(1,26) = 0.00001$, $p = 0.997$; and interaction $F(1,26) = 1.222$, $p = 0.279$; Newman-Keuls *post hoc* test RE 1 vs RE 2, Daun02 group: $p = 0.011$ and vehicle group $p = 0.402$). Inactive lever presses showed no significant differences between sessions (Newman-Keuls *post hoc* test; Daun 02: $\bar{x}$ EXT vs RE 1 $p = 0.785$, RE 1 vs RE 2 $p = 0.847$; Vehicle $\bar{x}$ EXT vs RE 1 $p = 0.903$, RE 1 vs RE 2 $p = 0.978$).

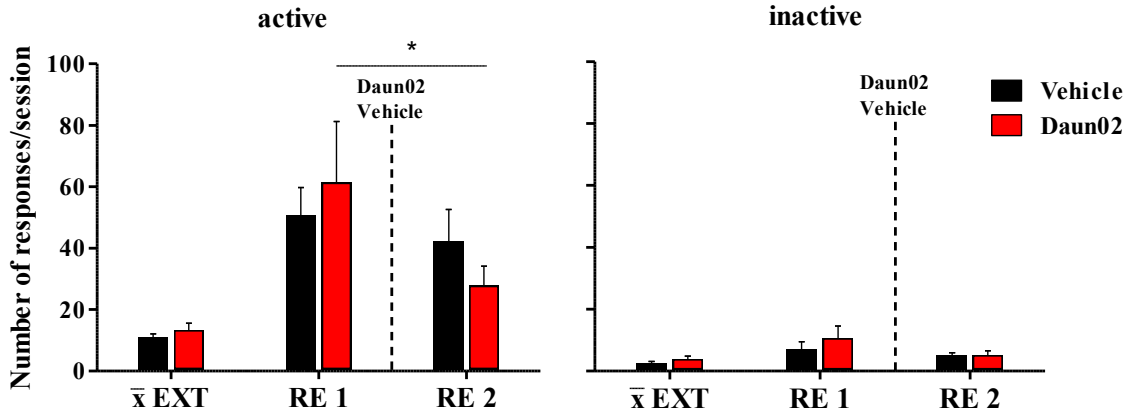

Figure 43) Active and inactive responses during cue-induced reinstatement before and after Daun02/vehicle infusions into the lateral OFC of saccharin trained rats compared to extinction

Daun02 infusion into the lateral OFC of saccharin trained animals after RE 1 caused a significant decrease in saccharin reward seeking in RE 2 (n = 7). However, infusion of a vehicle in the same location after RE 1 did not result in a significant alteration in the reward seeking response of saccharin trained animals (n = 8). No significant changes were detected for inactive lever presses for both groups. All values are expressed as mean ± SEM. * p = 0.011, Abbreviations: x̄ EXT = average of last extinction sessions, RE 1 = 1st cue - induced reinstatement, RE 2 = 2nd cue-induced reinstatement.

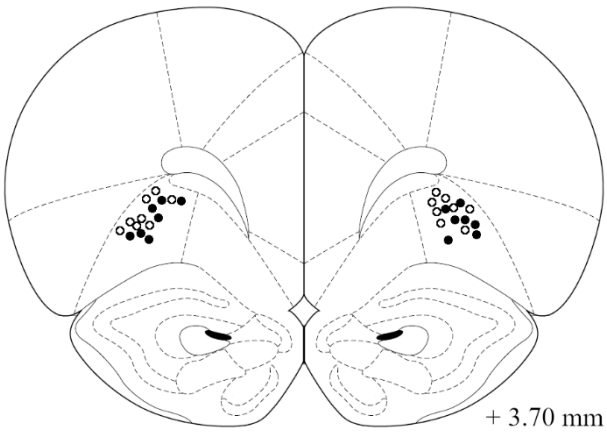

Figure 44) Infusion site mapping for saccharin trained animals

Approximate locations of Daun02 (full circle) and vehicle (empty circle) infusions into the lateral OFC of saccharin trained rats. Infusions were verified for + 3.70 mm anterior to bregma (Paxinos and Watson, 1998).

In order to examine the functional role of the ventral OFC in cue-induced reward seeking another batch of animals was trained to self-administer saccharin. Animals were again highly variable in their reward seeking for 0.2 % saccharin reaching 144 ± 29 lever presses on average over the last four training sessions. Self-administration was followed by extinction training until animals reached less than 20 % of their baseline response rate on average (11 ± 3) (Fig. 45).

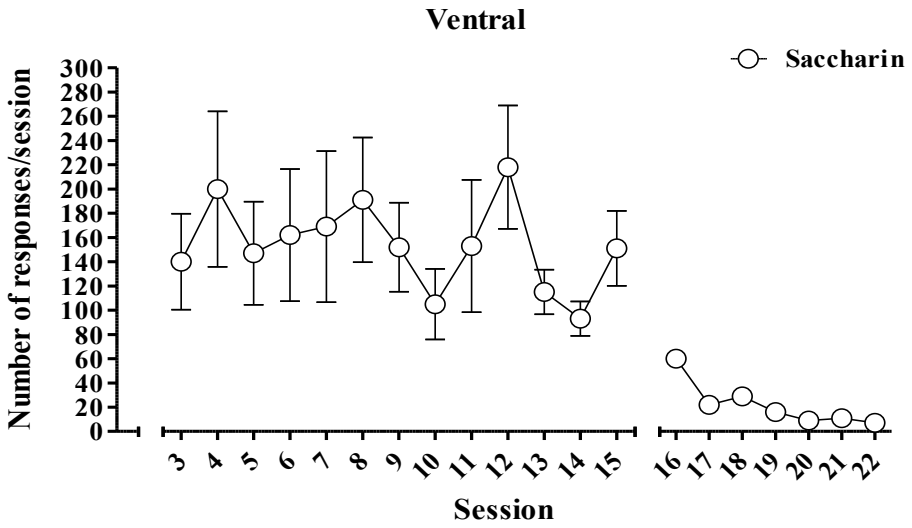

Figure 45) Saccharin self-administration training and extinction sessions for animals implanted into the ventral OFC; data for water deprivation (day 1 & 2) not shown

Displayed are lever press responses of animals trained to 0.2 % saccharin during self-administration training (days 3-15) and extinction training (days 16-22). Rats received a guide cannula implantation into the ventral OFC. Saccharin: n = 9; All values are expressed as mean ± SEM.

After successful extinction learning animals were implanted with a guide cannula in the ventral OFC. After a recovery period of seven days rats underwent their first cue-induced reinstatement session to activate the neuronal ensembles of interest within the ventral OFC. Again, animals were grouped according to their performance during self-administration, extinction and RE 1 into either Daun02 group or vehicle group. Each group displayed significantly increased response rates to the active lever during RE 1 compared to $\bar{x}$ EXT (Fig. 46) (two-way repeated measures ANOVA; saccharin ventral: main effect of sessions, F (1,14) = 17.087, p = 0.001; assigned groups, F (1,14) = 0.111, p = 0.744; and interaction F (1,14) = 0.859, p = 0.370; Newman-Keuls *post hoc* test $\bar{x}$ EXT vs RE 1, Daun02 group: p = 0.017 and vehicle group p = 0.004). Ninety minutes after onset of RE 1 animals received micro-infusions of either Daun02 or vehicle into the ventral OFC to target activated neuronal ensembles (see Fig. 47 for respective infusion locations). Then RE 2 was performed following a break of four days. Daun02 infused animals increased their response rate from 40 ± 6 lever presses in RE 1 to 58 ± 9 lever presses in RE 2. Vehicle treated animals decreased their lever presses from 46 ± 13 in RE 1 to 33 ± 11 in RE 2 (Fig. 46). However, none of these changes were statistically significant, even though Daun02 infused animals showed a trend comparing RE 1 and RE 2 (two-way repeated measures ANOVA; main effect of sessions, F (1,14) = 0.00001, p = 0.997; assigned groups, F (1,14) = 1.159, p = 0.300; and interaction F (1,14) = 5.656, p = 0.032; Newman-Keuls *post hoc* test RE 1 vs RE 2, Daun02 group: p = 0.066 and vehicle group p =

0.187). Responses on the inactive lever showed no significant differences for both groups. (Newman-Keuls *post hoc* test; Daun02: x̄ EXT vs RE 1 p = 0.815, RE 1 vs RE 2 p = 0.616; Vehicle x̄ EXT vs RE 1 p = 0.772, RE 1 vs RE 2 p = 0.936).

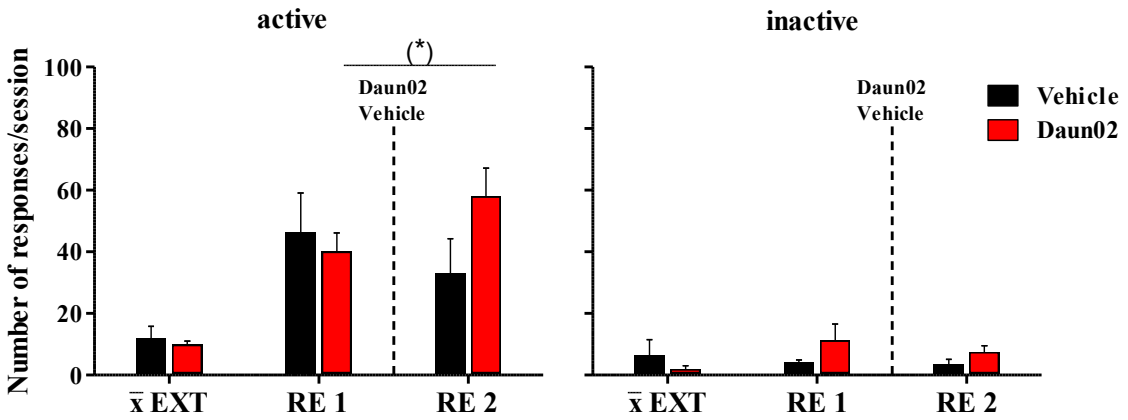

Figure 46) Active and inactive responses during cue-induced reinstatement before and after Daun02/vehicle infusions into the ventral OFC of saccharin trained rats compared to extinction

Neither Daun02 (n = 4) nor vehicle (n = 5) micro-infusions into the ventral OFC of saccharin trained animals caused a significant change in cue-induced saccharin seeking behaviour, however, a trend was detected comparing RE 1 and RE 2 within the Daun02 group. Inactive lever presses showed no significant differences. Values are expressed as mean ± SEM. (*) p = 0.066, Abbreviations: x̄ EXT = average of last extinction sessions, RE 1 = 1st cue - induced reinstatement, RE 2 = 2nd cue-induced reinstatement.

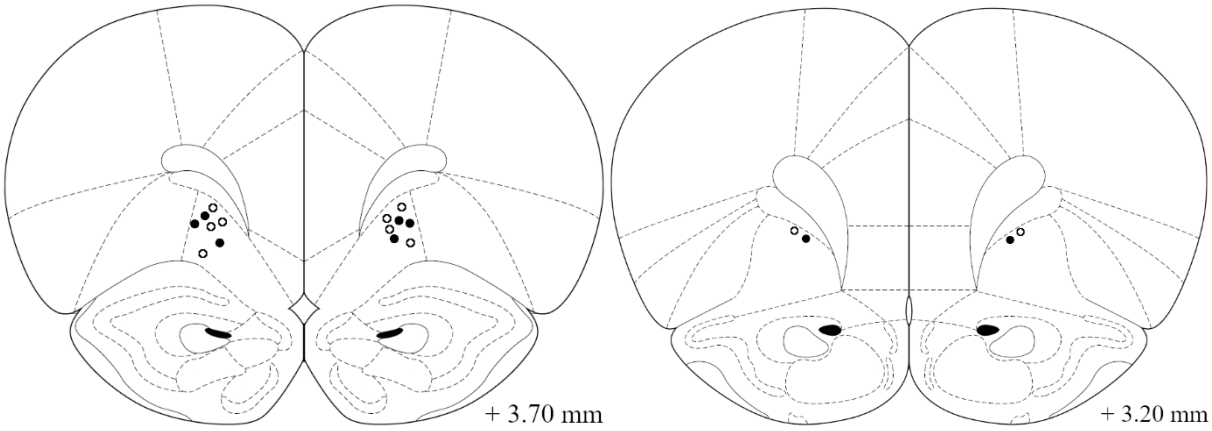

Figure 47) Infusion site mapping for saccharin trained animals

Approximate locations of Daun02 (full circle) and vehicle (empty circle) infusions into the ventral OFC of saccharin trained rats. Infusion were verified for + 3.70 mm to + 3.20 mm anterior to bregma (Paxinos and Watson, 1998).

3.4.2 Investigating the functional relevance of neuronal ensembles involved in cocaine reward seeking behaviour

Following the investigation of the functional role of neuronal ensembles activated by cue-induced saccharin seeking behaviour, the next set of experiments was designed to examine the same for cue-induced cocaine seeking. Therefore, animals were trained to self-administer cocaine by responding to an active lever, which they pressed 101 ± 14 times on average over the last four training sessions. During extinction animals reached below 20 % of baseline response rate with 15 ± 3 lever presses on average (Fig. 48).

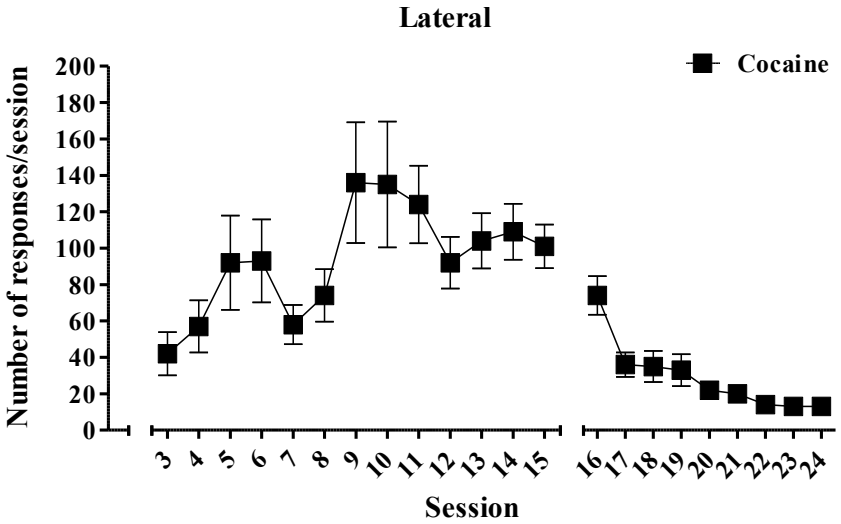

Figure 48) Cocaine self-administration training and extinction sessions for animals implanted into the lateral OFC; data for water deprivation (day 1 & 2) not shown

The graph depicts self-administration training (days 3-15) as well as extinction training (days 16-24) for 0.125 mg/kg cocaine trained animals. Rats were implanted with a guide cannula into the lateral OFC. Cocaine: n = 13; All values are expressed as mean ± SEM.

Afterwards all rats that were successfully conditioned to self-administer cocaine, were cannulated with guide cannulas into the lateral OFC. After surgery animals recovered for one week before they were subjected to RE 1, to activate neuronal ensembles responsible for cue-induced cocaine seeking. Animals were then divided into two groups (Daun02 and vehicle) according to their achievements during self-administration, extinction learning and RE 1. Two-way repeated measures ANOVA revealed significant main effect of the sessions ($F(1,22) = 32.076$, $p < 0.001$) but no significant effect of treatment ($F(1,22) = 1.054$, $p = 0.316$) or interaction ($F(1,22) = 0.109$, $p = 0.744$). Newman-Keuls *post hoc* test showed significant alterations between $\bar{x}$ EXT and RE 1 for both groups with $p < 0.001$ (Fig. 49). Daun02 or vehicle infusions into the lateral OFC were performed 30 min after the end of RE 1 (see Fig. 50 for

respective infusion placement). Four recovery days later animals underwent the second cue-induced reinstatement. Neither Daun02 group nor vehicle group displayed significant changes between RE 1 and RE 2 in their cocaine seeking behaviour (Fig. 49) (two-way repeated measures ANOVA; main effect of sessions, F (1,22) = 0.871, p = 0.361; assigned groups, F (1,22) = 1.227, p = 0.280; and interaction F (1,22) = 0.031, p = 0.862). Inactive lever presses were also not significantly different for both groups.

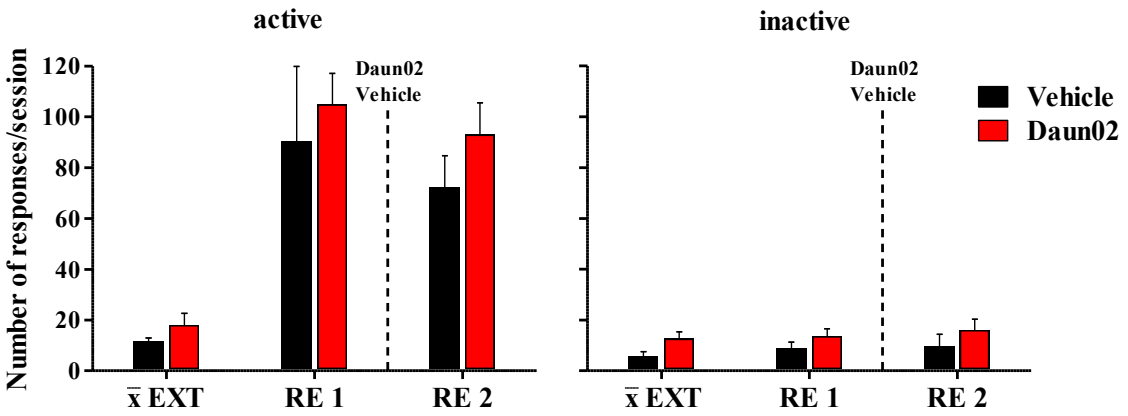

Figure 49) Active and inactive responses during cue-induced reinstatement before and after Daun02/vehicle infusions into the lateral OFC of cocaine trained rats compared to extinction

No significant changes were detected between RE 1 and RE 2 for Daun02 group (n = 7) or vehicle group (n = 6). Inactive lever presses showed no alterations. Values are expressed as mean ± SEM. Abbreviations: x̄ EXT = average of last extinction sessions, RE 1 = 1st cue - induced reinstatement, RE 2 = 2nd cue-induced reinstatement.

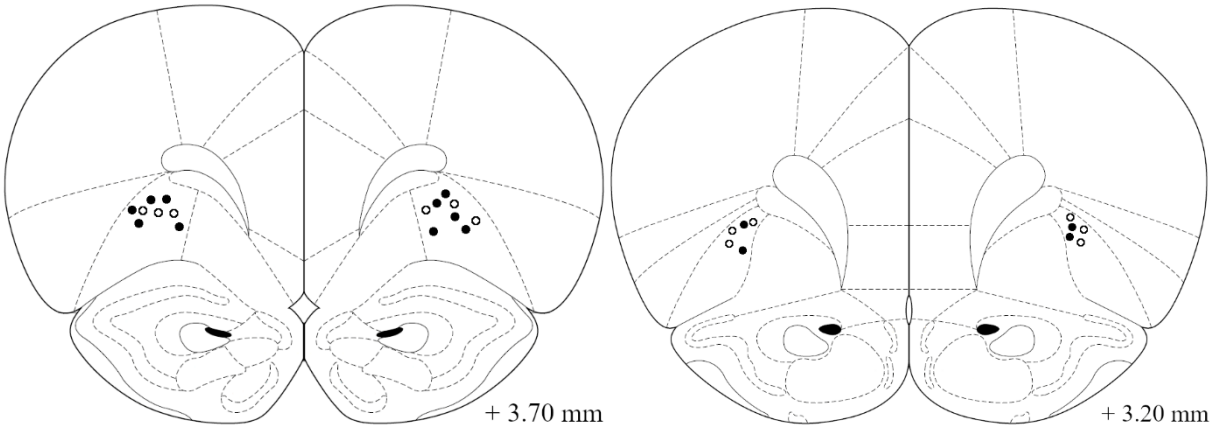

Figure 50) Mapping of infusion sites for cocaine trained rats

Approximate locations of Daun02 (full circle) and vehicle (empty circle) infusions into the lateral OFC of cocaine trained animals. Infusion were verified for + 3.70 mm to + 3.20 mm anterior to bregma (Paxinos and Watson, 1998).

To finish the investigation of OFC neuronal ensembles, another batch of animals was trained to self-administer cocaine. Animals reached a stable response rate at 84 ± 13 lever presses over the last four self-administration sessions. After nine days of extinction training the rats dropped below 20 % of baseline in their response rate with 11 ± 2 lever presses (Fig. 51).

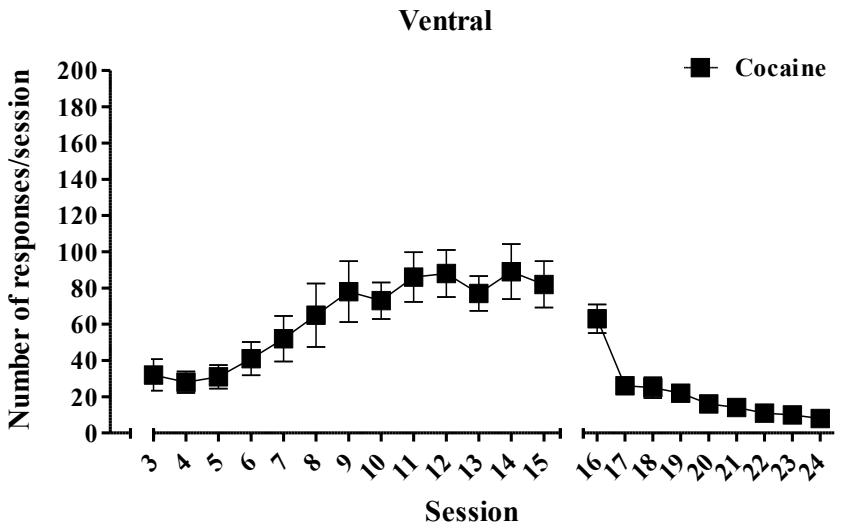

Figure 51) Cocaine self-administration training and extinction sessions for animals implanted into the ventral OFC; data for water deprivation (day 1 & 2) not shown

The graph shows active responses for 0.125 mg/kg cocaine during self-administration training (days 3-15) and extinction training (days 16-24). Animals received a guide cannula implantation into to ventral OFC. Cocaine: n = 12; All values are expressed as mean ± SEM.

At the end of their extinction training all animals were implanted with guide cannulas into the ventral OFC, which was followed by one week of recovery. Afterwards animals were subjected to the first cue-induced reinstatement. Grouping in Daun02 group and vehicle group was done according to performance during self-administration, extinction and RE 1. Both groups increased significantly in their cocaine seeking behaviour comparing $\bar{x}$ EXT vs RE 1 (Fig. 52) (two-way repeated measures ANOVA; cocaine ventral: main effect of sessions, $F(1,20) = 14.579$, $p = 0.001$; assigned groups, $F(1,20) = 0.143$, $p = 0.709$; and interaction $F(1,20) = 0.06$, $p = 0.809$; Newman-Keuls *post hoc* test $\bar{x}$ EXT vs RE 1, Daun02 group: $p = 0.01$ and vehicle group $p = 0.008$). Ninety minutes after start of RE 1 animals received their respective micro-infusion of Daun02 or vehicle in order to inactivate the previously active neuronal ensembles in the ventral OFC (see Fig. 53 for respective infusion locations). Five days later animals were tested in a second cue-induced reinstatement session. As can be seen in Fig. 52 none of the two groups changed in their reward seeking behaviour compared to RE 1 (two-way repeated measures ANOVA; cocaine ventral: main effect of sessions, $F(1,20) = 0.0003$, p

= 0.987; assigned groups, F (1,20) = 0.035, p = 0.853; and interaction F (1,20) = 0.019, p = 0.892). Responses to the inactive lever also showed no significant alterations.

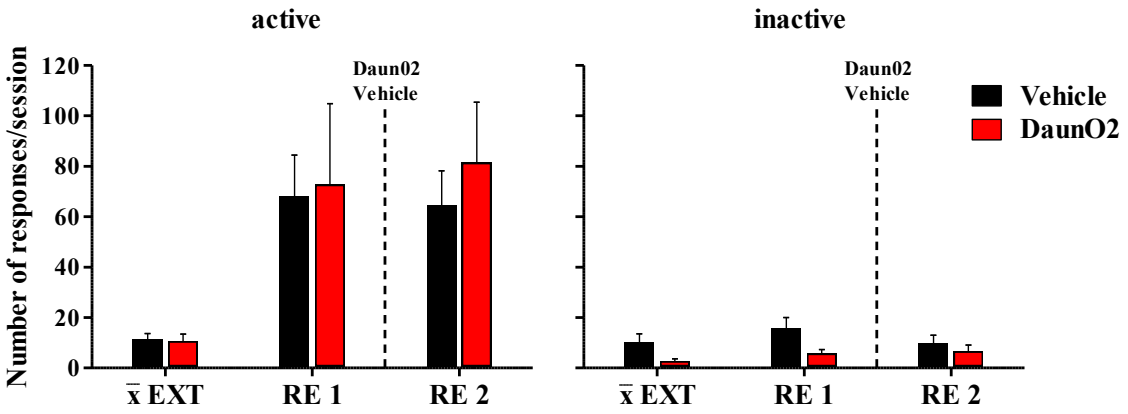

Figure 52) Active and inactive responses during cue-induced reinstatement before and after Daun02/vehicle infusions into the ventral OFC of cocaine trained rats compared to extinction

Neither Daun02 (n = 5) nor vehicle (n = 7) infusions into the ventral OFC of cocaine trained animals caused significant alterations. Inactive lever presses also showed no differences. Values are expressed as mean ± SEM. Abbreviations: x̄ EXT = average of last extinction sessions, RE 1 = 1st cue - induced reinstatement, RE 2 = 2nd cue-induced reinstatement.

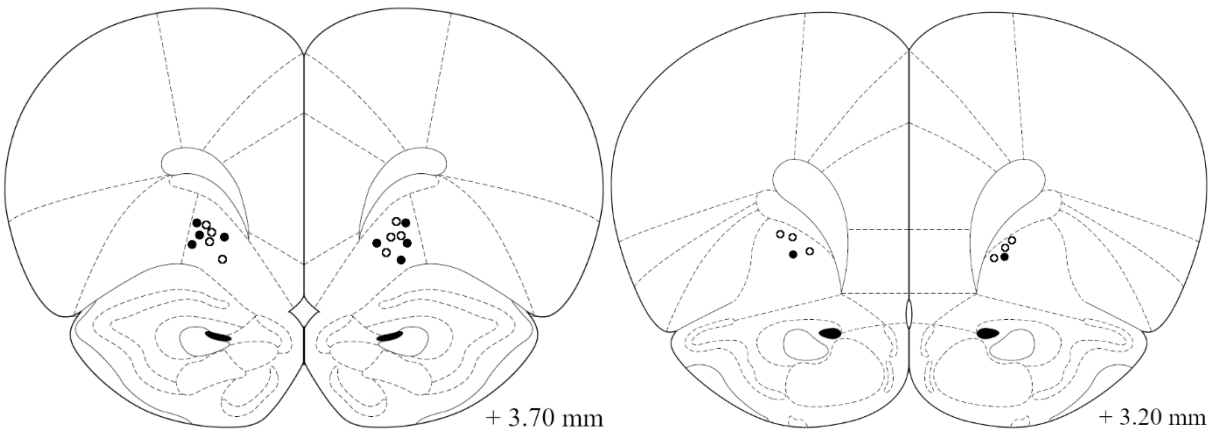

Figure 53) Location mapping of infusion sites for cocaine trained rats

Approximate locations of Daun02 (full circle) and vehicle (empty circle) infusions into the lateral OFC of cocaine trained animals. Infusion were verified for + 3.70 mm to + 3.20 mm anterior to bregma (Paxinos and Watson, 1998).

After examination of neuronal ensembles active during cue-induced saccharin and cocaine seeking behaviour the next set of experiments aimed to investigate those ensembles for cue-induced ethanol seeking. Therefore, animals were trained to self-administer ethanol following the same training schedule used before. Unfortunately, only a small number of animals showed ethanol seeking behaviour and successfully learned the task. Even after testing another self-

administration protocol rats still showed very low response rates on the active lever. With only around 40 % of animals successfully conditioning during self-administration training we decided to exclude ethanol from the functional validation of neuronal ensemble as the resulting benefits of the completed study would not justify the high number of rats needed to do so.

3.5 Study 3: Comparison of neuronal ensembles within the infralimbic cortex following reinstatement of saccharin and ethanol seeking behaviour

The following results are part of the publication "Choice for Drug or Natural Reward Engages Largely Overlapping Neuronal Ensembles in the Infralimbic Prefrontal Cortex", which was released in The Journal of Neuroscience, April 4, 2018 (Pfarr et al., 2018). Furthermore, they were published in Simone Pfarr's PhD thesis with the title "The Role of the Medial Prefrontal Cortex in Reward Seeking: Functional Evidence on Cellular and Molecular Mechanisms underlying Drug and Natural Reward Seeking" (Pfarr, 2018). All data (Fig. 54 - Fig. 58, Table 05 + 06) was generously provided by Simone and used with her permission as well as acquired, processed and analysed by her unless otherwise stated in either publication (Pfarr, 2018; Pfarr et al., 2018). Result analysis and interpretation was taken from either publication and re-written in own words, thus similarities cannot be excluded.

3.5.1 Study 3A: Two-reward operant conditioning for characterization of neuronal ensemble size following cue-induced reinstatement of EtOH or saccharin seeking behaviour

In order to compare neuronal ensembles activated by reinstatement of EtOH or saccharin seeking in the infralimbic cortex, animals were trained in the two-reward operant conditioning paradigm. Animals were thereby conditioned to self-administer EtOH and saccharin in presence of a discriminative cue (olfactory) in separate sessions. Reward availability was signalled by presentation of a visual cue (blink light). After all animals learned the task for both EtOH and saccharin, they were subjected to further self-administration sessions in pseudo-randomised order to achieve robust baseline responses for either reward. For both rewards animals reached a stable baseline with a similar response rate (EtOH: 88 ± 9; saccharin: 86 ± 13). Self-administration training was followed by extinction learning, where all animals showed fading of the non-reinforced response behaviour until they reached an average of 5 ± 1 lever presses

for either reward context (Fig. 54a). After extinction, animals were subjected to matched cue-induced reinstatement of reward seeking for EtOH and saccharin (RE 1+2). Animals pressed significantly more for EtOH (49 ± 4) than for saccharin (39 ± 4) (Fig. 54a, Table 05). Inactive lever responses showed no significant differences during baseline, extinction or reinstatement (Table 05). After each rat underwent one cue-induced reinstatement for either reward, they were grouped according to their performance and injected with retrograde tracers (results not shown). After a 5-day recovery period the animal's cue-induced reinstatement behaviour for the previously conditioned rewards EtOH or saccharin (RE 3) was examined (Fig. 54b). With 59 ± 4 lever presses on the active lever the EtOH group responded significantly more than the saccharin group with 40 ± 3 active lever presses (Table 05). Inactive lever presses, however, were not significantly different between groups.

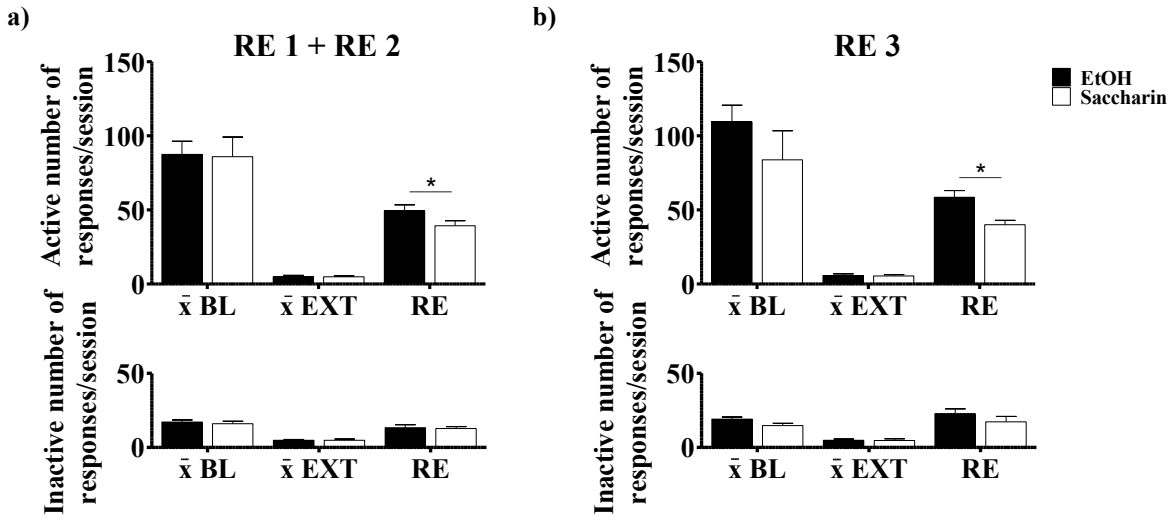

Figure 54) Average lever press responses during the different stages of the two-reward self-administration training paradigm to investigate ensemble size

a) The graph shows the average responses for the last self-administration and extinction sessions on the active and inactive lever for both rewards as well as the responses during the counterbalanced cue-induced reinstatement sessions (RE 1 + 2); n = 28. b) Displayed are the average active and inactive responses during conditioning and extinction training as well as during reward seeking for the previously associated rewards EtOH or saccharin (RE 3); n = 14/reward. All values are expressed as mean ± SEM. * $p < 0.05$, detailed statistical analysis can be found in Table 05, Abbreviations: $\bar{x}$ BL = average of the last self-administration sessions during baseline training, $\bar{x}$ EXT = average of last extinction sessions, RE = cue-induced reinstatement. Figure taken and adapted from (Pfarr, 2018; Pfarr et al., 2018).

						Newman-Keuls *post hoc* test						
	Repeated measures ANOVA					Within-group comparison			Between-group comparison		t-test (comparison active/inactive)	
Lever	**Test**	**df**	**Effect**	**F**	**p**	**Reward**	**Test**	**p**	**Test**	**p**	**Test**	**p**
Active RE 1 + RE 2	BL, EXT	1,54	**Reward**	0.01	0.917						**EtOH**	
			Session	107.94	0.0001	**EtOH**	BL, EXT	0.0001	BL	0.89	BL	0.0001
			Interaction	0.008	0.928	**Saccharin**	BL, EXT	0.0001	EXT	0.99	EXT	0.889
	EXT, RE1+2	1,54	**Reward**	3.468	0.068							
			Session	205.14	0.0001	**EtOH**	EXT, RE1+2	0.0001			RE 1+2	0.0001
			Interaction	3.246	0.077	**Saccharin**	EXT, RE1+2	0.0001	RE 1+2	0.01		
Inactive RE1 + RE2	BL, EXT	1,54	**Reward**	0.098	0.755						**Saccharin**	
			Session	159.09	0.0001	**EtOH**	BL, EXT	0.0002	BL	0.54	BL	0.0001
			Interaction	0.422	0.518	**Saccharin**	BL, EXT	0.0001	EXT	0.93	EXT	0.889
	EXT, RE1+2	1,54	**Reward**	0.029	0.865							
			Session	41.168	0.0001	**EtOH**	EXT, RE1+2	0.0002			RE 1+2	0.0001
			Interaction	0.078	0.78	**Saccharin**	EXT, RE1+2	0.0002	RE 1+2	0.75		
Active RE 3	BL, EXT	1,26	**Reward**	1.226	0.278						**EtOH**	
			Session	68.683	0.0001	**EtOH**	BL, EXT	0.0001	BL	0.12	BL	0.0001
			Interaction	1.334	0.259	**Saccharin**	BL, EXT	0.0002	EXT	0.99	EXT	0.586
	EXT, RE 3	1,26	**Reward**	9.576	0.005							
			Session	315.38	0.0001	**EtOH**	EXT, RE 3	0.0001			RE 3	0.0001
			Interaction	13.967	0.0009	**Saccharin**	EXT, RE 3	0.0001	RE 3	0.0001		
Inactive RE 3	BL, EXT	1,26	**Reward**	2.367	0.136						**Saccharin**	
			Session	107.27	0.0001	**EtOH**	BL, EXT	0.0001	BL	0.02	BL	0.0026
			Interaction	3.275	0.082	**Saccharin**	BL, EXT	0.0001	EXT	0.91	EXT	0.586
	EXT, RE 3	1,26	**Reward**	1.16	0.291							
			Session	37.699	0.0001	**EtOH**	EXT, RE 3	0.0002			RE 3	0.0003
			Interaction	1.101	0.304	**Saccharin**	EXT, RE 3	0.004	RE 3	0.14		

Table 05) Statistical analysis for two-reward operant conditioning - cFOS-ir/NeuN-ir co-localization

Statistical analysis was done using repeated measures ANOVA with subsequent Newman-Keuls *post hoc* tests. Two-tailed paired t-tests were utilised to compare active and inactive responses. Abbreviations: BL = average of the last self-administration sessions, EXT = average of last extinction sessions, RE = cue-induced reinstatement, df = degrees of freedom, F = F-value, p = p-value. Table taken and adapted from (Pfarr, 2018; Pfarr et al., 2018).

3.5.2 Study 3A: Immunohistochemical analysis of neuronal ensemble size

60 min after the end of cue-induced reinstatement session RE 3, rats were perfused and their brains processed to undergo double immunohistochemistry stainings. In order to characterize the population of previously activated cells, brain slices were exposed to an antibody against cFOS as well as an antibody against NeuN, to determine the size of the neuronal population (Fig. 55). For both groups of animals (EtOH, saccharin) all cFOS-ir positive neurons were quantified. Statistical analysis with a two-tailed, unpaired t-test revealed no significant difference in neuronal ensemble size between drug reward (14.9 % ± 0.58 %) and natural reward (15.32 % ± 0.63 %) ($t(1,26) = 0.49$, $p = 0.63$, n = 14/reward).

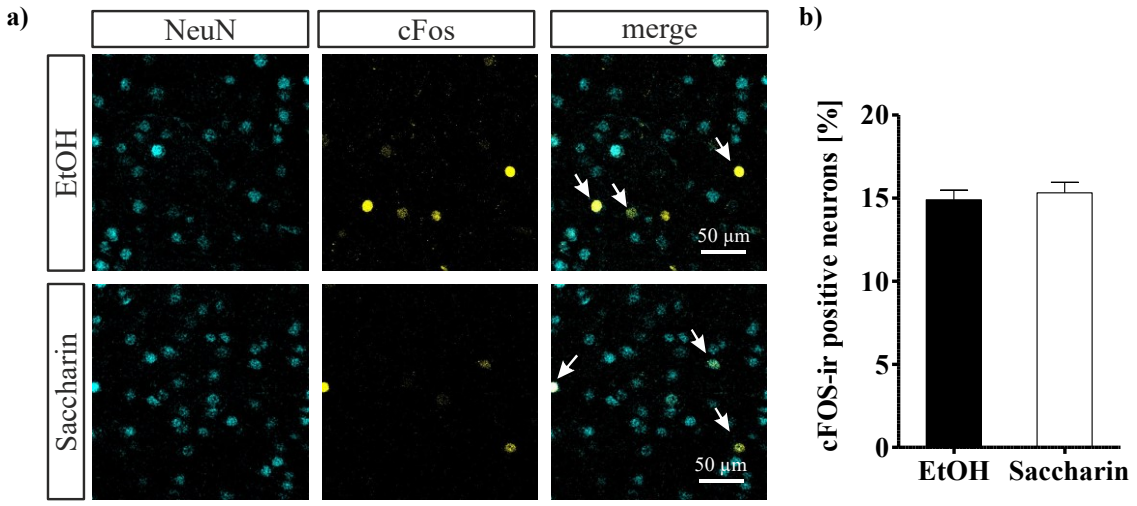

Figure 55) Co-localization of cFOS-ir positive and NeuN-ir positive cells in brain slices after ethanol or saccharin cue-induced reinstatement

a) Representative confocal laser scanning microscopy images of cFOS-ir/NeuN-ir double immunostainings (cFOS-ir = yellow, NeuN-ir = blue, cFOS-ir/NeuN-ir merge = green). Arrows indicate co-localization. b) Percentage of cFOS-ir positive neurons within the infralimbic cortex following EtOH or saccharin seeking. n = 14/reward; All values are expressed as mean ± SEM. Figure taken and adapted from (Pfarr, 2018; Pfarr et al., 2018).

3.5.3 Study 3B: Two-reward operant conditioning for characterization of neuronal ensemble distinctness following cue-induced reinstatement of natural and drug reward seeking

Investigation of neuronal ensemble size showed that neuronal ensembles that were induced during reinstatement of EtOH or saccharin seeking are of similar size (Fig. 55b). However, it is not clear whether these ensembles are identical or distinct from each other. This question could be answered with help of the two-reward conditioning model in combination with a double *c-fos* fluorescent *in situ* hybridization approach to investigate neuronal ensemble activation for both rewards within the same animal. Therefore, animals were again trained in the two-reward self-administration paradigm in order to learn to associate cues presented in the EtOH context with EtOH availability and cues presented in the saccharin context with saccharin availability. After achieving the task for both rewards, animals were trained in further pseudo-randomised self-administration sessions in order to acquire robust response rates for either reward. On average animals pressed 91 ± 11 times on the active lever for EtOH and 112 ± 12 times on the active lever for saccharin during the last self-administration sessions (Fig. 56a). The animal's motivation to achieve either reward was examined in course of the self-administration training with help of a progressive ratio test. During the test animals must progressively increase their responses on the active lever in order to receive their reward. The point at which their responding for the reward ceases, is the so-called breakpoint. Analysis revealed a significant difference between the breakpoint for both rewards, with the EtOH breakpoint being higher than that for saccharin ($t(1,46) = 3.122$, $p = 0.0031$, two-tailed, paired t-test; data not shown). After the conditioning phase rats were subjected to extinction training which resulted in continuous fading of non-reinforced response behaviour until animals reached an average of 8 ± 1 lever presses during the last extinction sessions. The counterbalanced cue-induced reinstatement sessions demonstrated significantly higher lever presses for the EtOH condition compared to the saccharin condition (EtOH: 49 ± 4, Saccharin: 36 ± 3) (Fig. 56a, Table 06). Following reinstatement rats were grouped according to their response during RE 1 + 2. Both groups were then subjected to a final reinstatement test, consisting of two 5 min reinstatement sessions separated by a 30 min break. Reinstatement was tested in a counterbalanced manner with one of the two groups starting with a cue-induced reinstatement session for EtOH seeking and the other beginning with a reinstatement session under saccharin conditions. From 24 animals tested only 14 reinstated successfully and were used for further analysis (EtOH: 15 ± 2, Saccharin: 12 ± 1) (Fig. 56b). Two-tailed unpaired t-tests revealed no significant differences

between the order of first vs. second cue-induced reinstatement for either reward (EtOH: t (1,12) = 0.73, p = 0.46; saccharin: t (1,12) = 0.07, p = 0.95). Despite the short duration of the reinstatement sessions (5 min each) animals were able to distinguish between active and inactive lever as it was shown by a significant difference in lever pressing for each reward (EtOH: t (1,13) = 8.33, p = 0.0001; saccharin: t (1,13) = 7.01, p = 0.0001, two-tailed, paired t-test). However, no significant difference could be observed between active lever presses for the reinstatement of EtOH and saccharin seeking (t (1,13) = 1.56, p = 0.14, two-tailed, paired t-test). As all animals were able to distinguish the two reward conditions and no difference between first and second reinstatement was found, data could be pooled for analysis.

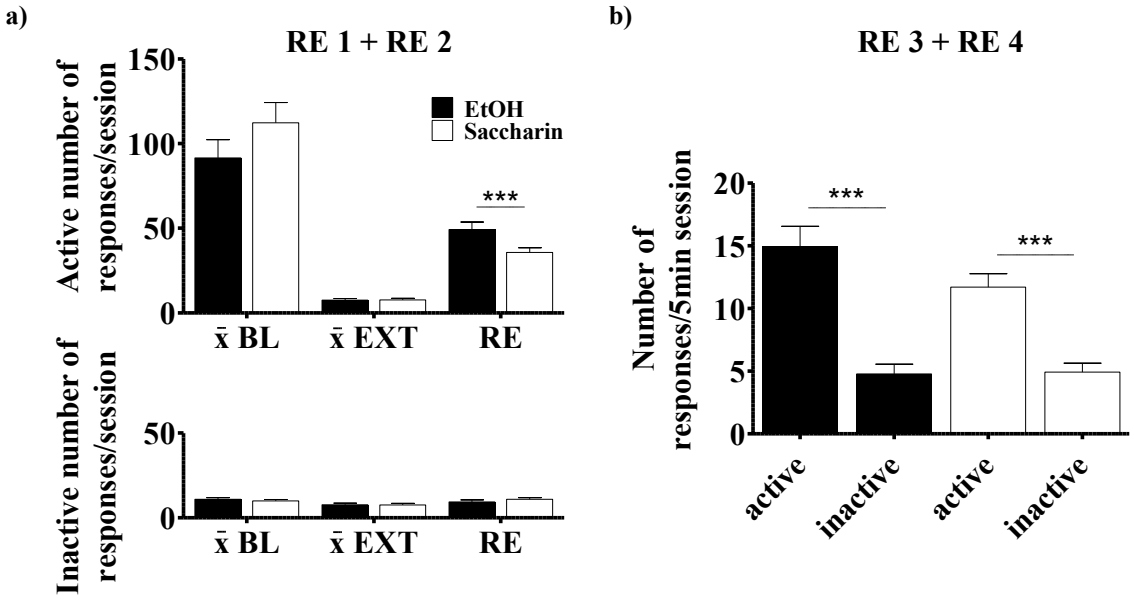

Figure 56) Average lever press responses during the different stages of the two-reward self-administration training paradigm to examine the distinctness of involved ensembles

a) Illustrated are the average responses for the last self-administration and extinction sessions on the active and inactive lever for both rewards as well as the responses during the counterbalanced cue-induced reinstatement sessions (RE 1 + 2); n = 24. b) The graph shows active and inactive responses during reinstatement RE 3 + 4 for both rewards; n = 14. All values are expressed as mean ± SEM. *** $p < 0.001$, detailed statistical analysis can be found in Table 06 and within the text, Abbreviations: $\bar{x}$ BL = average of the last self-administration sessions during baseline training, $\bar{x}$ EXT = average of last extinction sessions, RE = cue-induced reinstatement. Figure taken and adapted from (Pfarr, 2018; Pfarr et al., 2018).

						Newman-Keuls *post hoc* test						
	Repeated measures ANOVA					Within-group comparison			Between-group comparison		t-test (comparison active/inactive)	
Lever	**Test**	**df**	**Effect**	**F**	**p**	**Reward**	**Test**	**p**	**Test**	**p**	**Test**	**p**
Active	BL, EXT	1,46	**Reward**	1.547	0.219						**EtOH**	
			Session	146.81	0.0001	**EtOH**	BL, EXT	0.0001	BL	0.07	BL	0.0001
			Interaction	1.771	0.189	**Saccharin**	BL, EXT	0.0001	EXT	0.99	EXT	0.949
	EXT, RE1+2	1,46	**Reward**	5.551	0.023							
			Session	176.80	0.0001	**EtOH**	EXT, RE1+2	0.0002			RE1+2	0.0001
			Interaction	6.788	0.012	**Saccharin**	EXT, RE1+2	0.0001	RE	0.0009		
Inactive	BL, EXT	1,46	**Reward**	0.219	0.642						**Saccharin**	
			Session	16.127	0.0002	**EtOH**	BL, EXT	0.006	BL	0.48	BL	0.0001
			Interaction	0.336	0.565	**Saccharin**	BL, EXT	0.049	EXT	0.95	EXT	0.949
	EXT, RE1+2	1,46	**Reward**	0.394	0.533							
			Session	7.285	0.009	**EtOH**	EXT, RE1+2	0.195			RE1+2	0.0001
			Interaction	0.707	0.405	**Saccharin**	EXT, RE1+2	0.073	RE	0.31		

Table 06) Statistical analysis for two-reward operant conditioning - double fluorescent *in situ* hybridization

Statistical analysis was done using repeated measures ANOVA with subsequent Newman-Keuls *post hoc* tests. Two-tailed paired t-tests were utilised to compare active and inactive responses. Abbreviations: BL = average of the last self-administration sessions during baseline training, EXT = average of last extinction sessions, RE = cue-induced reinstatement, df = degrees of freedom, F = F-value, p = p-value. Table taken and adapted from (Pfarr, 2018; Pfarr et al., 2018).

3.5.4 Study 3B: Double *c-fos* fluorescent *in situ* hybridization following EtOH and saccharin cue-induced reinstatement

Following the second 5 min cue-induced reinstatement animals were sacrificed and their brains processed for further analysis with double fluorescent *in situ* hybridization. Hybridization was done using the RNAscope method. Nascent (unspliced) *c-fos* mRNA was detected with a probe called Rn-Fos-Intron1-C3 and mature (spliced) *c-fos* mRNA with the probe Rn-Fos-o1-C2. Each probe was labelled with a fluorescent marker (C2 with Alexa 488; C3 with Atto 647). After hybridization brain slices were counterstained with DAPI. Afterwards images were recorded and analysed (Fig. 57). The amount of spliced *c-fos* mRNA expressing neurons after reinstatement for EtOH or saccharin revealed no significant differences between the two groups (EtOH: 25 % ±1 % vs. saccharin 23.5 % ± 2 %; t (1,12) = 0.715, p = 0.4883;

two-tailed unpaired t-test). The expression of unspliced *c-fos* mRNA was also non-significant after EtOH or saccharin seeking for either population (EtOH: 49.4 % ± 2 % vs. saccharin: 50.6 % ± 2 %; t (1,12) = 0.44, p = 0.6706, two-tailed unpaired t-test). However, most interesting was the overlay of spliced and unspliced *c-fos* mRNA as it should indicate whether neuronal ensembles induced by EtOH and saccharin seeking are distinct or overlapping. Analysis of co-localized *c-fos* mRNA species revealed that about 50 % of both neuronal ensembles were overlapping with each other (Fig. 57b). Thereby the order in which the reinstatement was performed was irrelevant (t (1,12) = 1.19, p = 0.257, two-tailed unpaired t-test) (Fig. 57c).

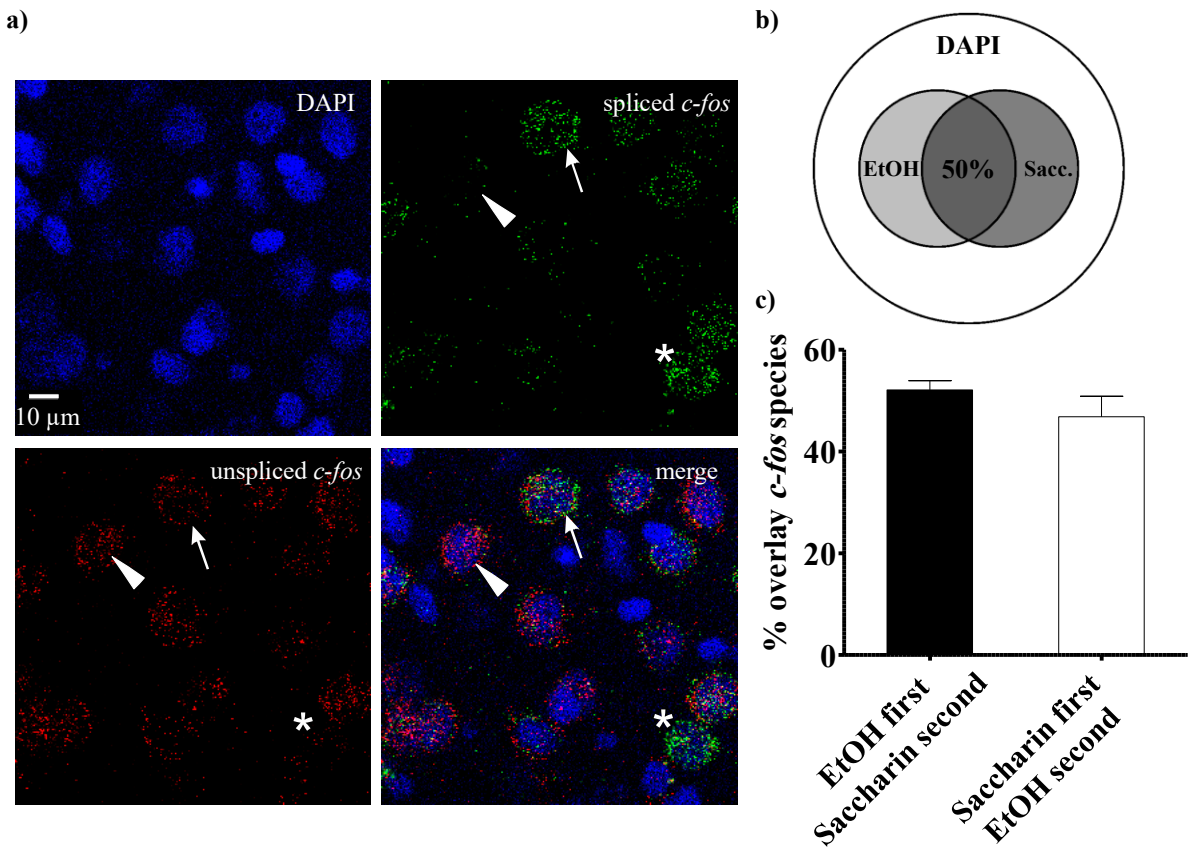

Figure 57) Fluorescent *in situ* hybridization for nascent and mature *c-fos* mRNA following cue-induced reinstatement of EtOH and saccharin seeking

a) Representative confocal laser scanning microscopy images of double *c-fos* fluorescent *in situ* hybridization staining for unspliced (red) and spliced (green) *c-fos* mRNA and counterstaining with DAPI (blue). A double positive cell is indicated by white arrows, a single positive neuron for spliced *c-fos* mRNA by asterisks and a single positive neuron for unspliced *c-fos* mRNA by white triangles. b) The Venn diagram shows the proportion of EtOH and saccharin neuronal ensembles in relation to the total cell population, indicated by DAPI. c) The graph displays the amount of co-localization for both *c-fos* species. All values are expressed as mean ± SEM., Abbreviation: Sacc. = saccharin. Figure taken and adapted from (Pfarr, 2018; Pfarr et al., 2018).

According to bootstrap analysis performed by Janine K. Reinert the investigated distribution of cells obtained during double *c-fos* fluorescent *in situ* hybridization is significantly different

from a cell population that was sampled randomly (Fig. 58), indicating highly robust data. It furthermore shows that the order of the reward condition reinstated first has no effect on the obtained results.

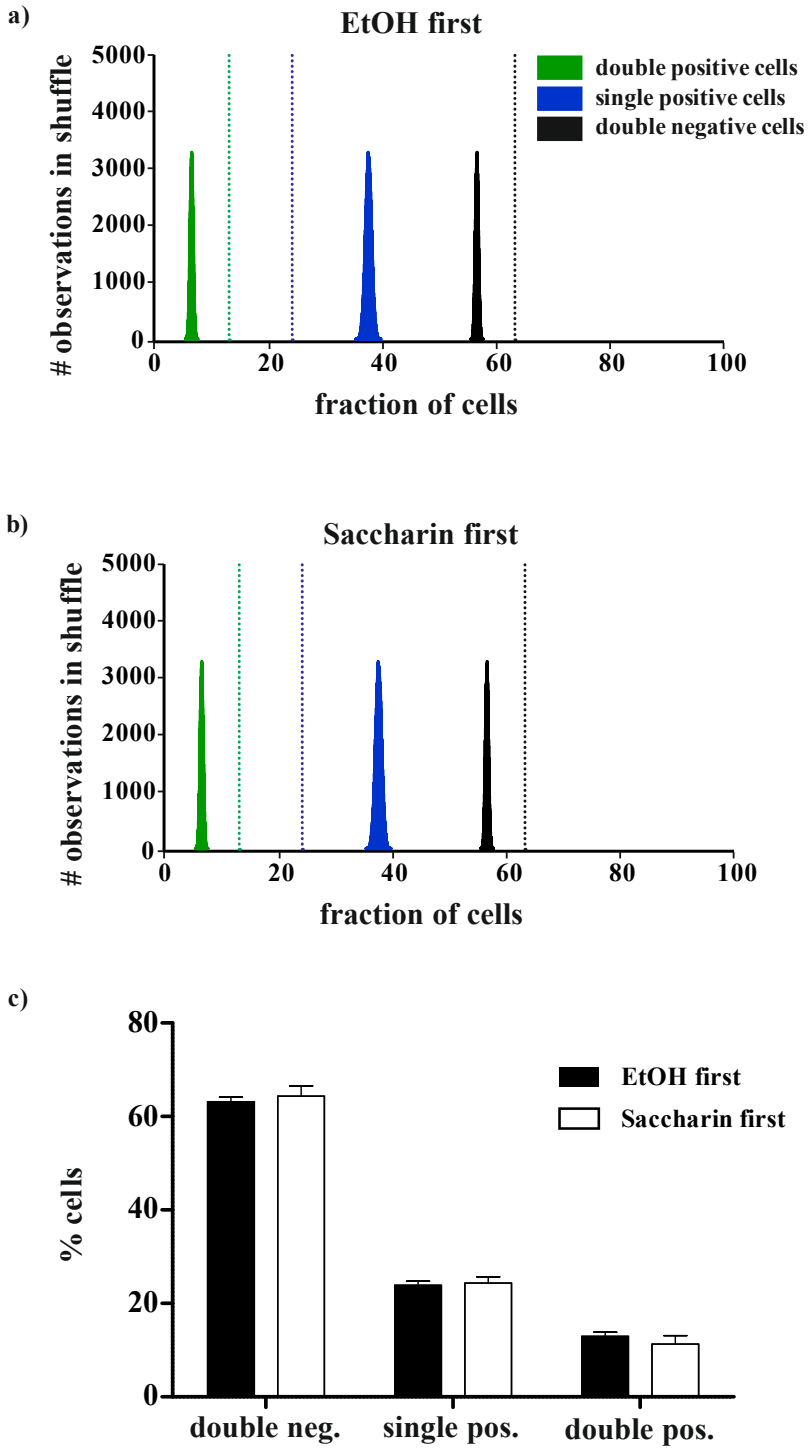

Figure 58) Bootstrap analysis of cell populations expressing both, one or none of the *c-fos* mRNA species examined

a)/b) Graphs of the random distribution of double positive, single positive and double negative cells after 100,000 shuffles. Cell fractions, that were experimentally obtained, are indicated by dashed vertical lines. c) Percentage of cells that are double negative, single positive or double positive for the *c-fos* mRNA species investigated. Values are expressed as mean ± SEM., Figure taken and adapted from (Pfarr, 2018; Pfarr et al., 2018).

3.6 Troubleshooting

Study 1C:

Study 1C had the aim to characterize the physiological properties of neuronal ensembles active during cue-induced reinstatement of reward seeking behaviour. *c-fos*-GFP transgenic rats were used in order to identify co-active cells in acute brain slices via GFP fluorescence. Unfortunately, the fluorescent microscope set up at our institute was not sensitive enough to detect the fluorescence emitted by GFP. For that reason, a collaboration with Dr. Peter Bengtson at the neurobiology division of the Interdisciplinary Centre for Neuroscience at Heidelberg University was established. In the following, we were able to perform our recordings in Heidelberg. However, behavioural training of the animals as well as cue-induced reinstatement of reward seeking behaviour still had to be conducted at the Central Institute of Mental Health in Mannheim. In order to perform electrophysiological recordings in Heidelberg, samples had to be transported to Dr. Bengtson's laboratory immediately after the cue-induced reinstatement test. Animals were perfused with a aCSF/20 % sucrose solution before the brain was extracted. Brains were placed into chilled and carbogen saturated aCSF/20 % sucrose solution to prevent and slow down cell death during transportation. In addition, samples were kept on ice inside an air-sealed and carbogen saturated transportation box. Transportation of the brains from Mannheim to Heidelberg took around 30 min. Including all steps from perfusion to transportation to slice preparation approximately 90 min passed between end of the experiment and the start of electrophysiological measurements. Because of the transportation process and all obstacles involved, cell health was less than ideal for electrophysiological examination (Fig. 59). Matters were complicated further by problems with one of the lasers of the fluorescence microscope, which aggravated identification of GFP positive neurons for a couple of weeks until the issue was solved. After nine months only eight healthy neurons (3 GFP negative and 5 GFP positive) could be recorded from 5 out of 40 rats. As a disproportionate number of animals, time and workload would have been needed to complete the experiment for all four rewards, it was decided to terminate further electrophysiological characterizations.

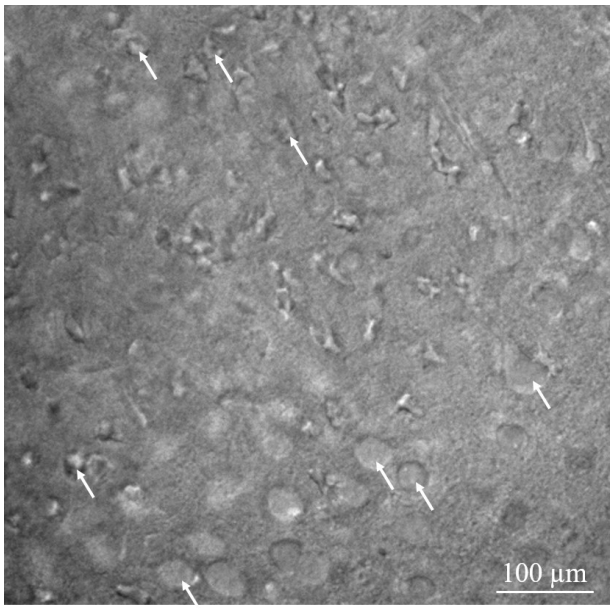

Figure 59) Differential interference contrast image of an acute OFC brain slice

The microscope image shows a segment of an acute OFC brain slice during electrophysiological examination. White arrows indicate dead or unhealthy neurons.

Study 2:

The validation of functional relevance of neuronal ensembles involved in reward seeking behaviour was done by using *c-fos*-lacZ transgenic rats breed on a Sprague-Dawley background. During Study 2 two main problems emerged, of which one was a behavioural issue and the other an equipment related one. The behavioural problem was expressed by a very high variability in lever press performance between animals trained to the same drug with a variation of up to 10 times. Also, individual animals displayed high day to day performance fluctuations during self-administration with increases or decreases of up to 10 x. In addition, a large proportion of animals was lever pressing below 20 times per session and therefore had to be excluded from the experiment (e.g., only about 40 % of ethanol trained animals conditioned successfully). Another proportion of animals was lost during cue-induced reinstatement as animals did not show increased reward seeking even though they successfully learned the self-administration procedure and also successfully completed extinction training. The complications during self-administration training and cue-induced reinstatement could be down to the well-known poor self-administration performance in Sprague Dawley rats, especially for ethanol. Another factor that might have affected behavioural performance were the long-lasting and still ongoing constructions at the Central Institute of Mental Health from 2016 until today. The construction noise could have had a negative impact on the animal's behaviour especially as rats were bred and raised in our own breeding facility.

The equipment related issue was present only in animals trained to cocaine self-administration as the catheter of some animals became dysfunctional after a couple of days despite proper maintenance. Animals, whose catheter became dysfunctional were re-implanted (paragraph 2.4.1.3). In this way most animals could be rescued for the experiment, however a proportion of animals had to be excluded from the experiment because the catheter was not working even after replacement. In order to examine the reason for the dysfunctional catheter a few animals were dissected and the implant analysed. The dissection revealed no problems with the implantation itself and also the catheter was still intact. However, the catheters became dysfunctional as part of the vein, the catheter was implanted in, grew around the catheter exit and blocked it. As this problem never happened that frequently or early in any of the other intravenous self-administration experiments of the thesis, it seemed that it was a specific problem with this transgenic rat strain.

4. DISCUSSION

The present thesis gives new insight into the involvement of neuronal ensembles in cue-induced reward seeking behaviour and proves distinctness of the investigated ensembles' features in a reward dependent manner.

Study 1A demonstrated that neuronal activity induced by cue-induced reward seeking behaviour for either natural rewards or drugs of abuse displayed broadly overlapping activation patterns within the extended reward system of rodents, especially within the PFC. The most prominent c-*fos* activation was detected within the OFC of animals conditioned to self-administer EtOH, saccharin, cocaine or nicotine. In addition to these similar activity patterns, distinct increases in *c-fos* expression were also observed for EtOH (BLA), Saccharin (VTA) and both psychostimulants (AcbC).

In order to investigate the reward-dependent distinctness of activated neuronal ensembles in greater detail, Study 1B examined their neurochemical composition within the OFC during cue-induced reinstatement of reward seeking behaviour. Immunohistochemical co-localization studies showed that ensembles activated during cue-induced reward seeking were entirely neuronal. Furthermore, the double immunohistochemistry approach could demonstrate that neuronal ensembles in the OFC were distinct in their neurochemical composition depending on the reward they were associated with. Whilst the natural reward saccharin was found to have approximately a similar amount of activation between glutamatergic and GABAergic neurons, EtOH associated ensembles recruited primarily GABAergic neurons whereas neuronal ensembles encoding for cocaine seeking behaviour were mainly glutamate driven.

Study 2 evaluated the functional relevance of identified ensembles and could reveal that the lateral OFC contains a functional ensemble responsible for the control of saccharin seeking. Furthermore, it showed that the ventral OFC contains a neuronal ensemble that might as well be involved in control of saccharin seeking behaviour. Animals that were trained to self-administer cocaine however showed no changes in cocaine seeking behaviour upon inactivation of neuronal ensembles within the lateral or ventral OFC.

A last set of experiments (Study 3) compared neuronal ensembles within the IL active during EtOH seeking and saccharin seeking. The study revealed that both neuronal ensembles were of similar size. A co-localization study of different *c-fos* mRNA species within the same animal furthermore showed that both the neuronal ensemble activated by EtOH cues and the neuronal ensemble activated by saccharin cues were distinct but also largely overlapping.

4.1 Study 1: Identification of neuronal ensembles within the extended reward system encoding for natural reward and drug reward seeking

4.1.1 Operant conditioning to identify neuronal ensembles within the extended reward system encoding for natural reward and drug reward seeking

In order to study neuronal ensembles involved in reward seeking behaviour the drug-self-administration and reinstatement model was used, as it is a valid and widely utilised model to investigate relapse-like behaviours (Epstein et al., 2006; Sanchis-Segura and Spanagel, 2006; Martin-Fardon R., 2012; Marchant et al., 2013; Spanagel, 2017). It furthermore presented itself as valuable model to examine neuronal ensembles active during reward seeking (Bossert et al., 2011; Fanous et al., 2012; Cruz et al., 2013; George and Hope, 2017; Pfarr et al., 2018; Warren et al., 2019; Kane et al., 2020). The model is essentially composed of three phases. During the operant conditioning phase animals learn to acquire stable reward self-administration, followed by an extinction phase during which their operant response behaviour gets extinguished. In a final step cue-induced reinstatement of the animal's reward seeking behaviour is tested.

Given the different reinforcement effects of the rewards used in this thesis, their concentrations had to be adjusted to rule out potential biases in neuronal ensemble activation due to simple increases in activity. An ethanol concentration of 10 % was predetermined and used as reference, since this concentration was reliably used in our laboratory for years. A small pilot study was then utilised to determine the concentration of the other rewards necessary to match the rat's performance during self-administration of 10 % ethanol. The resulting concentrations were 0.04 % for saccharin, 0.125 mg/kg for cocaine and 0.01 mg/kg for nicotine. Once all concentrations were determined, animals were trained in the operant self-administration paradigm.

During the first days of self-administration training animals slowly acquired the task of pressing a lever in order to receive a reward, which was paired with a cue light. Once the rats learned the association of lever pressing and reward delivery, their responding became more robust and they reached a stable baseline during the last five days of drug self-administration. On average responses for EtOH, cocaine and nicotine were roughly within the same range, whereas animals trained to saccharin pressed much higher, despite the low saccharin concentration determined during the pilot study. However, other self-administration studies investigating drugs of abuse and natural rewards also showed that responses for the natural reward (glucose/saccharin solution or sweetened condensed milk) can indeed be higher than

those for drugs of abuse, even though the concentrations used for the natural reward were quite high (Martin-Fardon and Weiss, 2014, 2017). In Study 1B animals showed higher variability in their response rate within each group, which could mainly be accounted for by the small number of animals used but could also have been influenced by the ongoing construction noise at our institute as described in paragraph 3.5; Study 2. However, none of these discrepancies (higher response rate for saccharin, high in-group variability in Study 1B) seemed to effect extinction learning as the rat's response rate dropped on their first extinction day and gradually continued to decrease until their response behaviour was extinguished. After successful extinction, which was achieved as soon as the animals presses less than 20 % of their baseline responses, the subject's cue-induced reinstatement of reward seeking behaviour was examined or another extinction session (Study 1A). Animals subjected to the cue-induced reinstatement session displayed a strong and robust reinstatement of their reward seeking behaviour compared to their average responses during the last four extinction sessions. All rats were therefore successfully conditioned to the cue light as re-exposure to the previously with reward availability associated stimulus triggered strong relapse-like behaviour with increases between 2.2- to 5.6-fold. Thereby the EtOH-paired light stimulus increased responses by 2.2-fold and 2.6-fold in studies 1A and 1B, respectively. The saccharin-paired cue increased lever presses by 2.6-fold (Study 1A) and 2.3-fold (Study 1B), whereas the nicotine-paired stimulus triggered a 3.0-fold increase. Reinstatement of reward seeking was strongest for cocaine-paired cue light presentation with elevations of 5.6-fold (Study 1A), 5.5-fold (Study 1B) and 5.0-fold (Study 1C). These results of cue-induced reinstatement demonstrated that the natural reward saccharin as well as the three drugs of abuse have reinforcement-enhancing effects on visual stimuli that were paired with the respective reward (Palmatier et al., 2006). Thereby the four rewards displayed differences in the strength of their ability to enhance reinforcing effects, with EtOH and saccharin having a similar effect, closely followed by nicotine and with the strongest effect shown by cocaine. This might be attributed to their different mechanisms of action, the distinct primary reinforcing effects and the dosage of the drugs used (Schuster and Thompson, 1969). Some studies however showed that rats, when given the choice, would almost always prefer saccharin over other drugs of abuse (Lenoir et al., 2007; Madsen and Ahmed, 2015; Pfarr et al., 2018). A study by Pfarr et al., 2018, on the other hand, showed that when the same rats were trained to a saccharin reward and an ethanol reward, reinstatement for ethanol would be significantly higher than for saccharin, despite similar responses during self-administration (Pfarr et al., 2018). These differences between studies imply that self-administration and reinstatement for natural rewards and drugs of abuse are complex processes, which are affected by multiple internal and external

factors, shifting the behavioural output in either direction. Nonetheless, re-exposure to the cue light had a similar reinforcement enhancing effect for the same drug between the different studies demonstrating methodological robustness. Thus, data within Study 1 can be reliably compared between batches.

For inactive lever presses no differences were detectable between extinction and reinstatement sessions, demonstrating that the animals had learned the different behavioural contingencies.

Animals, that were subjected to one more extinction session instead of a cue-induced reinstatement session (Study 1A), showed no significant differences in their behaviour compared to previous extinction sessions. Responses made on the inactive lever showed no differences as well.

The behavioural results discussed above demonstrate the successful acquisition of reward self-administration and establishment of a strong cue-reward association, which was able to elicit robust relapse-like behaviour upon cue re-exposure after a withdrawal-like phase. Therefore, the utilised drug-self-administration and reinstatement model provides a reliably and robust paradigm to investigate neuronal ensembles involved in reward seeking behaviour.

4.1.2 Study 1A: Mapping of *c-fos* mRNA expression patterns following natural reward and drug reward seeking

4.1.2.1 *c-fos* mRNA expression during cue-induced reinstatement of reward seeking

Environmental stimuli, that are paired with reward consumption and thus are associated with reward availability, become conditioned stimuli, which are able to control reward seeking behaviour (Lamb et al., 2016). Exposure to these cues results in increased neuronal activity within brain regions of the extended reward system that are involved in reward seeking and reward consumption (Kareken et al., 2012; Ranaldi, 2014). The activity pattern elicited by conditioned stimuli is thought to be similar to the neuronal response triggered by the drug itself, since conditioned and unconditioned responses are typically equal (Stewart et al., 1984; Van Hedger et al., 2018). One method to reliably map activity within the central nervous system is the analysis of *c-fos* mRNA expression patterns (Kovács, 2008).

In order to identify brain regions within the extended reward system activated by reward-associated cues, we used a radioactive *in situ* hybridization approach. *c-fos* mRNA mapping revealed overarching neuronal activation throughout the entire reward system. The activation

was mainly focused on the PFC, with broadly overlapping *c-fos* expression pattern for all four rewards. However, *c-fos* expression was also found on the subcortical level, where some regions displayed reward specific activation.

The strong activation of the PFC during reward seeking is consistent with its participation in high-level cognitive processing and limbic reward system modulation. Its specific involvement in compulsive behaviours, the drive to reward seeking and consumption, the strengthening of reward related memories, the attentional shift towards reward-related stimuli and decision making in anticipation of the reward make it a critical brain region during reward-learning and addiction development (Goldstein and Volkow, 2002, 2011; Wang et al., 2018). A more detailed analysis of PFC subregions revealed similar activation patterns between the different rewards, however, the intensity of their activation differed (Table 07). The most prominent change in activation within the PFC was displayed within the OFC with 1.6 to 3.8-fold increases compared to other prefrontal subregions. This finding confirms the crucial role of the OFC during reward seeking, which was demonstrated in previous studies examining different aspects of different drug seeking behaviours (Fuchs et al., 2004; Moorman, 2018; Reiner et al., 2020). It could also be shown that reward seeking increases *c-fos* expression within the OFC (Jupp et al., 2011; Bal et al., 2019). The second strongest activation was found within the cingulate cortex for alcohol, nicotine and saccharin trained animals, whereas for cocaine trained animals Cg activation was the third highest. Increased levels of *c-fos* expression during reward seeking were previously found for different drugs of abuse (Dayas et al., 2007; Hearing et al., 2008). Several studies investigated the involvement of Cg in reward seeking and could testify its importance during this behaviour (Baeg et al., 2009; Gremel et al., 2011; Madsen et al., 2012). Activity within the prelimbic cortex was the next highest activity for the rewards alcohol, saccharin and nicotine, whereas the prelimbic cortex showed the second highest activity in the PFC of cocaine trained animals. The prelimbic cortex was found to be critical in mediating reward seeking behaviour for different drugs and natural rewards (Ciccocioppo et al., 2001b; Schroeder et al., 2001; Schroeder and Kelley, 2002; Miller and Marshall, 2004; West et al., 2014; Whitaker et al., 2017). The infralimbic cortex, which was found to be strongly involved in reward seeking for various drugs like alcohol, heroin, cocaine or natural rewards (Bossert et al., 2011; Pfarr et al., 2015; Warren et al., 2016; Pfarr et al., 2018; Kane et al., 2020), showed second lowest activity within the PFC for all four rewards. For both PrL and IL increased neuronal activity was demonstrated during reward seeking behaviours (Dayas et al., 2007; Bossert et al., 2011; Pfarr et al., 2015; Suto et al., 2016; Warren et al., 2016; Kane et al., 2020). Lowest neuronal activity within the PFC was displayed by the agranular insular cortex.

Whereas saccharin and cocaine trained animals displayed no activation of the agranular insular cortex, both EtOH and nicotine trained animals showed increased *c-fos* expression within this brain region. A study by Campbell et al., 2019 showed that the insular cortex plays a causal role in relapse to reward seeking of EtOH (Campbell et al., 2019). The importance of the insular cortex during cue-induced nicotine seeking on the other hand was demonstrated in an inactivation study, which showed attenuated seeking behaviour after baclofen/muscimol treatment (Pushparaj et al., 2015). To our knowledge this is the first comprehensive study comparing *c-fos* mRNA expression between different PFC subregions following reward seeking for different drugs. However, Kufahl et al, 2009 investigated *c-fos* mRNA and cFOS protein expression within the prefrontal cortex of rats following cocaine seeking. *c-fos* mRNA *in situ* hybridization revealed strong activation throughout the entire PFC even though it was not able to show differences in expression between PFC subregions. Investigation of cFOS-ir within the different subregions of the PFC, however, revealed a quite similar expression pattern as it was found in the present study (Kufahl et al., 2009).

	Cg	**PrL**	**IL**	**OFC**	**IC**
EtOH	↑ (2)	↑ (3)	↑ (4)	↑ (1)	↑ (5)
Saccharin	↑ (2)	↑ (3)	↑ (4)	↑ (1)	=
Cocaine	↑ (3)	↑ (2)	↑ (4)	↑ (1)	=
Nicotine	↑ (2)	↑ (3)	↑ (4)	↑ (1)	↑ (5)

Table 07) Summary of *c-fos* activation within the PFC following cue-induced reward seeking

The table shows how neuronal activation changed within the PFC following reward seeking compared to control animals (Fig. 26). ↑ increase in activity, = no change in activity, numbers indicate the intensity of neuronal activation, whereby (1) symbolizes highest activity. Abbreviations: Cg = cingular cortex, PrL = prelimbic cortex, IL = infralimbic cortex, OFC = orbitofrontal cortex, IC = insular cortex.

On a subcortical level *c-fos* expression was more subtle and not as widespread as within the PFC. In return reward specific neuronal activation could be observed within distinct brain regions (Table 08). Of the subcortical brain regions investigated only the CPu showed similar activity patterns between the different rewards. The dorsal striatum was found to be crucial for goal-directed behaviours, habitual actions, reward learning and other drug-related behaviours (Reynolds et al., 2001; Bossert et al., 2009; Burton et al., 2015; Gremel and Lovinger, 2017; Oh et al., 2020) as well as to be directly involved in craving as dopamine levels in the dorsal striatum increase due to conditioned stimulus presentation (Volkow et al., 2006). Increased *c-fos* expression within the CPu was, for example, shown for context-induced induced methamphetamine seeking behaviour (Rubio et al., 2015).

	CPu	AcbC	AcbS	BLA	VTA
EtOH	↑	=	=	↑	=
Saccharin	↑	=	=	=	↓
Cocaine	↑	↑	=	=	=
Nicotine	↑	↑	=	=	=

Table 08) Summary of *c-fos* activation within subcortical brain regions following cue-induced reward seeking

Changes of neuronal activation within various subcortical brain regions following cue-induced reward seeking in comparison to control animals (Fig. 26). ↑ increase in activity, = no change in activity, ↓ decrease in activity. Abbreviations: AcbC = nucleus accumbens core, AcbS = nucleus accumbens shell, CPu = caudate putamen, BLA = basolateral amygdala, VTA = ventral tegmental area.

Except from the similarities displayed, activity mapping also revealed distinct changes in the reward system after re-exposure to the conditioned stimulus. Both psychostimulant trained animal groups, for example, displayed increased neuronal activity within the AcbC, a brain region, which plays a key role within the mesocorticolimbic dopamine system. The AcbC was shown to mediate reward processing and reward seeking for different psychostimulants, like cocaine, amphetamine and nicotine (Rocha and Kalivas, 2010; D'Souza and Markou, 2014; McGlinchey et al., 2016; Scheyer et al., 2016; Gao et al., 2017; Burton et al., 2018; Powell et al., 2019) and showed increased *c-fos* expression during reward seeking (Miller and Marshall, 2004; Cruz et al., 2014). EtOH and saccharin trained animals, on the other hand, showed no changes in neuronal activity within the AcbC. In addition, none of the reward-associated cues activated the AcbS, even though the nucleus accumbens was shown to be involved in cue-induced reinstatement behaviour in several studies (Dayas et al., 2007; Chaudhri et al., 2010; Sinclair et al., 2012; Millan et al., 2015). Nonetheless, involvement of the nucleus accumbens in different reward seeking behaviours was found to be highly inconsistent (Ciccocioppo et al., 2001a; Hamlin et al., 2006; Dayas et al., 2007; Marinelli et al., 2007) This could be due to several reasons, such as different training protocols and methodologies used to measure nucleus accumbens participation as well as masking localized effects by analysing subregions as single anatomical structure (Marinelli et al., 2007). These localized effects on nucleus accumbens could not only be shown for reward seeking (Hamlin et al., 2006; Hamlin et al., 2007) but also for acute drug exposure (Brenhouse and Stellar, 2006).

For EtOH a discrete increase was found within the BLA, which was already shown to be crucial during context-induced and cue-induced alcohol seeking (Marinelli et al., 2010; Sciascia et al., 2015). In addition, the BLA was found to mediate anxiety-driven alcohol consumption and relapse behaviour (Varodayan et al., 2017). BLA *c-fos* expression levels were also found

to be significantly increased following re-exposure to EtOH associated context (Marinelli et al., 2007).

Even though the VTA is known to play a major role in motivation and reward, especially in the processing of stimuli that are reward related (Volkow and Morales, 2015), none of our reward-associated cues increased activity within the VTA. Saccharin trained rats even displayed decreased activity compared to the control group. However, even if dopaminergic neurons of the VTA get activated by reward-predicting cues they also get inhibited when the expected reward does not appear (Volkow and Morales, 2015). As no rewards are delivered during our reinstatement paradigm, inhibition of VTA neurons could be an explanation for the basal *c-fos* mRNA levels detected.

4.1.2.2 *c-fos* mRNA expression during extinction

For all four rewards one group of animals was tested in an additional extinction session to examine activity levels during this condition. Interestingly, the activity pattern expressed during the extinction condition was quite similar to the pattern displayed during reward seeking behaviour. The PFC also seems to play a key role during extinction learning as it showed high and overlapping activation for all four reward conditions (Table 09). Again, the OFC was the subregion with the highest activity followed by the cingulate cortex, the prelimbic cortex (EtOH, Cocaine, Nicotine) and the infralimbic cortex (EtOH, Cocaine, Nicotine). For saccharin trained animals the infralimbic cortex showed slightly higher activation than the prelimbic cortex. Aside from overlaps on the cortical level, the dorsal striatum as subcortical region, also seems to be crucially involved during extinction since it displayed increased activity (Table 10).

	Cg	PrL	IL	OFC	IC
EtOH	↑ (2)	↑ (3)	↑ (4)	↑ (1)	=
Saccharin	↑ (2)	↑ (4)	↑ (3)	↑ (1)	=
Cocaine	↑ (2)	↑ (3)	↑ (4)	↑ (1)	=
Nicotine	↑ (2)	↑ (3)	↑ (4)	↑ (1)	↑ (5)

Table 09) Summary of *c-fos* activation within the PFC during extinction

The table shows how neuronal activation changed within the PFC during extinction compared to control animals (Fig. 27). ↑ increase in activity, = no change in activity, numbers indicate the intensity of neuronal activation, whereby (1) symbolizes highest activity. Abbreviations: Cg = cingular cortex, PrL = prelimbic cortex, IL = infralimbic cortex, OFC = orbitofrontal cortex, IC = insular cortex.

	CPu	AcbC	AcbS	BLA	VTA
EtOH	↑	=	=	↑	=
Saccharin	↑	=	=	↑	=
Cocaine	↑	=	=	=	=
Nicotine	↑	=	=	=	=

Table 10) Summary of *c-fos* activation within subcortical brain regions following extinction

Changes of neuronal activation within various subcortical brain regions following extinction in comparison to control animals (Fig. 27). ↑ increase in activity, = no change in activity, ↓ decrease in activity. Abbreviations: AcbC = nucleus accumbens core, AcbS = nucleus accumbens shell, CPu = caudate putamen, BLA = basolateral amygdala, VTA = ventral tegmental area.

Some distinct chances could also be observed for EtOH and saccharin within the BLA and for nicotine in the insular cortex. The question now is how reinstatement and extinction conditions recruit similar brain regions and display similar activation strength. During the development of an addiction different learning processes are initiated. The most crucial ones thereby are learning processes involved in the establishment of cue- and context associations that are linked to certain behaviours such as reward "wanting", reward seeking and reward-taking. The information of learned associations, their predictive value and the respective behaviours are encoded in specific patterns and stored in the respective brain regions (Hyman et al., 2006). During phases of abstinence these memories can get reactivated by the reward-associated stimuli and trigger relapse of reward seeking and reward taking behaviour (Bossert et al., 2013), a phenomenon that is studied by the reinstatement model, which was used in this thesis. This model is also based on extinction training during which the animals learn to inhibit their responses to reward-associated contexts, so called extinction learning (Knackstedt et al., 2010). Thus, during the operant conditioning paradigm animals establish different memories that are either associated with reward or that are associated with extinction. Warren et al. (2016)

was able to demonstrate that these memories are not only distinct from each other but that they are encoded by specific neuronal ensembles which co-exist within the same brain region. The same group not only demonstrated this phenomenon for natural rewards but also showed that memories for opposing behaviours can intermingle within the same brain area for drugs of abuse (Warren et al., 2019). Taking together the evidence from such studies the overlapping activity patterns between the extinction and reinstatement condition could be explained. Furthermore, *c-fos* expression in these brain regions can to some extend also be initiated by processes that are identical between the two procedures such as animal handling, animal transport and experimental context (Asanuma et al., 1992; Asanuma and Ogawa, 1994).

4.1.2.3 Summary

Study 1A provided new insights into brain regions active during cue-induced reinstatement of reward seeking behaviour and during extinction learning. Re-exposure to environmental cues that were previously associated with reward availability triggered broadly overlapping *c-fos* expression within the prefrontal cortex of rats conditioned to self-administer natural rewards and drugs of abuse. Thereby the most prominent activation was found within the OFC. At the subcortical level, reward seeking induced overlapping activation within the dorsal striatum for all four rewards. In addition to these similarities, different rewards also showed distinct activation, such as increased activity in the BLA in EtOH trained animals or elevated *c-fos* expression within the AcbC of psychostimulant-trained animals.

Interestingly, the expression pattern did not differ much between the reinstatement and the extinction condition, suggesting that similar brain regions encode reward-related and extinction-related memories.

4.1.3 Study 1B: Immunohistochemical analysis of neuronal ensembles following cue-induced reinstatement of reward seeking behaviour

Mapping *c-fos* mRNA expression patterns during cue-induced reinstatement of reward seeking behaviour revealed similar neuronal activation for natural rewards and drugs of abuse. Highest activity was thereby demonstrated for the prefrontal cortex with peak *c-fos* mRNA levels within the OFC. However, with the method used no differentiation was possible with regard to cell types involved. For this reason, the cellular composition of cue-responsive

ensembles within the OFC was investigated with a double antibody staining approach where cFOS was labelled in combination with other cell-type-specific markers. The antibodies used to examine co-localizations with cFOS were anti-NeuN, anti-GFAP, anti-CaMKII and anti-GAD67. anti-NeuN is used on a regular basis to reliably identify mature neurons, as it binds to the antigen neuronal nuclei (NeuN), which is located inside the neuronal nucleus. The nuclear protein was identified as gene product of FOX-3 and functions as neuronal splicing regulator. It is thereby present throughout the entire vertebrate nervous system (Kim et al., 2009; Duan et al., 2016). In order to detect neuroglia, an antibody against GFAP was used. The filament protein is mainly expressed in mature astrocytes but also plays an important role in the cytoskeleton during the development of these cells. Thereby the intermediate filament protein not only fulfils a structural role but is also important for astrocyte function (Middeldorp and Hol, 2011; Brenner, 2014). GFAP is therefore an ideal candidate for astrocyte identification. To determine whether the cue-response cells were of excitatory or inhibitory nature antibodies against CaMKII and GAD67 were used. Excitatory neurons can be labelled with an antibody against CaMKII. This kinase has four different isoforms (alpha, beta, gamma, delta) of which alpha is the most abundant isoform in the adult forebrain. Therefore, an antibody against this isoform was used. CaMKII is essential for a variety of neuronal functions ranging from neurotransmitter synthesis and release to learning and memory. Even though GABAergic cells express αCaMKII in the central amygdala, it can be reliably used to label excitatory neurons in the PFC (Benson et al., 1992; Yamauchi, 2005; Broccoli et al., 2018). Inhibitory neurons are dependent on glutamic acid decarboxylases (GADs) as these enzymes synthetize the neurotransmitter GABA by decarboxylation of glutamate. GADs are therefore highly correlated with GABAergic neurotransmission. There are two different isoforms of GADs, which are GAD67 and GAD65. GAD67 is thereby responsible for the generation of over 90 % of basal GABA levels in the cerebral cortex as it is constitutively active (Lee et al., 2019). The usage of an antibody against GAD67 to detect inhibitory neurons is therefore trustworthy.

A first step in the investigation of ensembles was to determine their distribution within the OFC. cFOS-ir was thereby detected to be evenly distributed throughout the entire OFC. Despite its even distribution, cFOS-ir was not densely packed but rather showed a clustered arrangement compared to NeuN-ir. A similar observation was made by Gonzales et al. (2020) who was able to demonstrate that ensembles expressing IEGs showed spatially defined cluster formations (Gonzales et al., 2020). Even though the study focused on IEG expression on a subcortical level after acute cocaine exposure, the results give an insight on how IEG expression and therefore neuronal ensembles might be spatially organized in other brain regions as well.

At the beginning, quantification of the number of different cell-types (neurons, inhibitory cells, excitatory cells) within the OFC between the different groups was conducted, independent of their activation status. Cell number counts revealed an equal number of neurons within the OFC for all three reward conditions. Only the number of neurons counted for the control group was larger compared to reward groups within the ventral OFC (EtOH, saccharin, cocaine) and the lateral OFC (cocaine). The behavioural paradigm tested is based on reward learning, which like every form of learning and memory involves some form of neuronal plasticity. Neuronal plasticity focuses mainly on changes in the intrinsic excitability of neurons or on synaptic plasticity, where synaptic connections are strengthened, formed or eliminated and entire dendrite or axon formations remodelled, rather than on numeral changes (Hyman et al., 2006). Chronic drug consumption, however, can result in neurodegeneration in case of EtOH (Fadda and Rossetti, 1998). Chronic cocaine use, on the other hand, does not cause neuronal damage (Goodman and Sloviter, 1993). These findings and the rather short period of drug self-administration in the present experimental setup make it unlikely that the reduced number of neurons within the OFC was caused by reward consumption or reward learning. A simple explanation for the phenomenon might be the selection of segments analysed and the manual counting of cells. Quantification of excitatory cells showed equal numbers between all four conditions tested. For inhibitory cells however the number of cells counted for the EtOH group and the saccharin group was significantly higher compared to the other conditions. As such short reward consumption should not influence the number of inhibitory cells within the OFC, the results could be explained by the suboptimal GAD67 staining quality, the random selection of segments analysed and the manual counting or a combination of all three.

The central nervous system is involved in integration of environmental information, processing of these signals and in the coordination and response to these inputs, which manifest as behavioural outputs. All these actions require neuronal activation, which can be examined by monitoring *c-fos* expression (Herrera and Robertson, 1996; Cruz et al., 2015). The initiation of reward seeking behaviour by reward-associated cues also induces *c-fos* expression. By monitoring cFOS expression within the OFC, neuronal activation of this region can be examined (Bal et al., 2019). As cFOS can also be expressed in neuroglia (Hisanaga et al., 1990; Herrera and Robertson, 1996) co-expression of cFOS-ir with either NeuN-ir or GFAP-ir was monitored. All cFOS-ir positive cells detected were also NeuN-ir positive. This and the negative co-localization of cFOS-ir and GFAP-ir proved that ensembles activated by cue-induced reward seeking were entirely neuronal. Neuronal activation triggered by reward seeking behaviour was significantly higher for all three reward seeking conditions compared to the control group,

which confirms previous findings of this thesis (Study 1A). The results furthermore demonstrated increased neuronal activation in both the ventral and lateral OFC, whereby both subregions showed similar activation levels, indicating equal involvement in the tested behaviour. Similar findings were made for cue-induced cocaine seeking behaviour (Bal et al., 2019). Within the reward seeking group, saccharin trained animals showed a significantly higher neuronal activation than groups trained to EtOH or cocaine, indicating the activation of a larger neuronal ensemble within the OFC. Whether the ensemble activated by saccharin seeking is in fact the largest of the three ensembles can however not be finally concluded from the present data as neuronal ensembles encoding a specific behaviour can span across several brain areas (Holtmaat and Caroni, 2016). However, saccharin seeking activated the most neurons within the OFC according to cFOS-ir/NeuN-ir co-localization. Within the population of excitatory cells EtOH and cocaine trained animals showed higher activation compared to saccharin trained rats and controls, percentagewise, with control animals having the lowest activation of all four conditions. One could therefore argue that cue-induced seeking for drugs of abuse activated more neurons within the population of excitatory cells than reward seeking for the natural reward saccharin. As discussed earlier, stimuli that were previously associated with rewards have a high potential to increase activity in the PFC. Pyramidal neurons, which are the primary excitatory cells within the PFC (Kamigaki, 2019), undergo dendritic spine plasticity upon drug exposure in key brain regions of the reward system such as the medial PFC. These morphological changes lead to alterations in synaptic connectivity and thus may result in the behavioural consequences that can be observed after repeated drug exposure (Robinson and Kolb, 1999; Robinson et al., 2001; Robinson and Kolb, 2004). Furthermore, the formation of synaptic plasticity in pyramidal neurons seems to be concurrent to the establishing of drug-associated memories (Otis and Mueller, 2017). Thus, retrieval of these memories during cue-induced drug seeking increased the activity within the population of excitatory neurons. For the population of inhibitory interneurons activity was also significantly reduces in control animals compared to rats trained to self-administer a reward. Interestingly, the EtOH group, in contrast to the cocaine or saccharin group, showed increased activity within the population of inhibitory interneurons during reward seeking. Even though the two carbon molecule EtOH can interact with a large diversity of different molecular and cellular targets (Abrahao et al., 2017), it was found that acute EtOH exposure results in potentiation of GABAergic neurotransmission through significant alterations of GABA release (Weiner and Valenzuela, 2006). Furthermore, the drug is able to increase the function of $GABA_A$ receptors, whereby their sensitivity to EtOH seems to be dependent on subunit expression and thus receptor composition or density (Harris

and Mihic, 2004). In addition, EtOH is able to block glutamatergic neurotransmission shifting the excitation/inhibition balance towards inhibition (Huang et al., 2012). As acute EtOH exposure favours GABAergic neurotransmission it might be possible that this effect is also reflected during the seeking behaviour for this drug, shown in increased activity in the GABAergic cell population.

In order to identify reward seeking specific neuronal activation, basal activity levels displayed by the control animals were subtracted from activity levels demonstrated by the reinstatement group. Analysis of the resulting data revealed that a vast majority of active neurons within the EtOH group were GABAergic interneurons whereas only one quarter to one third of neurons were glutamatergic pyramidal neurons. The second group of animals that was trained to seek for cocaine, showed the exact opposite picture with the majority of active neurons being glutamatergic pyramidal neurons and less than one quarter being GABAergic interneurons. Saccharin trained animals on the other hand showed a balanced amount of glutamatergic and GABAergic neurons being active during reward seeking behaviour. As mentioned before, the increased activity of GABAergic interneurons within the EtOH group and the increased activity of glutamatergic pyramidal neurons within the cocaine group could interrelate with the effects of the drug on GABAergic or glutamatergic neurotransmission, respectively (Stewart et al., 1984; Van Hedger et al., 2018). However, the present results contrast a previous study where the neurochemical composition of neuronal ensembles of EtOH trained animals was investigated in the medial PFC. Pfarr et al., 2015 showed that for both the infralimbic cortex and the prelimbic cortex the majority of active neurons was glutamatergic and only a fraction of active cells GABAergic (Pfarr et al., 2015). Even though the total number of inhibitory cells counted for cocaine trained animals was significantly lower than that for the other two groups of animals (EtOH and saccharin), no effect on the present analysis is expected since it accounts for the number of active cells and co-localizations. Furthermore, the number of active cells (cFOS-ir positive) within the GAD67 staining showed no significant differences between the reward trained groups. The number of cFOS-ir/GAD67-ir co-localized cells, however, was significantly increased for EtOH trained animals. As the number of active cells within the double staining of cFOS-ir and GAD67-ir showed no differences a methodological error cannot explain the contrasting result. Unfortunately, there are no comprehensive studies comparing the cellular composition of prefrontal cortex subregions that include the OFC. However, one study investigated parvalbumin expressing interneurons, which are the PFC's primary inhibitory interneurons, within the prelimbic cortex and OFC. The data showed that the density of these principal inhibitory interneurons was about five times higher in the OFC

than in the prelimbic cortex (Lee and Lee, 2021). This discrepancy in interneuron density could be one explanation for the increased amount of active GABAergic cells within the OFC during EtOH reward seeking compared to the amount active cells within the medial PFC. Furthermore, even though the medial PFC and the OFC share similar connections with other brain regions, they are anatomically but most importantly functionally distinct areas (Chudasama and Robbins, 2003; Golebiowska and Rygula, 2017; Miyazaki et al., 2020). The study conducted by Pfarr et al. (2015) also showed that the neuronal ensembles active during cue-induced reward seeking within the PrL and IL were smaller, 12.7 % and 11.2 % respectively (Pfarr et al., 2015), compared to neuronal ensembles investigated in the present study (18 % - 37 %). Other studies also reported smaller neuronal ensembles within the IL, active during heroin or natural reward seeking (Bossert et al., 2011; Warren et al., 2016). Only one other study investigated neuronal ensembles active during cue-induced reward seeking within the OFC. The group investigated both the proportion of neurons active during the heroin seeking and their neurochemical composition. With only 12 % cFOS-ir positive neurons, Fanous et al., 2012 identified a neuronal ensemble smaller than the ensembles investigated in the present study. However, with a neurochemical composition of 55 % excitatory and 10 % inhibitory neurons, the neuronal ensemble also demonstrated a unique reward-specific composition (Fanous et al., 2012). The discrepancies between published data and the present results could be due to several reasons. First data analysis was focused on segments with high cFOS-ir, thus generating a potential bias towards higher overall activity, resulting in larger ensembles percentagewise. Second, a crucial component in accessing ensemble composition is the quantification method used, including the threshold set to pre-empt false positive results. Thus, different quantification parameters used, could have resulted in the observed discrepancies. Third, differences with neuronal ensembles of the IL can be explained by the fact that both areas are discrete and might therefore show differential activity during reward seeking (Chudasama and Robbins, 2003; Golebiowska and Rygula, 2017; Miyazaki et al., 2020). Thus, the results obtained in this study should not be viewed as contrary to published data but should rather be seen as valuable addition to our knowledge about PFC subregions and their complex and distinct functional involvement in reward seeking behaviour.

4.1.3.1 Summary

To our knowledge, this is the first comprehensive study that investigated the cell-type specific composition of neuronal ensembles involved in cue-induced reinstatement of reward seeking behaviour for different rewards. Overall, Study 1B showed that neuronal ensembles in the OFC that respond to cue re-exposure are composed of crucial yet small subsets of neurons, a phenomenon, which was already demonstrated for other brain regions (Bossert et al., 2011; Cruz et al., 2014; Pfarr et al., 2015). Moreover, co-localization of cFOS-ir with cell-type specific markers could demonstrate that neuronal ensembles active during cue-induced reward seeking displayed a distinct neurochemical composition depending on the reward that was associated with the presented stimulus. Whereas neuronal ensembles activated by the saccharin associated cue showed a balanced contribution of excitatory (glutamatergic) and inhibitory (GABAergic) neurons, ETOH and cocaine cue-induced ensembles demonstrated an opposing neurochemical composition. The ensemble activated by ETOH associated cues was mainly inhibitory, whereas the ensemble induced by cocaine associated cues was primarily excitatory. Therefore, all interventions, whether scientific or therapeutic, targeting neuronal ensembles involved in reward seeking should account for their distinct neurochemical composition.

4.1.4 Study 1C: Characterization of the physiological properties of GFP positive (active) versus GFP negative (inactive) neurons after reinstatement of reward seeking

4.1.4.1 cFOS-ir and GFP-ir co-localization

Physiological characterization of neuronal ensembles was dependent on the rapid transcription and translation of the GFP coding sequence upon neuronal activation. The co-localization of cFOS-ir and GFP-ir thereby investigated the robustness of GFP expression driven by the *c-fos* promoter. With 100 % of GFP-ir positive neurons being cFOS-ir positive and with 83 % of the cFOS-ir positive population being GFP-ir positive, the *c-fos*-GFP transgenic rats were proven to be a reliable model to characterize physiological properties of neuronal ensembles active during cue-induced reward seeking.

4.1.4.2 Whole-cell patch clamp analysis to characterize physiological properties of neuronal ensembles

Learning and memory processes are crucial for the association of external stimuli with rewards and their availability. An important factor during these learning and memory processes are alterations in neuronal connectivity and efficacy (Cruz et al., 2013). In order to examine the physiological properties of neurons involved in ensemble formation, which were activated by cue-induced reward seeking, acute brain slices of *c-fos*-GFP transgenic rats were taken. Whole-cell recordings of GFP-positive neurons were obtained from these slices and compared with recordings from nearby GFP-negative (inactive) cells. The described procedure was successfully used in previous studies to investigate neuronal ensembles involved in different reward related behaviours. However, as discussed in detail in paragraph 3.6; Study 1C, the health of recorded cells was less than ideal for electrophysiological measurements due to the huge time gap between the end of the experiments and the actual start of the recordings. Therefore, recordings of only eight neurons were successful and yielded in robust data. The recorded neurons, three of which were GFP negative and five were GFP positive, emanated from only five animals. The obtained results, however, did not show any differences between GFP positive and GFP negative neurons, which would be in line with previous findings (Ziminski et al., 2017). Nonetheless, considering the low number of animals, the number of neurons recorded and the involved circumstances the obtained data from the present electrophysiological study is unfortunately not conclusive and does therefore not allow for an in-depth comparison of physiological properties between GFP positive and GFP negative neurons. We are therefore dependent on findings from the literature.

The first study to examine synaptic alterations in *c-fos*-GFP transgenic rats was conducted by Cifani et al. (2012). The group investigated synaptic alterations in medial PFC neurons, which displayed activation during stress-induced reinstatement of food seeking behaviour. In addition to a reduction in current ratios of α-amino-3-hydroxy-5-methyl-4-isoxazolepropionic acid (AMPA) and NMDA receptors, the scientists found that GFP positive neurons also showed increased paired-pulse facilitation (Cifani et al., 2012b). Another study examined the excitability of neuronal ensemble participating neurons in the prelimbic cortex after food self-administration. The group discovered that GFP positive neurons displayed increased excitability whereas GFP negative neurons showed decreased excitability after operant learning (Whitaker et al., 2017). Only one study so far focused also on alterations within the OFC. The group around Joseph Ziminski (2017) investigated how cue-activated neurons differ in their

excitability compared to surrounding non-active neurons. They could show that the sucrose cue was able to trigger activation of nerve cells in both brain regions investigated, the AcbS and the OFC. However, in contrast to GFP positive neurons within the AcbS, GFP positive neurons within the OFC did not display increased excitability in comparison to nearby GFP negative cells (Ziminski et al., 2017).

4.1.4.3 Summary

As the only study investigating physiological properties of active OFC neuronal ensembles was conducted in mice and used a different experimental procedure, we were eager to examine neuronal ensembles active during cue-induced reinstatement of reward seeking in the OFC of rats. Unfortunately, due to the circumstances described in paragraph 3.6; Study 1C, the number of animals and neurons that were successfully recorded was too small to obtain conclusive results. Elimination of all obstacles involved would allow a replication of the whole-cell patch clamp experiments in rats undergoing cue-induced reinstatement of reward seeking, however, this was beyond the scope of this thesis.

4.2 Study 2: Validation of functional neuronal ensembles encoding for natural reward and drug reward seeking behaviour

4.2.1 Investigating the functional relevance of neuronal ensembles involved in saccharin reward seeking behaviour

The first neuronal ensemble that was investigated for its functional relevance was the one encoding for cue-induced saccharin seeking. Ensembles of both the ventral as well as the lateral OFC were examined. At the beginning of the experiment animals had to undergo the usual training paradigm for operant conditioning. During the self-administration phase rats of each group displayed high variability in their response rate between each other. Furthermore, individual animals also showed somewhat to high variability in their response behaviour from one training session to the next. This was true for the ventral OFC and for the lateral OFC group. One reason for this high variance in their behaviour might have been ongoing construction noise at the institute as described in detail in paragraph 3.5; Study 2. Another issue that might have had an influence on the behavioural performance of the animals was the rat strain used in

combination with the specific transgene. Experience in our laboratory showed that *c-fos*-lacZ transgenic Sprague Dawley rats displayed lower susceptibility towards acquisition of the operant training paradigm and they also showed lower motivation towards reward consumption then other rat strains. There were no specific experiments conducted to further investigate these observations, however, several studies demonstrated behavioural differences between rat strains and even rats of the same strain, that were obtained from different breeding facilities displayed variations. Differences could be observed for behaviours such as locomotor activity, anxiety related behaviours, stress response, acoustic startle response, play behaviour and reward consumption as well as for the rewarding effect of a drug (Gauvin et al., 1993; Glowa and Hansen, 1994; Stöhr et al., 1998; Goepfrich et al., 2013; Northcutt and Nwankwo, 2018). Emphasis should thereby be put on the strain differences observed for reward consumption and the differences in the effect the same reward can have between different strains. Furthermore, it is well known that even within the same strain there are individual differences detectable for susceptibility to drug dependence, a phenomenon also observed in human addicts (Mandt et al., 2008). Despite the great variance shown by some animals, they all acquired the task and also displayed successful extinction learning as their responses gradually dropped below the 20 % threshold of the animal's baseline response rate. After implantation of the guide cannulas all animals were examined for their cue-induced reinstatement of reward seeking behaviour. Both groups of animals (ventral and lateral) as well as their subgroups (vehicle and Daun02) showed strong and robust reinstatement of saccharin seeking compared to their responses during the extinction phase with average increases of 3.9- to 4.6-times. Therefore, association of the cue light with reward availability was successful as reward seeking was elicited and the ensemble responsible for the relapse-like behaviour could be targeted by Daun02 inactivation.

Right after the cue-induced reinstatement session animals were infused with either vehicle or Daun02 into the lateral or ventral part of the OFC depending on their group assignment. After a recovery period they underwent the 2nd reinstatement test to investigate the functional relevance of ensembles activated during the 1st reinstatement. The vehicle infused group of rats for both OFC subregions displayed no significant changes of response behaviour compared to the 1st reinstatement, meaning that neither one of the chemical compounds (DMSO and Tween-80), that were used to dissolve Daun02, nor the intracranial infusion had an effect on the animal's reward seeking behaviour. Infusion of Daun02 into the lateral OFC, however, resulted in a behavioural change during the second reinstatement. Animals that received Daun02 showed a significant decrease in saccharin seeking, demonstrating the functional role of a specific subset of neurons that was synchronously activated by the saccharin-paired stimulus. Infusion

of Daun02 into the ventral part of the OFC, on the other hand resulted in an increase in reward seeking compared to the first reinstatement. The increase was not significant but showed a behavioural trend ($p = 0.066$). Even though animal numbers were low, the observed opposing effect between lateral and ventral OFC could indicate differential roles for the two subregions of the OFC.

Previous studies investigating the different subregions of the OFC revealed divergence on the anatomical as well as high heterogeneity on the functional level. Existing anatomical data indicates that both the ventral and the lateral OFC receive their main input from different cortical as well as subcortical regions. However, brain regions such as agranular insular cortex, mediodorsal nucleus as well as the submedial nucleus innervate both areas (Reep et al., 1996; McCracken and Grace, 2007; Alcaraz et al., 2016; Lichtenberg et al., 2017). An in-depth connection study showed wide ranging similarities for projection targets between the medial OFC and the ventral OFC on both the cortical as well as subcortical level. Both regions also have much higher interconnections with one another than with the lateral OFC (Hoover and Vertes, 2011). The lateral OFC however also shares similar projection targets with the other OFC subregions. Lateral and medial OFC innervate the nucleus accumbens and BLA, which on the other hand share less connections with the ventral OFC (Rempel-Clower, 2007; Schilman et al., 2008; Hoover and Vertes, 2011; Malvaez et al., 2019; Wang et al., 2019). Ventral and lateral OFC both send projections to the primary somatosensory cortex (Hoover and Vertes, 2011; Banerjee et al., 2020). All three subregions have a common target with the caudate putamen. Interestingly, the location of projections to the caudate putamen corresponds to the location of the different subregions from medial to lateral (Schilman et al., 2008). As the medial and ventral OFC share a good deal of projection targets it is proposed that these brain regions might be a functional unit and may functionally deviate from the lateral part of the OFC, which would coincide with the present results. Some scientists even suggested that medial OFC and ventral OFC might function as link between the medial PFC and the lateral OFC (Hoover and Vertes, 2011; Izquierdo, 2017).

The investigation of OFC function in addiction research was so far mainly done using lesion studies, pharmacological interventions or viral approaches (Fuchs et al., 2004; Lasseter et al., 2009; den Hartog et al., 2016; Arguello et al., 2017; Izquierdo, 2017; Bianchi et al., 2018; Arinze and Moorman, 2020; Reiner et al., 2020). Whereas some studies focused on the entire region there are several studies targeting subregions of the OFC. The deactivation of the lateral OFC showed decreases in cocaine-primed, cocaine-paired context-induced, cocaine-paired cue-induced and EtOH-paired cue-induced reinstatement (Fuchs et al., 2004; Lasseter et al., 2009;

den Hartog et al., 2016; Arguello et al., 2017; Arinze and Moorman, 2020). The role of the ventral OFC in reward seeking however remains unclear as most functional studies target lateral and ventral OFC in combination (Bal et al., 2019). Since the medial and ventral OFC are proposed to form a functional unit (Izquierdo, 2017) one might however get an idea of ventral OFC function by observing the functional involvement of the medial OFC in reward seeking behaviour. Having said this, inactivation of the medial OFC does not give a clear picture of its function as different studies showed opposing results (Fuchs et al., 2004; Arinze and Moorman, 2020). However, the methodologies used in the mentioned studies were unspecific and targeted the entire brain region. Since D.O. Hebb proposed that brain processes and resulting behaviours are not mediated by all cells of a specific brain region, but that information is rather processed by subpopulations of cells, inactivation of these so-called ensembles might provide an even better understanding of brain region function (Hebb, 1949; Cruz et al., 2015). Several research groups already investigated neuronal ensemble function within the medial PFC (Bossert et al., 2011; Pfarr et al., 2015; Suto et al., 2016; Warren et al., 2016; Warren et al., 2019; Kane et al., 2020) but so far only one paper was published examining ensembles of the OFC in reward seeking. The group around Sanya Fanous found that inactivation of the lateral part of the OFC after heroin-associated cue re-exposure attenuated heroin-paired cue-induced reinstatement (Fanous et al., 2012), matching results obtained in this study. However, the experimental protocol used by Fanous et al., 2012 differed substantially from the one used in this study.

4.2.2 Investigating the functional relevance of neuronal ensembles involved in cocaine reward seeking behaviour

The functional relevance of OFC ensembles during cue-induced reinstatement of cocaine reward seeking was also examined with help of the Daun02 inactivation method. During the acquisition of drug self-administration behaviour, animals also displayed high variability in response behaviour as described before in the saccharin group. Variability between animals but also high variability for individual animals on a day-to-day basis could be observed. Issues could have been the ongoing construction noise (paragraph 3.6; Study 2) and the phenotype of the rat strain as explained in detail in 4.2.1. However, the behavioural fluctuations could also be explained by problems that occurred with the intravenous catheter (paragraph 3.6; Study 2). Despite those issues all rats learned the task and acquired a stable baseline of cocaine self-administration. In the following extinction training the response rate for both groups of animals (lateral and ventral) dropped below 20 % of their baseline lever response, marking successful

extinction of reward seeking behaviour. In order to mimic relapse-like conditions animals were subjected to a cue-induced reinstatement test, after successful intracranial implantation of guide cannulas. For both groups of animals (ventral and lateral) as well as their subgroups (vehicle and Daun02) re-exposure to the cue associated with cocaine triggered a strong and robust reward seeking response with increases of 5.8 to 7.9 times. Thus, the cue light was successfully paired with cocaine availability and activation of the responsible ensemble elicited strong relapse-like behaviour, which could then be targeted by Daun02 inactivation. Targeting of the ventral and lateral OFC ensemble by vehicle infusion had no effect on cocaine seeking behaviour during the 2nd reinstatement. As no significant changes were observed, both DMSO and Tween-80 as well as the infusion itself had no impact on reward seeking behaviour. Daun02 induced inactivation of neuronal ensembles, that were activated during the 1st cue-induced reinstatement, did not result in changes of cocaine seeking, neither for the lateral nor for the ventral OFC. This finding opposes results from other studies that found decreases in cocaine reward seeking after cocaine-primed, cocaine-paired context-induced, cocaine-paired cue-induced reinstatement. However, these studies targeted the entire lateral part of the OFC by lesions, pharmacological interventions or optogenetic inhibition (Fuchs et al., 2004; Lasseter et al., 2009; Arguello et al., 2017). They can therefore only be partially compared with the present results, as Daun02 inactivation should only target previously active neuronal ensembles. One study, however, targeted the lateral OFC during reward seeking and was able to show that selective inactivation of a neuronal ensemble in this subregion reduced cue-induced heroin seeking (Fanous et al., 2012). However, the protocol used by Fanous et al. (2012) was distinct from the one used in the present study. The research group around Sanya Fanous did not subject their animals to an extinction learning paradigm in the operant boxes but rather kept their animals in their home cages during the withdrawal phase. Neuronal ensembles were activated by a so-called extinction test of 15 min where animals were exposed to heroin context and cues for 15 min. After an additional 75 min in their home cage Daun02 or vehicle were infused (Fanous et al., 2012). In view of these differences in the experimental procedure a comparison of the obtained data is only partially possible. For the ventral OFC however, no comparable studies exist. There are some studies on silencing of the medial OFC, which is proposed to build a functional unit with the ventral OFC (Izquierdo, 2017), but those studies are not conclusive as they show varying outcomes (Fuchs et al., 2004; Arinze and Moorman, 2020). Compared to neuronal ensembles involved in cue-induced saccharin seeking the ensembles targeted during cue-induced cocaine seeking do not seem to be functionally relevant for the behaviour as neither inactivation of the ventral OFC ensemble nor of the lateral OFC ensemble was able to affect

reward seeking behaviour in the present study. However, the comprehensive examination of neuronal activation within the extended reward system in Study 1A demonstrated that the OFC is crucially involved in reward seeking behaviour. In addition to this finding several other studies were able to prove the importance of the OFC during reward seeking behaviour (Fuchs et al., 2004; Lasseter et al., 2009; Arguello et al., 2017; Bal et al., 2019; Arinze and Moorman, 2020; Hernandez et al., 2020). One explanation for the contrasting result could be the circumstance that neurons forming a neuronal ensemble that encodes a specific behaviour can be located in several brain areas (Holtmaat and Caroni, 2016). Mapping of neuronal activity by *c-fos* mRNA expression resulted not only in a broadly overlapping activity pattern between the different rewards but also in distinct changes for the unique rewards. Cocaine seeking, for example, distinctly activated neurons in the AcbC. Theoretically it is possible that the ensemble relevant for cocaine seeking not only comprises neurons within the OFC but also within the AcbC. Thus, it is possible that even though parts of the ensemble were silenced, inactivation of neurons within the lateral or ventral OFC by Daun02 was not sufficient to impact cocaine seeking as the behaviour could have been rescued by other parts of the ensemble. As saccharin trained animals did not show any unique activation pattern within other brain regions of the extended reward system, the ensemble responsible for cue-induced saccharin seeking might be restricted to the lateral or ventral OFC. Thus, inactivation of the lateral or ventral OFC neuronal ensemble was sufficient to alter response behaviour.

4.2.3 Summary

Taken together, this is the first study to investigate the impact of neuronal ensemble specific inactivation within the lateral and ventral OFC following cue-induced reinstatement of reward seeking behaviour. Saccharin reward seeking thereby appears to be regulated by neuronal ensembles in both the ventral and lateral OFC in opposing manner. The ventral OFC ensemble seems to have an inhibitory effect on reward seeking, whereas the lateral OFC ensemble exhibits enhancing impact on reward seeking behaviour. However, due to the lack of statistical significance for the ventral OFC, this interpretation should be taken with caution. In contrast, reward seeking for cocaine does not appear to involve neuronal ensembles within the lateral or ventral OFC, that are crucial for the behaviour, as silencing of neuronal ensembles within either subregion had no effect. Nevertheless, more data need to be generated to draw a conclusion, as low animal numbers and high behavioural variability could conceal an effect.

4.3 Study 3: Comparison of neuronal ensembles within the infralimbic cortex following reinstatement of saccharin and ethanol seeking behaviour

The following discussion was composed based on the discussions and conclusions of Simone Pfarr's publications "Choice for Drug or Natural Reward Engages Largely Overlapping Neuronal Ensembles in the Infralimbic Prefrontal Cortex" and "The Role of the Medial Prefrontal Cortex in Reward Seeking: Functional Evidence on Cellular and Molecular Mechanisms underlying Drug and Natural Reward Seeking" and used with her permission (Pfarr, 2018; Pfarr et al., 2018). Even though the essence of the discussions was re-written in own words, similarities cannot be excluded.

4.3.1 Two-reward operant conditioning for characterization of neuronal ensemble size and distinctness following cue-induced reinstatement of EtOH or saccharin seeking behaviour

In order to study neuronal ensembles encoding reward seeking behaviour for two different rewards within the same animal, a new operant conditioning protocol had to be implemented. The two-reward operant conditioning protocol was developed based on the drug-self-administration and reinstatement model, a valid and widely used model to investigate relapse-like behaviours (Epstein et al., 2006; Sanchis-Segura and Spanagel, 2006; Martin-Fardon R., 2012; Marchant et al., 2013; Spanagel, 2017). Similar to previous experiments discussed in this thesis, the two-reward conditioning approach was composed of a self-administration phase, an extinction phase and multiple cue-induced reinstatement tests. In contrast to previous experiments however, self-administration was first performed for EtOH and saccharin separately before sessions were randomised to reach a stable baseline. Like discussed previously reward concentrations had to be adjusted to rule out potential biases towards one reward. Due to the different reinforcement effect, saccharin concentrations were thus adjusted to match the animal's performance during EtOH self-administration. Whereas reward availability was signalled by a visual cue for both rewards, a discriminative olfactory cue was used to allow for reward differentiation. Behavioural data showed that rats learned the behavioural task for both reward conditions, as a robust baseline was reached during self-administration. Thereby animals displayed no bias towards one of the rewards. After extinction, where response behaviour was successfully extinguished, both groups of animals showed

robust reinstatement of reward seeking for both Study 3A and 3B. Interestingly, reinstatement revealed a clear bias of the animals towards the drug of abuse EtOH, indicating a higher motivation of the animals towards EtOH. Inactive lever presses and reinstatement of reward seeking clearly demonstrated that animals were able to learn the two different reward contingencies. Thus, the behavioural data indicates that the two-reward conditioning paradigm can be used as a tool to identify neuronal ensembles encoding for different rewards within the same animal.

4.3.2 Study 3A: Immunohistochemical analysis of neuronal ensemble size

For the investigation of neuronal ensembles encoding reward seeking behaviour for two different rewards within the same animal, first the size of each ensemble was analysed. Similar to Study 1B an immunohistochemical co-localization approach was used. Therefore, an antibody against cFOS was utilised, as cFOS is a good marker of neuronal activity (Herrera and Robertson, 1996; Cruz et al., 2013; Cruz et al., 2015). Neurons were labelled with an antibody against NeuN, which can be reliably used for this matter (Duan et al., 2016). Co-localization analysis revealed that the neuronal ensemble activated for both rewards following cue-induced reinstatement was of the same size (approximately 15 %). In comparison with the neuronal ensembles identified within the OFC following cue-induced reinstatement of EtOH or saccharin seeking, the IL ensembles were much smaller. As discussed before this could be due to different reasons (paragraph 4.1.3). The most likely explanation being the distinctness of the two brain regions investigated and the therefore possible differential activity expressed during reward seeking (Chudasama and Robbins, 2003; Golebiowska and Rygula, 2017; Miyazaki et al., 2020). Other studies investigating neuronal ensembles within the IL cortex following reward seeking behaviour, identified ensembles comprising 4 % - 11 % of the neuronal population (Bossert et al., 2011; Pfarr et al., 2015; Warren et al., 2016). An explanation for this discrepancy could be the use of a more complex behavioural paradigm compared to the before mentioned studies. Whereas these studies utilised highly distinct predictive stimuli, the present protocol involved both discriminative (olfactory) and distinct (visual) cues in combination with two different rewards. Thus, neuronal ensembles involved in this more complex reward seeking behaviour might simply recruit more neurons to accomplish the task, resulting in the observed larger neuronal ensemble size.

4.3.3 Study 3B: Double *c-fos* fluorescent *in situ* hybridization following EtOH and saccharin cue-induced reinstatement

In order to characterize the shared and distinct properties of the neuronal ensembles that were previously identified during EtOH and saccharin seeking within the IL in the same animal a double fluorescent *in situ* hybridization approach was used. The two-reward operant conditioning paradigm was therefore slightly modified to make use of different *c-fos* mRNA species. Spliced *c-fos* mRNA was thereby used to identify the neuronal ensemble active during cue-induced reinstatement for the first reward, and unspliced *c-fos* mRNA to detect the ensemble encoding reward seeking during the second cue-induced reinstatement (paragraph 2.2.5 + 2.3.1; Study 3). Co-localization analysis of both *c-fos* mRNA species revealed that both ensembles are distinct but also show a large overlap with about 50 %. Thus, neurons active during reward seeking for both rewards seem to encode parts of the behaviour that are shared, such as the animals approach behaviour in response to the predictive cue or the intrinsic motivation for reward consumption. However, the overlap of neuronal ensembles was not surprising as several studies demonstrated that distinct memories, such as different contexts or adverse events, might be linked by shared neuronal ensembles (Cai et al., 2016; Rashid et al., 2016; Josselyn and Frankland, 2018). Despite the observed similarities, each neuronal ensemble also comprised a distinct part, which might encode for reward specific properties, such as the different modes of action on the nervous system exhibited by the two rewards and the different sensations they produce (taste/smell).

4.3.4 Summary

In summary, investigation of the neuronal ensembles encoding EtOH and saccharin seeking behaviours revealed that the two ensembles were not only similar in size but largely overlapped. However, the identified ensembles did not only display shared properties, but were reward-specific and exhibited distinct properties. The findings therefore show that memories are not only encoded by sparsely distributed neuronal ensembles, but that these ensembles may link memories via their shared properties. Thus, the IL encodes different reward seeking behaviours involving neuronal ensembles able to store and recall overlapping and distinct components of the underlying memories. With the introduction of the two-reward operant conditioning paradigm, Study 3 demonstrated that investigation of different reward seeking behaviours within the same animal is reliably possible. The method therefore provides the possibility to

study co-existing neuronal ensembles within the same brain region, making it an interesting tool for future studies dealing with linked memories.

4.4 Study limitations

Reviewing the results of this thesis one must keep in mind that all methods used to identify and characterize neuronal ensembles that are specific to cue-induced reward seeking behaviour are based on *c-fos* expression with a limited temporal resolution. Thus, all methods used from radioactive *in situ* hybridizations, immunohistochemical co-localizations, whole cell patch clamp recording to Daun02 inactivation not only focused on strongly activated cells during reward seeking behaviour but detected all neuronal activity during the entire test session. Consequently, all external stimuli as well as behaviours conducted by the animal during the respective test session trigger neuronal activation. All methods used therefore not only detect active cells responsible for cue-induced reward seeking but also cells activated by handling stress, contextual cues, the cue presentation, the lever press behaviour and others. Therefore, a collective of neuronal ensembles is identified and targeted by the used methods, which makes it impossible to differentiate between neuronal ensembles encoding a specific behaviour as the individual cells cannot be assigned to a distinct ensemble. Hence, it would be a great advantage for further investigations to monitor neuronal activity with a greater time resolution in order to being able to differentiate between neuronal ensembles involved in the various events.

The usage of the Daun02 inactivation method has its own limitations. As it is based on *c-fos* promotor activation the method targets all highly active cell expressing cFOS and ß-galactosidase. Behaviours that do not require high levels of *c-fos* expression furthermore remain under the radar and cannot be silenced by the Daun02 method (Cruz et al., 2013). In addition, the Daun02 inactivation method leads to permanent inactivation of strongly activated neurons in the targeted region as they undergo apoptosis (Pfarr et al., 2015). Thus, one cannot investigate different neuronal ensembles within the same animal. Hence, further studies would profit from the development of an inactivation method whose effect could be reversed and neuronal ensembles could be switched on and off to study their effects on various behaviours.

5. CONCLUSION

Human behaviour is driven by rewards, which can be associated with certain contexts and discriminative cues. The conditioned cues develop a predictive value for the individual and are thus able to trigger strong motivational states leading to reward seeking. In case of drugs of abuse, this mechanism can result in addiction development. A deeper understanding of the cellular and molecular mechanisms behind the associative learning processes is therefore necessary to help affected individuals to prevent drug relapse and thus break through the addiction cycle. It is hypothesized that cells synchronously active during the memorization process form so called neuronal ensembles, which encode specific cue-reward associations. In order to advance our knowledge about neuronal ensembles involved in cue-induced reward seeking for natural rewards and drugs of abuse, the present thesis aimed to identify and characterize the shared and distinct properties of these synchronously active cells.

Re-exposure to reward-associated cues induced overlapping activity patterns for different rewards throughout the reward system. The PFC, especially its orbitofrontal part, displayed prominent neuronal activity during the behaviour. Thus, its role as key player of the limbic reward system as well as its critical involvement in reward-related behaviours was confirmed. However, each cue-reward association also triggered distinct neuronal ensemble activation, suggesting reward-specific involvement of certain brain regions. Furthermore, examination of neuronal activation during extinction revealed largely overlapping activity patterns similar to those displayed during cue-induced reinstatement, proving the co-existents of different memories within the same brain areas.

A more detailed investigation of identified neuronal ensembles within the orbitofrontal cortex revealed a distinct reward-related neurochemical composition. Each reward tested therefore recruited a unique constellation of neurons, each with specific neurotransmitter phenotypes. These findings give new insight about the neurochemical distinctness of neuronal ensembles in reward seeking and provide evidence that interventions or potential therapies that target reward-related memories should be cell-type specific.

Silencing of neurons active during saccharin seeking revealed a neuronal ensemble within the lateral OFC, which showed functional relevance for the behaviour. Furthermore, our data indicates that an ensemble within the ventral OFC might also be involved in saccharin reward seeking. Thus, both ensembles seem to exhibit an opposing effect on reward seeking, confirming the functional heterogeneity of OFC subregions.

Furthermore, examination of neuronal ensembles encoding for a natural reward and a drug of abuse within the same animal revealed that both ensembles are largely overlapping but comprise distinct components for each reward (Pfarr, 2018; Pfarr et al., 2018).

In summary, the findings gathered in this work provide new insight into the shared and distinct properties of neuronal ensembles encoding reward seeking behaviours for natural rewards and drugs of abuse. Thus, they provide new knowledge about potential cellular mechanisms behind associative learning processes and addiction memory. They furthermore underline the importance of the PFC in relapse like behaviours and identified it as a potential target for therapeutical interventions, both on a pharmacological and behavioural level. A successful therapy form, able to attenuate maladaptive behaviours, is exposure therapy. Individuals are thereby exposed to discriminative cues, which were associated with reward seeking and substance abuse, and due to absence of the predicted outcome, e.g., reward availability, the behaviour gets extinguished. As the approach has a few downsides such as behavioural suppression without memory alteration, potential of no long-lasting behavioural extinction and averseness against cravings triggered by cue exposure, additional extinction promoting methods have to be used (Pizzimenti and Lattal, 2015). One method could be the use of pharmacological treatments targeting the underlying cellular and molecular pathways of addiction memories, such as the neuronal ensembles identified within this thesis.

However, the results obtained by this thesis have shown, that the mechanisms involved are substantially more complex and further studies are needed to further elucidate the role of the distinct reward specific components, to precisely address them in a pharmacological treatment. Thus, two experiments are proposed in the following chapter to gain further insight into the role neuronal ensembles in reward seeking.

6. OUTLOOK

As mentioned previously the methods used in this thesis have their own minor limitations. First, the *c-fos* expression approach has a limited temporal resolution, which could be improved by techniques allowing for precise and timely controlled identification of neuronal activation. Second, the Daun02 method targets all active cells expressing *c-fos* in combination with lacZ, independent of their neurochemical phenotype. In order to functionally validate neuronal ensembles in a cell-type specific manner, techniques targeting active neurons of a specific neurochemical phenotype need to be utilised. Two experimental approaches fulfilling these criteria are proposed in the following.

6.1 CAMPARI method

The first experiment aims to circumvent the restricted temporal resolution of *c-fos* induction and therefore work around the limitation of our methods to also detect cellular activity induced by events as e.g., responses to stress, handling procedure et cetera. An alternative approach to reach this goal involves a calcium modulated photoactivatable ratiometric integrator protein (CaMPARI). This method is based on a viral approach utilising the recombinant adeno-associated virus rAAV2/1-hSynapsin1-CaMPARI, which enables expression of CaMPARI in infected cells. CaMPARI is a green fluorescent protein, which irreversibly converts to a red fluorescent conformation in presence of sufficient calcium influx, induced by neuronal activity, and precise experimenter-controlled light exposure (405 nm). The technique therefore allows precise and timely controlled identification of active neurons via a red fluorescent signal (Fosque et al., 2015; Zolnik et al., 2017). To apply this approach to our drug-self-administration and reinstatement model, animals need to be stereotactically injected with the rAAV into the OFC and get implanted with an optic fibre above the same region. During cue-induced reward seeking, presentation of the discriminative visual cue will directly be coupled with a 405 nm light pulse, provided by the optic fibre. If now sufficient intracellular calcium concentrations, which are induced in cells of neuronal ensembles encoding reward seeking behaviour, and the 405 nm light stimulus coincide, CaMPARI undergoes a green-red conversion, which exclusively labels neurons mediating the behaviour tested during the task (Fig. 60).

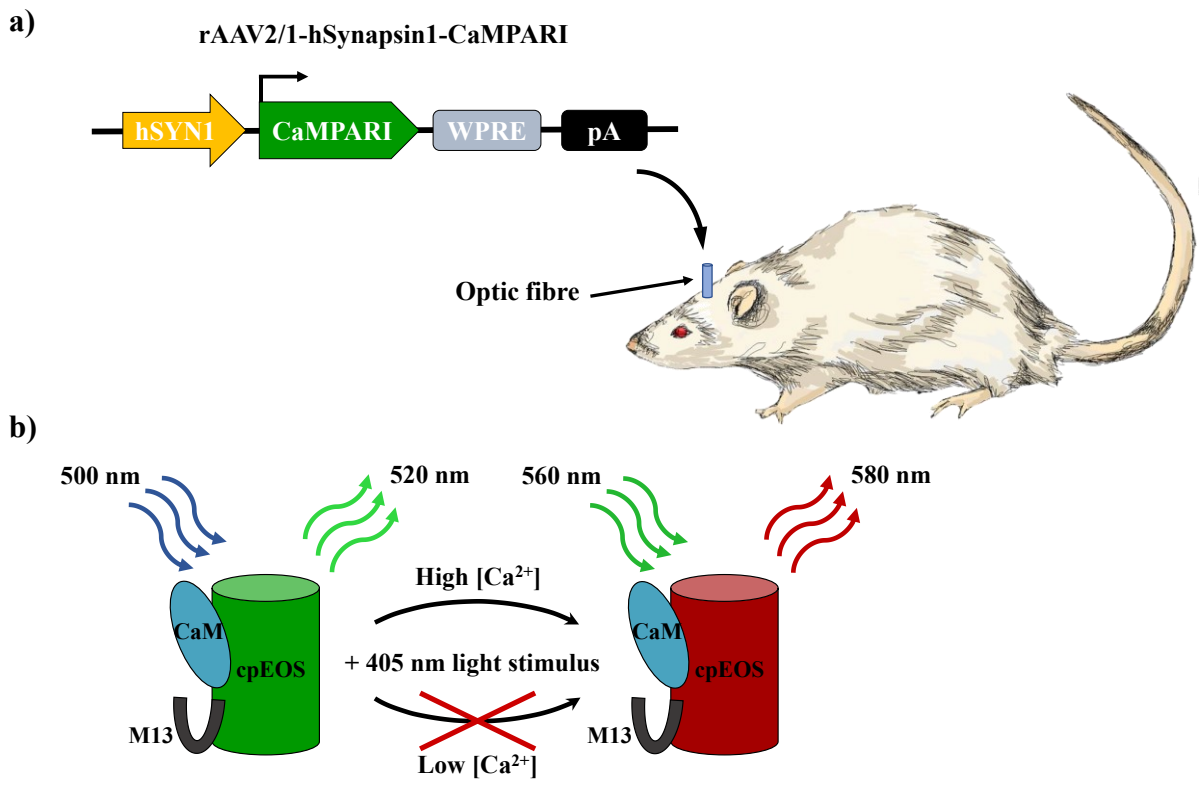

Figure 60) Schematic representation of the CaMPARI method

a) After reward self-administration training rats are injected with a rAAV2/1-hSynapsin1-CaMPARI construct into the brain region of interest, which enables expression of CaMPARI under control of the hSYN1 promoter. The injection is directly followed by implantation of an optic fibre above the brain region, to enable light delivery. After surgery and recovery, rats undergo retraining of reward self-administration and extinction, which will be followed by cue-induced reinstatement of reward seeking. b) During reinstatement cue light presentation will be coupled with the external 405 nm light stimulus and neuronal ensembles encoding the tested behaviour get activated, leading to increased intracellular calcium concentrations. Both events, high calcium concentrations and the 405 nm light stimulus will result in the green-red conversion of CaMPARI, allowing identification of active neurons. Abbreviations: hSYN1 = human synapsin1 promoter, CaMPARI = calcium modulated photoactivatable ratiometric integrator, WPRE = woodchuck hepatitis virus post-transcriptional regulatory element, pA = SV40 polyadenylation signal, CaM = calmodulin, M13 = M13 peptide, cpEOS = circularly permuted photoactivatable green to red fluorescent protein. Adapted and modified from (Fosque et al., 2015), Rat picture used and modified with permission from Wolfgang Sommer.

6.2 Cell-type specific silencing of active neurons using a Cre-dependent viral gene transfer approach

The viral construct (rAAV-CRAM-d2tTA::TRE-FLEX-hM4Di-mCherry) proposed for the following experimental approach was generated by Dr. Ana M.M. Oliveira, who inserted the hM4Di-mCherry expression cassette into the rAAV-RAM-d2tTA::TRE-FLEX-MCS obtained from addgene (plasmid#84467).

In order to clarify the role of the reward-specific neurochemical composition of neuronal ensembles involved in cue-induced reward seeking, neuronal ensembles can be silenced in a

cell-type specific manner. This can be achieved by utilisation of CaMKII-Cre or GAD1-Cre transgenic rats in combination with an rAAV-CRAM-d2tTA::TRE-FLEX-hM4Di-mCherry viral gene transfer (Fig. 61a). The cre-dependent robust activity marking system (CRAM) is extremely sensitive and allows the manipulation of Cre-expressing cells. Its sensitivity is achieved by an activity-regulated promoter, which is induced only in presence of strong neuronal activation. In addition, the construct comprises a modified tetracycline (Tet)-Off-system allowing for an optimized temporal control and thus high selectivity (Sørensen et al., 2016). Furthermore, the effector sequence, comprised of hM4D(GI)-mCherry, is expressed under control of a tTA-responsive element (TRE)-promoter and dependent on Cre-recombinase, allowing the deactivation of active cells. In order to apply this method to our drug-self-administration and reinstatement model, CaMKII-Cre or GAD1-Cre rats are injected with rAAV-CRAM-d2tTA::TRE-FLEX-hM4Di-mCherry into the brain region of interest. Thus, hM4Di will only be expressed in either glutamatergic (CaMKII) or GABAergic (GAD1) neurons and activated cells can be inhibited in their activity during drug-seeking behaviour. Expression is furthermore controlled by the Tet-Off-system (Fig. 61b) (Gossen et al., 1995). The destabilized tetracycline transactivator (d2tTA), whose expression is controlled by the P_{RAM} promoter, induces expression of the effector gene cassette by binding to the TRE. However, binding of d2tTA to TRE can be inhibited by the presence of doxycycline (Sorensen et al., 2016). Thus, expression of hM4D, a modified human M4 muscarinic receptor, can be temporally controlled by removal of doxycycline, allowing expression only during cue-induced reward seeking. This tight control of the CRAM-system will result in expression of hM4D only in glutamatergic (CaMKII) or GABAergic (GAD1) neurons of the neuronal ensemble encoding for cue-induced reward seeking. hM4D can be activated by clozapine-N-oxide (CNO), a hM4D agonist, which will result in a dramatically reduced excitability potential (Ferguson et al., 2011; Zhang et al., 2018; Tanimura et al., 2019). Thus, intraperitoneal injection of CNO before the second cue-induced reinstatement test, will result in silencing of glutamatergic (CaMKII) or GABAergic (GAD1) neurons active during the first reinstatement, allowing their functional investigation in the second reward seeking test.

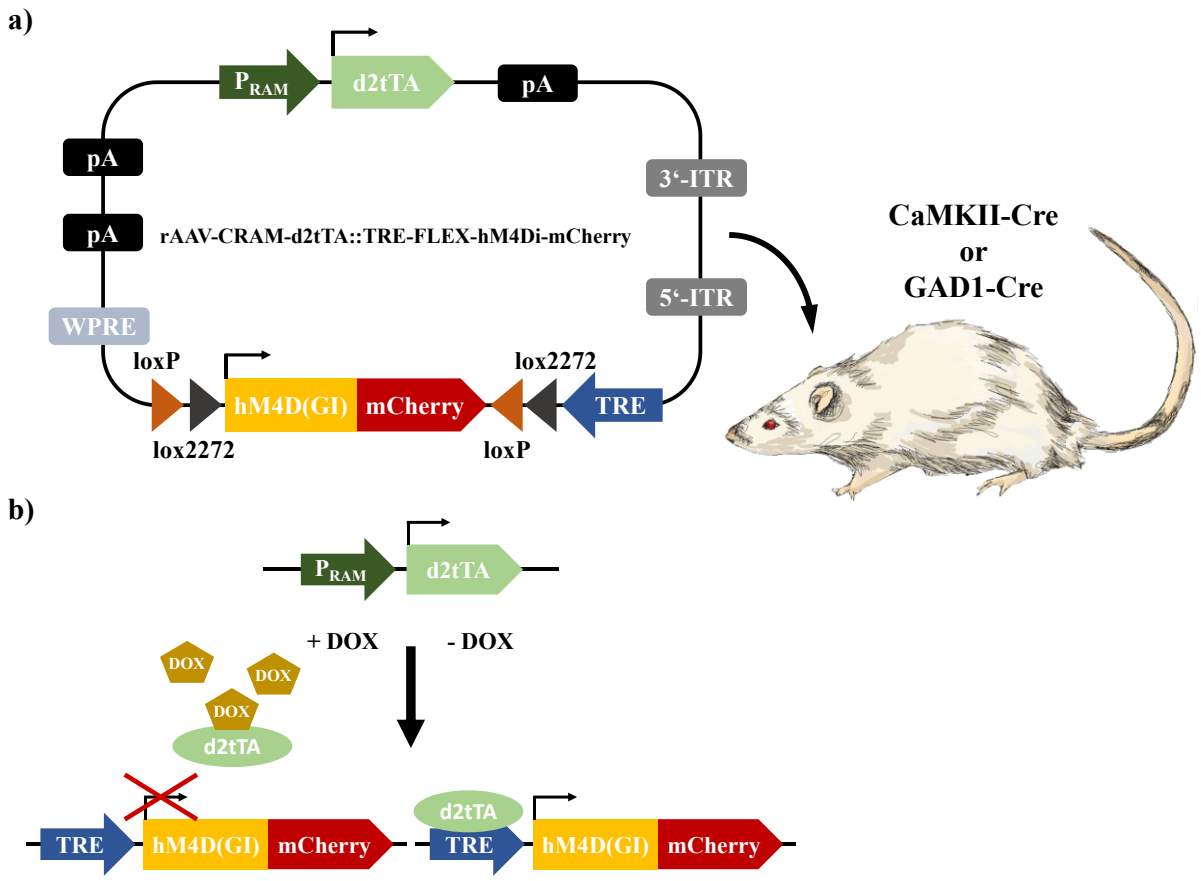

Figure 61) Schematic representation of the viral rAAV-CRAM-d2tTA::TRE-FLEX-hM4Di-mCherry construct and the Tet-OFF system

a) Scheme of the viral rAAV-CRAM construct with all crucial genetic elements indicated. The virus is injected in the OFC of CaMKII-Cre or CAD1-Cre transgenic rats, as the effector cassette (hM4D(GI)-mCherry) can only be expressed in glutamatergic or GABAergic neurons producing Cre-recombinase. Effector expression, however, is also controlled by the TRE-promoter, which is dependent on the P_{RAM}-promoter inducing d2tTA expression. b) Illustration of the Tet-OFF system and its control of effector expression. The TRE-promoter requires binding of d2tTA to induce expression of hM4D(GI)-mCherry. d2tTA, whose expression is induced by P_{RAM}, can be bound by the antibiotic doxycycline (DOX), which prevents binding to TRE. Doxycycline administration therefore inhibits effector expression. Abbreviations: P_{RAM} = Robust activity marking promoter, d2tTA = destabilized tetracycline transactivator, pA = SV40 polyadenylation signal, 3'-ITR = 3' inverted terminal repeat, 5'-ITR = 5' inverted terminal repeat, TRE = tTA-responsive element promoter, lox2272/loxP = recombination sites, mCherry = coding sequence for the red fluorescent protein mCherry, hM4D(GI) = coding sequence for modified human M4 muscarinic receptor, WPRE = woodchuck hepatitis virus post-transcriptional regulatory element. Adapted and modified from (Sørensen et al., 2016), Viral construct generated by Ana M.M. Oliveira, Rat picture used and modified with permission from Wolfgang Sommer.

7. REFERENCES

Abernathy K, Chandler LJ, Woodward JJ (2010) Alcohol and the prefrontal cortex. Int Rev Neurobiol 91:289-320.

Abrahao KP, Salinas AG, Lovinger DM (2017) Alcohol and the Brain: Neuronal Molecular Targets, Synapses, and Circuits. Neuron 96:1223-1238.

Adinoff B (2004) Neurobiologic processes in drug reward and addiction. Harv Rev Psychiatry 12:305-320.

Agell N, Bachs O, Rocamora N, Villalonga P (2002) Modulation of the Ras/Raf/MEK/ERK pathway by Ca2+, and Calmodulin. Cellular Signalling 14:649-654.

Alberts B JA, Lewis J, et al. (2002) Molecular Biology of the Cell. Available from: https://www.ncbi.nlm.nih.gov/books/NBK26822/ New York: Garland Science.

Alcaraz F, Marchand AR, Courtand G, Coutureau E, Wolff M (2016) Parallel inputs from the mediodorsal thalamus to the prefrontal cortex in the rat. European Journal of Neuroscience 44:1972-1986.

Alessi DR, Saito Y, Campbell DG, Cohen P, Sithanandam G, Rapp U, Ashworth A, Marshall CJ, Cowley S (1994) Identification of the sites in MAP kinase kinase-1 phosphorylated by p74raf-1. EMBO J 13:1610-1619.

American Psychiatric Association (2013) Diagnostic and Statistical Manual of Mental Disorders (DSM-5), Fifth Edition. Washington, DC.

Angel P, Karin M (1991) The role of Jun, Fos and the AP-1 complex in cell-proliferation and transformation. Biochim Biophys Acta 1072:129-157.

Anthony J, Warner L, Kessler R (1994) Comparative Epidemiology of Dependence on Tobacco, Alcohol, Controlled Substances, and Inhalants: Basic Findings From the National Comorbidity Survey. Experimental and Clinical Psychopharmacology 2:244-268.

Arguello AA, Richardson BD, Hall JL, Wang R, Hodges MA, Mitchell MP, Stuber GD, Rossi DJ, Fuchs RA (2017) Role of a Lateral Orbital Frontal Cortex-Basolateral Amygdala Circuit in Cue-Induced Cocaine-Seeking Behavior. Neuropsychopharmacology : official publication of the American College of Neuropsychopharmacology 42:727-735.

Arias-Carrión O, Pöppel E (2007) Dopamine, learning, and reward-seeking behavior. Acta Neurobiol Exp (Wars) 67:481-488.

Arinze I, Moorman DE (2020) Selective impact of lateral orbitofrontal cortex inactivation on reinstatement of alcohol seeking in male Long-Evans rats. Neuropharmacology 168:108007.

Arnold DL, Krewski D, Munro IC (1983) Saccharin: a toxicological and historical perspective. Toxicology 27:179-256.

Asanuma M, Ogawa N (1994) Pitfalls in assessment of c-fos mRNA expression in the brain: effects of animal handling. Rev Neurosci 5:171-178.

Asanuma M, Ogawa N, Hirata H, Chou H, Tanaka K, Mori A (1992) Opposite effects of rough and gentle handling with repeated saline administration on c-fos mRNA expression in the rat brain. J Neural Transm Gen Sect 90:163-169.

Atzendorf J, Rauschert C, Seitz NN, Lochbuhler K, Kraus L (2019) The Use of Alcohol, Tobacco, Illegal Drugs and Medicines. Dtsch Arztebl Int 116:577-584.

Azevedo FA, Carvalho LR, Grinberg LT, Farfel JM, Ferretti RE, Leite RE, Jacob Filho W, Lent R, Herculano-Houzel S (2009) Equal numbers of neuronal and nonneuronal cells make the human brain an isometrically scaled-up primate brain. J Comp Neurol 513:532-541.

Bading H, Hardingham GE, Johnson CM, Chawla S (1997) Gene Regulation by Nuclear and Cytoplasmic Calcium Signals. Biochemical and Biophysical Research Communications 236:541-543.

Baeg EH, Jackson ME, Jedema HP, Bradberry CW (2009) Orbitofrontal and anterior cingulate cortex neurons selectively process cocaine-associated environmental cues in the rhesus monkey. J Neurosci 29:11619-11627.

Bahrami S, Drabløs F (2016) Gene regulation in the immediate-early response process. Advances in Biological Regulation 62:37-49.

Bal A, Gerena J, Olekanma DI, Arguello AA (2019) Neuronal activation in orbitofrontal cortex subregions: Cfos expression following cue-induced reinstatement of cocaine-seeking behavior. Behav Neurosci 133:489-495.

Banerjee A, Parente G, Teutsch J, Lewis C, Voigt FF, Helmchen F (2020) Value-guided remapping of sensory cortex by lateral orbitofrontal cortex. Nature 585:245-250.

Barbosa FF, Silva RH (2018) Chapter 18 - Immediate-Early Gene Expression in Neural Circuits Related to Object Recognition Memory. In: Handbook of Behavioral Neuroscience (Ennaceur A, de Souza Silva MA, eds), pp 261-271: Elsevier.

Barros VN, Mundim M, Galindo LT, Bittencourt S, Porcionatto M, Mello LE (2015) The pattern of c-Fos expression and its refractory period in the brain of rats and monkeys. Front Cell Neurosci 9.

Barth AL, Gerkin RC, Dean KL (2004) Alteration of neuronal firing properties after in vivo experience in a FosGFP transgenic mouse. The Journal of neuroscience : the official journal of the Society for Neuroscience 24:6466-6475.

Bear M, Connors B, Paradiso M (2016) Neuroscience: Exploring the brain: Fourth edition. Philadelphia: Wolters Kluwer.

Bechara A (2005) Decision making, impulse control and loss of willpower to resist drugs: a neurocognitive perspective. Nat Neurosci 8:1458-1463.

Bengtson CP, Bading H (2012) Nuclear calcium signaling. Adv Exp Med Biol 970:377-405.

Benowitz NL (2010) Nicotine addiction. N Engl J Med 362:2295-2303.

Benson DL, Isackson PJ, Gall CM, Jones EG (1992) Contrasting patterns in the localization of glutamic acid decarboxylase and Ca2+/calmodulin protein kinase gene expression in the rat central nervous system. Neuroscience 46:825-849.

Berridge KC (2003) Pleasures of the brain. Brain and Cognition 52:106-128.

Berridge KC, Kringelbach ML (2008) Affective neuroscience of pleasure: reward in humans and animals. Psychopharmacology (Berl) 199:457-480.

Berridge KC, Kringelbach ML (2015) Pleasure systems in the brain. Neuron 86:646-664.

Berridge KC, Robinson TE (2016) Liking, wanting, and the incentive-sensitization theory of addiction. Am Psychol 71:670-679.

Berridge KC, Robinson TE, Aldridge JW (2009) Dissecting components of reward: 'liking', 'wanting', and learning. Curr Opin Pharmacol 9:65-73.

Bianchi PC, Carneiro de Oliveira PE, Palombo P, Leão RM, Cogo-Moreira H, Planeta CDS, Cruz FC (2018) Functional inactivation of the orbitofrontal cortex disrupts context-induced reinstatement of alcohol seeking in rats. Drug Alcohol Depend 186:102-112.

Bossert JM, Marchant NJ, Calu DJ, Shaham Y (2013) The reinstatement model of drug relapse: recent neurobiological findings, emerging research topics, and translational research. Psychopharmacology 229:453-476.

Bossert JM, Wihbey KA, Pickens CL, Nair SG, Shaham Y (2009) Role of dopamine D(1)-family receptors in dorsolateral striatum in context-induced reinstatement of heroin seeking in rats. Psychopharmacology 206:51-60.

Bossert JM, Stern AL, Theberge FRM, Cifani C, Koya E, Hope BT, Shaham Y (2011) Ventral medial prefrontal cortex neuronal ensembles mediate context-induced relapse to heroin. Nature neuroscience 14:420-422.

Boulougouris V, Dalley JW, Robbins TW (2007) Effects of orbitofrontal, infralimbic and prelimbic cortical lesions on serial spatial reversal learning in the rat. Behav Brain Res 179:219-228.

Brenhouse HC, Stellar JR (2006) c-Fos and ΔFosB expression are differentially altered in distinct subregions of the nucleus accumbens shell in cocaine-sensitized rats. Neuroscience 137:773-780.

Brenner M (2014) Role of GFAP in CNS injuries. Neuroscience letters 565:7-13.

Broccoli L, Uhrig S, von Jonquieres G, Schönig K, Bartsch D, Justice NJ, Spanagel R, Sommer WH, Klugmann M, Hansson AC (2018) Targeted overexpression of CRH receptor subtype 1 in central amygdala neurons: effect on alcohol-seeking behavior. Psychopharmacology 235:1821-1833.

Bundeskriminalamt (2018) Rauschgiftkriminalität, Bundeslagebild 2018, Seite 29 und 30.

Burton AC, Nakamura K, Roesch MR (2015) From ventral-medial to dorsal-lateral striatum: neural correlates of reward-guided decision-making. Neurobiology of learning and memory 117:51-59.

Burton AC, Bissonette GB, Vazquez D, Blume EM, Donnelly M, Heatley KC, Hinduja A, Roesch MR (2018) Previous cocaine self-administration disrupts reward expectancy encoding in ventral striatum. Neuropsychopharmacology : official publication of the American College of Neuropsychopharmacology 43:2350-2360.

Cai DJ et al. (2016) A shared neural ensemble links distinct contextual memories encoded close in time. Nature 534:115-118.

Campbell EJ, Flanagan JPM, Walker LC, Hill M, Marchant NJ, Lawrence AJ (2019) Anterior Insular Cortex is Critical for the Propensity to Relapse Following Punishment-Imposed Abstinence of Alcohol Seeking. J Neurosci 39:1077-1087.

Caprioli D, Venniro M, Zhang M, Bossert JM, Warren BL, Hope BT, Shaham Y (2017) Role of Dorsomedial Striatum Neuronal Ensembles in Incubation of Methamphetamine Craving after Voluntary Abstinence. The Journal of neuroscience : the official journal of the Society for Neuroscience 37:1014-1027.

Carelli RM, Williams JG, Hollander JA (2003) Basolateral amygdala neurons encode cocaine self-administration and cocaine-associated cues. The Journal of neuroscience : the official journal of the Society for Neuroscience 23:8204-8211.

Carelli RM, King VC, Hampson RE, Deadwyler SA (1993) Firing patterns of nucleus accumbens neurons during cocaine self-administration in rats. Brain Res 626:14-22.

Carlén M (2017) What constitutes the prefrontal cortex? Science 358:478-482.

Castillo-Morales A, Monzón-Sandoval J, de Sousa AA, Urrutia AO, Gutierrez H (2016) Neocortex expansion is linked to size variations in gene families with chemotaxis, cell-cell signalling and immune response functions in mammals. Open Biol 6:160132.

Causton HC, Ren B, Koh SS, Harbison CT, Kanin E, Jennings EG, Lee TI, True HL, Lander ES, Young RA (2001) Remodeling of yeast genome expression in response to environmental changes. Mol Biol Cell 12:323-337.

Chang JY, Zhang L, Janak PH, Woodward DJ (1997) Neuronal responses in prefrontal cortex and nucleus accumbens during heroin self-administration in freely moving rats. Brain Res 754:12-20.

Chappel CI (1992) A review and biological risk assessment of sodium saccharin. Regul Toxicol Pharmacol 15:253-270.

Chase EA, Tait DS, Brown VJ (2012) Lesions of the orbital prefrontal cortex impair the formation of attentional set in rats. Eur J Neurosci 36:2368-2375.

Chaudhri N, Sahuque LL, Schairer WW, Janak PH (2010) Separable roles of the nucleus accumbens core and shell in context- and cue-induced alcohol-seeking. Neuropsychopharmacology : official publication of the American College of Neuropsychopharmacology 35:783-791.

Chudasama Y, Robbins TW (2003) Dissociable contributions of the orbitofrontal and infralimbic cortex to pavlovian autoshaping and discrimination reversal learning: further evidence for the functional heterogeneity of the rodent frontal cortex. The Journal of neuroscience : the official journal of the Society for Neuroscience 23:8771-8780.

Ciccocioppo R, Sanna PP, Weiss F (2001a) Cocaine-predictive stimulus induces drug-seeking behavior and neural activation in limbic brain regions after multiple months of abstinence: reversal by D(1) antagonists. Proceedings of the National Academy of Sciences of the United States of America 98:1976-1981.

Ciccocioppo R, Sanna PP, Weiss F (2001b) Cocaine-predictive stimulus induces drug-seeking behavior and neural activation in limbic brain regions after multiple months of abstinence: Reversal by D₁ antagonists. Proceedings of the National Academy of Sciences 98:1976.

Cifani C, Koya E, Navarre BM, Calu DJ, Baumann MH, Marchant NJ, Liu QR, Khuc T, Pickel J, Lupica CR, Shaham Y, Hope BT (2012a) Medial prefrontal cortex neuronal activation and synaptic alterations after stress-induced reinstatement of palatable food seeking: a study using c-fos-GFP transgenic female rats. The Journal of neuroscience : the official journal of the Society for Neuroscience 32:8480-8490.

Cifani C, Koya E, Navarre BM, Calu DJ, Baumann MH, Marchant NJ, Liu Q-R, Khuc T, Pickel J, Lupica CR, Shaham Y, Hope BT (2012b) Medial prefrontal cortex neuronal activation and synaptic alterations after stress-induced reinstatement of palatable food seeking: a

study using c-fos-GFP transgenic female rats. The Journal of neuroscience : the official journal of the Society for Neuroscience 32:8480-8490.

Cohen S, Greenberg ME (2008) Communication between the synapse and the nucleus in neuronal development, plasticity, and disease. Annu Rev Cell Dev Biol 24:183-209.

Cooper S, Robison AJ, Mazei-Robison MS (2017) Reward Circuitry in Addiction. Neurotherapeutics 14:687-697.

Cregler LL (1989) Adverse health consequences of cocaine abuse. J Natl Med Assoc 81:27-38.

Crombag HS, Shaham Y (2002) Renewal of drug seeking by contextual cues after prolonged extinction in rats. Behav Neurosci 116:169-173.

Cruz FC, Javier Rubio F, Hope BT (2015) Using c-fos to study neuronal ensembles in corticostriatal circuitry of addiction. Brain Res 1628:157-173.

Cruz FC, Koya E, Guez-Barber DH, Bossert JM, Lupica CR, Shaham Y, Hope BT (2013) New technologies for examining the role of neuronal ensembles in drug addiction and fear. Nat Rev Neurosci 14:743-754.

Cruz FC, Babin KR, Leao RM, Goldart EM, Bossert JM, Shaham Y, Hope BT (2014) Role of nucleus accumbens shell neuronal ensembles in context-induced reinstatement of cocaine-seeking. The Journal of neuroscience : the official journal of the Society for Neuroscience 34:7437-7446.

D'Souza MS, Markou A (2014) Differential role of N-methyl-D-aspartate receptor-mediated glutamate transmission in the nucleus accumbens shell and core in nicotine seeking in rats. European Journal of Neuroscience 39:1314-1322.

Dajas-Bailador F, Wonnacott S (2004) Nicotinic acetylcholine receptors and the regulation of neuronal signalling. Trends in Pharmacological Sciences 25:317-324.

Dalley JW, Cardinal RN, Robbins TW (2004) Prefrontal executive and cognitive functions in rodents: neural and neurochemical substrates. Neuroscience & Biobehavioral Reviews 28:771-784.

Dalton GL, Wang NY, Phillips AG, Floresco SB (2016) Multifaceted Contributions by Different Regions of the Orbitofrontal and Medial Prefrontal Cortex to Probabilistic Reversal Learning. J Neurosci 36:1996-2006.

Davis S, Bozon B, Laroche S (2003) How necessary is the activation of the immediate early gene zif268 in synaptic plasticity and learning? Behavioural Brain Research 142:17-30.

Dayas CV, Liu X, Simms JA, Weiss F (2007) Distinct patterns of neural activation associated with ethanol seeking: effects of naltrexone. Biological psychiatry 61:979-989.

de Guglielmo G, Crawford E, Kim S, Vendruscolo LF, Hope BT, Brennan M, Cole M, Koob GF, George O (2016) Recruitment of a Neuronal Ensemble in the Central Nucleus of the Amygdala Is Required for Alcohol Dependence. The Journal of neuroscience : the official journal of the Society for Neuroscience 36:9446-9453.

de Wit H, Stewart J (1981) Reinstatement of cocaine-reinforced responding in the rat. Psychopharmacology (Berl) 75:134-143.

den Hartog C, Zamudio-Bulcock P, Nimitvilai S, Gilstrap M, Eaton B, Fedarovich H, Motts A, Woodward JJ (2016) Inactivation of the lateral orbitofrontal cortex increases drinking in ethanol-dependent but not non-dependent mice. Neuropharmacology 107:451-459.

DePoy LM, McClung CA, Logan RW (2017) Neural Mechanisms of Circadian Regulation of Natural and Drug Reward. Neural Plast 2017:5720842.

Deutsche Hauptstelle für Suchtfragen e.V. (2013) Tabakabhängigkeit, Suchtmedizinische Reihe, Band 2. In. Deutsche Hauptstelle für Suchtfragen e. V., Westenwall 4, 59065 Hamm.

Die Drogenbeauftragte der Bundesregierung (2019) Drogen- und Suchtbericht 2019. In. Die Drogenbeauftragte der Bundesregierung beim Bundesministerium für Gesundheit 11055 Berlin.

Dixon ML, Thiruchselvam R, Todd R, Christoff K (2017) Emotion and the prefrontal cortex: An integrative review. Psychol Bull 143:1033-1081.

Dorr A, Sled JG, Kabani N (2007) Three-dimensional cerebral vasculature of the CBA mouse brain: a magnetic resonance imaging and micro computed tomography study. Neuroimage 35:1409-1423.

Drake LR, Scott PJH (2018) DARK Classics in Chemical Neuroscience: Cocaine. ACS Chem Neurosci 9:2358-2372.

Drevets WC (2007) Orbitofrontal cortex function and structure in depression. Ann N Y Acad Sci 1121:499-527.

Duan W, Zhang YP, Hou Z, Huang C, Zhu H, Zhang CQ, Yin Q (2016) Novel Insights into NeuN: from Neuronal Marker to Splicing Regulator. Mol Neurobiol 53:1637-1647.

Dudley R (2000) Evolutionary origins of human alcoholism in primate frugivory. Q Rev Biol 75:3-15.

Ellenbroek BA, Cools AR (1990) Animal models with construct validity for schizophrenia. Behav Pharmacol 1:469-490.

Ellwein LB, Cohen SM (1990) The Health Risks of Saccharin Revisited. Critical Reviews in Toxicology 20:311-326.

Epstein DH, Preston KL, Stewart J, Shaham Y (2006) Toward a model of drug relapse: an assessment of the validity of the reinstatement procedure. Psychopharmacology (Berl) 189:1-16.

Everitt BJ, Robbins TW (2005) Neural systems of reinforcement for drug addiction: from actions to habits to compulsion. Nature Neuroscience 8:1481-1489.

Everitt BJ, Hutcheson DM, Ersche KD, Pelloux Y, Dalley JW, Robbins TW (2007) The Orbital Prefrontal Cortex and Drug Addiction in Laboratory Animals and Humans. Annals of the New York Academy of Sciences 1121:576-597.

Everitt BJ, Belin D, Economidou D, Pelloux Y, Dalley JW, Robbins TW (2008) Review. Neural mechanisms underlying the vulnerability to develop compulsive drug-seeking habits and addiction. Philos Trans R Soc Lond B Biol Sci 363:3125-3135.

Fadda F, Rossetti ZL (1998) Chronic ethanol consumption:from neuroadaptation to neurodegeneration. Prog Neurobiol 56:385-431.

Fan H, Pan X, Wang R, Sakagami M (2017) Differences in reward processing between putative cell types in primate prefrontal cortex. PLoS One 12:e0189771-e0189771.

Fanous S, Goldart EM, Theberge FRM, Bossert JM, Shaham Y, Hope BT (2012) Role of orbitofrontal cortex neuronal ensembles in the expression of incubation of heroin

craving. The Journal of neuroscience : the official journal of the Society for Neuroscience 32:11600-11609.

Feng Z, Kong L-Y, Qi Q, Ho S-L, Tiao N, Bing G, Han Y-F (2001) Induction of unspliced c-fos messenger RNA in rodent brain by kainic acid and lipopolysaccharide. Neuroscience Letters 305:17-20.

Ferguson SM, Eskenazi D, Ishikawa M, Wanat MJ, Phillips PEM, Dong Y, Roth BL, Neumaier JF (2011) Transient neuronal inhibition reveals opposing roles of indirect and direct pathways in sensitization. Nature Neuroscience 14:22-24.

Fettes P, Schulze L, Downar J (2017) Cortico-Striatal-Thalamic Loop Circuits of the Orbitofrontal Cortex: Promising Therapeutic Targets in Psychiatric Illness. Front Syst Neurosci 11:25-25.

Fetz EE (1999) Real-time control of a robotic arm by neuronal ensembles. Nat Neurosci 2:583-584.

Filip M, Frankowska M, Zaniewska M, Gołda A, Przegaliński E (2005) The serotonergic system and its role in cocaine addiction. Pharmacol Rep 57:685-700.

Florio M, Huttner WB (2014) Neural progenitors, neurogenesis and the evolution of the neocortex. Development 141:2182-2194.

Fosque BF, Sun Y, Dana H, Yang CT, Ohyama T, Tadross MR, Patel R, Zlatic M, Kim DS, Ahrens MB, Jayaraman V, Looger LL, Schreiter ER (2015) Neural circuits. Labeling of active neural circuits in vivo with designed calcium integrators. Science 347:755-760.

Fuchs RA, Evans KA, Parker MP, See RE (2004) Differential involvement of orbitofrontal cortex subregions in conditioned cue-induced and cocaine-primed reinstatement of cocaine seeking in rats. J Neurosci 24:6600-6610.

Funk D, Coen K, Tamadon S, Hope BT, Shaham Y, Lê AD (2016) Role of Central Amygdala Neuronal Ensembles in Incubation of Nicotine Craving. The Journal of neuroscience : the official journal of the Society for Neuroscience 36:8612-8623.

Gall CM, Hess US, Lynch G (1998) Mapping Brain Networks Engaged by, and Changed by, Learning. Neurobiology of Learning and Memory 70:14-36.

Gandolfi D, Cerri S, Mapelli J, Polimeni M, Tritto S, Fuzzati-Armentero M-T, Bigiani A, Blandini F, Mapelli L, D'Angelo E (2017) Activation of the CREB/c-Fos Pathway during Long-Term Synaptic Plasticity in the Cerebellum Granular Layer. Front Cell Neurosci 11:184-184.

Gao XJ, Yuan K, Cao L, Yan W, Luo YX, Jian M, Liu JF, Fang Q, Wang JS, Han Y, Shi J, Lu L (2017) AMPK signaling in the nucleus accumbens core mediates cue-induced reinstatement of cocaine seeking. Sci Rep 7:1038.

García Pardo MP, Roger Sánchez C, De la Rubia Ortí JE, Aguilar Calpe MA (2017) Animal models of drug addiction. Adicciones 29:278-292.

Gauvin DV, Moore KR, Holloway FA (1993) Do rat strain differences in ethanol consumption reflect differences in ethanol sensitivity or the preparedness to learn? Alcohol 10:37-43.

George O, Hope BT (2017) Cortical and amygdalar neuronal ensembles in alcohol seeking, drinking and withdrawal. Neuropharmacology 122:107-114.

Girgenti MJ, Wohleb ES, Mehta S, Ghosal S, Fogaca MV, Duman RS (2019) Prefrontal cortex interneurons display dynamic sex-specific stress-induced transcriptomes. Transl Psychiatry 9:292-292.

Glowa JR, Hansen CT (1994) Differences in response to an acoustic startle stimulus among forty-six rat strains. Behav Genet 24:79-84.

Goepfrich AA, Gluch C, Friemel CM, Schneider M (2013) Behavioral differences in three Wistar Han rat lines for emotional reactivity, cognitive processing and ethanol intake. Physiol Behav 110-111:102-108.

Goldstein RA, DesLauriers C, Burda AM (2009) Cocaine: history, social implications, and toxicity--a review. Dis Mon 55:6-38.

Goldstein RZ, Volkow ND (2002) Drug addiction and its underlying neurobiological basis: neuroimaging evidence for the involvement of the frontal cortex. The American journal of psychiatry 159:1642-1652.

Goldstein RZ, Volkow ND (2011) Dysfunction of the prefrontal cortex in addiction: neuroimaging findings and clinical implications. Nat Rev Neurosci 12:652-669.

Golebiowska J, Rygula R (2017) Lesions of the Orbitofrontal but Not Medial Prefrontal Cortex Affect Cognitive Judgment Bias in Rats. Frontiers in behavioral neuroscience 11:51-51.

Gonzales BJ, Mukherjee D, Ashwal-Fluss R, Loewenstein Y, Citri A (2020) Subregion-specific rules govern the distribution of neuronal immediate-early gene induction. Proceedings of the National Academy of Sciences of the United States of America 117:23304-23310.

Goodman JH, Sloviter RS (1993) Cocaine neurotoxicity and altered neuropeptide Y immunoreactivity in the rat hippocampus; a silver degeneration and immunocytochemical study. Brain Res 616:263-272.

Gordon JW, Scangos GA, Plotkin DJ, Barbosa JA, Ruddle FH (1980) Genetic transformation of mouse embryos by microinjection of purified DNA. Proceedings of the National Academy of Sciences of the United States of America 77:7380-7384.

Gossen M, Freundlieb S, Bender G, Müller G, Hillen W, Bujard H (1995) Transcriptional Activation by Tetracyclines in Mammalian Cells. Science 268:1766-1769.

Gremel CM, Lovinger DM (2017) Associative and sensorimotor cortico-basal ganglia circuit roles in effects of abused drugs. Genes Brain Behav 16:71-85.

Gremel CM, Young EA, Cunningham CL (2011) Blockade of opioid receptors in anterior cingulate cortex disrupts ethanol-seeking behavior in mice. Behav Brain Res 219:358-362.

Haber SN, Fudge JL, McFarland NR (2000) Striatonigrostriatal pathways in primates form an ascending spiral from the shell to the dorsolateral striatum. J Neurosci 20:2369-2382.

Hamlin AS, Blatchford KE, McNally GP (2006) Renewal of an extinguished instrumental response: Neural correlates and the role of D1 dopamine receptors. Neuroscience 143:25-38.

Hamlin AS, Newby J, McNally GP (2007) The neural correlates and role of D1 dopamine receptors in renewal of extinguished alcohol-seeking. Neuroscience 146:525-536.

Hansson AC, Gründer G, Hirth N, Noori HR, Spanagel R, Sommer WH (2019) Dopamine and opioid systems adaptation in alcoholism revisited: Convergent evidence from positron

emission tomography and postmortem studies. Neuroscience & Biobehavioral Reviews 106:141-164.

Harris RA, Mihic SJ (2004) Alcohol and inhibitory receptors: unexpected specificity from a nonspecific drug. Proceedings of the National Academy of Sciences of the United States of America 101:2-3.

Hearing MC, See RE, McGinty JF (2008) Relapse to cocaine-seeking increases activity-regulated gene expression differentially in the striatum and cerebral cortex of rats following short or long periods of abstinence. Brain structure & function 213:215-227.

Hebb DO (1949) The organization of behaviour: a neuropsychological theory. New York: Wiley.

Heidbreder CA, Groenewegen HJ (2003) The medial prefrontal cortex in the rat: evidence for a dorso-ventral distinction based upon functional and anatomical characteristics. Neurosci Biobehav Rev 27:555-579.

Heilig M, Barbier E, Johnstone AL, Tapocik J, Meinhardt MW, Pfarr S, Wahlestedt C, Sommer WH (2017) Reprogramming of mPFC transcriptome and function in alcohol dependence. Genes Brain Behav 16:86-100.

Heimer L, Alheid GF, de Olmos JS, Groenewegen HJ, Haber SN, Harlan RE, Zahm DS (1997) The accumbens: beyond the core-shell dichotomy. J Neuropsychiatry Clin Neurosci 9:354-381.

Herman AI, DeVito EE, Jensen KP, Sofuoglu M (2014) Pharmacogenetics of nicotine addiction: role of dopamine. Pharmacogenomics 15:221-234.

Hernandez JS, Moorman DE (2020) Orbitofrontal Cortex Encodes Preference for Alcohol. eNeuro 7:ENEURO.0402-0419.2020.

Hernandez JS, Binette AN, Rahman T, Tarantino JD, Moorman DE (2020) Chemogenetic Inactivation of Orbitofrontal Cortex Decreases Cue-induced Reinstatement of Ethanol and Sucrose Seeking in Male and Female Wistar Rats. Alcoholism: Clinical and Experimental Research 44:1769-1782.

Herrera DG, Robertson HA (1996) Activation of c-fos in the brain. Prog Neurobiol 50:83-107.

Hika B, Al Khalili Y (2020) Neuronatomy, Prefrontal Association Cortex. In: StatPearls. Treasure Island (FL): StatPearls Publishing; Copyright © 2020, StatPearls Publishing LLC.

Hisanaga K, Sagar SM, Hicks KJ, Swanson RA, Sharp FR (1990) c-fos proto-oncogene expression in astrocytes associated with differentiation or proliferation but not depolarization. Brain Res Mol Brain Res 8:69-75.

Hoffman GE, Smith MS, Verbalis JG (1993) c-Fos and related immediate early gene products as markers of activity in neuroendocrine systems. Front Neuroendocrinol 14:173-213.

Holtmaat A, Caroni P (2016) Functional and structural underpinnings of neuronal assembly formation in learning. Nature Neuroscience 19:1553-1562.

Hoover WB, Vertes RP (2007) Anatomical analysis of afferent projections to the medial prefrontal cortex in the rat. Brain Struct Funct 212:149-179.

Hoover WB, Vertes RP (2011) Projections of the medial orbital and ventral orbital cortex in the rat. Journal of Comparative Neurology 519:3766-3801.

Huang J-J, Yen C-T, Tsai M-L, Valenzuela CF, Huang C (2012) Acute ethanol exposure increases firing and induces oscillations in cerebellar Golgi cells of freely moving rats. Alcoholism, clinical and experimental research 36:2110-2116.

Huber RS, Subramaniam P, Kondo DG, Shi X, Renshaw PF, Yurgelun-Todd DA (2019) Reduced lateral orbitofrontal cortex volume and suicide behavior in youth with bipolar disorder. Bipolar Disord 21:321-329.

Hyman SE, Malenka RC, Nestler EJ (2006) NEURAL MECHANISMS OF ADDICTION: The Role of Reward-Related Learning and Memory. Annual Review of Neuroscience 29:565-598.

Ikemoto S, Bonci A (2014) Neurocircuitry of drug reward. Neuropharmacology 76 Pt B:329-341.

Institute for Health Metrics and Evaluation (2017) Global Burden of Disease Study 2017, Global Health Data Exchange. In. Retrieved from http://ghdx.healthdata.org/gbd-results-tool on 13.05.2020.

Izquierdo A (2017) Functional Heterogeneity within Rat Orbitofrontal Cortex in Reward Learning and Decision Making. J Neurosci 37:10529-10540.

Josselyn SA, Frankland PW (2018) Memory Allocation: Mechanisms and Function. Annu Rev Neurosci 41:389-413.

Jupp B, Krstew E, Dezsi G, Lawrence AJ (2011) Discrete cue-conditioned alcohol-seeking after protracted abstinence: pattern of neural activation and involvement of orexin$_1$ receptors. British journal of pharmacology 162:880-889.

Jurado J, Fuentes-Almagro CA, Prieto-Alamo MJ, Pueyo C (2007) Alternative splicing of c-fos pre-mRNA: contribution of the rates of synthesis and degradation to the copy number of each transcript isoform and detection of a truncated c-Fos immunoreactive species. BMC Mol Biol 8:83-83.

Kalivas PW, Volkow ND (2005) The neural basis of addiction: a pathology of motivation and choice. Am J Psychiatry 162:1403-1413.

Kamigaki T (2019) Prefrontal circuit organization for executive control. Neuroscience Research 140:23-36.

Kane L, Venniro M, Quintana-Feliciano R, Madangopal R, Rubio FJ, Bossert JM, Caprioli D, Shaham Y, Hope BT, Warren BL (2020) Fos-expressing neuronal ensemble in rat ventromedial prefrontal cortex encodes cocaine seeking but not food seeking in rats. Addiction Biology n/a:e12943.

Kareken DA, Grahame N, Dzemidzic M, Walker MJ, Lehigh CA, O'Connor SJ (2012) fMRI of the brain's response to stimuli experimentally paired with alcohol intoxication. Psychopharmacology 220:787-797.

Kariisa M, Scholl L, Wilson N, Seth P, Hoots B (2019) Drug Overdose Deaths Involving Cocaine and Psychostimulants with Abuse Potential - United States, 2003-2017. MMWR Morb Mortal Wkly Rep 68:388-395.

Karila L, Gorelick D, Weinstein A, Noble F, Benyamina A, Coscas S, Blecha L, Lowenstein W, Martinot JL, Reynaud M, Lépine JP (2008) New treatments for cocaine dependence: a focused review. Int J Neuropsychopharmacol 11:425-438.

Kasof GM, Mandelzys A, Maika SD, Hammer RE, Curran T, Morgan JI (1995) Kainic acid-induced neuronal death is associated with DNA damage and a unique immediate-early gene response in c-fos-lacZ transgenic rats. J Neurosci 15:4238-4249.

Kelley AE, Berridge KC (2002) The neuroscience of natural rewards: relevance to addictive drugs. J Neurosci 22:3306-3311.

Kesner RP, Churchwell JC (2011) An analysis of rat prefrontal cortex in mediating executive function. Neurobiology of Learning and Memory 96:417-431.

Kim KK, Adelstein RS, Kawamoto S (2009) Identification of neuronal nuclei (NeuN) as Fox-3, a new member of the Fox-1 gene family of splicing factors. J Biol Chem 284:31052-31061.

Kiyatkin EA, Rebec GV (1997) Activity of presumed dopamine neurons in the ventral tegmental area during heroin self-administration. Neuroreport 8:2581-2585.

Klitenick MA, Deutch AY, Churchill L, Kalivas PW (1992) Topography and functional role of dopaminergic projections from the ventral mesencephalic tegmentum to the ventral pallidum. Neuroscience 50:371-386.

Knackstedt LA, Moussawi K, Lalumiere R, Schwendt M, Klugmann M, Kalivas PW (2010) Extinction training after cocaine self-administration induces glutamatergic plasticity to inhibit cocaine seeking. The Journal of neuroscience : the official journal of the Society for Neuroscience 30:7984-7992.

Koob GF, Volkow ND (2010) Neurocircuitry of addiction. Neuropsychopharmacology 35:217-238.

Koruza K, Mahon BP, Blakeley MP, Ostermann A, Schrader TE, McKenna R, Knecht W, Fisher SZ (2019) Using neutron crystallography to elucidate the basis of selective inhibition of carbonic anhydrase by saccharin and a derivative. J Struct Biol 205:147-154.

Kotz D, Böckmann M, Kastaun S (2018) The Use of Tobacco, E-Cigarettes, and Methods to Quit Smoking in Germany. Deutsches Arzteblatt international 115:235-242.

Kovács KJ (1998) Invited review c-Fos as a transcription factor: a stressful (re)view from a functional map. Neurochemistry International 33:287-297.

Kovács KJ (2008) Measurement of immediate-early gene activation- c-fos and beyond. J Neuroendocrinol 20:665-672.

Koya E, Margetts-Smith G, Hope BT (2016) Daun02 Inactivation of Behaviorally Activated Fos-Expressing Neuronal Ensembles. Curr Protoc Neurosci 76:8.36.31-38.36.17.

Koya E, Uejima JL, Wihbey KA, Bossert JM, Hope BT, Shaham Y (2009a) Role of ventral medial prefrontal cortex in incubation of cocaine craving. Neuropharmacology 56 Suppl 1:177-185.

Koya E, Golden SA, Harvey BK, Guez-Barber DH, Berkow A, Simmons DE, Bossert JM, Nair SG, Uejima JL, Marin MT, Mitchell TB, Farquhar D, Ghosh SC, Mattson BJ, Hope BT (2009b) Targeted disruption of cocaine-activated nucleus accumbens neurons prevents context-specific sensitization. Nat Neurosci 12:1069-1073.

Kringelbach ML (2005) The human orbitofrontal cortex: linking reward to hedonic experience. Nature Reviews Neuroscience 6:691-702.

Kufahl PR, Zavala AR, Singh A, Thiel KJ, Dickey ED, Joyce JN, Neisewander JL (2009) c-Fos expression associated with reinstatement of cocaine-seeking behavior by response-contingent conditioned cues. Synapse 63:823-835.

Kumar M, Chail M (2019) Sucrose and saccharin differentially modulate depression and anxiety-like behavior in diabetic mice: exposures and withdrawal effects. Psychopharmacology 236:3095-3110.

LaLumiere RT, Smith KC, Kalivas PW (2012) Neural circuit competition in cocaine-seeking: roles of the infralimbic cortex and nucleus accumbens shell. The European journal of neuroscience 35:614-622.

Lamb RJ, Schindler CW, Pinkston JW (2016) Conditioned stimuli's role in relapse: preclinical research on Pavlovian-Instrumental-Transfer. Psychopharmacology 233:1933-1944.

Lanahan A, Worley P (1998) Immediate-early genes and synaptic function. Neurobiol Learn Mem 70:37-43.

Lasseter HC, Ramirez DR, Xie X, Fuchs RA (2009) Involvement of the lateral orbitofrontal cortex in drug context-induced reinstatement of cocaine-seeking behavior in rats. The European journal of neuroscience 30:1370-1381.

Laubach M, Amarante LM, Swanson K, White SR (2018) What, If Anything, Is Rodent Prefrontal Cortex? eNeuro 5:ENEURO.0315-0318.2018.

Lee CR, Tepper JM (2009) Basal ganglia control of substantia nigra dopaminergic neurons. J Neural Transm Suppl:71-90.

Lee J, Lee K (2021) Parvalbumin-expressing GABAergic interneurons and perineuronal nets in the prelimbic and orbitofrontal cortices in association with basal anxiety-like behaviors in adult mice. Behav Brain Res 398:112915.

Lee S-E, Lee Y, Lee GH (2019) The regulation of glutamic acid decarboxylases in GABA neurotransmission in the brain. Archives of Pharmacal Research 42:1031-1039.

Lenoir M, Serre F, Cantin L, Ahmed SH (2007) Intense sweetness surpasses cocaine reward. PLoS One 2:e698-e698.

Leutgeb S, Leutgeb JK, Barnes CA, Moser EI, McNaughton BL, Moser MB (2005) Independent codes for spatial and episodic memory in hippocampal neuronal ensembles. Science 309:619-623.

Lichtenberg NT, Pennington ZT, Holley SM, Greenfield VY, Cepeda C, Levine MS, Wassum KM (2017) Basolateral Amygdala to Orbitofrontal Cortex Projections Enable Cue-Triggered Reward Expectations. The Journal of neuroscience : the official journal of the Society for Neuroscience 37:8374-8384.

Limpens JH, Damsteegt R, Broekhoven MH, Voorn P, Vanderschuren LJ (2015) Pharmacological inactivation of the prelimbic cortex emulates compulsive reward seeking in rats. Brain Res 1628:210-218.

Lin D, Boyle MP, Dollar P, Lee H, Lein ES, Perona P, Anderson DJ (2011) Functional identification of an aggression locus in the mouse hypothalamus. Nature 470:221-226.

London ED, Ernst M, Grant S, Bonson K, Weinstein A (2000) Orbitofrontal Cortex and Human Drug Abuse: Functional Imaging. Cerebral Cortex 10:334-342.

Lüscher C, Ungless MA (2006) The mechanistic classification of addictive drugs. PLoS Med 3:e437.

Madsen HB, Ahmed SH (2015) Drug versus sweet reward: greater attraction to and preference for sweet versus drug cues. Addiction Biology 20:433-444.

Madsen HB, Brown RM, Short JL, Lawrence AJ (2012) Investigation of the neuroanatomical substrates of reward seeking following protracted abstinence in mice. J Physiol 590:2427-2442.

Malvaez M, Shieh C, Murphy MD, Greenfield VY, Wassum KM (2019) Distinct cortical-amygdala projections drive reward value encoding and retrieval. Nature neuroscience 22:762-769.

Mandt BH, Schenk S, Zahniser NR, Allen RM (2008) Individual differences in cocaine-induced locomotor activity in male Sprague-Dawley rats and their acquisition of and motivation to self-administer cocaine. Psychopharmacology 201:195-202.

Marchant NJ, Li X, Shaham Y (2013) Recent developments in animal models of drug relapse. Current opinion in neurobiology 23:675-683.

Marinelli PW, Funk D, Juzytsch W, Lê AD (2010) Opioid receptors in the basolateral amygdala but not dorsal hippocampus mediate context-induced alcohol seeking. Behavioural brain research 211:58-63.

Marinelli PW, Funk D, Juzytsch W, Li Z, Lê AD (2007) Effects of opioid receptor blockade on the renewal of alcohol seeking induced by context: relationship to c-fos mRNA expression. Eur J Neurosci 26:2815-2823.

Markram H, Toledo-Rodriguez M, Wang Y, Gupta A, Silberberg G, Wu C (2004) Interneurons of the neocortical inhibitory system. Nature Reviews Neuroscience 5:793-807.

Martin-Fardon R, Weiss F (2014) Blockade of hypocretin receptor-1 preferentially prevents cocaine seeking: comparison with natural reward seeking. Neuroreport 25:485-488.

Martin-Fardon R, Weiss F (2017) Perseveration of craving: effects of stimuli conditioned to drugs of abuse versus conventional reinforcers differing in demand. Addiction biology 22:923-932.

Martin-Fardon R. WF (2012) Modeling Relapse in Animals. In: Behavioral Neurobiology of Alcohol Addiction. Current Topics in Behavioral Neurosciences (Sommer W. SR, ed), pp 403-432. Berlin, Heidelberg: Springer.

Mayford M (2013) The search for a hippocampal engram. Philos Trans R Soc Lond B Biol Sci 369:20130161-20130161.

McCracken CB, Grace AA (2007) High-frequency deep brain stimulation of the nucleus accumbens region suppresses neuronal activity and selectively modulates afferent drive in rat orbitofrontal cortex in vivo. The Journal of neuroscience : the official journal of the Society for Neuroscience 27:12601-12610.

McCubrey JA, Steelman LS, Chappell WH, Abrams SL, Wong EWT, Chang F, Lehmann B, Terrian DM, Milella M, Tafuri A, Stivala F, Libra M, Basecke J, Evangelisti C, Martelli AM, Franklin RA (2007) Roles of the Raf/MEK/ERK pathway in cell growth, malignant transformation and drug resistance. Biochimica et biophysica acta 1773:1263-1284.

McGlinchey EM, James MH, Mahler SV, Pantazis C, Aston-Jones G (2016) Prelimbic to Accumbens Core Pathway Is Recruited in a Dopamine-Dependent Manner to Drive Cued Reinstatement of Cocaine Seeking. J Neurosci 36:8700-8711.

Meil WM, See RE (1996) Conditioned cued recovery of responding following prolonged withdrawal from self-administered cocaine in rats: an animal model of relapse. Behav Pharmacol 7:754-763.

Merlino GT (1991) Transgenic animals in biomedical research. Faseb j 5:2996-3001.

Middeldorp J, Hol EM (2011) GFAP in health and disease. Prog Neurobiol 93:421-443.

Milde-Langosch K (2005) The Fos family of transcription factors and their role in tumourigenesis. Eur J Cancer 41:2449-2461.

Millan EZ, Reese RM, Grossman CD, Chaudhri N, Janak PH (2015) Nucleus Accumbens and Posterior Amygdala Mediate Cue-Triggered Alcohol Seeking and Suppress Behavior During the Omission of Alcohol-Predictive Cues. Neuropsychopharmacology : official publication of the American College of Neuropsychopharmacology 40:2555-2565.

Miller CA, Marshall JF (2004) Altered Prelimbic Cortex Output during Cue-Elicited Drug Seeking. The Journal of Neuroscience 24:6889.

Miller EK, Cohen JD (2001) An integrative theory of prefrontal cortex function. Annu Rev Neurosci 24:167-202.

Minogianis E-A, Servonnet A, Filion M-P, Samaha A-N (2019) Role of the orbitofrontal cortex and the dorsal striatum in incentive motivation for cocaine. Behavioural Brain Research 372:112026.

Miyazaki K, Miyazaki KW, Sivori G, Yamanaka A, Tanaka KF, Doya K (2020) Serotonergic projections to the orbitofrontal and medial prefrontal cortices differentially modulate waiting for future rewards. Sci Adv 6:eabc7246.

Moorman DE (2018) The role of the orbitofrontal cortex in alcohol use, abuse, and dependence. Prog Neuropsychopharmacol Biol Psychiatry 87:85-107.

Moorman DE, Aston-Jones G (2015) Prefrontal neurons encode context-based response execution and inhibition in reward seeking and extinction. Proceedings of the National Academy of Sciences of the United States of America 112:9472-9477.

Moorman DE, James MH, McGlinchey EM, Aston-Jones G (2015) Differential roles of medial prefrontal subregions in the regulation of drug seeking. Brain Res 1628:130-146.

Morgan JI, Cohen DR, Hempstead JL, Curran T (1987) Mapping patterns of c-fos expression in the central nervous system after seizure. Science 237:192.

Murphy MJM, Deutch AY (2018) Organization of afferents to the orbitofrontal cortex in the rat. The Journal of comparative neurology 526:1498-1526.

Nakao T, Okada K, Kanba S (2014) Neurobiological model of obsessive–compulsive disorder: Evidence from recent neuropsychological and neuroimaging findings. Psychiatry and Clinical Neurosciences 68:587-605.

Nicolelis MAL, Fanselow EE, Ghazanfar AA (1997) Hebb's Dream: The Resurgence of Cell Assemblies. Neuron 19:219-221.

Nonkes LJP, van Bussel IPG, Verheij MMM, Homberg JR (2011) The interplay between brain 5-hydroxytryptamine levels and cocaine addiction. Behavioural Pharmacology 22:723-738.

Northcutt KV, Nwankwo VC (2018) Sex differences in juvenile play behavior differ among rat strains. Dev Psychobiol 60:903-912.

Oades RD, Halliday GM (1987) Ventral tegmental (A10) system: neurobiology. 1. Anatomy and connectivity. Brain Research Reviews 12:117-165.

Oh H, Lee J, Gosnell SN, Patriquin M, Kosten T, Salas R (2020) Orbitofrontal, dorsal striatum, and habenula functional connectivity in psychiatric patients with substance use problems. Addictive Behaviors 108:106457.

Öngür D, Price JL (2000) The Organization of Networks within the Orbital and Medial Prefrontal Cortex of Rats, Monkeys and Humans. Cerebral Cortex 10:206-219.

Otis JM, Mueller D (2017) Reversal of Cocaine-Associated Synaptic Plasticity in Medial Prefrontal Cortex Parallels Elimination of Memory Retrieval. Neuropsychopharmacology : official publication of the American College of Neuropsychopharmacology 42:2000-2010.

Palmatier MI, Evans-Martin FF, Hoffman A, Caggiula AR, Chaudhri N, Donny EC, Liu X, Booth S, Gharib M, Craven L, Sved AF (2006) Dissociating the primary reinforcing and reinforcement-enhancing effects of nicotine using a rat self-administration paradigm with concurrently available drug and environmental reinforcers. Psychopharmacology (Berl) 184:391-400.

Palombo P, Leao RM, Bianchi PC, de Oliveira PEC, Planeta CdS, Cruz FC (2017) Inactivation of the Prelimbic Cortex Impairs the Context-Induced Reinstatement of Ethanol Seeking. Front Pharmacol 8:725-725.

Pardo-Garcia TR, Garcia-Keller C, Penaloza T, Richie CT, Pickel J, Hope BT, Harvey BK, Kalivas PW, Heinsbroek JA (2019) Ventral Pallidum Is the Primary Target for Accumbens D1 Projections Driving Cocaine Seeking. The Journal of Neuroscience 39:2041.

Parikh V, Naughton SX, Shi X, Kelley LK, Yegla B, Tallarida CS, Rawls SM, Unterwald EM (2014) Cocaine-induced neuroadaptations in the dorsal striatum: glutamate dynamics and behavioral sensitization. Neurochem Int 75:54-65.

Parsons LH, Hurd YL (2015) Endocannabinoid signalling in reward and addiction. Nat Rev Neurosci 16:579-594.

Paxinos G, Watson C (1998) The rat brain in stereotaxic coordinates. Academic Press, Inc. 525 B Street, Suite 1900, San Diego, California 92101-4495, USA.

Peoples LL, West MO (1996) Phasic firing of single neurons in the rat nucleus accumbens correlated with the timing of intravenous cocaine self-administration. The Journal of neuroscience : the official journal of the Society for Neuroscience 16:3459-3473.

Pérez-Cadahía B, Drobic B, Davie JR (2011) Activation and function of immediate-early genes in the nervous system. Biochem Cell Biol 89:61-73.

Peters J, LaLumiere RT, Kalivas PW (2008) Infralimbic prefrontal cortex is responsible for inhibiting cocaine seeking in extinguished rats. J Neurosci 28:6046-6053.

Pfarr S (2018) The Role of the Medial Prefrontal Cortex in Reward Seeking: Functional Evidence on Cellular and Molecular Mechanisms underlying Drug and Natural Reward Seeking In: Ruprecht-Karls-Universität Heidelberg.

Pfarr S, Meinhardt MW, Klee ML, Hansson AC, Vengeliene V, Schönig K, Bartsch D, Hope BT, Spanagel R, Sommer WH (2015) Losing Control: Excessive Alcohol Seeking after Selective Inactivation of Cue-Responsive Neurons in the Infralimbic Cortex. J Neurosci 35:10750-10761.

Pfarr S, Schaaf L, Reinert JK, Paul E, Herrmannsdorfer F, Roßmanith M, Kuner T, Hansson AC, Spanagel R, Korber C, Sommer WH (2018) Choice for Drug or Natural Reward Engages Largely Overlapping Neuronal Ensembles in the Infralimbic Prefrontal Cortex. J Neurosci 38:3507-3519.

Picciotto MR, Addy NA, Mineur YS, Brunzell DH (2008) It is not "either/or": activation and desensitization of nicotinic acetylcholine receptors both contribute to behaviors related to nicotine addiction and mood. Prog Neurobiol 84:329-342.

Pierce RC, Kumaresan V (2006) The mesolimbic dopamine system: the final common pathway for the reinforcing effect of drugs of abuse? Neurosci Biobehav Rev 30:215-238.

Pizzimenti CL, Lattal KM (2015) Epigenetics and memory: causes, consequences and treatments for post-traumatic stress disorder and addiction. Genes Brain Behav 14:73-84.

Poulin JF, Caronia G, Hofer C, Cui Q, Helm B, Ramakrishnan C, Chan CS, Dombeck DA, Deisseroth K, Awatramani R (2018) Mapping projections of molecularly defined dopamine neuron subtypes using intersectional genetic approaches. Nat Neurosci 21:1260-1271.

Powell GL, Leyrer-Jackson JM, Goenaga J, Namba MD, Piña J, Spencer S, Stankeviciute N, Schwartz D, Allen NP, Del Franco AP, McClure EA, Olive MF, Gipson CD (2019) Chronic treatment with N-acetylcysteine decreases extinction responding and reduces cue-induced nicotine-seeking. Physiol Rep 7:e13958-e13958.

PubMed.gov NLoM (2020) In. Retrieved from https://pubmed.ncbi.nlm.nih.gov/?term=neuronal%20ensembles on 24.10.2020: National Center for Biotechnology Information, 8600 Rockville Pike Bethesda, MD 20894 USA

Pushparaj A, Kim AS, Musiol M, Trigo JM, Le Foll B (2015) Involvement of the rostral agranular insular cortex in nicotine self-administration in rats. Behavioural Brain Research 290:77-83.

Radnikow G, Feldmeyer D (2018) Layer- and Cell Type-Specific Modulation of Excitatory Neuronal Activity in the Neocortex. Front Neuroanat 12:1-1.

Rajkowska G, Miguel-Hidalgo JJ (2007) Gliogenesis and glial pathology in depression. CNS Neurol Disord Drug Targets 6:219-233.

Ranaldi R (2014) Dopamine and reward seeking: the role of ventral tegmental area. Rev Neurosci 25:621-630.

Rashid AJ, Yan C, Mercaldo V, Hsiang H-LL, Park S, Cole CJ, De Cristofaro A, Yu J, Ramakrishnan C, Lee SY, Deisseroth K, Frankland PW, Josselyn SA (2016) Competition between engrams influences fear memory formation and recall. Science (New York, NY) 353:383-387.

Reep RL, Corwin JV, King V (1996) Neuronal connections of orbital cortex in rats: topography of cortical and thalamic afferents. Experimental Brain Research 111:215-232.

Rehm J, Room R, Graham K, Monteiro M, Gmel G, Sempos CT (2003) The relationship of average volume of alcohol consumption and patterns of drinking to burden of disease: an overview. Addiction 98:1209-1228.

Rehm J, Gmel Sr GE, Gmel G, Hasan OSM, Imtiaz S, Popova S, Probst C, Roerecke M, Room R, Samokhvalov AV, Shield KD, Shuper PA (2017) The relationship between different

dimensions of alcohol use and the burden of disease—an update. Addiction 112:968-1001.

Rehm J, Baliunas D, Borges GLG, Graham K, Irving H, Kehoe T, Parry CD, Patra J, Popova S, Poznyak V, Roerecke M, Room R, Samokhvalov AV, Taylor B (2010) The relation between different dimensions of alcohol consumption and burden of disease: an overview. Addiction (Abingdon, England) 105:817-843.

Rehn S, Onuma T, Rooney KB, Boakes RA (2018) Sodium saccharin can be more acceptable to rats than pure saccharin. Behavioural Processes 157:188-191.

Reilly MT, Noronha A, Goldman D, Koob GF (2017) Genetic studies of alcohol dependence in the context of the addiction cycle. Neuropharmacology 122:3-21.

Reiner DJ, Lofaro OM, Applebey SV, Korah H, Venniro M, Cifani C, Bossert JM, Shaham Y (2020) Role of Projections between Piriform Cortex and Orbitofrontal Cortex in Relapse to Fentanyl Seeking after Palatable Food Choice-Induced Voluntary Abstinence. The Journal of neuroscience : the official journal of the Society for Neuroscience 40:2485-2497.

Rempel-Clower NL (2007) Role of Orbitofrontal Cortex Connections in Emotion. Annals of the New York Academy of Sciences 1121:72-86.

Reynolds JN, Hyland BI, Wickens JR (2001) A cellular mechanism of reward-related learning. Nature 413:67-70.

Riceberg JS, Shapiro ML (2017) Orbitofrontal Cortex Signals Expected Outcomes with Predictive Codes When Stable Contingencies Promote the Integration of Reward History. The Journal of neuroscience : the official journal of the Society for Neuroscience 37:2010-2021.

Richardson CL, Tate WP, Mason SE, Lawlor PA, Dragunow M, Abraham WC (1992) Correlation between the induction of an immediate early gene, zif/268, and long-term potentiation in the dentate gyrus. Brain Res 580:147-154.

Roberto M, Varodayan FP (2017) Synaptic targets: Chronic alcohol actions. Neuropharmacology 122:85-99.

Roberts AC (2006) Primate orbitofrontal cortex and adaptive behaviour. Trends Cogn Sci 10:83-90.

Robinson TE, Berridge KC (1993) The neural basis of drug craving: An incentive-sensitization theory of addiction. Brain Research Reviews 18:247-291.

Robinson TE, Kolb B (1999) Alterations in the morphology of dendrites and dendritic spines in the nucleus accumbens and prefrontal cortex following repeated treatment with amphetamine or cocaine. European Journal of Neuroscience 11:1598-1604.

Robinson TE, Kolb B (2004) Structural plasticity associated with exposure to drugs of abuse. Neuropharmacology 47:33-46.

Robinson TE, Gorny G, Mitton E, Kolb B (2001) Cocaine self-administration alters the morphology of dendrites and dendritic spines in the nucleus accumbens and neocortex. Synapse 39:257-266.

Rocha A, Kalivas PW (2010) Role of the prefrontal cortex and nucleus accumbens in reinstating methamphetamine seeking. Eur J Neurosci 31:903-909.

Rodríguez-Arellano JJ, Parpura V, Zorec R, Verkhratsky A (2016) Astrocytes in physiological aging and Alzheimer's disease. Neuroscience 323:170-182.

Rolls ET (2015) Taste, olfactory, and food reward value processing in the brain. Prog Neurobiol 127-128:64-90.

Root DH, Fabbricatore AT, Ma S, Barker DJ, West MO (2010) Rapid phasic activity of ventral pallidal neurons during cocaine self-administration. Synapse (New York, NY) 64:704-713.

Rubio FJ, Liu Q-R, Li X, Cruz FC, Leão RM, Warren BL, Kambhampati S, Babin KR, McPherson KB, Cimbro R, Bossert JM, Shaham Y, Hope BT (2015) Context-induced reinstatement of methamphetamine seeking is associated with unique molecular alterations in Fos-expressing dorsolateral striatum neurons. The Journal of neuroscience : the official journal of the Society for Neuroscience 35:5625-5639.

Rudebeck PH, Rich EL (2018) Orbitofrontal cortex. Curr Biol 28:R1083-r1088.

Rudy B, Fishell G, Lee S, Hjerling-Leffler J (2011) Three groups of interneurons account for nearly 100% of neocortical GABAergic neurons. Dev Neurobiol 71:45-61.

Russo SJ, Nestler EJ (2013) The brain reward circuitry in mood disorders. Nat Rev Neurosci 14:609-625.

Sakurai K, Zhao S, Takatoh J, Rodriguez E, Lu J, Leavitt AD, Fu M, Han B-X, Wang F (2016) Capturing and Manipulating Activated Neuronal Ensembles with CANE Delineates a Hypothalamic Social-Fear Circuit. Neuron 92:739-753.

Sams-Dodd F (1999) Phencyclidine in the social interaction test: an animal model of schizophrenia with face and predictive validity. Rev Neurosci 10:59-90.

Sams-Dodd F (2006) Strategies to optimize the validity of disease models in the drug discovery process. Drug Discovery Today 11:355-363.

Sanchis-Segura C, Spanagel R (2006) Behavioural assessment of drug reinforcement and addictive features in rodents: an overview. Addict Biol 11:2-38.

Scheyer AF, Loweth JA, Christian DT, Uejima J, Rabei R, Le T, Dolubizno H, Stefanik MT, Murray CH, Sakas C, Wolf ME (2016) AMPA Receptor Plasticity in Accumbens Core Contributes to Incubation of Methamphetamine Craving. Biol Psychiatry 80:661-670.

Schilling K, Luk D, Morgan JI, Curran T (1991) Regulation of a fos-lacZ fusion gene: a paradigm for quantitative analysis of stimulus-transcription coupling. Proceedings of the National Academy of Sciences of the United States of America 88:5665-5669.

Schilman EA, Uylings HBM, Graaf YG-d, Joel D, Groenewegen HJ (2008) The orbital cortex in rats topographically projects to central parts of the caudate–putamen complex. Neuroscience Letters 432:40-45.

Schmidt HD, Pierce RC (2010) Cocaine-induced neuroadaptations in glutamate transmission: potential therapeutic targets for craving and addiction. Ann N Y Acad Sci 1187:35-75.

Schönig K, Weber T, Frömmig A, Wendler L, Pesold B, Djandji D, Bujard H, Bartsch D (2012) Conditional gene expression systems in the transgenic rat brain. BMC Biol 10:77-77.

Schroeder BE, Kelley AE (2002) Conditioned Fos expression following morphine-paired contextual cue exposure is environment specific. Behav Neurosci 116:727-732.

Schroeder BE, Binzak JM, Kelley AE (2001) A common profile of prefrontal cortical activation following exposure to nicotine- or chocolate-associated contextual cues. Neuroscience 105:535-545.

Schuster CR, Thompson T (1969) Self administration of and behavioral dependence on drugs. Annu Rev Pharmacol 9:483-502.

Sciascia JM, Reese RM, Janak PH, Chaudhri N (2015) Alcohol-Seeking Triggered by Discrete Pavlovian Cues is Invigorated by Alcohol Contexts and Mediated by Glutamate Signaling in the Basolateral Amygdala. Neuropsychopharmacology : official publication of the American College of Neuropsychopharmacology 40:2801-2812.

Seitz N-N, Lochbühler K, Atzendorf J, Rauschert C, Pfeiffer-Gerschel T, Kraus L (2019) Trends In Substance Use And Related Disorders. Deutsches Arzteblatt international 116:585-591.

Sesia T, Bizup B, Grace AA (2014) Nucleus accumbens high-frequency stimulation selectively impacts nigrostriatal dopaminergic neurons. Int J Neuropsychopharmacol 17:421-427.

Settell ML, Testini P, Cho S, Lee JH, Blaha CD, Jo HJ, Lee KH, Min H-K (2017) Functional Circuitry Effect of Ventral Tegmental Area Deep Brain Stimulation: Imaging and Neurochemical Evidence of Mesocortical and Mesolimbic Pathway Modulation. Front Neurosci 11:104-104.

Shaham Y, Stewart J (1995) Stress reinstates heroin-seeking in drug-free animals: an effect mimicking heroin, not withdrawal. Psychopharmacology (Berl) 119:334-341.

Sheng M, Greenberg ME (1990) The regulation and function of c-fos and other immediate early genes in the nervous system. Neuron 4:477-485.

Shepard JD, Bossert JM, Liu SY, Shaham Y (2004) The anxiogenic drug yohimbine reinstates methamphetamine seeking in a rat model of drug relapse. Biol Psychiatry 55:1082-1089.

Shields CN, Gremel CM (2020) Review of Orbitofrontal Cortex in Alcohol Dependence: A Disrupted Cognitive Map? Alcohol Clin Exp Res.

Shuldiner AR (1996) Transgenic Animals. New England Journal of Medicine 334:653-654.

Simmons JM, Richmond BJ (2007) Dynamic Changes in Representations of Preceding and Upcoming Reward in Monkey Orbitofrontal Cortex. Cerebral Cortex 18:93-103.

Sinclair CM, Cleva RM, Hood LE, Olive MF, Gass JT (2012) mGluR5 receptors in the basolateral amygdala and nucleus accumbens regulate cue-induced reinstatement of ethanol-seeking behavior. Pharmacol Biochem Behav 101:329-335.

Sladky R, Höflich A, Atanelov J, Kraus C, Baldinger P, Moser E, Lanzenberger R, Windischberger C (2012) Increased neural habituation in the amygdala and orbitofrontal cortex in social anxiety disorder revealed by FMRI. PLoS One 7:e50050-e50050.

Sleezer BJ, Castagno MD, Hayden BY (2016) Rule Encoding in Orbitofrontal Cortex and Striatum Guides Selection. J Neurosci 36:11223-11237.

Sleezer BJ, LoConte GA, Castagno MD, Hayden BY (2017) Neuronal responses support a role for orbitofrontal cortex in cognitive set reconfiguration. Eur J Neurosci 45:940-951.

Sompolinsky H (2014) Computational neuroscience: beyond the local circuit. Current Opinion in Neurobiology 25:xiii-xviii.

Sørensen AT, Cooper YA, Baratta MV, Weng F-J, Zhang Y, Ramamoorthi K, Fropf R, LaVerriere E, Xue J, Young A, Schneider C, Gøtzsche CR, Hemberg M, Yin JCP, Maier SF, Lin Y (2016) A robust activity marking system for exploring active neuronal ensembles. Elife 5:e13918.

Spanagel R (2009) Alcoholism: A Systems Approach From Molecular Physiology to Addictive Behavior. Physiological Reviews 89:649-705.

Spanagel R (2017) Animal models of addiction. Dialogues Clin Neurosci 19:247-258.

Spanagel R, Weiss F (1999) The dopamine hypothesis of reward: past and current status. Trends Neurosci 22:521-527.

Sporns O, Tononi G, Kötter R (2005) The human connectome: A structural description of the human brain. PLoS Comput Biol 1:e42-e42.

Stalnaker TA, Liu T-L, Takahashi YK, Schoenbaum G (2018) Orbitofrontal neurons signal reward predictions, not reward prediction errors. Neurobiology of learning and memory 153:137-143.

Stewart J, de Wit H, Eikelboom R (1984) Role of unconditioned and conditioned drug effects in the self-administration of opiates and stimulants. Psychol Rev 91:251-268.

Stöhr T, Schulte Wermeling D, Weiner I, Feldon J (1998) Rat strain differences in open-field behavior and the locomotor stimulating and rewarding effects of amphetamine. Pharmacol Biochem Behav 59:813-818.

Strahlendorf HK, Barnes CD (1983) Control of substantia nigra pars reticulata neurons by the nucleus accumbens. Brain Res Bull 11:259-263.

Sudhinaraset M, Wigglesworth C, Takeuchi DT (2016) Social and Cultural Contexts of Alcohol Use: Influences in a Social-Ecological Framework. Alcohol Res 38:35-45.

Sullivan RJ, Hagen EH (2002) Psychotropic substance-seeking: evolutionary pathology or adaptation? Addiction 97:389-400.

Sullivan RJ, Hagen EH, Hammerstein P (2008) Revealing the paradox of drug reward in human evolution. Proc Biol Sci 275:1231-1241.

Suto N, Laque A, De Ness GL, Wagner GE, Watry D, Kerr T, Koya E, Mayford MR, Hope BT, Weiss F (2016) Distinct memory engrams in the infralimbic cortex of rats control opposing environmental actions on a learned behavior. Elife 5:e21920.

Tanimura A, Du Y, Kondapalli J, Wokosin DL, Surmeier DJ (2019) Cholinergic Interneurons Amplify Thalamostriatal Excitation of Striatal Indirect Pathway Neurons in Parkinson's Disease Models. Neuron 101:444-458.e446.

Tepper JM, Lee CR (2007) GABAergic control of substantia nigra dopaminergic neurons. In: Progress in Brain Research (Tepper JM, Abercrombie ED, Bolam JP, eds), pp 189-208: Elsevier.

Trask S, Shipman ML, Green JT, Bouton ME (2017) Inactivation of the Prelimbic Cortex Attenuates Context-Dependent Operant Responding. The Journal of neuroscience : the official journal of the Society for Neuroscience 37:2317-2324.

Trulson ME, Ulissey MJ (1987) Chronic cocaine administration decreases dopamine synthesis rate and increases [3H] spiroperidol binding in rat brain. Brain Res Bull 19:35-38.

Tsukada H, Kreuter J, Maggos CE, Unterwald EM, Kakiuchi T, Nishiyama S, Futatsubashi M, Kreek MJ (1996) Effects of binge pattern cocaine administration on dopamine D1 and D2 receptors in the rat brain: an in vivo study using positron emission tomography. The Journal of neuroscience : the official journal of the Society for Neuroscience 16:7670-7677.

U.S. Department of Health and Human Services (2010) A Report of the Surgeon General: How Tobacco Smoke Causes Disease: What It Means to You. In. U.S. Department of Health and Human Services, Centers for Disease Control and Prevention, National Center for Chronic Disease Prevention and Health Promotion, Office on Smoking and Health.

U.S. Department of Health and Human Services (2014) The Health Consequences of Smoking—50 Years of Progress; A Report of the Surgeon General; Executive Summary. In. U.S. Department of Health and Human Services, Public Health Service, Office of the Surgeon General, Rockville, MD.

United Nations (2019) World Drug Report 2019. In. United Nations publication, Sales No. E.19.XI.8.

Uylings HB, Groenewegen HJ, Kolb B (2003) Do rats have a prefrontal cortex? Behav Brain Res 146:3-17.

Van De Werd HJ, Uylings HB (2008) The rat orbital and agranular insular prefrontal cortical areas: a cytoarchitectonic and chemoarchitectonic study. Brain Struct Funct 212:387-401.

van Duuren E, Lankelma J, Pennartz CMA (2008) Population coding of reward magnitude in the orbitofrontal cortex of the rat. The Journal of neuroscience : the official journal of the Society for Neuroscience 28:8590-8603.

van Duuren E, van der Plasse G, Lankelma J, Joosten RNJMA, Feenstra MGP, Pennartz CMA (2009) Single-cell and population coding of expected reward probability in the orbitofrontal cortex of the rat. The Journal of neuroscience : the official journal of the Society for Neuroscience 29:8965-8976.

Van Hedger K, Keedy SK, Mayo LM, Heilig M, de Wit H (2018) Neural responses to cues paired with methamphetamine in healthy volunteers. Neuropsychopharmacology : official publication of the American College of Neuropsychopharmacology 43:1732-1737.

Varodayan FP, Bajo M, Soni N, Luu G, Madamba SG, Schweitzer P, Roberto M (2017) Chronic alcohol exposure disrupts CB(1) regulation of GABAergic transmission in the rat basolateral amygdala. Addiction biology 22:766-778.

Vengeliene V, Bilbao A, Molander A, Spanagel R (2008) Neuropharmacology of alcohol addiction. Br J Pharmacol 154:299-315.

Volkow ND, Fowler JS (2000) Addiction, a Disease of Compulsion and Drive: Involvement of the Orbitofrontal Cortex. Cerebral Cortex 10:318-325.

Volkow ND, Morales M (2015) The Brain on Drugs: From Reward to Addiction. Cell 162:712-725.

Volkow ND, Fowler JS, Wang G-J (2003) The addicted human brain: insights from imaging studies. J Clin Invest 111:1444-1451.

Volkow ND, Wang G-J, Fowler JS, Tomasi D, Telang F (2011) Addiction: beyond dopamine reward circuitry. Proceedings of the National Academy of Sciences of the United States of America 108:15037-15042.

Volkow ND, Fowler JS, Wang GJ, Hitzemann R, Logan J, Schlyer DJ, Dewey SL, Wolf AP (1993) Decreased dopamine D2 receptor availability is associated with reduced frontal metabolism in cocaine abusers. Synapse 14:169-177.

Volkow ND, Wang G-J, Telang F, Fowler JS, Logan J, Childress A-R, Jayne M, Ma Y, Wong C (2006) Cocaine Cues and Dopamine in Dorsal Striatum: Mechanism of Craving in Cocaine Addiction. The Journal of Neuroscience 26:6583.

Volkow ND, Fowler JS, Wolf AP, Schlyer D, Shiue CY, Alpert R, Dewey SL, Logan J, Bendriem B, Christman D, et al. (1990) Effects of chronic cocaine abuse on postsynaptic dopamine receptors. Am J Psychiatry 147:719-724.

von Wartburg JP (1990) [Considering the psychotropic effect of alcohol]. Ther Umsch 47:399-404.

Wall NR, Neumann PA, Beier KT, Mokhtari AK, Luo L, Malenka RC (2019) Complementary Genetic Targeting and Monosynaptic Input Mapping Reveal Recruitment and Refinement of Distributed Corticostriatal Ensembles by Cocaine. Neuron 104:916-930.e915.

Wallis JD (2011) Cross-species studies of orbitofrontal cortex and value-based decision-making. Nature neuroscience 15:13-19.

Wan C, Zhihuan N, Yaoxuan L, Jianping H, Chunxia C, Luying H (2017) Role of Dopamine Signaling in Drug Addiction. Current Topics in Medicinal Chemistry 17:2440-2455.

Wang JX, Kurth-Nelson Z, Kumaran D, Tirumala D, Soyer H, Leibo JZ, Hassabis D, Botvinick M (2018) Prefrontal cortex as a meta-reinforcement learning system. Nat Neurosci 21:860-868.

Wang Z, Yue L, Cui C, Liu S, Wang X, Li Y, Ma L (2019) Top-down control of the medial orbitofrontal cortex to nucleus accumbens core pathway in decisional impulsivity. Brain Structure and Function 224:2437-2452.

Warren BL, Suto N, Hope BT (2017) Mechanistic Resolution Required to Mediate Operant Learned Behaviors: Insights from Neuronal Ensemble-Specific Inactivation. Front Neural Circuits 11:28-28.

Warren BL, Mendoza MP, Cruz FC, Leao RM, Caprioli D, Rubio FJ, Whitaker LR, McPherson KB, Bossert JM, Shaham Y, Hope BT (2016) Distinct Fos-Expressing Neuronal Ensembles in the Ventromedial Prefrontal Cortex Mediate Food Reward and Extinction Memories. The Journal of neuroscience : the official journal of the Society for Neuroscience 36:6691-6703.

Warren BL, Kane L, Venniro M, Selvam P, Quintana-Feliciano R, Mendoza MP, Madangopal R, Komer L, Whitaker LR, Rubio FJ, Bossert JM, Caprioli D, Shaham Y, Hope BT (2019) Separate vmPFC Ensembles Control Cocaine Self-Administration Versus Extinction in Rats. The Journal of neuroscience : the official journal of the Society for Neuroscience 39:7394-7407.

Wee S, Wang Z, He R, Zhou J, Kozikowski AP, Woolverton WL (2006) Role of the increased noradrenergic neurotransmission in drug self-administration. Drug and Alcohol Dependence 82:151-157.

Weiner JL, Valenzuela CF (2006) Ethanol modulation of GABAergic transmission: The view from the slice. Pharmacology & Therapeutics 111:533-554.

Weiss F, Maldonado-Vlaar CS, Parsons LH, Kerr TM, Smith DL, Ben-Shahar O (2000) Control of cocaine-seeking behavior by drug-associated stimuli in rats: effects on recovery of extinguished operant-responding and extracellular dopamine levels in amygdala and nucleus accumbens. Proceedings of the National Academy of Sciences of the United States of America 97:4321-4326.

West EA, Saddoris MP, Kerfoot EC, Carelli RM (2014) Prelimbic and infralimbic cortical regions differentially encode cocaine-associated stimuli and cocaine-seeking before and following abstinence. The European journal of neuroscience 39:1891-1902.

Whitaker LR, Warren BL, Venniro M, Harte TC, McPherson KB, Beidel J, Bossert JM, Shaham Y, Bonci A, Hope BT (2017) Bidirectional Modulation of Intrinsic Excitability in Rat Prelimbic Cortex Neuronal Ensembles and Non-Ensembles after Operant Learning. The Journal of neuroscience : the official journal of the Society for Neuroscience 37:8845-8856.

White FJ, Kalivas PW (1998) Neuroadaptations involved in amphetamine and cocaine addiction. Drug Alcohol Depend 51:141-153.

Wilcox CE, Teshiba TM, Merideth F, Ling J, Mayer AR (2011) Enhanced cue reactivity and fronto-striatal functional connectivity in cocaine use disorders. Drug and alcohol dependence 115:137-144.

Willcocks AL, McNally GP (2013) The role of medial prefrontal cortex in extinction and reinstatement of alcohol-seeking in rats. Eur J Neurosci 37:259-268.

Willner P, Muscat R, Papp M (1992) Chronic mild stress-induced anhedonia: a realistic animal model of depression. Neurosci Biobehav Rev 16:525-534.

Wilson CRE, Gaffan D, Browning PGF, Baxter MG (2010) Functional localization within the prefrontal cortex: missing the forest for the trees? Trends Neurosci 33:533-540.

Wink M (2003) Evolution of secondary metabolites from an ecological and molecular phylogenetic perspective. Phytochemistry 64:3-19.

Wink M (2018) Plant Secondary Metabolites Modulate Insect Behavior-Steps Toward Addiction? Front Physiol 9:364.

Wise RA (2009) Roles for nigrostriatal--not just mesocorticolimbic--dopamine in reward and addiction. Trends Neurosci 32:517-524.

Wise SP (2008) Forward frontal fields: phylogeny and fundamental function. Trends Neurosci 31:599-608.

Wolffgramm J, Heyne A (1995) From controlled drug intake to loss of control: the irreversible development of drug addiction in the rat. Behav Brain Res 70:77-94.

Wonders CP, Anderson SA (2006) The origin and specification of cortical interneurons. Nature Reviews Neuroscience 7:687-696.

World Health Organization (2018) Alcohol. In. Retrieved from https://www.who.int/news-room/fact-sheets/detail/alcohol on 06.05.2020.

World Health Organization (2019) Tobacco. In. Retrieved from https://www.who.int/news-room/fact-sheets/detail/tobacco on 11.05.2020.

Xu P, Chen A, Li Y, Xing X, Lu H (2019) Medial prefrontal cortex in neurological diseases. Physiol Genomics 51:432-442.

Xue Y-X, Chen Y-Y, Zhang L-B, Zhang L-Q, Huang G-D, Sun S-C, Deng J-H, Luo Y-X, Bao Y-P, Wu P, Han Y, Hope BT, Shaham Y, Shi J, Lu L (2017) Selective Inhibition of Amygdala Neuronal Ensembles Encoding Nicotine-Associated Memories Inhibits Nicotine Preference and Relapse. Biological psychiatry 82:781-793.

Yamauchi T (2005) Neuronal Ca²⁺/Calmodulin-Dependent Protein Kinase II—Discovery, Progress in a Quarter of a Century, and Perspective: Implication for Learning and Memory. Biological and Pharmaceutical Bulletin 28:1342-1354.

Zhang G-W, Shen L, Zhong W, Xiong Y, Zhang LI, Tao HW (2018) Transforming Sensory Cues into Aversive Emotion via Septal-Habenular Pathway. Neuron 99:1016-1028.e1015.

Ziminski JJ, Hessler S, Margetts-Smith G, Sieburg MC, Crombag HS, Koya E (2017) Changes in Appetitive Associative Strength Modulates Nucleus Accumbens, But Not Orbitofrontal Cortex Neuronal Ensemble Excitability. The Journal of neuroscience : the official journal of the Society for Neuroscience 37:3160-3170.

Zolnik TA, Sha F, Johenning FW, Schreiter ER, Looger LL, Larkum ME, Sachdev RNS (2017) All-optical functional synaptic connectivity mapping in acute brain slices using the calcium integrator CaMPARI. The Journal of physiology 595:1465-1477.

8. SUPPLEMENTARY

7.1 Supplementary Materials & Methods

7.1.1 Antibodies

Anti-GAD67 Antibody, clone 1G10.2	Merck KGaA
Anti-Glial Fibrillary Acidic Protein Antibody, clone GA5	Merck KGaA
Anti-NeuN Antibody, clone A60 #MAB377	Merck KGaA
beta Galactosidase Polyclonal Antibody-5	Thermo Fisher Scientific Inc.
CaMKII alpha Monoclonal Antibody (6G9)	Thermo Fisher Scientific Inc.
c-Fos (9F6) Rabbit mAb #2250	Cell Signaling Technology, Inc.
Donkey anti-Mouse IgG (H+L) Highly Cross-Adsorbed Secondary Antibody, Alexa Fluor 594	Thermo Fisher Scientific Inc.
Donkey anti-Mouse IgG (H+L) Highly Cross-Adsorbed Secondary Antibody, Alexa Fluor 488	Thermo Fisher Scientific Inc.
Donkey anti-Mouse IgG (H+L) Highly Cross-Adsorbed Secondary Antibody, Alexa Fluor 405	Thermo Fisher Scientific Inc.
Donkey anti-Rabbit IgG (H+L) Highly Cross-Adsorbed Secondary Antibody, Alexa Fluor 594	Thermo Fisher Scientific Inc.
Donkey anti-Rabbit IgG (H+L) Highly Cross-Adsorbed Secondary Antibody, Alexa Fluor 488	Thermo Fisher Scientific Inc.
Donkey anti-Rabbit IgG (H+L) Highly Cross-Adsorbed Secondary Antibody, Alexa Fluor 568	Thermo Fisher Scientific Inc.
GFP Monoclonal Antibody (3E6)	Thermo Fisher Scientific Inc.

Table 11) List of antibodies

7.1.2 Drugs

(-)-Nicotine ditartrate (S)-3-(1-Methyl-2-pyrrolindinyl) pyridine $C_{10}H_{14}N_2 \bullet 2C_4H_6O_6$	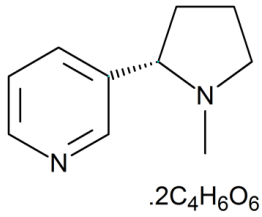	Santa Cruz Biotechnology, Inc.
Cocaine hydrochloride 2b-Carbomethoxy -3b-benzoyloxy tropane hydrochloride $C_{17}H_{21}NO_4 \bullet HCl$	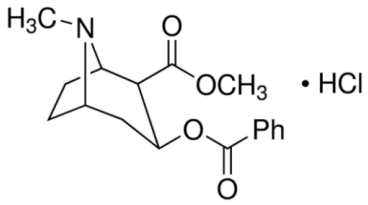	Sigma-Aldrich, Inc.
Daun02 [3-nitro-4-[(2S,3R,4S,5R,6R)-3,4,5-trihydroxy-6-(hydroxymethyl) oxan-2-yl] oxyphenyl] methyl N-[(2S,3S,4S,6R)-6-[(3-acetyl-3,5,12-trihydroxy-10-methoxy-6,11-dioxo-2,4-dihydro-1H-tetracen-1-yl) oxy]-3-hydroxy-2-methyloxan-4-yl] carbamate $C_{41}H_{44}N_2O_{20}$	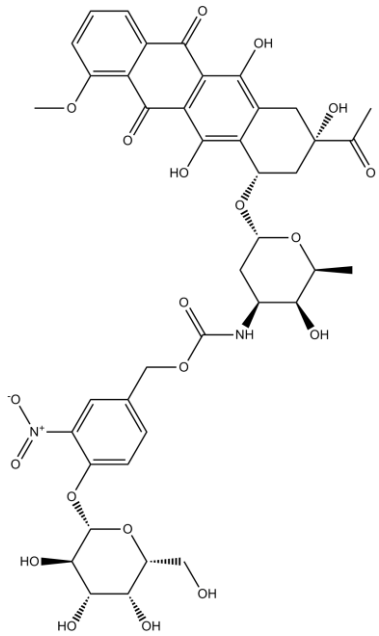	
Ethanol C_2H_6O	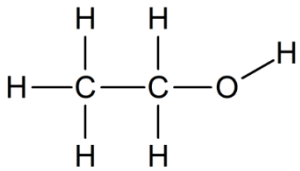	Sigma-Aldrich, Inc.
Saccharin sodium salt hydrate 2,3-Dihydro-3-oxobenzisosulfonazole sodium salt $C_7H_4NNaO_3S \bullet xH_2O$	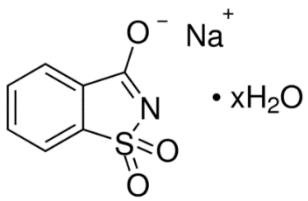	Sigma-Aldrich, Inc.

Table 12) List of rewards and active compounds used for self-administration and infusion

7.1.3 Solutions

0.1 M HCl	Dilute 1 M HCl stock solution 1:10 to working concentration with sterile water.
0.1 M Triethanolamine pH 8.0 (1 litre)	Mix 13.3 ml Triethanolamine with sterile water and adjust pH using HCl.
1 M HCl stock solution (1 litre)	Mix 84 ml concentrated HCl (12 M) with 800 ml sterile water and adjust volume.
1 x PBS	Dilute 10 x PBS 1:10 to the desired working concentration with sterile water.
1 x TBS (1 litre)	Dissolve 6.05 g Tris and 8.76 g NaCl in 800 ml deionized water. Adjust pH to 7.6 with 1 M HCl and adjust volume.
10 x Grundmix	For 10 ml of 10 x Grundmix mix: 2 ml 1 M Tris-HCl pH 7.6 2 ml 50 X Denhardt's solution 2 ml yest tRNA (25 mg/ml) 2 ml poly-A-RNA (5mg/ml) 0.2 ml 0.5 M EDTA pH 8.0 1.8 ml sterile H2O Mix well, sterile filter, and divide into 500 µl aliquots and store at -20°C
10 x PBS pH 7.4 (5 litres)	Dissolve the following chemicals in 4 l of water and adjust pH to 7.4: 400g NaCl 145g Na_2HPO_4 * 2 H_2O 10g KH_2PO_4 10g KCl Adjust volume, aliquot and autoclave.

2 x Prehybridization Buffer (100 ml)	Mix the following reagents: 10ml 1M Tris-HCl pH 7.6 10ml 0.5M EDTA pH 8.0 10ml 50x Denhardt's 5ml yeast tRNA (25mg/ml) 4ml 1M NaCl 61ml sterile water Divide into 25 ml aliquots and store at -20°C.
4 % PFA in PBS pH 7.0 (2 litres)	Dissolve 80 g PFA in 800 ml sterile water with help of small amounts of NaOH. Add 200 ml 10 x PBS and adjust pH to 7.0 with concentrated $HCl_{(aq)}$. Adjust volume and filter the solution.
aCSF (125 mM NaCl, 25 mM $NaHCO_3$, 2.5 mM KCl, 1.25 mM NaH_2PO_4, 10 mM Glucose, 2 mM $CaCl_2$, 1 mM $MgCl_2$)	Mix the following reagents for aCSF: 14.61 g NaCl 4.20 g $NaHCO_3$ 0.37 g KCl 0.39 g NaH_2PO_4 3.60 g Glucose 4 ml 1 M $CaCl_2$ 2 ml 1 M $MgCl_2$ Adjusted volume to 2 litres.
Blocking solution	7.5 % Donkey serum + 2.5 % BSA in TBS 0.2 % Triton X-100
EtOH (70 %, 80 %, 95 %)	70 % ethanol: Mix 700 ml absolute ethanol with 300 ml sterile water. 80 % ethanol: Mix 800 ml absolute ethanol with 200 ml water. 95 % ethanol: Mix 950 ml absolute ethanol with 50 ml sterile water.

Sucrose saline (87 mM NaCl, 25 mM $NaHCO_3$, 2.5 mM KCl, 1.25 mM NaH_2PO_4, 10 mM Glucose, 62 mM Sucrose, 0.5 mM $CaCl_2$, 7 mM $MgSO_4$, 0.01 mM Pyruvate)	Dissolve the following reagents in ultrapure H_2O: 10.17 g NaCl 4.20 g $NaHCO_3$ 0.37 g KCl 0.39 g NaH_2PO_4 3.60 g Glucose 42.45 g Sucrose 1 ml 1 M $CaCl_2$ 14 ml 1 M $MgSO_4$ 0.2 ml Pyruvate Adjust volume to 2 litres.
TBS 0.2 % Triton X-100 (1 litre)	Add 10 ml of a 20 % Triton-X 100 solution to 990 ml 1 x TBS and mix well.

Table 13) List of solutions and preparation protocols

7.2 Supplementary Results

7.2.1 Immunohistochemical analysis of neuronal ensembles following cue-induced reinstatement of reward seeking behaviour

For the neurochemical characterization of co-active cells during reward seeking behaviour animals had to acquire robust reward self-administration, which was followed by the cue-induced reinstatement test after an extinction phase. Afterwards animals were sacrificed and the brain region of interest, the OFC, treated with different antibody combinations to characterize the different cell types involved in ensemble formation. After image acquisition the immune reactivity of the different antibodies was counted (Table 14) and the resulting data analysed. Statistics for cell number comparisons, active cell comparisons and co-localization comparisons are displayed in tables 15-20. A comparison of the total number of cells counted in the investigated segments showed no significant differences between the three rewards neither for neurons nor for excitatory cells counted for each OFC subregion. However, there were significantly less inhibitory cells counted for the cocaine and the control group. Furthermore, the number of neurons counted for the control group within the ventral OFC was significantly larger than the number of neurons counted for the three rewards. In addition, the number of neurons in the lateral OFC of the control group was significantly larger than that of the EtOH group (Table 16).

Comparison of combined cFOS-ir positive counts, which represent previously active cells, showed that all groups of animals that were trained to reward self-administration had significantly higher activity levels compared to the control condition. Within the reward trained groups, no differences in active cells counted were detected. Only the number of active cells for the lateral OFC within the cocaine group was significantly lower than that of the ventral OFC for EtOH and saccharin trained animals (Table 17). Investigating each staining individually for active cells counted, it was found that for the NeuN staining the saccharin trained group had significantly more cFOS-ir counted than the EtOH or Cocaine trained group of rats. Furthermore, there were significantly less active neurons counted in control animals compared to all other groups (Table 18 cFOS-ir (NeuN)). For the GAD67 staining the control group showed significantly less activation compared to the other groups of animals (Table 18 cFOS-ir (GAD67)/cFOS-ir (CaMKII)). Within the CaMKII staining the cFOS-ir count for control animals was lower but not significantly different from the other groups of animals.

Furthermore, cell activity counts between the different antibody stainings was compared within each reward or control condition (Table 19). Within the EtOH group there were no differences in cFOS-ir positive cell counts detectable between the different antibody stainings. Counting of active cells for the saccharin trained group of animals revealed significantly higher amounts of active cells for the NeuN staining in the ventral OFC (GAD67/CaMKII ventral) and the lateral OFC (CaMKII lateral). For cocaine trained animals no differences in the activity counting were found between antibody stainings. A significantly higher amount of cFOS-ir was counted within the CaMKII-staining for controls compared to the other two antibody stainings. Only marginal differences in activity counts could be observed between the different stainings, which might to be considered during the interpretation of results, but overall the obtained cell counts should be reliable.

The overlay between cFOS-ir and NeuN-ir revealed that all cFOS-ir positive cells were also NeuN-ir positive. This was the case for all four reward conditions. However, differences could be observed for the percentage of neurons active during the different reward seeking or control conditions. The control group showed a significantly lower percentage of neurons being active within the lateral or ventral OFC than all three reward seeking groups. However, within the group of animals subjected to cue-induced reward seeking the saccharin trained animals displayed a significantly higher percentage of active cells within the neuronal population than EtOH or cocaine trained rats (Table 20). Co-localization of cFOS-ir and GAD67-ir also showed substantial overlap between these two biomarkers. Comparison of the percentage of merged immune-reactivity for cFOS and GAD67 within the population of inhibitory cells revealed that a significantly increased percentage of inhibitory cells was active during EtOH reward seeking compared to all other conditions. Furthermore, the control group showed a significantly lower percentage of inhibitory cells being active for both OFC subregions compared to all other groups that were trained to reward self-administration. The percentage of active neurons within the population of excitatory cells was significantly increased for EtOH and cocaine trained animals compared to saccharin trained animals and the control group. However, control animals also displayed a significantly decreased percentage of active excitatory cells within the OFC compared to saccharin trained rats (Table 20).

A		NeuN-ir		GAD67-ir		CaMKII-ir	
		ventral	lateral	ventral	lateral	ventral	lateral
EtOH	Mean	136	122	53	50	105	91
	SEM	3.85	5.56	4.19	4.47	4.86	5.65
Saccharin	Mean	144	130	53	53	112	97
	SEM	5.16	4.84	1.69	2.36	5.48	3.79
Cocaine	Mean	143	128	38	38	104	89
	SEM	4.47	3.85	2.45	2.28	4.75	4.67
Control	Mean	163	146	32	33	115	102
	SEM	5.61	7.40	1.67	1.51	6.14	4.74

B		cFOS-ir (NeuN)		cFOS-ir (GAD67)		cFOS-ir (CaMKII)	
		ventral	lateral	ventral	lateral	ventral	lateral
EtOH	Mean	72	64	82	77	78	71
	SEM	2.22	3.04	4.25	4.89	2.61	3.93
Saccharin	Mean	98	84	68	67	69	59
	SEM	6.05	5.01	4.23	3.97	4.08	4.49
Cocaine	Mean	69	64	71	66	80	66
	SEM	3.49	2.53	5.37	3.28	3.56	3.80
Control	Mean	49	43	52	48	67	62
	SEM	1.70	2.82	2.36	1.91	3.17	4.10

C		cFOS-ir/NeuN-ir Merge		cFOS-ir/GAD67-ir Merge		cFOS-ir/CaMKII-ir Merge	
		ventral	lateral	ventral	lateral	ventral	lateral
EtOH	Mean	53	53	47	46	60	61
	SEM	1.02	0.93	2.62	2.96	2.96	3.11
Saccharin	Mean	67	64	27	27	52	50
	SEM	2.41	2.12	2.73	2.77	2.00	3.41
Cocaine	Mean	48	50	26	27	68	63
	SEM	1.67	1.32	1.98	2.56	1.64	3.04
Control	Mean	30	30	16	16	42	41
	SEM	1.60	1.09	1.16	1.15	1.21	2.31

Table 14) Number of cells labelled by the different antibodies within the OFC after cue-induced reinstatement and percentage of co-localized cells within each population

Displayed are the average number (mean) of labelled cells and the standard error of mean (SEM) counted for the different subregions of the OFC (ventral OFC and lateral OFC) as well as the percentage of active cells within each cell population. A) Number of neurons (NeuN), inhibitory cells (GAD67) and excitatory cells (CaMKII) counted for animals trained to the different rewards. B) Displayed are the number of cells active (cFOS positive) within the group of cells shown in A). C) Depicts the percentage of merged active cells within each cell population (NeuN-ir positive, GAD67-ir positive or CaMKII-ir positive).

	Two-way ANOVA			
	df	Effect	F	p
NeuN-ir	90	Reward	8.805	0.000035
		Subregion	17.018	0.000082
		Interaction	0.030	0.992922
GAD67-ir	70	Reward	23.838	0.000000
		Subregion	0.021	0.886436
		Interaction	0.177	0.911460
CaMKII-ir	76	Reward	2.475	0.067859
		Subregion	15.635	0.000171
		Interaction	0.012	0.998141
cFOS-ir (NeuN)	90	Reward	47.082	0.000000
		Subregion	8.790	0.003877
		Interaction	0.552	0.648291
cFOS-ir (GAD67)	70	Reward	17.670	0.000000
		Subregion	1.887	0.173925
		Interaction	0.123	0.946308
cFOS-ir (CaMKII)	76	Reward	4.528	0.005646
		Subregion	11.534	0.001089
		Interaction	0.545	0.652744
EtOH	58	Reward	5.325	0.007532
		Subregion	4.866	0.031361
		Interaction	0.088	0.916120
Saccharin	62	Staining	19.810	0.000000
		Subregion	4.282	0.042696
		Interaction	0.848	0.433132
Cocaine	62	Staining	1.321	0.274188
		Subregion	7.453	0.008233
		Interaction	0.947	0.393296
Control	54	Staining	23.617	0.000000
		Subregion	4.758	0.033530
		Interaction	0.025	0.975395
cFOS-ir/NeuN-ir Merge	90	Reward	155.571	0.000000
		Subregion	0.175	0.676399
		Interaction	0.849	0.470750
cFOS-ir/GAD67-ir Merge	70	Reward	56.974	0.000000
		Subregion	0.018	0.893275
		Interaction	0.149	0.929808
cFOS-ir/CaMKII-ir Merge	76	Reward	33.605	0.000000
		Subregion	1.118	0.293642
		Interaction	0.347	0.791369

Table 15) Statistics for the comparison of cell numbers, number of active cells between rewards/between stainings and percentage of merged immune reactivity within the respective population

Table 15 shows the results of a two-way ANOVA analysis for the comparison of cells labelled (NeuN-ir, GAD67-ir and CaMKII-ir), the number of active cells (cFOS-ir positive) between rewards (cFOS-ir (NeuN); cFOS-ir (GAD67); cFOS-ir (CaMKII))/between stainings (EtOH; Saccharin; Cocaine; Control) and the percentage of merges between cFOS-ir and the respective cell-type specific immune reactivity population. Abbreviations: df = degrees of freedom, F = F-value, p = p-value.

Newman-Keuls *post hoc* test									
Reward	**Sub-region**	**NeuN**							
EtOH	ventral		0.203154	0.504545	0.444362	0.358522	0.481279	0.002925	0.471778
EtOH	lateral	0.203154		0.030135	0.449370	0.036618	0.413288	0.000120	0.015437
Sacc	ventral	0.504545	0.030135		0.240464	0.844679	0.161766	0.026894	0.741852
Sacc	lateral	0.444362	0.449370	0.240464		0.214053	0.697818	0.000384	0.182317
Cocaine	ventral	0.358522	0.036618	0.844679	0.214053		0.167168	0.029087	0.858287
Cocaine	lateral	0.481279	0.413288	0.161766	0.697818	0.167168		0.000204	0.105847
Control	ventral	0.002925	0.000120	0.026894	0.000384	0.029087	0.000204		0.023823
Control	lateral	0.471778	0.015437	0.741852	0.182317	0.858287	0.105847	0.023823	
		GAD67							
EtOH	ventral		0.770120	0.965512	0.980329	0.003102	0.002605	0.000191	0.000226
EtOH	lateral	0.770120		0.520151	0.890917	0.008235	0.003983	0.000479	0.000660
Sacc	ventral	0.965512	0.520151		0.997493	0.002237	0.001592	0.000172	0.000201
Sacc	lateral	0.980329	0.890917	0.997493		0.004098	0.003829	0.000186	0.000262
Cocaine	ventral	0.003102	0.008235	0.002237	0.004098		0.926065	0.399629	0.293356
Cocaine	lateral	0.002605	0.003983	0.001592	0.003829	0.926065		0.507392	0.485649
Control	ventral	0.000191	0.000479	0.000172	0.000186	0.399629	0.507392		0.809768
Control	lateral	0.000226	0.000660	0.000201	0.000262	0.293356	0.485649	0.809768	
		CaMKII							
EtOH	ventral		0.269912	0.342317	0.668665	0.817136	0.245909	0.356181	0.896319
EtOH	lateral	0.269912		0.044552	0.383433	0.290601	0.845176	0.018228	0.266338
Sacc	ventral	0.342317	0.044552		0.234385	0.464007	0.034781	0.672350	0.502130
Sacc	lateral	0.668665	0.383433	0.234385		0.639667	0.533720	0.132312	0.492539
Cocaine	ventral	0.817136	0.290601	0.464007	0.639667		0.287242	0.377752	0.831257
Cocaine	lateral	0.245909	0.845176	0.034781	0.533720	0.287242		0.013044	0.299271
Control	ventral	0.356181	0.018228	0.672350	0.132312	0.377752	0.013044		0.366164
Control	lateral	0.896319	0.266338	0.502130	0.492539	0.831257	0.299271	0.366164	

Table 16) Statistical analysis for cell number comparisons

Table 16 shows the results of the Newman-Keuls *post hoc* analysis for the comparison of the number of cells counted for the different antibody stainings (NeuN, GAD67, CaMKII) and the different rewards investigated. Numbers represent the p-value. Abbreviation: Sacc = saccharin.

		Two-way ANOVA			
		df	Effect	F	p
cFOS-ir		90	Reward	28.852	0.000000
			Subregion	14.967	0.000139
			Interaction	0.207	0.891482
Newman-Keuls *post hoc* test					
EtOH	ventral		0.298807	0.439711	0.234860	0.316002	0.011514	0.000020	0.000026
EtOH	lateral	0.298807		0.086031	0.902400	0.736428	0.143053	0.000196	0.000008
Sacc	ventral	0.439711	0.086031		0.077409	0.177873	0.000961	0.000026	0.000032
Sacc	lateral	0.234860	0.902400	0.077409		0.533468	0.251147	0.000215	0.000017
Cocaine	ventral	0.316002	0.736428	0.177873	0.533468		0.120494	0.000036	0.000020
Cocaine	lateral	0.011514	0.143053	0.000961	0.251147	0.120494		0.010934	0.000270
Control	ventral	0.000020	0.000196	0.000026	0.000215	0.000036	0.010934		0.167206
Control	lateral	0.000026	0.000008	0.000032	0.000017	0.000020	0.000270	0.167206	

Table 17) Statistical analysis of cFOS-ir reward/control-specific

Table 17 shows the results of a two-way ANOVA and Newman-Keuls *post hoc* analysis for the combined cFOS-ir counts for all stainings in a reward/control specific manner. Values for the Newman-Keuls *post hoc* analysis represent the p-value. Abbreviations: df = degrees of freedom, F = F-value, p = p-value.

Newman-Keuls *post hoc* test									
Reward	**Sub-region**	**cFOS-ir (NeuN)**							
EtOH	ventral		0.352426	0.000116	0.019742	0.656937	0.506767	0.000545	0.000130
EtOH	lateral	0.352426		0.000118	0.001779	0.349606	0.994347	0.013105	0.000968
Sacc	ventral	0.000116	0.000118		0.013067	0.000147	0.000123	0.000121	0.000118
Sacc	lateral	0.019742	0.001779	0.013067		0.016171	0.002760	0.000123	0.000121
Cocaine	ventral	0.656937	0.349606	0.000147	0.016171		0.611755	0.001403	0.000153
Cocaine	lateral	0.506767	0.994347	0.000123	0.002760	0.611755		0.004962	0.000541
Control	ventral	0.000545	0.013105	0.000121	0.000123	0.001403	0.004962		0.291924
Control	lateral	0.000130	0.000968	0.000118	0.000121	0.000153	0.000541	0.291924	
		cFOS-ir (GAD67)							
EtOH	ventral		0.416911	0.091300	0.089249	0.175478	0.072826	0.000159	0.000125
EtOH	lateral	0.416911		0.270231	0.309419	0.326606	0.294777	0.000686	0.000166
Sacc	ventral	0.091300	0.270231		0.854294	0.569982	0.914115	0.031433	0.005506
Sacc	lateral	0.089249	0.309419	0.854294		0.731448	0.826943	0.027945	0.006053
Cocaine	ventral	0.175478	0.326606	0.569982	0.731448		0.764144	0.010016	0.001319
Cocaine	lateral	0.072826	0.294777	0.914115	0.826943	0.764144		0.018597	0.006185
Control	ventral	0.000159	0.000686	0.031433	0.027945	0.010016	0.018597		0.443430
Control	lateral	0.000125	0.000166	0.005506	0.006053	0.001319	0.006185	0.443430	
		cFOS-ir (CaMKII)							
EtOH	ventral		0.194398	0.183617	0.007245	0.839179	0.121529	0.134005	0.028380
EtOH	lateral	0.194398		0.640241	0.173453	0.290523	0.685120	0.651169	0.366115
Sacc	ventral	0.183617	0.640241		0.316298	0.203640	0.798785	0.678694	0.529832
Sacc	lateral	0.007245	0.173453	0.316298		0.004910	0.411160	0.440757	0.576040
Cocaine	ventral	0.839179	0.290523	0.203640	0.004910		0.104410	0.126891	0.021270
Cocaine	lateral	0.121529	0.685120	0.798785	0.411160	0.104410		0.823715	0.475287
Control	ventral	0.134005	0.651169	0.678694	0.440757	0.126891	0.823715		0.616050
Control	lateral	0.028380	0.366115	0.529832	0.576040	0.021270	0.475287	0.616050	

Table 18) Statistical analysis for active cell number comparisons

Table 18 displays the results of the Newman-Keuls *post hoc* analysis for the comparison of active cells (cFOS-ir positive) counted for the different antibody stainings (NeuN, GAD67, CaMKII) and the different rewards investigated. Numbers show the p-value. Abbreviation: Sacc = saccharin

Newman-Keuls *post hoc* test							
IR	**Sub-region**	**EtOH**					
NeuN	ventral		0.307570	0.215260	0.308444	0.372030	0.956776
NeuN	lateral	0.307570		0.013283	0.069164	0.047823	0.159226
GAD67	ventral	0.215260	0.013283		0.622528	0.546814	0.272337
GAD67	lateral	0.308444	0.069164	0.622528		0.745971	0.528877
CaMKII	ventral	0.372030	0.047823	0.546814	0.745971		0.499656
CaMKII	lateral	0.956776	0.159226	0.272337	0.528877	0.499656	
		Saccharin					
NeuN	ventral		0.056021	0.000465	0.000433	0.000376	0.000136
NeuN	lateral	0.056021		0.054399	0.067110	0.029615	0.004020
GAD67	ventral	0.000465	0.054399		0.880249	0.890821	0.375355
GAD67	lateral	0.000433	0.067110	0.880249		0.955023	0.236702
CaMKII	ventral	0.000376	0.029615	0.890821	0.955023		0.453026
CaMKII	lateral	0.000136	0.004020	0.375355	0.236702	0.453026	
		Cocaine					
NeuN	ventral		0.767984	0.720102	0.484396	0.131087	0.742469
NeuN	lateral	0.767984		0.674856	0.962268	0.051784	0.818194
GAD67	ventral	0.720102	0.674856		0.540033	0.114976	0.692554
GAD67	lateral	0.484396	0.962268	0.540033		0.047368	0.973449
CaMKII	ventral	0.131087	0.051784	0.114976	0.047368		0.066029
CaMKII	lateral	0.742469	0.818194	0.692554	0.973449	0.066029	
		Control					
NeuN	ventral		0.340528	0.448472	0.738976	0.000381	0.006639
NeuN	lateral	0.340528		0.142330	0.285090	0.000141	0.000356
GAD67	ventral	0.448472	0.142330		0.519000	0.001573	0.018566
GAD67	lateral	0.738976	0.285090	0.519000		0.000251	0.004751
CaMKII	ventral	0.000381	0.000141	0.001573	0.000251		0.211613
CaMKII	lateral	0.006639	0.000356	0.018566	0.004751	0.211613	

Table 19) Statistical analysis of cell activity counts between different antibody stainings within each reward group

Table 19 gives an overview of the statistical results of the Newman-Keuls *post hoc* analysis for the comparison of differences between cFOS-ir counting between the three antibody co-stainings within each reward group. Values represent the p-value.

Newman-Keuls *post hoc* test									
Reward	**Sub-region**	**cFOS-ir/NeuN-ir Merge**							
EtOH	ventral		0.958091	0.000144	0.000119	0.156360	0.297114	0.000144	0.000118
EtOH	lateral	0.958091		0.000106	0.000118	0.229952	0.515584	0.000118	0.000123
Sacc	ventral	0.000144	0.000106		0.186162	0.000123	0.000118	0.000121	0.000118
Sacc	lateral	0.000119	0.000118	0.186162		0.000118	0.000144	0.000123	0.000121
Cocaine	ventral	0.156360	0.229952	0.000123	0.000118		0.419420	0.000113	0.000106
Cocaine	lateral	0.297114	0.515584	0.000118	0.000144	0.419420		0.000106	0.000144
Control	ventral	0.000144	0.000118	0.000121	0.000123	0.000113	0.000106		0.712965
Control	lateral	0.000118	0.000123	0.000118	0.000121	0.000106	0.000144	0.712965	
		cFOS-ir/GAD67-ir Merge							
EtOH	ventral		0.664400	0.000151	0.000125	0.000128	0.000112	0.000127	0.000123
EtOH	lateral	0.664400		0.000112	0.000152	0.000125	0.000116	0.000128	0.000127
Sacc	ventral	0.000151	0.000112		0.917472	0.925591	0.928135	0.010571	0.009422
Sacc	lateral	0.000125	0.000152	0.917472		0.787421	0.979398	0.007670	0.008118
Cocaine	ventral	0.000128	0.000125	0.925591	0.787421		0.966375	0.006068	0.009507
Cocaine	lateral	0.000112	0.000116	0.928135	0.979398	0.966375		0.012789	0.010310
Control	ventral	0.000127	0.000128	0.010571	0.007670	0.006068	0.012789		0.846136
Control	lateral	0.000123	0.000127	0.009422	0.008118	0.009507	0.010310	0.846136	
		cFOS-ir/CaMKII-ir Merge							
EtOH	ventral		0.851866	0.025769	0.014948	0.184992	0.714068	0.000172	0.000128
EtOH	lateral	0.851866		0.042000	0.016384	0.161830	0.552785	0.000141	0.000130
Sacc	ventral	0.025769	0.042000		0.559254	0.000568	0.015945	0.027117	0.014067
Sacc	lateral	0.014948	0.016384	0.559254		0.000194	0.004400	0.043781	0.036779
Cocaine	ventral	0.184992	0.161830	0.000568	0.000194		0.215378	0.000125	0.000121
Cocaine	lateral	0.714068	0.552785	0.015945	0.004400	0.215378		0.000128	0.000125
Control	ventral	0.000172	0.000141	0.027117	0.043781	0.000125	0.000128		0.642535
Control	lateral	0.000128	0.000130	0.014067	0.036779	0.000121	0.000125	0.642535	

Table 20) Statistical analysis for the percentage of merged immune reactivity

Table 20 shows the results of the Newman-Keuls *post hoc* analysis for the comparison of the percentage of active cells within each cell population (NeuN-ir positive, GAD67-ir positive or CaMKII-ir positive) for each of the rewards investigated. Numbers represent the p-value. Abbreviation: Sacc = saccharin